

Electron Spin-Spin Coupling
from Multireference CI Wave Functions

Inaugural-Dissertation

zur

Erlangung des Doktorgrades der
Mathematisch-Naturwissenschaftlichen Fakultät
der Heinrich-Heine-Universität Düsseldorf

vorgelegt von

Natalie Gilka

aus Bydgoszcz (Polen)

April 2008

Aus dem Institut für Theoretische Chemie und Computerchemie
der Heinrich-Heine-Universität Düsseldorf

Gedruckt mit der Genehmigung der
Mathematisch-Naturwissenschaftlichen Fakultät
der Heinrich-Heine-Universität Düsseldorf

Referentin:	Prof. Dr. Christel M. Marian
Korreferent:	Prof. Dr. Walter Thiel
Externer Referent:	Prof. Dr. Frank Neese

Tag der mündlichen Prüfung: 23.06.2008

Contents

Introduction	1
1 Framework	3
1.1 Electron Spin-Spin Coupling: General Framework	4
1.1.1 Primary Concepts	4
1.1.2 Assessment of the Experimental Framework	7
1.1.3 Historically: Calculations of Electron Spin-Spin Coupling	10
1.1.4 Present Theoretical Work	13
1.1.5 Conclusion: Concerted Considerations	19
1.2 Theoretical Chemistry at Düsseldorf – SFB 663	20
1.3 Computational Considerations	22
1.4 Program Frame	25
1.5 Theoretical Concepts	28
1.5.1 Expression of the Operator	28
Wigner-Eckart Theorem	30
Second Quantization	31
1.5.2 Matrix Elements	33
Algorithm: η -Pattern: spin-free	33
Algorithm: η -Pattern: spin-dependent	35
1.6 Experimental Formulation	36
1.7 Final Remarks	38
2 Computational Structure	41
2.1 Program Structure	41
2.2 Calculation of Matrix Elements	45
2.2.1 Spin-Spin Operator	48
2.2.2 Derivation – Part (I)	52
Selection Rules	52
Contribution of Closed Shells	55
Permutational Relation	57
2.2.3 Derivation – Part (II)	61
Anticommutation	62
Insertion of Resolution of Identity	63
Sequence of Spin Terms	63
$\Delta S = 2$	66
$\Delta S = 1$	67

$\Delta S = 0$	68
2.2.4 Implemented Formulas	75
2.2.5 Spatial Integrals	78
Principal scheme	79
Existing Approach in Dalton	81
2.3 Implementation	83
2.3.1 Program Execution	91
2.4 Conclusion	92
3 Calculations	93
3.1 O ₂	94
3.1.1 One- vs. Two-Center Contributions	95
3.1.2 Augmented vs. Non-Augmented Basis Sets	97
3.1.3 Effect of Selected Reference Configurations	98
3.1.4 Convergence with Reference Space	100
3.1.5 Evaluation of Results for O ₂	102
3.2 NH	103
3.3 All-trans Polyenes	104
3.3.1 Discussion of MOs	108
3.3.2 Hexatriene: Comparison of DFT/MRCI, HF/MRCI, and CASSCF	111
3.3.3 DFT/MRCI: Basis Set Comparison	113
3.3.4 DFT/MRCI: Results for C ₆ H ₈ – C ₁₆ H ₃₄	115
3.3.5 All-trans Polyenes: Conclusions	116
3.4 Conclusion	117
Summary and Outlook	119
List of Tables	121
List of Figures	123
Acknowledgement	141

Introduction

Understanding the laws of nature and elucidating their functioning is the fundamental motivation in the natural sciences. In the evolution of life, this functioning is strongly determined by our main natural source of energy, the sun. On a biochemical level, sunlight initiates a multitude of processes involving excited states of molecules, thereby constituting the driving force in the astonishing complexity of what we simply call “living”.

These processes usually involve direct excitation of molecular systems, followed by subsequent de-excitation through a variety of possible mechanisms. Considering especially the numerous pathways molecules in biological environments can follow in redistributing their excess energy, it is not surprising to reflect that we are far from understanding the functioning of biological organisms. Nonetheless, concerted efforts from both the experimental and theoretical sides constitute a promising approach, successively revealing facets of the entire composition.

The theoretical community has a profound record of success in the consideration of systems at equilibrium. Investigation of excited states, in particular the consideration of reaction mechanisms, necessitates entirely different approaches, however. A molecule undergoes conformational reorientations accompanied by changes in the structure of its energy levels, opening possibilities for intricate energy redistributions and coupling to different states, conceivably involving neighbouring molecules. Excitation from the singlet to the triplet manifold can be a crucial aspect in this process and necessitates the consideration of spin interactions. From a theoretical perspective, this involves the evaluation of spin coupling effects frequently small in magnitude, the conceptual origin of which lies in the consideration of special relativity.

The group of Theoretical and Computational Chemistry at the University of Düsseldorf provides profound competence in the sophisticated electronic structure treatment of excited states of medium-sized systems through the efficient DFT/MRCI approach [1]. This is combined with considerable experience in the calculation of spin-orbit coupling effects employing the program SPOCK [2–4]. This expertise is brought to applications in the Sonderforschungsbereich (SFB) 663 “Molecular Response to Electronic Excitation”. The incentive of the SFB 663 is the investigation of processes of photostability and photoreactivity; its particular strength lies in the interdisciplinary approach of experimental and theoretical fields.

The present work is motivated by an extension of the capabilities of our group. It

presents the development and theoretical consideration of the calculation of coupling effects between the spins of unpaired electrons (*spin-spin coupling*). The impact of this work is twofold: First, electron spin-spin interaction, like spin-orbit interaction, constitutes a possible coupling mechanism in processes of excitation and de-excitation. Understanding the origin of these transitions is mandatory for an explanation of biochemical reactions. Second, spin-spin coupling can be employed as a means of investigating the structure of excited states. The magnitude of this interaction is an indicator of the distance between unpaired electrons. This has already been employed in an experimental context and the combination with the theoretical approach is particularly promising for obtaining insight into the location of radical electrons in molecular systems, thereby clarifying processes of energy dissipation.

Calculations in the field of electron spin-spin coupling have been very limited. This observation is related to the high demand that the implementation of this operator poses, motivated by its complicated structure. The present work represents one of the first efforts in the implementation of this effect based on a computational treatment that considers dynamical as well as non-dynamical correlation contributions and allows for the computation of medium-sized systems. It is novel as it is one of the few approaches that considers the relevant correlation effects on an equal basis, allows for the calculation of excited states due to its multireference approach, and furthermore enables the consideration of larger systems due to the efficient selecting algorithm of the underlying correlation treatment. The present work will thereby not only assist in the ultimate elucidation of the intricate biochemical mechanisms present in photoactive systems but will advance an understanding of the properties of this effect itself.

Chapter 1

Framework

$$\hat{\mathcal{H}}\Psi = i\hbar\frac{\partial}{\partial t}\Psi$$

The field of theoretical chemistry is concerned with the task of solving the Schrödinger equation which is given above in its most general form. The Schrödinger equation represents the Coulomb interactions between charged particles on a quantum mechanical level as described by the action of the Hamiltonian $\hat{\mathcal{H}}$ on the wave function Ψ . Fundamental aspects underlying this task have been extensively covered in literature [5–7]. The Schrödinger equation in itself does not account for relativistic effects, thereby in its most profound deficiency failing to describe the quantity of spin. One of the first attempts at a unified description of relativistic as well as quantum mechanical effects was formulated through the Dirac equation [8, 9] which is valid for a single particle of spin 1/2 and thereby constitutes a starting point for a unification of these theories on a molecular level. Nevertheless, the extension of the Dirac equation to a many-particle system is not straightforward and the field of theoretical chemistry has observed considerable effort in the development of approximate treatments of relativistic effects. A beautiful introduction is given by Moss [10], while Faegri and Dylla [11] cover contemporary efforts and developments in the field of relativistic quantum mechanics.

For a consistent overview over the more basic aspects in the field of theoretical chemistry, the reader is encouraged to refer to beforehand mentioned literature [5–7, 10, 11]. Within this thesis, I will restrict myself to the introduction of concepts and notions specific to this work which may extend beyond fundamental aspects familiar to most quantum chemists. I will refer frequently to available literature, though, so as to enable the reader to acquire a more detailed knowledge where desired.

Prelude

The following sections are intended as a reflection on more general aspects, embedding the computational treatment of electron spin-spin coupling into an experimental as well as historical context. I will start out with an introduction of the most important concepts and characteristics concerning electron spin-spin interactions (Section *Primary Concepts*). Subsequently, I will turn to the experimental side of the observation of this effect, discussing in particular its investigation and relevance in the context of experimental work (Section *Assessment of the Experimental Framework*). The following

sections will be concerned with a discussion of the theoretical side, starting out with an illustration of the historical origins in the calculation of electron spin-spin coupling (Section *Historically: Calculations of Electron Spin-Spin Coupling*), and subsequently discussing in detail the contemporary efforts in this field (Section *Present Theoretical Work*). I will finish with a brief reflection on the concerted efforts in theory and experiment (Section *Concerted Considerations*).

1.1 Electron Spin-Spin Coupling: General Framework

1.1.1 Primary Concepts

The observation and explanation of the effect of electron spin-spin coupling is historically in close vicinity to the emergence of quantum mechanics itself.

The experimental foundation of electron spin lies in the famous measurement of the magnetic moment of a beam of silver atoms by Stern and Gerlach in 1921 [12, 13]. The origin for the observed well-defined transition which suggested a quantization of the magnetic moment of the silver atoms was then unknown. A theoretical discussion of the anomalous Zeeman effect in alkali atoms, in particular the reflection on the relevance of inner shell electrons, caused Pauli to conclude that the observed effect is attributable solely to the valence electron and thereby led him to the postulation of a fourth electronic quantum number [14]. His work was shortly after interpreted by Uhlenbeck and Goudsmit [15, 16] as an intrinsic angular momentum of the electron (for a more detailed review of the experimental discovery, see e.g., Ch. 2 in [17]). The theoretical basis of the effect of electron spin was laid by Dirac in 1928 with the relativistic description of the motion of a single electron [8, 9, 18]. An approximate extension to a system of more than one electron followed subsequently by Breit [19, 20]. By 1957, the transitions observable in electron spectra were already well understood and a comprehensive discussion of atomic terms in the Hamiltonian was given in the influential work by Bethe and Salpeter [21].

A detailed discussion of the parallel experimental and theoretical development of electron paramagnetic resonance (EPR) is presented in a review by Neese and Munzarová, *Historical Aspects of EPR Parameter Calculations*, in [22]. This review illustrates comprehensively the connections and mutual influences between theory and experiment and provides a concise overview of the historical path in theoretical developments. I will therefore restrict myself to highlighting a few points of major relevance and refer to the above mentioned work for the entire picture.

The concept of fundamental influence in the theoretical treatment of transitions experimentally observable in EPR spectra was the introduction of the effective spin Hamiltonian in the early 1950s. The theoretical description of molecular systems from first principles proved to be highly demanding at the time of the emergence of EPR, and a simpler concept was required to assist experimentalists in a theoretical interpretation

of spectral transitions. The fundamental idea lay in the introduction of a fictitious Hamiltonian containing solely spin-dependent operators. The theoretically demanding effects of correlation were absorbed into numerical parameters, the values of which were obtained by comparison with experiment. I refer to McWeeny [23] for a thorough discussion of the underlying theory of the spin Hamiltonian formalism, but would like to stress that this “effective Hamiltonian” is *not* the electronic Hamiltonian of the system under consideration but a construct introduced on the basis of a simplified analysis of experimental data. As McWeeny remarked in this respect: “*It [the spin Hamiltonian] provides an attractive formal prescription for “absorbing” the complexities of a detailed energy calculation into a few numerical parameters [...]. The use of spin Hamiltonians in many areas of chemical physics is now commonplace, but we must always remember they provide the means of fitting observed results and identifying parameter values within a certain theoretical scheme – they do not provide a “first principles” method of calculating anything.*” (McWeeny [23], p. 30).

The concept of the spin Hamiltonian was and still is of major relevance in the analysis of experimental data as it enables experimentalists to interpret complicated spectra on the basis of a limited number of parameters. Extensive literature has been written, particularly in the 1960s and 1970s, which establishes the connection between the theoretical concept of spin Hamiltonian parameters and experimental observations, discusses spectra of individual systems as well as classes of systems, and analyzes experimentally observed transitions with respect to selection rules, considerations of symmetry and possible influences of the surrounding environment [24–31]. Among these, I would like to point out in particular the comprehensive discussion of organic as well as inorganic systems by Weltner [24] which reflects a thorough investigation of contemporary experimental and theoretical work, furthermore the monograph by Abragam and Bleaney [25] which constitutes a detailed discussion of effects observable in transition metal spectra, and the review by Langhoff and Kern [27] which considers aspects closer to the computational level, discussing the evaluation of matrix elements and the analytic calculation of integral expressions. A particular focus on triplet systems is provided by the extensive assessment of McGlynn, Azumi and Kinoshita [29].

The general principle behind the investigation of transitions in atomic and molecular systems is the observation of minor deviations of the energetics from the predictions on the basis of a purely electrostatic Hamiltonian. The cause of these deviations lies in coupling effects involving electron and/or nuclear momenta which can theoretically only be accounted for in the framework of a relativistic description [10, 11]. These coupling effects may give rise to splittings of levels which are degenerate in a nonrelativistic consideration of the system and may furthermore affect the energetic position of individual levels. Due to the small magnitude of these deviations, the computational approach consists frequently of a consideration of individual coupling terms on the basis of perturbation theory. Assuming the nonrelativistic Hamiltonian as the unperturbed description of a system composed of electrons and nuclei, the perturbing relativistic effects are most commonly described through the terms of the well-established Breit-Pauli Hamiltonian, originating in the work by respective persons [19, 20, 32] (for a

concise derivation of this operator, the reader is furthermore referred to [10,11]). The Breit-Pauli Hamiltonian, which constitutes an approximate consideration of the relativistic interactions, possesses the distinct advantage of allowing for a straightforward interpretation of its individual terms with regard to physical interactions.

The early introduction of a fictitious spin Hamiltonian was motivated from an experimental perspective, simplifying the interpretation of spectral observations. At the same time, the theoretical foundation of these transitions was accepted to originate in the relativistic description of the electron. This suggested the possibility of relating individual spin Hamiltonian parameters to (approximate) expressions derived from the full relativistic Hamiltonian. The connection between spin Hamiltonian parameters and terms of the Breit-Pauli Hamiltonian was indeed accomplished by Harriman in 1978 [33], and his work has therefore to be referred to as of particular significance, establishing a direct relationship between the first principles approach of the theoretician and the effective, phenomenological description of the experimentalist. (For further theoretical considerations on the spin Hamiltonian, the reader is referred to [23], while [24–31] cover issues of higher relevance to the experimental interpretation.)

One of the terms introduced through the derivation of the Breit-Pauli Hamiltonian can be recognized as describing the interaction of the spins of two electrons. Naturally, electron spin-spin interaction can only occur in systems with a spin S of $S \geq 1$. The coupling of electron spins potentially causes a splitting of electronic states with identical spin quantum number S but differing projections M_S , thereby possibly partially lifting the degeneracy present in a nonrelativistic calculation. As this effect arises independent of the presence of external fields, it is commonly denoted “zero-field splitting” (ZFS). Phenomenologically, the experimentally observable effect of zero-field splittings is parametrized in the framework of the spin Hamiltonian by the zero-field coupling constants D and E . In the case of a triplet, which is the most frequently considered one, we may observe depending on the symmetry of the system a splitting into two or into three distinct levels, the nomenclature of which is illustrated in Fig. 1.1.

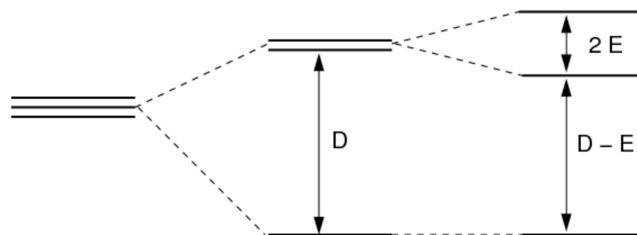


Figure 1.1: General picture of the splitting of a triplet state

A distinctly complicating aspect in the theoretical assessment of zero-field splittings lies in the fact that in the case of this observable, *two different* physical effects can contribute. The coupling of electron spin with orbital angular momentum is referred to as *spin-orbit coupling (SO)* and may, depending on the system, contribute in first

and/or in second order to the splitting. The coupling between spins of different electrons is denoted *spin-spin coupling* (*SS*) and contributes in first order [33]. The critical point herein is the observation that second-order SO and first-order SS coupling exhibit an identical mathematical structure, therefore causing these two effects to be experimentally indistinguishable. In theoretical literature, a differentiation between the two possible origins of zero-field splitting is frequently encountered by assignment of corresponding subindices, thereby specifying coupling constants D_{SS}/E_{SS} vs. D_{SO}/E_{SO} . Depending on the system, one or the other effect may predominate, otherwise, a balanced description of both is required to obtain quantitative agreement with experiment.

1.1.2 Assessment of the Experimental Framework

In the analysis of experimental EPR spectra, the physical coupling effects essential for a qualitative description, parametrized by corresponding spin-Hamiltonian parameters, are [34]:

- Interaction of the electron dipole moment with an external magnetic field (Zeeman effect) which is parametrized through the so-called “g-tensor”.
- Interaction between electronic and nuclear spins which is parametrized by the hyperfine coupling constant A .
- Effect of zero-field splitting (ZFS), lifting the degeneracy between spin components in states of $S \geq 1$ as parametrized by the zero-field splitting constants D and E .
- Interaction of the nuclear quadrupole moment Q with the electric field gradient q at the nucleus (for nuclear spins with $I \geq 1$), parametrized by the nuclear quadrupole coupling constant given as the product eqQ (e : electron charge).
- Interaction of the nuclear dipole moment with an external magnetic field (nuclear Zeeman effect), parametrized by the chemical shielding σ .

The order of magnitude of the observed transitions may assume as much as several hundred wave numbers in the case of electron Zeeman splittings (in particular in the presence of considerable spin-orbit coupling effects), a few wave numbers in the case of zero-field effects, less than one wave number in the case of hyperfine couplings, and less than a hundredth of a wave number in the case of nuclear quadrupole and nuclear Zeeman splittings. Computational investigations in literature have until recently strongly focussed on the calculation of hyperfine couplings (in particular in the context of transition metals) and g-tensors. For a detailed discussion of the historical development in these fields, the reader is once again referred to the review by Neese and Munzarová [34], while contributions in the entire volume provide a notion of the range of present achievements [22]. Efforts in the calculation of zero-field splittings have been moderate in comparison ([34] and discussion in Chs. 1.1.3, 1.1.4).

Since the advent of EPR as a spectroscopic method in the 1950s, the focus in the computational developments was strongly influenced by contemporary experimental possibilities. The first applications of EPR consisted of observations of hyperfine couplings in transition metal ions, while the interest from the side of organic chemistry originated in the investigation of π -systems in aromatic radicals. Parallel studies continued in the three different fields of organic radicals, transition metal ions and small inorganic radicals [34]. For a period of several decades, the technological possibilities were constrained to continuous wave (cw) EPR of limited spectral and time resolution. The development of pulse EPR techniques in combination with the technological improvement of operating at higher and higher frequencies was of substantial impact on the experimental field of EPR spectroscopy. The introduction of commercially available high-field EPR spectrometers in the early 1990s induced a high interest into the application of EPR spectroscopy and led to a substantial effort into the further development and improvement of sophisticated techniques which still continues [35, 36]. The high resolution achievable with pulse/cw high-field/high-frequency EPR spectroscopy provides the experimentalist with means of establishing remarkably detailed information about the system under study. The potential of this technique covers the investigation of interactions on a shorter range, thereby revealing information about electronic states and couplings of electron and nuclear momenta, as well as assessing long-range interactions which may extend to several (5-8) nanometers [35, 37, 38], thereby providing means of evaluating information concerning electron spin distributions as well as separations between coupling electronic/nuclear centers. For an introductory summary, I refer to the article by Calle et al. [39], while a comprehensive treatise of the historical development of EPR techniques as well as a review of modern methods is encountered in Schweiger and Jeschke [35]. A recent special issue in *Magnetic Resonance in Chemistry* offers a notion of the diverse research efforts conducted in this area at present [36].

Regarding electron spin-spin coupling, the particular relevance for EPR investigations lies in the interpretation of zero-field splittings in terms of distances of coupling electron centers. The spin-spin operator exhibits a strong dependence on the interelectronic distance as the Hamiltonian structure entails an r_{ij}^{-3} coupling between electrons i, j (see Eq. (1.2) and accompanying discussion in Ch. 1.3). The experimental interpretation is based on the spin Hamiltonian approach, thereby adopting a simplified theoretical description in the framework of which experimental parameters are fitted. The principal concept has been described comprehensively in literature [35, 40], complemented by reviews [41, 42] and advanced discussions of the accessible distance range and limitations as well as precision and sensitivity of present EPR experiments [37]. With respect to most recent work, I would like to point to the review by Jeschke and Polyhach [38] (and references therein). The particularly high interest in the last decade in the combination of EPR spectroscopy and electron-electron distance interpretation can possibly be attributed to its applicability to biological systems. Structures of biomolecules are frequently assessed by X-ray crystallography and/or high-resolution NMR. While X-ray crystallography requires the system to be crystallizable, NMR on the other hand imposes restrictions with respect to the size of the biological system under investigation. EPR spectroscopy is establishing itself in this respect as an advantageous complement,

as it can be applied to biological systems in their natural conformation and is sufficiently sensitive for characterization of large biomolecular complexes, as well as having the advantage of assessing a distance range ($\lesssim 5$ nm) which is on the order of the size of the system [38]. In general, hyperfine and spin-spin coupling effects can be interpreted in terms of spin distributions and distance measurements. The introduction of spin labels provides additionally the possibility to selectively mark molecular sites by attaching paramagnetic centers, frequently nitroxides. A consecutive EPR spectroscopic investigation reveals information about orientation and geometry of the nitroxide-labeled protein domains (see [37] and references therein, as well as again [35,40]). An experimental elucidation is universally assisted by sophisticated techniques which enable a separation of experimental signals, thereby facilitating a high spectroscopic resolution. The timescale accessible by EPR spectroscopy furthermore allows the detection and investigation of transient intermediates in their biologically active state, a point of particular relevance in the elucidation of mechanistics underlying biological processes. Combining different available strategies finally enables the experimentalist to deduce previously unaccessible information about the system. Latest developments entail the assessment of geometric information on the structure of macromolecules beyond straightforward distance distributions, as is discussed in the combination of spin-labeling with experimental orientation selection, supported by simulations of the spectra, by Polyhach et al. [43]. Another recent example for the ingenious combination of experimental techniques, aided by considerate data analysis, can be encountered in the work of Savitsky et al. [44]. This group studied bacterial photosynthetic reaction centers and was able not only to obtain information about the electronic structure of the redox partners but also about the three-dimensional orientation of the radical-pair system $P_{865}^+Q_A^-$, encompassing distances to about 5 nm. Thereby, the three-dimensional structure of the charge-separated primary electron donors P_{865}^+ and acceptors Q_A^- in reaction centers from the purple photosynthetic bacterium *Rhodobacter sphaeroides* was solved, and a small light-induced reorientation of the acceptor discovered which had escaped previous investigations. The resolution achievable and information content deducible is an impressive reflection on the advances in the field of EPR spectroscopy accomplished in the last 15 – 20 years.

A point of high relevance with respect to the experimental treatment of electron spin-spin coupling from the viewpoint of the theoretician is the realization that although experimental techniques have developed to a high degree of sophistication, the theoretical structures experimentalists employ are usually still based on the spin Hamiltonian approach in an approximation which is entitled “dipolar electron-electron interaction”, or alternatively “point-dipole model”. Electron spin-spin coupling is therein reduced to the physical picture of localized electrons of distinct distance. Effects of correlation and delocalization are neglected in this approximation as we are basically considering two point charges on different sites of a molecular system with the interaction being described by classical electromagnetics. In experimental literature, the limitations of this approach are noted and discussed as restrictions on the lower limit of the accessible distance range [37]: “A lower limit is imposed by the exchange contribution to the coupling between the two electron spins. Neglect of the through-space isotropic exchange

coupling may cause significant errors for distances below 1.5 nm, [...]. [Isotropic and anisotropic] contributions cannot be separated from the dipole-dipole coupling by any means, and at present they cannot be predicted with sufficient precision by quantum-chemical computations. Special care should be taken in studies on conjugated systems, where the isotropic exchange coupling can be significant for distances up to at least 3.6 nm.” Evaluating this statement from the theoretician’s perspective, we have to consider that the terminology employed stems out of an experimental context. The notion of “exchange coupling” for example refers to a term in the spin Hamiltonian that is included on the basis of a phenomenological treatment and does not arise from true spin interactions in the Hamiltonian (see [33], p. 190). Accounting for these for the theoretician slightly unfamiliar concepts, we recognize nonetheless that from the experimental side, deficiencies on the level of calculation and data analysis are distinctly noted. In particular the failure of an approximation based on localized electrons in the treatment of conjugated systems is recognized. In the reflection of experimental progress, two aspects clearly point to the necessity of improved theoretical concepts and computational considerations. On the one hand, the increased sensitivity on the experimental side provides more detailed information which should in its precision be met by the level of sophistication in calculations. On the other hand, considering the heightened interest and increased possibilities in the experimental investigation of biologically relevant compounds, one has to reflect about the nature of these systems. Catalytically relevant metal complexes may comply with the assumption of localized spin radicals; for delocalized conjugated molecules, like porphyrins, porphyrin-derived systems like corroles and corrins, as well as for carotenoidal systems which are of pronounced relevance in photoactive processes, a “dipolar electron-electron approximation” will very likely fail, and the question for computational treatments which account for high-level correlation as well as possibly a multireference character of the underlying system is posed.

1.1.3 Historically: Calculations of Electron Spin-Spin Coupling

Theoretical assessments of electron spin-spin coupling were and still are in general based on a perturbative treatment of the Breit-Pauli spin-spin Hamiltonian (see Ch. 1.3), a legitimate approach given the magnitude of this effect.

Computational considerations of zero-field splittings (spin-orbit and spin-spin) date back as far as the 1950s/1960s and were motivated by experimental investigations. An early work by Hameka in 1959 [45] evaluated the spin-spin contribution to the zero-field splitting of benzene in first-order perturbation theory, restricted to a consideration of the π -electron system employing Hückel MOs. The wave function consisted of Slater orbitals, incorporating as an empirical parameter the experimental C-C bond length of this system. At that time, experimental ZFS values for benzene were not available, but a very recent EPR investigation by Hutchison and Mangum on naphthalene [46] existed. The symmetry of the lowest triplet state was not known with certainty; Hameka calculated a spin-spin coupling constant of $D = 0.15 \text{ cm}^{-1}$ for a state of ${}^3B_{2u}$ symmetry and

$D = 0.09 \text{ cm}^{-1}$ for a state of ${}^3B_{1u}$ symmetry¹. In 1963, Boorstein and Gouterman [47] conducted a theoretical study on the ZFS in aromatic hydrocarbons (benzene, naphthalene, anthracene, phenanthrene, triphenylene, coronene), again based on a π -electron Hückel-MO approximation, employing a wave function parametrized with respect to configurational mixing. Their calculated spin-spin coupling constant of $D = 0.159 \text{ cm}^{-1}$ for benzene was in astonishingly good agreement with recent computational assessments of Vahtras et al. in 2002 [48], who reported a value of $D = 0.1583 \text{ cm}^{-1}$. At the time of the study of Boorstein and Gouterman, experimental values for the investigated systems were already available, indicating the experimental advancement in the field of EPR spectroscopy. The agreement between theory and experiment was reported to be satisfactory for benzene, naphthalene and anthracene, but declined substantially for the larger polyenes. Considering the simplicity in the theoretical treatment, the calculated results for the smaller systems were of encouraging accordance with experimental work.

The first *ab initio* calculation of electron spin-spin coupling was accomplished by Kayama in 1965 on the molecular system of O_2 [49] (according to Langhoff and Davidson [50]). Kayama compared the results as obtained under different constructions of the wave function, motivated by schemes which were employed by other groups. The electron spin-spin coupling for a single configuration wave function composed from Slater orbitals yielded a value of $D_{SS} = 1.510 \text{ cm}^{-1}$, thereby in favourable agreement with present computational considerations of Vahtras et al. [48] ($D_{SS} = 1.455 \text{ cm}^{-1}$). Employing a p -electron CI wave function which was considered to be the best theoretical approach assessed in their study resulted in noticeably stronger deviations, though ($D_{SS} = 0.94 \text{ cm}^{-1}$). Early EPR investigations by Tinkham and Strandberg [51] established an experimental value for the zero-field splitting in O_2 of $\lambda = \frac{1}{2}D = 1.981 \text{ cm}^{-1}$; this naturally comprises spin-orbit and spin-spin effects. The case of O_2 proved to be computationally distinctly more demanding than benzene, for which the spin-spin coupling was considered to be the predominant contribution to its zero-field splitting and the spin-orbit coupling of negligible relevance, thereby usually omitting its calculation. For O_2 , it was not clear that either of these experimentally indistinguishable effects could be neglected in a computational treatment. The theoretical consideration of O_2 by Kayama was therefore followed by an animated prolonged effort in the investigation of the contribution of spin-orbit vs. spin-spin coupling to the zero-field splitting in this system [52–57]. The ongoing discussion was seemingly resolved in 1974 by Langhoff [58], who calculated the spin-orbit and spin-spin contribution employing configuration interaction wave functions.

Further computational investigations of this period encompass for example calculations on O_2 and SO by Veseth and Lofthus [56], on NH , NF , PH , PF , NCl and SO by Wayne and Colburn [59], on N_2 and CO by Sink et al. [60], NH , OH^+ , PH , SH^+ by Palmieri and Sink, on benzene by Luzanov and Poltavets [61]. For a concise overview over the computational efforts of this time, I refer to [24, 29]. Acknowledging a major contribution to the field, I would like to point out though the extensive work of Langhoff, partly in

¹Subsequently, it was established that contrary to the speculations of Hameka based on spin-orbit calculations, the lowest triplet was of ${}^3B_{1u}$ symmetry.

collaboration with Davidson and Kern, in the 1980s joined by Ellenbogen, Feller, Borden, who conducted investigations on numerous systems, basing their spin-orbit and spin-spin calculations on a configuration interaction treatment, in combination with a sophisticated analysis (SO and SS in O₂ [58], SO in CH₂ [62], SS in benzene [63], SS in C₂ [64], SO in CH₂O [65], SO and SS in CH₂O [66], SS in pyrazine [67], SS in vinylmethylene [68]; see further the review of Langhoff and Kern in [69]).

The efforts in the 1960s – 1980s in the calculation of electron spin-spin coupling in organic and inorganic systems can adequately be grouped into two categories: On the one hand, *ab initio* investigations on small systems, commonly diatomics, on the other hand, investigations on aromatic hydrocarbons, frequently employing a semi-empirical approach confined to the π -electron system. Calculations on transition metal ions usually neglected the spin-spin contribution to the zero-field splitting as the spin-orbit effect was considered to be predominant [70](p. 330). Based on a historical assessment and comparison with experimentally available zero-field splittings, the initial impression is formed that those early calculations frequently resulted in astonishingly satisfactory results. As Vahtras et al. [48] pointed out with reference to Langhoff et al. [63] though, a more detailed analysis of the computational treatment of aromatic systems indicates the agreement of the semi-empirical π -electron approximation to be accidental. Langhoff et al. considered electron spin-spin coupling in benzene based on a CI wave function, investigating in particular the dependence on the size of the CI space and relevance of particular excitations. A distinct difficulty in the balanced description of the spin density of benzene was found and small deviations from the hexagonal symmetry were reported to have a substantial effect. Electron correlation was considered to be of dominant relevance, as their large CI calculation yielded a spin-spin coupling of $D = 0.1676 \text{ cm}^{-1}$ as compared to an experimental value of $D = 0.1580 \text{ cm}^{-1}$ and a value of $D = 0.1087 \text{ cm}^{-1}$ for a single-reference calculation. Their conclusion stated the necessity of including a considerably larger number of configurations in the computational treatment for an appropriate characterization. Difficulties in the description of the spin density were furthermore reported subsequently by Feller et al. [68] in the context of a multireference treatment of modest size on vinylmethylene. As this group states in their initial discussion of calculations of zero-field splittings: “*Past attempts to compute molecular zfs parameters by ab initio methods have shown these properties can be quite sensitive to the electronic distribution in the molecule. Thus, convergence of the theoretical estimate of D and E with regard to quality of CI and basis set size is sometimes discouragingly slow.*” They relate their difficulties in the calculation of spin-spin couplings in vinylmethylene to a particularly flat potential energy surface in combination with a high sensitivity of the spin density on the difference between C-C bond lengths. “*Therefore, a relatively small error in the calculated equilibrium geometry could lead to a large error in the spin density and, hence, in D.*”

In recent years, the advance in computational methods in combination with a considerable improvement in available computer resources resulted in an unprecedented level of sophistication in the theoretical assessment of molecular systems, extending meanwhile to calculations on small biological units. It is in these circumstances, partly motivated

by the heightened interest from the experimental side, that a revived concern with the evaluation of electron spin-spin coupling is initiated.

1.1.4 Present Theoretical Work

In the last decade, the number of groups involved in the calculation of electron spin-spin coupling has been limited. My intention is to review the investigations of this period, only briefly noting work of minor significance while referring in more detail to contributions of higher relevance, highlighting therein points of particular interest. I will start out with the assessment of predominantly first-principles *ab initio* investigations and will finish with a brief discussion of the characteristics of the prevalent theoretical method. Subsequently, I will turn to an evaluation of approaches originating from the area of density functional theory.

Mählmann and Klessinger [71] published in 2000 spin-orbit and spin-spin calculations on a series of carbenes (carbene, tetramethyleneethane, twisted ethylene, ring-opened oxirane biradical) within a multireference scheme based on spin-adapted CSFs, albeit in the context of their semiempirical MNDQC-CI treatment. In the same year, Bomfleur et al. [72] employed a single-configuration spin-coupled valence bond function for the calculation of benzene and naphthalene, in reasonable agreement with experiment, analyzing their results in a subsequent publication [73] in terms of spin-correlation functions.

On a higher level of sophistication, Mitrushenkov, Palmieri and Tarroni [74] presented in 2003 a scheme for the calculation of spin-orbit and spin-spin effects based on internally contracted CI wave functions derived from the MOLPRO [75] implementation and applied it to the test cases of atomic oxygen O and the O⁺ ion. Subsequent publications involving Spielfiedel, Palmieri and Mitrushenkov [76, 77] applied this method in the calculation of excited states and transition matrix elements in H₂. Unfortunately, calculations on larger systems with this promising approach were not noted.

Michl [78] introduced in 1996 in the first publication of a continuing series the algebraic “2-electrons-in-2-orbitals” model in its extension to spin-orbit effects in biradicaloid systems, considering one-electron as well as two-electron interactions. In 1998, Havlas, Downing and Michl [79] evaluated spin-orbit and spin-spin effects in CH₂ and SiH₂, employing wave functions of different quality on the CASSCF and CI level, interpreting the results on the basis of their “2-in-2” model. The investigations on CH₂ should be pointed out in particular as they constitute an extensive analysis of the quality of the computational approach in its impact on the magnitude of electron spin-spin coupling. Correlation treatments under consideration include ROHF, CIS, CASSCF(6,6), CISD and CISDTQ, while the basis set size covers the range from STO-3G over 6-31G* to cc-pVTZ. A slow convergence of the results of spin-spin coupling with the basis set size is noted, as well as a distinct sensitivity to the description of electron correlation; a questionable value of CIS and CASSCF(6,6) is stated. The authors recommend at least a correlation on the level of CISD in combination with a

triple- ζ basis for quantitative results. As a further point, the dependence of spin-orbit and spin-spin effects on the bonding angle H-C-H was analyzed in detail. Further articles of this series entail calculation and analysis of spin-orbit and spin-spin effects in carbenes [80] (CH_2 , CHF, CHCl, CHBr; CASSCF(8,6)/cc-pVDZ), ground and excited triplets of *m*-xylylene [81] (CASSCF(6,6)/cc-pVDZ; Havlas and Michl), nitrenes, phosphinidenes, and arsinidenes [82] ($\text{CH}_3\text{-N}$, $\text{CH}_3\text{-P}$, $\text{CH}_3\text{-As}$, $\text{SiH}_3\text{-N}$, $\text{SiH}_3\text{-P}$, $\text{SiH}_3\text{-As}$; CASSCF(12,11)/cc-pVTZ; Havlas, K \acute{y} vala, Michl). Analysis in the framework of the “2-in-2” model usually confirmed the applicability of this algebraic approach. The latest work in 2005 considers the reactive intermediates triplet dimethylnitrenium, dimethylphosphenium and dimethylarsenium cations [83] ($[\text{CH}_3\text{-N-CH}_3]^+$, $[\text{CH}_3\text{-P-CH}_3]^+$, $[\text{CH}_3\text{-As-CH}_3]^+$; Havlas, K \acute{y} vala, Michl) within a CASSCF(14,14)/cc-pVTZ treatment. The contribution of spin-orbit vs. spin-spin coupling in these systems isoelectronic to the corresponding carbene $[\text{CH}_3\text{-C-CH}_3]$ was investigated and again satisfactory agreement with the “2-in-2” model stated.

Particular relevance in the high-level correlation treatment of electron spin-spin coupling should be attributed to the efforts around its evaluation within an MCSCF treatment in the program DALTON [84]. Since 2002, various persons contributed to more than ten publications based on this implementation, the most frequently noted ones being Vahtras, Minaev, Loboda, Ruud and Ågren [48, 85–95]. The first publication in this context by Vahtras et al. [48] considered zero-field splittings (spin-orbit and spin-spin) on O_2 , investigating furthermore the internuclear dependence of D_{SO}/D_{SS} , as well as the calculation of spin-spin effects on benzene (this work was already noted in the discussion of the historical efforts on these systems), providing highly satisfactory agreement with experimental values. Loboda et al. [85] investigated subsequently spin-spin coupling effects in linear polyacenes (naphthalene, anthracene, naphthacene) based on a consideration of the π -electron space, but limited to a RAS instead of a CAS treatment in the two larger systems. Agreement of the D value with experiment was reasonable, while the E splitting value, not surprisingly enough considering its distinctly small magnitude, constituted a more problematic case. Pentacene was calculated on the basis of an ROHF approach. In this context, the essential relevance of electron correlation was stated, as Loboda et al. observed in the comparison of a restricted open-shell approach with a consideration of the full π -electron active space roughly an increase in the magnitude of spin-spin coupling by a factor of two. Evaluations of electron spin-spin coupling embedded in a polarized continuum model (PCM), thereby incorporating effects of the surrounding solvent environment, were presented on pyrazine and quinoline [86] as well as subsequently on pyridine, pyrazine, pyrimidine, quinoline [91]. Experimental data available for pyrazine showed reasonable agreement. Further studies include the diatomics H_2 [87], He_2 [88], Li_2 [93], NH [92], as well as triatomic systems, with focus on HCN and O_3 [90]. Calculations on the larger system of *p*-dichlorobenzene [94] showed good agreement with experimental values, on the other hand investigations on a series of benzene derivatives [89] proved to be more problematic. In *p*-dibromobenzene, a deviation by almost a factor of two is noted, which is attributed to the presence of the heavier atom Br and the increased contribution of second-order spin-orbit effects. Equally high deviations for aniline are speculated

to originate in the presence of environmental effects in the experimental consideration within a *p*-xylene host crystal. Free-base porphyrin constitutes the largest system investigated by Loboda et al. [95]. The calculation of zero-field splittings is performed in this case within an ROHF treatment, though, which, as was observed in the context of linear polyacenes, may be problematic in its deficiencies in the description of correlation effects. The predicted theoretical value is found in distinct disagreement with experimental assessments (exp.: $D = 0.0435 \text{ cm}^{-1}$, $E = 0.0063 \text{ cm}^{-1}$, measurement in *n*-octane matrix; calc.: $D = 0.016 \text{ cm}^{-1}$, $E = 0.0021 \text{ cm}^{-1}$).

In considering the most relevant *ab initio* efforts in the calculation of electron spin-spin coupling, it can be noted that the two major distinct groups (Havlas, Michl et al. on the one hand, the group employing DALTON on the other hand) both predominantly operate in the framework of CASSCF. In evaluating the characteristics of this approach, I may start out with quoting Rubio-Pons et al. [89] who summarized the implicit deficiencies encountered in the context of calculations on benzene derivatives: “*Limitations of the CASSCF method are obvious and well known; the wave functions blow up rapidly in size with increasing active spaces and, except for benzene, for which two well-defined π -electron active spaces can be utilized, there is no beforehand-given choice for the other species, and one has to rely on an analysis of bonding character and calculated natural occupation numbers. Furthermore, CASSCF excludes a large part of the dynamic correlation effect.*” CASSCF as a method constitutes a sophisticated correlation treatment which accounts appropriately for non-dynamical correlation. A distinct disadvantage lies in the considerable restrictions on the active space, which manifests itself already within a molecular system of limited size, as was recognized by Rubio-Pons et al. Furthermore, CASSCF does not consider dynamical correlation appropriately, which could possibly be a particularly severe limitation in the case of electron spin-spin coupling, reflecting here from a principal perspective the strong dependence on the interelectronic distance of the underlying operator while noting at the same time the observed sensitivity to a balanced description of the spin density. These issues raise the interest in a computational consideration of electron spin-spin coupling in the framework of a method which may meet associated demands. A further point that should be mentioned with respect to the implementations within DALTON as well as in the treatment by Havlas and Michl is the restriction to the evaluation of expectation values, thereby neglecting couplings between different states. It is usually assumed that this approach is legitimate, as Havlas et al. pointed out though [79]: “*We also ignore all elements of the spin-spin dipolar coupling operator that connect different states. It is hoped that these neglects are acceptable when the properties of the lowest triplet are to be described, even though we realize that in at least one case (predissociation of NH) first-order spin-spin dipole induced singlet-quintet state mixing is known to dominate over second-order spin-orbit induced mixing of the same states.*”. Without investigation of this aspect, it is not possible to exclude its relevance.

The heightened attention that density functional theory (DFT) has received in recent years propagated into the field of computational evaluation of EPR spectroscopic parameters. Again, initial efforts focussed more on the calculation of *g*-tensors and

hyperfine coupling constants [34]. The first application of DFT in the calculation of electron spin-spin coupling is attributed to Petrenko et al. [96] in 2002. The theoretical basis for their evaluation lies in an analogy to Hartree-Fock theory. As was shown early by Dirac [97], the two-particle density function can be exactly expressed through one-particle density functions in the case of a single-determinant description. McWeeny [23](p. 85–90), [98] applied this reduction on the spin-spin coupling function in the description of the Breit-Pauli Hamiltonian, thereby obtaining an expression in which the two-electron quantity of electron spin-spin coupling is entirely determined by one-electron spin densities. Petrenko et al. replaced the HF-one particle density with the spin-density as obtained in their DFT calculation on CH_2 and thereby transferred the formalism of McWeeny into the framework of DFT. As the authors stated with respect to the validity of this approach: “*To our knowledge, the validity of DFT-based calculations for reproduction of the observed ZFS parameters D and E has not been tested up to now.*” The results of their practically motivated approach were satisfactory though, even if in slightly worse agreement with experiment than the *ab initio* calculations of Havlas et al. [79].

Shoji et al. [99] based their evaluation of electron spin-spin coupling in the framework of DFT on the calculation of spin natural orbitals (SNO). The triplet states of organic biradicals were expressed as a simple antisymmetrized product of respective two singly occupied SNOs and the expectation value over the Breit-Pauli spin-spin operator was evaluated. In the context of a restricted Hartree-Fock formalism, it is well known [27, 100] and will be proved in detail in Ch. 2.2.2 that the contribution of closed shells to electron spin-spin coupling vanishes and only open shells enter the equation. The expression to be evaluated therefore involves solely the two open shells in the case of a single determinant of triplet symmetry. It is presumably on this analogy that Shoji et al. base their approach. Their calculations on a series of carbenes of different size were in good agreement for smaller systems, distinct discrepancies with experimentally predicted values were obtained in some cases for the larger systems, not entirely surprising considering the observations of Loboda et al. on linear polyacenes [85].

The most extensive investigations in the calculation of EPR parameters within a DFT approach were undertaken by Neese. His access to the field of computational chemistry originated from the direction of bioinorganic chemistry and is strongly motivated by a purpose-driven application. Employing computational methods as supportive means, closely accompanying the interpretation of experimental work, characterizes his approach. Strongly influenced by the relevance of individual parameters in the context of bioinorganic chemistry, his work in the computational evaluation of EPR spectroscopic quantities has evolved continuously and comprises meanwhile several investigations in the calculation on g -tensors, hyperfine coupling constants, as well as zero-field splittings. Commonly, but not exclusively, Neese employs DFT, as this method has a high potential especially in the consideration of larger systems, and operates frequently in collaboration with experimental groups [101–111]; recent work encompasses furthermore consideration of environmental effects in an QM/MM approach [112, 113]. A comprehensive contribution [114] analyzes the evaluation of coupling effects and EPR

parameters in transition metal chemistry while numerous reviews on the interface of computational and spectroscopic investigations [102, 115–120] discuss applicability, limitations and examples of present approaches. The efforts of Neese in the evaluation of zero-field splittings focussed until recently onto the contribution of spin-orbit coupling as the effect of electron spin-spin interactions was historically considered to be negligible in transition metal chemistry [70] (p. 330), an opinion that perpetuated in this area for decades. Only recently has this assumption started to be questioned by Neese, and his theoretical investigation in 2006 [108] on $\text{Mn}[(\text{acac})_3]$ yielded a contribution of electron spin-spin coupling of $\sim 1 \text{ cm}^{-1}$, thereby accounting for 40 % of the overall zero-field splitting, which even allowing for an error in the computational assessment of a factor of 2–3 indicates it to be far from negligible in this system. As the calculation of electron spin-spin coupling has been so far predominantly an area of the organic chemist, Neese’s results may motivate an interest in the field of transition metal chemistry.

Neese’s most recent approaches to the computational evaluation of zero-field splittings encompass therefore not only spin-orbit effects but consider furthermore spin-spin interactions. I would like to point in this context to two recent reviews, the first of which discusses the theoretical evaluation of zero-field splittings (spin-orbit and spin-spin) [119]. In particular the connection established between experimentally observed transitions and the magnitude of individual EPR parameters for different cases of field strength may be of value to the theoretician. The second is concerned more comprehensively with the theoretical approach and computational evaluation of the most relevant coupling effects manifest in EPR spectra, accompanied by practical aspects of the calculation, illustrated with results of individual case studies [121]. Highlighted here should be in the context of spin-spin coupling the discussion of the experimentally employed “point-dipole approximation”, as it represents the very seldom reflection on this approximation from the perspective of the theoretician, illustrating underlying assumptions and neglected terms on the basis of the Breit-Pauli spin-spin Hamiltonian.

Neese’s computational approach to the calculation of electron spin-spin coupling employs the same theoretical concept as Petrenko et al., based on the spin-density formalism of McWeeny. His implementation evaluates this quantity in the framework of DFT as well as CASSCF. The previously discussed reduction of the two-particle spin-density into an antisymmetrized product of one-particle density functions is exact in the formalism of Hartree Fock. Its validity in the context of DFT has not been established, as is acknowledged by Petrenko et al. as well as Neese [108]: “*It is unknown what kind of error is introduced by this approximation. Its main justification may remain for some time to come that, at least to the best of the author’s knowledge, it is without practical alternative at the present level of sophistication of DFT.*” In the case of a CASSCF wave function, the two-particle spin-density does not factorize in the indicated way, and the application of this scheme is therefore an approximate treatment. Presumably in the analogy to Hartree-Fock constituting a mean-field approach and the employed scheme for the calculation of electron spin-spin coupling being exact in the case of Hartree-Fock, Neese denotes his approach “spin-spin mean-field approximation”. This

should not be mistaken though with the well-established spin-orbit mean-field approximation [17, 122, 123], which is based on a different theoretical foundation. Neese's first investigation of electron spin-spin coupling together with Sinnecker in 2006 [124] constitutes a comprehensive study and will be discussed in more detail motivated by the general relevance of its conclusions. In the first part, it assesses the validity of his approach in calculations on O_2 in the internuclear distance range of 1.0 Å to 2.0 Å, based on CASSCF, UHF, restricted DFT (RODFT) and unrestricted DFT (UDFT), comparing with the exact (i.e., no spin-spin mean-field approximation) CASSCF results of Vahtras et al. [48]. The overall agreement of the CASSCF calculations of Sinnecker and Neese with the results of Vahtras et al. is satisfactory and indicates the applicability of Neese's mean-field approach in this system at equilibrium geometry. A breakdown upon increased internuclear distance is noted though, which is attributed to the strongly increased non-dynamical correlation effects. With respect to the spin-spin mean-field approach in the context of DFT, the authors note a better performance of restricted as compared to unrestricted calculations. Furthermore, a series of fifteen triplet carbenes as well as benzene and the polyacenes naphthalene, anthracene and tetracene were computationally assessed in the framework of RODFT and UDFT. These test systems were chosen on the basis of existing experimental and/or theoretical data and comparisons were included in the work. The evaluation of the series of triplet carbenes revealed considerable discrepancies between a restricted and an unrestricted approach. While the RODFT calculations showed reasonable agreement with experimental values, distinct difficulties were observed in the case of an unrestricted treatment. This point was therefore further investigated in a computational assessment of H_2CO . By comparison with a series of CASSCF and multireference calculations, it was concluded that UB3LYP provides a very realistic description of the spin distribution, indeed slightly better than ROB3LYP. The predicted spin-spin couplings differed almost by a factor of two though, with ROB3LYP being in better agreement with experimental data. The authors compared spin populations of different orbitals and noted a minute amount of spin polarization contained in the unrestricted Kohn-Sham determinant, which they concluded to be responsible for the large difference between unrestricted and restricted solutions. As an important point of the work, the authors state an extreme sensitive reaction of ZFS to the calculated spin distribution. The good performance of the restricted open-shell Kohn-Sham methods was speculated to be attributable to a certain amount of error compensation. The study on benzene yielded a coupling parameter D in satisfactory agreement with experiment while the values for the polyacenes were underestimated by approximately a factor of two, which is consistent with the observation of Loboda et al. [85] in the comparison of ROHF and CASSCF on these systems, thereby indicating the necessity of an explicitly correlated treatment beyond DFT. As a result of their investigations, the authors conclude a satisfactory validity of their spin-spin DFT approach in the study of triplet states and diradicals in large biologically relevant molecules, and state its deficiency in extended π -systems: "*In situations with large medium- and long-ranged electron-electron correlation effects, ab initio methods will probably turn out to be preferable over DFT methods and, in our opinion, efforts toward their efficient development and implementation are well-invested.*"

Subsequent work by Ganyushin and Neese [125] applies their approach furthermore to S_2 and SO, while computational considerations of transition metals (Mn-complexes) are encountered in [108, 111] (the latter work has already been noted in the assessment of the relevance of spin-spin couplings in transition metals).

1.1.5 Conclusion: Concerted Considerations

The last decade has seen a considerable development in EPR spectroscopy, meanwhile enabling investigations on biological systems of distinct size. From the perspective of the experimentalist, the significance of computational methods is recognized, as discussed by Möbius et al. [126] who emphasize the importance of quantum-chemical interpretations of experimental data in their review of high-field EPR spectroscopy, applied to biological systems. Due to the size of the system under consideration, the computational approach consists frequently of advanced semi-empirical methods and/or DFT. Multiple examples for a beneficial combination of DFT and experimental assessments [103–107, 110–113, 127–129] support the general applicability and value of this method.

Nonetheless, two main aspects have to be recognized in the computational consideration of electron spin-spin coupling. First, from the approach of the pure experimentalist, the employed theoretical model is usually of a strongly simplified structure. It is frequently based on the “point-dipole approximation”, which is restricted to an application to well-localized electron distributions of distinct distance (see discussion in Ch. 1.1.2 as well as theoretical assessment by Neese [121]). A further point of discomfort for the theoretician in this respect is the observation that in experimental evaluations of electron spin-spin coupling, the quantity of the g -tensor frequently appears together with the D value in the same expression (see for example [37, 38, 43, 44]), as was already criticized by Neese [121]. The application of a more sophisticated computational approach should therefore be of distinct relevance in the experimental context, especially considering the advance and level of sophistication meanwhile attained in EPR spectroscopy. Second, from the approach of the theoretician, it has to be recognized that the calculation of electron spin-spin coupling necessitates a highly sophisticated computational treatment as an exceptional sensitivity of this effect on the description of the spin density is observed. A considerable demand on the correct description of the spin distribution was already early on noted by Langhoff et al. [63] as well as Feller et al. [68] and recently supported by Sinnecker and Neese [124]. Difficulties were furthermore reported in the description of extended π -systems with DFT based approaches, as the explicit treatment of non-dynamical correlation effects is beyond the scope of this method. It is therefore particularly in those systems which do not satisfactorily comply with assumptions underlying the experimentally employed point-dipole approximation that the application of high-level correlation beyond DFT is of significant relevance.

The most important point to be emphasized in the context of a computational approach is that based on existing evidence, satisfactory agreement with excitation energies or other properties may not necessarily indicate a reliable calculation of electron spin-

spin interactions as this effect exhibits a considerably stronger sensitivity on the spin distribution.

Interlude

Recent years observed promising efforts in the field of theoretical chemistry, at the same time, the heightened interest in the experimental community can possibly be considered a motivating aspect. Nonetheless, the computational investigation of electron spin-spin coupling is still at an early stage, and a comprehensive understanding of the characteristics of this quantity has still to be gained. The number of sophisticated investigations, in particular concerning systems of a moderate molecular size, is limited and it is here that the strongest demand for computational development is noted.

After this more general reflection on the framework accompanying the theoretical consideration of electron spin-spin coupling, I will turn specifically to the interests and capabilities of the group of Theoretical Chemistry of Christel M. Marian at the University of Düsseldorf as this constitutes the environment for the present work. After discussing the scientific context, I will illustrate the motivation and in particular the promising potential that is provided in the computational competence of this group for the investigation of electron spin-spin coupling in the systems of interest.

1.2 Theoretical Chemistry at Düsseldorf – SFB 663

The group of Theoretical Chemistry at the University of Düsseldorf is centrally embedded in the Sonderforschungsbereich (SFB) 663 “Molecular Response to Electronic Excitation”, an interdisciplinary project funded by the Deutsche Forschungsgemeinschaft (DFG) which is the main institution for external support of research at universities and public research centers in Germany. The purpose of an SFB in general is the initiation of interdisciplinary cooperation in the context of a common long-term project, involving a distinct number of groups rooted in differing scientific fields. The incentive of the SFB 663 in particular is the investigation of photostability, photoreactivity and photoprotection, aiming at the elucidation of transient intermediates and reaction pathways in the context of biologically relevant processes of photoexcitation and de-excitation. A particular strength of the SFB 663 therein is the breadth of theoretical and experimental methods involved, with participation of groups situated in the field of organic and macromolecular chemistry, biochemistry, biophysics, molecular biology, as well as physical and theoretical chemistry.

The group of Marian provides in the DFT/MRCI approach, which will be discussed in Ch. 1.4, a sophisticated means for the investigation of excited states of multireference character. Expertise in the context of spin-orbit and vibronic coupling allows the assessment of de-excitation mechanisms caused by these effects. It is in this framework that the development of an advanced means of evaluation of electron spin-spin coupling effects is embedded. Collaboration with W. Lubitz who employs high-resolution EPR spectroscopy, thereby providing information about spin density distributions and

structural aspects, constitutes great promise for a common experimental and theoretical assessment of transient triplet states. The group of W. Lubitz introduces valuable expertise in the EPR/ENDOR investigation of biological systems [44, 127, 130–145], their experimental investigations frequently being supported by computational assessments, commonly reverting to DFT based methods, partly in collaboration with Neese.

Of particular interest in the framework of the SFB 663 is the investigation of carotenoids as they are of central significance in biological systems. Their dual purpose comprises the functionality as effective quenchers for reactive triplet species as well as singlet oxygen in most biological species while furthermore in photosynthetic organisms, carotenoids as part of the antenna system constitute a functional unit in the energy-transfer process. The detailed mechanism underlying the singlet-triplet transitions associated with their biological activity is unknown and of major interest in the SFB 663. The complex activity of carotenoids in biologically relevant circumstances is certainly closely related to position and characteristics of its excited states. The experimental assessment of these states, in particular of the so-called “dark states”, is very difficult, though, as these states usually exhibit very short lifetimes (tens of femtoseconds to at most a few picoseconds); furthermore, one-photon transitions are symmetry forbidden for excitations from the ground to some of the excited states, therefore preventing the direct spectroscopic access to those.

Recently, extensive investigations by Marian [146,147] in the framework of the DFT/MRCI approach provided valuable insight into the characteristics of this system. A detailed computational study revealed the predominant multireference character of the lowest singlet state S_1 , the triplet state T_2 and the singlet state S_3 , as well as to a lesser extent of S_2 and T_1 . For example, for S_1 , the major configuration defines 26 % of the state, while at the same time three more states of similar relevance contribute noticeably (15 %, 12 %, 10 %). Furthermore, it was found that the description of S_1 as well as T_2 is dominated by double excitations from the ground state, a contribution that is still non-negligible in the states T_1 and S_3 . This investigation has to be analyzed in the context of the methodological approach, and in particular in its relevance for a calculation of electron spin-spin coupling. The strength of the DFT/MRCI lies in its computational assessment of even medium-sized systems on a sophisticated level. This efficiency is realized through a shortened configuration expansion as dynamical correlation effects are already partly accounted for through the DFT ansatz by employing Kohn-Sham orbitals. Non-dynamical correlation is described by the multireference approach which in its implementation of a configuration selecting scheme further contributes considerably to a limitation in the size of the configuration space. Assessing the systems under investigation and the questions posed in the framework of the SFB 663, it has to be recognized that it is a combination of different aspects that poses challenges on the computational description. The systems are from the perspective of the theoretician of considerable size, thereby preventing in particular the application of CASSCF-based methods since the required active spaces likely exceed present computational possibilities. A considerable multireference character as observable through significant configuration mixing necessitates a reliable description of non-dynamical

correlation effects, which are beyond the scope of DFT. Furthermore, it should be mentioned that the calculation of excited states is commonly approached within the context of a further popular method (TDDFT) which is conceptually based on linear response theory. Due to the distinct double-excitation character of the investigated singlet and triplet states, this method cannot be applied in the present case. It is the combination of these aspects that places the demand on the computational description and explains the difficulties in previous theoretical assessments. After elucidation of the characteristics in the electronic structure, the next questions to be approached concern the electron distribution in excited states and the coupling effects responsible for the fast singlet–triplet transitions in this system. It is in this context that electron spin-spin coupling may assist in the clarification, in combination with a high-level correlation treatment in the framework of the DFT/MRCI approach.

Interlude

Having established the general environment and motivation of the present work, I will turn now to a stronger mathematical/computational level. In the following section, I will discuss the characteristics of the Breit-Pauli spin-spin operator. My intention is to point out differences in the mathematical structure in comparison to the nonrelativistic Hamiltonian in order to illustrate where the challenges and difficulties in the calculation of electron spin-spin coupling could possibly lie. Subsequently, I will turn to aspects concerning the present implementation of electron spin-spin coupling (Sec. *Program Frame*, Ch. 1.4). In particular, I will introduce the computational efforts in the group of Theoretical Chemistry at the University of Düsseldorf. I will give an overview over the program structure electron spin-spin coupling is embedded in, pointing out issues in the existing environment and programming decisions made in the context of the whole package which strongly influence the spin-spin implementation.

1.3 Computational Considerations

In the framework of the Breit-Pauli Hamiltonian, electron spin-spin interaction is described through the operator expression:

$$\hat{\mathcal{H}}_{SS}^{BP} = g_e^2 \mu_B^2 \alpha^2 \sum_{i < j}^N \left\{ -\frac{8\pi}{3} \delta(\mathbf{r}_{ij}) \hat{\mathbf{s}}_i \hat{\mathbf{s}}_j + \frac{\hat{\mathbf{s}}_i \cdot \hat{\mathbf{s}}_j}{\hat{r}_{ij}^3} - \frac{3(\hat{\mathbf{s}}_i \cdot \hat{\mathbf{s}}_j)(\hat{\mathbf{r}}_{ij} \cdot \hat{\mathbf{r}}_{ij})}{\hat{r}_{ij}^5} \right\}, \quad (1.1)$$

given in atomic units, with the g-factor of the free electron g_e , the Bohr magneton μ_B , and the fine structure constant α . Summation in the electron indices i, j is over all electrons N .

The first term of the Breit-Pauli spin-spin operator constitutes a Fermi-contact type interaction which is nonvanishing when the two electrons coincide. Terms two and three represent a dipole-dipole interaction, analogous to the interaction between two magnetic moments in classical physics. As the Fermi-contact type interaction does not contribute to the magnitude of the zero-field splitting but solely causes an identical

energetic shift of the components of a spin state S it is usually neglected.

For the subsequent discussion of the computational demands related to the structure of the operator, it is advantageous to write it in terms of its tensor components, close to its actual computational treatment (for discussion of aspects of the tensor formulation, see Ch. 1.5.1):

$$\begin{aligned} \hat{\mathcal{H}}_{SS} = & -g_e^2 \mu_B^2 \alpha^2 \sum_i^N \sum_{j<i}^N \left[\frac{1}{2} \left\{ \frac{2\hat{z}_{ij}^2 - \hat{x}_{ij}^2 - \hat{y}_{ij}^2}{\hat{r}_{ij}^5} \right\} \{2\hat{s}_i^0 \hat{s}_j^0 + \hat{s}_i^{+1} \hat{s}_j^{-1} + \hat{s}_i^{-1} \hat{s}_j^{+1}\} \right. \\ & + \frac{3}{2} \left\{ \frac{\hat{x}_{ij}^2 - \hat{y}_{ij}^2}{\hat{r}_{ij}^5} \right\} \{ \hat{s}_i^{-1} \hat{s}_j^{-1} + \hat{s}_i^{+1} \hat{s}_j^{+1} \} \\ & + i \left\{ \frac{3\hat{x}_{ij} \hat{y}_{ij}}{\hat{r}_{ij}^5} \right\} \{ \hat{s}_i^{-1} \hat{s}_j^{-1} - \hat{s}_i^{+1} \hat{s}_j^{+1} \} \\ & + \frac{1}{\sqrt{2}} \left\{ \frac{3\hat{x}_{ij} \hat{z}_{ij}}{\hat{r}_{ij}^5} \right\} \{ \hat{s}_i^{-1} \hat{s}_j^0 + \hat{s}_i^0 \hat{s}_j^{-1} - \hat{s}_i^{+1} \hat{s}_j^0 - \hat{s}_i^0 \hat{s}_j^{+1} \} \\ & \left. + i \frac{1}{\sqrt{2}} \left\{ \frac{3\hat{y}_{ij} \hat{z}_{ij}}{\hat{r}_{ij}^5} \right\} \{ \hat{s}_i^{-1} \hat{s}_j^0 + \hat{s}_i^0 \hat{s}_j^{-1} + \hat{s}_i^{+1} \hat{s}_j^0 + \hat{s}_i^0 \hat{s}_j^{+1} \} \right]. \quad (1.2) \end{aligned}$$

Different albeit equivalent formulations of $\hat{\mathcal{H}}_{SS}$ are found in the literature. I chose here to express the spin part in terms of spherical operators while the grouping of the spatial part as linear combinations of its cartesian components is influenced by arguments of symmetry. The operator is given in atomic units, it should be mentioned, though, that especially in physics literature, Planck units are commonly chosen which differ from atomic units by the speed of light c being defined as $c = 1$ instead of $c = \alpha^{-1}$, consequently resulting in a prefactor of $-g_e^2 \mu_B^2$ with $\mu_B = \frac{e}{2m_e}$. Furthermore, I chose in my work to deviate from the commonly encountered notation in the spin operator indices which refers to electrons as well as operator components through subscripts. Especially within the intricate derivation of Ch. 2, an unambiguous identification of these quantities is mandatory, and the reference to the operator component will therefore appear as a superscript throughout. With respect to the expression of the spherical spin operator components, it has to be noted that prevalent formulations may differ in signs and prefactors. The convention employed in above equation defines the spin operator components as tensor operators which are related to their cartesian counterparts by the following relationships:

$$\hat{s}^{+1} = -\frac{1}{\sqrt{2}}(\hat{s}^x + i\hat{s}^y), \quad \hat{s}^0 = \hat{s}^z, \quad \hat{s}^{-1} = \frac{1}{\sqrt{2}}(\hat{s}^x - i\hat{s}^y). \quad (1.3)$$

To illustrate the additional issues arising in the context of the spin-spin operator, I compare to the nonrelativistic Hamiltonian in the Born-Oppenheimer approximation describing the motion of N electrons in the field of M nuclei:

$$\hat{\mathcal{H}}_{BO} = -\sum_i^N \frac{1}{2} \nabla_i^2 - \sum_i^N \sum_A^M \frac{Z_A}{r_{iA}} + \sum_i^N \sum_{j<i}^N \frac{1}{r_{ij}} \quad (1.4)$$

The most demanding evaluation in the case of this purely electrostatic Hamiltonian is the contribution of the electron-electron interaction which corresponds to the last term in above equation. In comparison, the spin-spin operator is like the spin-free operator a full two-electron operator and we are faced with a computational demand on equally high a level. No approximations are rigorously investigated and established so far, and the implementation of the exact evaluation is therefore mandatory for an assessment of the validity of possible future simplifications.

A simple but obvious structural difference between spin-spin versus spin-free electrostatic operator lies in the number of terms that have to be evaluated: While the latter exhibits a single term related to the electron-electron interaction, the former consists in the above formulation of five terms. Furthermore, each of these terms comprises a space as well as a spin dependent part, whereas the nonrelativistic Hamiltonian depends on space only. Connected to this observation is the issue of nonvanishing coupling elements between different quantum states: All terms of the Hamilton operator belong to the totally symmetric irreducible representation. In the case of a spin-free operator, this imposes identical spatial symmetry on two interacting states, while in the case of a spin-dependent operator, no such selection rule necessarily holds for the space part only but instead the product of spatial *and* spin symmetry of interacting states has to be totally symmetric. The individual spatial components of the spin-spin operator will, depending on the point group of the system, likely fall into different irreducible representations, thereby enabling the spin-spin operator, in contrast to the spin-free operator, to couple multiple different spatial symmetries. Furthermore, related to the presence of spin dependent factors, additional coupling is introduced between states of different spin quantum number S and/or its projections of differing M_S value as the selection rule imposed by the spin part is $\Delta S/\Delta M_S = 0, \pm 1, \pm 2$. Consequently, we observe now a coupling between the degenerate components of a spin state, at the same time, the coupling of states with different spin quantum numbers is introduced. Therefore, with respect to the possible nonvanishing matrix elements between quantum states, we notice the introduction of additional coupling due to the space as well as the spin part, thereby greatly exacerbating the complexity of the computational evaluation.

Turning to the structure of individual terms, the different dependence of spin-free vs. spin-spin operator on r_{ij} has to be noted. While the Coulomb term of the purely electrostatic Hamiltonian exhibits an $\propto r_{ij}^{-1}$ dependence, a dependence on r_{ij}^{-3} in the spin-spin operator is observed. As an r_{ij}^{-3} operator is in principle unbounded, this poses the question of the convergence properties of the spin-spin operator which may manifest itself within a variational treatment in instabilities, an issue that is of minor relevance in the context of first-order perturbation theory, though. Another aspect following from the stronger singularity of the operator, with higher relevance on the level of the present calculations, is the possibly increased demand on the quality of basis set and computational consideration, imposed by the demand of describing more singular an electron cusp: Since matrix elements over the spin-spin Hamiltonian exhibit a distinctly stronger dependence on the interelectron distance, it is not obvious that a wave function which satisfactorily describes the Coulomb cusp is necessarily

sufficient with respect to a description of the electron spin-spin cusp. One should be aware of this aspect in the context of quality and reliability of calculations. Particular observations concerning basis set effects and composition of the wave function relating to the different structure of the spin-spin operator will be discussed in the context of calculations on O_2 (see Ch. 3.1).

Further issues of relevance, stronger on the level of the actual implementation, which I would like to point out are: In case of the spin-free Hamiltonian which commutes with the operator of the spin, it is advantageous to employ an algorithm based on spin eigenfunctions (*configuration state functions* – CSFs) as opposed to determinants since this allows for the application of selection rules in the spin quantum number. In the case of a spin-dependent operator, both, an implementation based on determinants as well as an implementation based on CSFs, is accompanied by complications. In the case of determinants, one has to be conscientious with respect to a proper evaluation of the spin interaction. Algorithms based on CSFs on the other hand have to realize an intelligent implementation in order to be computationally feasible. In any case, additional thought has to be given to the processing of spin functions. Considering the calculation of the space part, the actual spatial integrals can be obtained via the evaluation of second derivatives of Coulomb integrals. As several of the existing quantum chemistry programs do already possess implementations of second-order derivatives, obtaining these integrals does not pose a strong demand from an implementational point of view. Nonetheless, the calculation of second-order derivatives as compared to undifferentiated integrals constitutes a computational expense that can be six times higher, depending on the algorithm.

Finally, I finish the consideration of computational aspects of the spin-spin operator on a more general note: Research has been performed for some considerable time on the evaluation of the Coulomb operator. Computational chemists have meanwhile a good impression of the scope and limitations of contemporary approaches and approximations. On the other hand, research in the framework of spin-spin coupling has been limited, and especially recognizing the strongly differing structure, it is not obvious that the experience gained in the context of the electrostatic Hamiltonian is readily extensible to the case of the spin-spin operator. There is a strong need for reliable investigations in this respect.

1.4 Program Frame

The group of Christel M. Marian at the University of Düsseldorf has a strong connection to the programming package DFT/MRCI which was written by Stefan Grimme and Mirko Waletzke, University of Münster [1]. This program possesses an *ab initio* MRCI branch which works with Hartree-Fock orbitals obtained from a previous TURBOMOLE-DSCF [148,149] run, as well as a DFT/MRCI branch which differs from the former in employing Kohn-Sham orbitals and a modified empirical Hamiltonian. The subsequent multireference calculation constitutes a selecting MRCI: After generation of the CI space from the specified references, relevant configurations are selected based

on their contribution to the reference space as evaluated perturbationally. The distinctive advantage of this approach lies in the reduction of the size of the calculation by exclusion of configurations of minor relevance. Employing configuration selection compels the implementation of a configuration-driven, as opposed to an integral-driven, algorithm: On the computational level, functions $|\Psi\rangle$ are stored as vectors of configurations $|\Xi\rangle$, as indicated in Fig. 1.2. The matrix element (ME) $\langle\Psi_k|O|\Psi_l\rangle$ is calculated by comparing configurations pairwise and adding up the contribution from each pair. What further data has to be accessed is therefore determined by the pair of configurations that is immediately evaluated. Details of the algorithm will be illustrated in Ch. 2; the discussion in this section will slightly simplify aspects of the processing.

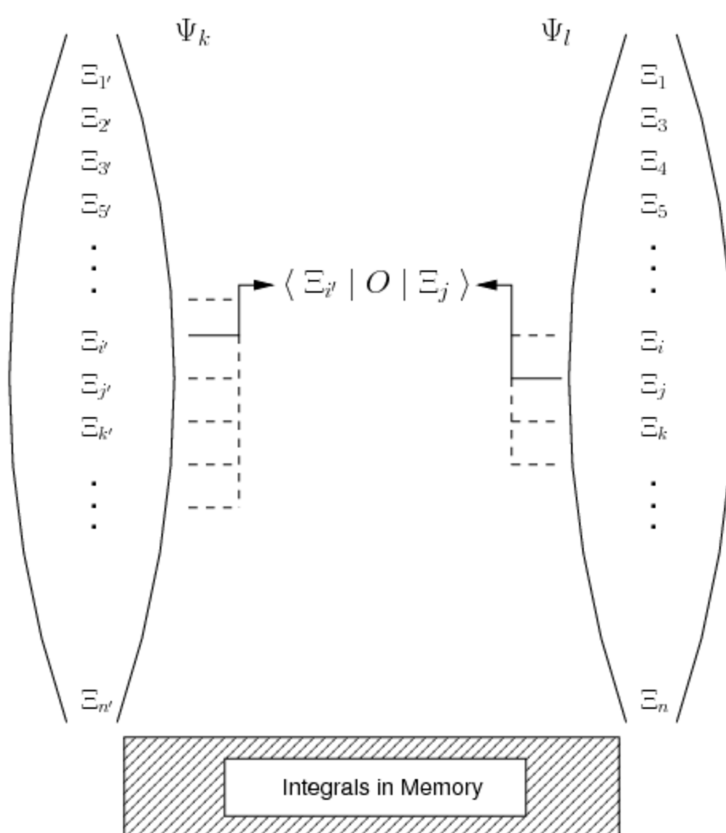


Figure 1.2: Pairwise comparison of configurations

An integral-driven algorithm, as is realized in “direct CI”, processes instead lists of integrals; in this case, the specific integral determines which configurations have to be evaluated. Since we deleted some configurations out of the state vector, we do not store a consecutive sequence of configurations anymore. Therefore, we cannot predict at which position of a vector a particular configuration appears but would have to search step-by-step through a list instead, which would be computationally too laborious. One major consequence of a configuration-driven algorithm is the necessity to

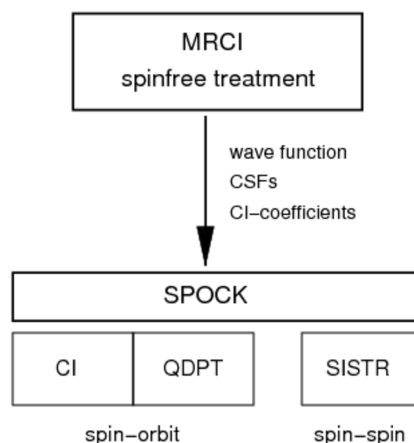


Figure 1.3: Connection of MRCI, SPOCK, SPOCK.SISTR

store all possible integrals in memory. Before comparing two configurations, we are not in the possession of the information which integral(s) need to be processed, furthermore, it would be too time consuming to load integrals from disk. We therefore have to provide all integrals readily accessible in memory, which can become a serious limitation on the size of the calculation. Approximate schemes exist to reduce the storage space necessary for the spatial integrals, one of which, the *RI-approximation* [150,151], has been implemented in the case of the Grimme/Waletzke DFT/MRCI. Since there has been limited interest in the field of spin-spin coupling until recently, no well-established analogous schemes for spatial spin-spin integrals exist as to this stage though.

The DFT/MRCI-program constitutes the first step of a subsequent high-correlation treatment of spin-dependent effects in the group of Theoretical and Computational Chemistry at the University of Düsseldorf (see Fig. 1.3). Built onto the Grimme/Waletzke DFT/MRCI resides the SPIN-ORBIT-COUPLING KIT (SPOCK) [2–4] which is on its implementational level in parts based on the former. SPOCK calculates spin-orbit interactions between the previously obtained MRCI-wave functions, providing a quasi-degenerate perturbational (QDPT) as well as a spin-orbit-CI algorithm (SOC) within the spin-orbit mean field approximation [122,152]. Again, determined by the use of the preselected MRCI-wave functions, a configuration driven algorithm is compulsory. Since we employ a spin-dependent operator, thought has to be invested into coping with the aspect of spin though. It was chosen to base the algorithm on the implementation of $M_S = S$ spin functions while the matrix elements between spin functions for which $M_S \neq S$ can be obtained via the Wigner-Eckart theorem (see p. 30ff in Ch. 1.5.1). Relevant aspects of the algorithm will be illustrated in Ch. 2 while further details beyond can be found in [153].

This work presents the derivation and implementation of SPOCK.SISTR, the *spin-spin treatment*. SPOCK.SISTR constitutes an extension of SPOCK, enabling the calculation of electron spin-spin effects subsequent to an MRCI-, parallel to a possible spin-orbit

calculation. The implementation is conceptually strongly related to the QDPT-spin-orbit treatment. The main difference and point of labour as well as novelty lies in the extension of algorithm and implementation to the treatment of a two-electron operator as opposed to the one-electron mean-field treatment in the case of the spin-orbit branch. At the beginning of the project, it was not clear if the procedure employed in the spin-orbit case is applicable to the spin-spin operator. Now, the first major step is taken to show that it is indeed in principle possible, and this work will hopefully be taken further at the University of Düsseldorf, assessing the full scope and possibilities of the project.

Interlude

The previous sections intended to convey the overall context of the present work, addressing the level of the general motivation, the particular scientific interests in this group, as well as establishing an impression of the demands and challenges on a level closer to the computational treatment.

The remaining part of this chapter focusses on detailed aspects. Ch. 1.5 is dedicated to the introduction of concepts and algorithms assisting in the theoretical and computational consideration of the spin-spin operator. This chapter therefore constitutes the basis for an in-depth understanding of the derivation of the spin-spin implementation (Ch. 2). The path I will follow herein is to start on the level of the operator itself, motivating its particular formulation as employed in this work as well as introducing auxiliary concepts (Sections *Wigner-Eckart Theorem* and *Second Quantization*). Subsequently, I will turn to the level of evaluation of individual matrix elements, introducing the η -pattern formalism which constitutes a concept of central relevance in the spin-orbit and spin-spin implementation. I will discuss its spin-free manifestation before turning to the spin-dependent algorithm as realized in SPOCK.

Having established the relevant theoretical and computational concepts, I will illustrate in Ch. 1.6 the phenomenological description on a mathematical level and relate it to the theoretically employed Hamiltonian. The chapter will conclude with reflections on principal issues in the present implementation (Ch. 1.7).

1.5 Theoretical Concepts

1.5.1 Expression of the Operator

The spin-spin operator can be written in terms of tensor operators of the space and spin part as follows:

$$\hat{\mathcal{H}}_{SS}^{BP} = g_e^2 \mu_B^2 \alpha^2 \sum_{i < j}^N \left\{ \frac{\hat{\mathbf{s}}_i \cdot \hat{\mathbf{s}}_j}{\hat{r}_{ij}^3} - \frac{3(\hat{\mathbf{s}}_i \cdot \hat{\mathbf{s}}_j)(\hat{\mathbf{r}}_{ij} \cdot \hat{\mathbf{r}}_{ij})}{\hat{r}_{ij}^5} \right\} \quad (1.5)$$

$$= g_e^2 \mu_B^2 \alpha^2 \sum_{i < j}^N \sum_m (-1)^m \hat{r}_{ij}^{-5} \cdot [\hat{\mathbf{s}}_i \otimes \hat{\mathbf{s}}_j]_m^{(2)} \cdot 3 [\hat{\mathbf{r}}_{ij} \otimes \hat{\mathbf{r}}_{ij}]_{-m}^{(2)} \quad (1.6)$$

$$= g_e^2 \mu_B^2 \alpha^2 \sum_{i < j}^N \left\{ \left\{ \hat{\mathbf{s}}_i^{(1)} \otimes \hat{\mathbf{s}}_j^{(1)} \right\}^{(2)} \otimes \hat{D}_{ij}^{(2)} \right\}^{(0)}. \quad (1.7)$$

The parenthesized superscripts denote the rank of the underlying tensorial structure, the index m refers to its components, $\hat{\mathbf{s}}_{i/j}$ designate spin tensors of rank one while the traceless tensor operator of rank two \hat{D}_{ij} can be expressed as:

$$\hat{D}_{ij} = -\frac{1}{\hat{r}_{ij}^5} \begin{pmatrix} 3\hat{x}_{ij}^2 - \hat{r}_{ij}^2 & 3\hat{x}_{ij}\hat{y}_{ij} & 3\hat{x}_{ij}\hat{z}_{ij} \\ 3\hat{x}_{ij}\hat{y}_{ij} & 3\hat{y}_{ij}^2 - \hat{r}_{ij}^2 & 3\hat{y}_{ij}\hat{z}_{ij} \\ 3\hat{x}_{ij}\hat{z}_{ij} & 3\hat{y}_{ij}\hat{z}_{ij} & 3\hat{z}_{ij}^2 - \hat{r}_{ij}^2 \end{pmatrix}. \quad (1.8)$$

The dipole-dipole interaction can thereby be viewed as the coupling of a spin tensor of rank two with a space tensor of rank two to give an operator of rank zero. The motivation for the consideration of the spin-spin operator as a tensor construct lies in the computational advantages that can be exploited in this reformulation: Choosing to recast the tensor operators through their irreducible components permits the application of the Wigner-Eckart theorem (WET). This theorem establishes relationships between irreducible tensor components and thereby allows for an expression of components through one another, resulting in a saving in the number of terms that have to be evaluated directly.

The irreducible components of the second-rank spin tensor operator $\hat{T}^{(2)}$ are specified as:

$$\begin{aligned} \hat{T}_{+2}^{(2)} &= \hat{s}_i^{+1} \hat{s}_j^{+1} \\ \hat{T}_{+1}^{(2)} &= \frac{1}{\sqrt{2}} \{ \hat{s}_i^0 \hat{s}_j^{+1} + \hat{s}_i^{+1} \hat{s}_j^0 \} \\ \hat{T}_0^{(2)} &= \frac{1}{\sqrt{6}} \{ 2\hat{s}_i^0 \hat{s}_j^0 + \hat{s}_i^{+1} \hat{s}_j^{-1} + \hat{s}_i^{-1} \hat{s}_j^{+1} \} \\ \hat{T}_{-1}^{(2)} &= \frac{1}{\sqrt{2}} \{ \hat{s}_i^{-1} \hat{s}_j^0 + \hat{s}_i^0 \hat{s}_j^{-1} \} \\ \hat{T}_{-2}^{(2)} &= \hat{s}_i^{-1} \hat{s}_j^{-1}. \end{aligned} \quad (1.9)$$

We can thereby rewrite the spin-spin operator as given in Eq. (1.2) as follows:

$$\begin{aligned} \hat{\mathcal{H}}_{SS} &= -g_e^2 \mu_B^2 \alpha^2 \sum_i^N \sum_{j < i}^N \left[\frac{1}{2} \left\{ \frac{2\hat{z}_{ij}^2 - \hat{x}_{ij}^2 - \hat{y}_{ij}^2}{\hat{r}_{ij}^5} \right\} \{ 2\hat{s}_i^0 \hat{s}_j^0 + \hat{s}_i^{+1} \hat{s}_j^{-1} + \hat{s}_i^{-1} \hat{s}_j^{+1} \} \right. \\ &\quad + \frac{3}{2} \left\{ \frac{\hat{x}_{ij}^2 - \hat{y}_{ij}^2}{\hat{r}_{ij}^5} \right\} \{ \hat{s}_i^{-1} \hat{s}_j^{-1} + \hat{s}_i^{+1} \hat{s}_j^{+1} \} \\ &\quad + i \left\{ \frac{3\hat{x}_{ij}\hat{y}_{ij}}{\hat{r}_{ij}^5} \right\} \{ \hat{s}_i^{-1} \hat{s}_j^{-1} - \hat{s}_i^{+1} \hat{s}_j^{+1} \} \\ &\quad \left. + \frac{1}{\sqrt{2}} \left\{ \frac{3\hat{x}_{ij}\hat{z}_{ij}}{\hat{r}_{ij}^5} \right\} \{ \hat{s}_i^{-1} \hat{s}_j^0 + \hat{s}_i^0 \hat{s}_j^{-1} - \hat{s}_i^{+1} \hat{s}_j^0 - \hat{s}_i^0 \hat{s}_j^{+1} \} \right] \end{aligned}$$

$$\begin{aligned}
& +i \frac{1}{\sqrt{2}} \left\{ \frac{3\hat{y}_{ij}\hat{z}_{ij}}{\hat{r}_{ij}^5} \right\} \left\{ \hat{s}_i^{-1}\hat{s}_j^0 + \hat{s}_i^0\hat{s}_j^{-1} + \hat{s}_i^{+1}\hat{s}_j^0 + \hat{s}_i^0\hat{s}_j^{+1} \right\} \quad (1.10) \\
= & -g_e^2\mu_B^2\alpha^2 \sum_i^N \sum_{j<i}^N \left[\sqrt{\frac{3}{2}} \left\{ \frac{2\hat{z}_{ij}^2 - \hat{x}_{ij}^2 - \hat{y}_{ij}^2}{\hat{r}_{ij}^5} \right\} \left\{ \hat{T}_0^{(2)} \right\} \right. \\
& + \frac{3}{2} \left\{ \frac{\hat{x}_{ij}^2 - \hat{y}_{ij}^2}{\hat{r}_{ij}^5} \right\} \left\{ \hat{T}_{-2}^{(2)} + \hat{T}_{+2}^{(2)} \right\} \\
& + i \left\{ \frac{3\hat{x}_{ij}\hat{y}_{ij}}{\hat{r}_{ij}^5} \right\} \left\{ \hat{T}_{-2}^{(2)} - \hat{T}_{+2}^{(2)} \right\} \\
& + \left\{ \frac{3\hat{x}_{ij}\hat{z}_{ij}}{\hat{r}_{ij}^5} \right\} \left\{ \hat{T}_{-1}^{(2)} - \hat{T}_{+1}^{(2)} \right\} \\
& \left. + i \left\{ \frac{3\hat{y}_{ij}\hat{z}_{ij}}{\hat{r}_{ij}^5} \right\} \left\{ \hat{T}_{-1}^{(2)} + \hat{T}_{+1}^{(2)} \right\} \right]. \quad (1.11)
\end{aligned}$$

In the general case of an irreducible tensor operator $\hat{T}_q^{(k)}$ of rank k and component q , and denoting an eigenstate with angular momentum j , magnetic quantum number m and possible additional quantum numbers α as $|\alpha j m\rangle$, we observe nonvanishing matrix elements $\langle \alpha' j' m' | T_q^{(k)} | \alpha j m \rangle$ only if the selection rules:

$$|j - k| \leq j' \leq j + k \quad (1.12)$$

$$m' = q + m \quad (1.13)$$

are obeyed. With $k = 2$ in the case of the spin-spin operator, we notice therefore that there is no coupling $j = 0/j = 0$ (singlet–singlet), $j = 0/j = 1$ (singlet–triplet), $j = \frac{1}{2}/j = \frac{1}{2}$ (doublet–doublet).

Wigner-Eckart Theorem

In the evaluation of matrix elements over irreducible spin tensor components, the application of the Wigner-Eckart theorem (WET) is of crucial relevance. A matrix element $\langle \alpha' j' m' | T_q^{(k)} | \alpha j m \rangle$ over an irreducible tensor $\hat{T}_q^{(k)}$ can according to the WET be expressed as:

$$\langle \alpha', j' m' | T_q^{(k)} | \alpha, j m \rangle = \langle jk; mq | jk; j' m' \rangle \frac{\langle \alpha' j' || T^{(k)} || \alpha j \rangle}{\sqrt{2j+1}}. \quad (1.14)$$

The *Clebsch-Gordan coefficients* $\langle jk; mq | jk; j' m' \rangle$ (see [6]) denote coupling coefficients between angular momentum states and are tabulated in literature [154]. Further details referring to tensors, tensorial methods and the WET can be found in Silver [155].

The relevance of the WET in the present case is the expression of a tensorial matrix element through the *reduced matrix element* (RME) $\langle \alpha' j' || T^{(k)} || \alpha j \rangle$ which is independent of the quantum numbers m, m' and q . Therefore, if we consider further matrix

elements between states with identical quantum number j, j' but differing magnetic quantum numbers m'', m''' , we can formulate:

$$\langle \alpha', j' m''' | T_{q'}^{(k)} | \alpha, j m'' \rangle = \frac{\langle jk; m'' q' | jk; j' m''' \rangle}{\langle jk; m q | jk; j' m' \rangle} \langle \alpha', j' m' | T_q^{(k)} | \alpha, j m \rangle. \quad (1.15)$$

The quotient of two Clebsch-Gordan coefficients is denoted as a scaled Wigner-Eckart coefficient.

Concretely in the application of the WET in the present implementation, I give the calculation of the spin-spin interaction between two triplet states as an example: In principle, we have to set up a $\{3 \times 3\}$ matrix between the $M_S = -1, 0, +1$ components of the triplet state. What is actually implemented is an evaluation of each space component with the spin component $\hat{T}_0^{(2)}$ between the triplet states with $M_S = S = +1$; we therefore only calculate one spin-coupling element of the matrix. Subsequently, the appropriate combination with the spin components $\hat{T}_{-2}^{(2)}, \hat{T}_{-1}^{(2)}, \hat{T}_{+1}^{(2)}, \hat{T}_{+2}^{(2)}$ is obtained via the WET without having to evaluate the other spin parts directly.

Since the implementation of our spin-spin program evaluates matrix elements over $M_S = S$ -states, the reference MEs that we have to consider with respect to the application of the WET represent the subcase $j = m, j' = m'$. McWeeny [98] has derived scaled Wigner-Eckart coefficients for irreducible tensor operators $\hat{T}^{(1)}, \hat{T}^{(2)}$ for this particular subcase, denoting his coefficients as “scaled $3j$ symbols”. We have employed his tabulated scaled $3j$ symbols, given in table III of his work, in our implementation.²

Second Quantization

The derivation of the implemented formulas in Ch. 2 will employ the formalism of second quantization. The most important notions and relationships are introduced in this section, for a comprehensive presentation the reader is referred to [7].

In second quantization, operators and wave functions are expressed through the construct of creation and annihilation operators; inherent properties like the antisymmetry of the wave function are represented through the algebra of these operators. For simplicity, I will introduce relevant concepts in the context of a spin-free formalism, the adaptation to a spin-dependent scheme is straightforward and will occur at the end of this section.

A determinant in the basis $\{\phi_P\}$ of M orthonormal spin orbitals can be written as a general *occupation number vector* (ONV) $|k\rangle$:

$$|k\rangle = |k_1, k_2, \dots, k_M\rangle, \quad k_P = \begin{cases} 1 & \phi_P \text{ occupied} \\ 0 & \phi_P \text{ unoccupied} \end{cases} \quad (1.16)$$

²Note that his table exhibits a sign error: In the entry $S_a = S, S_b = S + 2, M_a = M, M_b = M \pm 1$, it should read $[(S \pm M + 1)(S \mp M + 1)(S \pm M + 2)(S \pm M + 3)]$.

with the *occupation number* k_P denoting the occupation 1 or 0 of spin orbital P . A creation operator a_P^\dagger operates on the spin orbital ϕ_P as follows:

$$a_P^\dagger |k_1, k_2, \dots, 0_P, \dots, k_M\rangle = \Gamma_P^k |k_1, k_2, \dots, 1_P, \dots, k_M\rangle \quad (1.17)$$

$$a_P^\dagger |k_1, k_2, \dots, 1_P, \dots, k_M\rangle = 0, \quad (1.18)$$

thereby generating an electron in ϕ_P if it is unoccupied, resulting in zero else. The phase factor Γ_P^k is equal to +1 if the number of occupied spin orbitals to the left in the ON vector is even, and -1 if it is odd. Conversely, the action of an annihilation operator a_P is defined as:

$$a_P |k_1, k_2, \dots, 0_P, \dots, k_M\rangle = 0 \quad (1.19)$$

$$a_P |k_1, k_2, \dots, 1_P, \dots, k_M\rangle = \Gamma_P^k |k_1, k_2, \dots, 1_P, \dots, k_M\rangle. \quad (1.20)$$

The following *anticommutation relations* are defined:

$$\{a_P^\dagger, a_Q^\dagger\} = 0 \quad (1.21)$$

$$\{a_P, a_Q\} = 0 \quad (1.22)$$

$$\{a_P^\dagger, a_Q\} = \delta_{PQ}. \quad (1.23)$$

These relations determine the algebra of creation and annihilation operators and are a direct consequence of the mathematical properties imposed on the fermionic system.

One-electron operators are expressed in second quantization as:

$$\hat{f} = \sum_{PQ} \langle P|f|Q\rangle a_P^\dagger a_Q = \sum_{PQ} f_{PQ} a_P^\dagger a_Q \quad (1.24)$$

while *two-electron operators* are introduced as:

$$\hat{g} = \frac{1}{2} \sum_{PQRS} g_{PQRS} a_P^\dagger a_R^\dagger a_S a_Q \quad (1.25)$$

(see [7], especially Eqs. (1.4.2) and (1.4.15)).

As a simpler example, the spin-free Hamiltonian in the Born-Oppenheimer approximation is therefore formulated in second quantization as:

$$\hat{\mathcal{H}} = \sum_{PQ} h_{PQ} a_P^\dagger a_Q + \frac{1}{2} \sum_{PQRS} g_{PQRS} a_P^\dagger a_R^\dagger a_S a_Q. \quad (1.26)$$

In the framework of spin-dependent operators, it is advantageous to adapt the notation and refer to spin quantum numbers explicitly. As it is common practice, I will operate with a restricted formalism in which a spin orbital is formulated as a product of spatial and spin eigenfunctions. A compound index is employed, referring to the orbital part through lower-case Roman letters r, s while lower-case Greek letters ρ, σ

denote the spin state, thereby identifying spin orbitals as $\phi_{r\rho}$, $\phi_{s\sigma}$. The formalism of creation/annihilation operators introduced so far is straightforwardly adaptable to this change in notation, thereby for example in the case of the anticommutation rule given in Eq. (1.23) rewriting to:

$$\{a_{r\rho}^\dagger, a_{s\sigma}\} = \delta_{rs}\delta_{\rho\sigma}. \quad (1.27)$$

1.5.2 Matrix Elements

Algorithm: η -Pattern: spin-free

In 1975 Wetmore and Segal introduced a scheme for the efficient evaluation of CI-matrix elements [156]. The basic idea is to avoid the time-consuming step of descending onto the level of determinants in the comparison of configurations. A crucial element in the realization of this intention is the recognition that the difference in occupation between two arbitrary configurations can be expressed through a limited number of possible *excitation patterns*. It is in those excitation patterns that ultimately the spin-coupling information of the associated CSFs is encapsulated. The interaction associated with each pattern can be precalculated once, which reduces the computational labour in the actual evaluation to the recognition of the concrete pattern of the pair of configurations in question and retrieving from memory the interaction element associated with this pattern. I will subsequently outline the crucial aspects of the work of Wetmore and Segal before illustrating the extension to the spin-orbit operator.

A *configuration* will denote solely the spatial occupation of molecular orbitals. Associated with a single configuration can be more than one *configuration state function* (CSF) which represents an eigenfunction with valid S , M_S values. Following the convention of Wetmore and Segal, a CSF is expressed as a linear combination of determinants Δ_i as:

$$|S, M_S, \omega, w\rangle = \sum_i c_i(S, M_S, \omega) \Delta_i(M_S, w) \quad (1.28)$$

with w representing the space occupation vector while ω refers to the spin eigenfunction. Introducing in the notation of Wetmore and Segal the spin-conserving excitation operator:

$$\hat{E}_i^j = \sum_\sigma a_{i\sigma}^\dagger a_{j\sigma}, \quad (1.29)$$

the matrix element between two CSFs $|\omega, w\rangle$, $|\omega', w'\rangle$ over this operator is obtained as:

$$\langle \omega', w' | \hat{E}_i^j | \omega, w \rangle = \eta(\omega', w'; \omega, w). \quad (1.30)$$

The η -coefficient constitutes a single number representing the spin interaction of the CSFs $|\omega, w\rangle$, $|\omega', w'\rangle$. It is computed by evaluating the spin occupation vectors of the determinants associated with respective CSFs and can be precalculated ahead of the actual program run and retrieved from memory during the calculation. The application

of this scheme to two-electron operators was introduced employing the insertion of the resolution of identity:

$$\begin{aligned} \langle \omega', w' | E_i^j E_k^l | \omega, w \rangle &= \sum_{\omega''} \langle \omega', w' | E_i^j | \omega'', w'' \rangle \langle \omega'', w'' | E_k^l | \omega, w \rangle \\ &= \boldsymbol{\eta}(\omega', w'; w'')_{\omega''} \cdot \boldsymbol{\eta}(w''; \omega, w)_{\omega''} \end{aligned} \quad (1.31)$$

with the contraction of the vectors $\boldsymbol{\eta}$ over the dimension in ω'' . The summation in w'' vanishes as the particular excitation indices i, j, k, l constitute a selection in w'' . Note that at this point, I deviate from the notation of Wetmore and Segal as I chose to refer to the bra with indices grouped on the left of the bracketed expression accompanying an η -coefficient while indices grouped on the right, separated by a semicolon, refer to the ket. The dimension ω'' along which contraction is performed is denoted by a subscript. This deviation from the original notation of Wetmore and Segal is introduced for reasons of clarity in the case of the more complex spin-spin formulation, as it will be employed in Ch. 2.

A crucial saving intrinsic in this approach is that the value of η depends solely on number and positions of open-shell electrons of the two CSFs involved while shells empty or doubly occupied in both CSFs do not contribute to the value of η . Indeed, as the *sequence* of open shells is common to CSFs exhibiting an identical configuration, the notion of *excitation patterns* can already be applied on the level of configurations. A brief introduction of this scheme including the computationally efficient realization as binary numbers follows.

Configurations are stored as occupation vectors of MOs, constituting a sequence of 0, 1, 2, depending on the occupation of the individual molecular orbital. According to Wetmore and Segal, the difference between two occupation vectors is expressed as a so-called excitation pattern. The identification of excitation patterns is performed by bitwise comparison of occupations of bra and ket and the resulting pattern is stored as a binary number. The following example illustrates the underlying principle in the comparison of two occupation number vectors:

$$\begin{array}{r} \text{ONV 1} \quad 1 \ 0 \ 1 \ 1 \ 0 \ 1 \ 2 \ 2 \ 2 \ 2 \\ \text{ONV 2} \quad 1 \ 1 \ 0 \ 1 \ 0 \ 1 \ 2 \ 2 \ 2 \ 2 \\ \hline \quad \quad 1 \ 0 \ 0 \ 1 \quad 1 \\ = 1 \cdot 2^4 + 0 \cdot 2^3 + 0 \cdot 2^2 + 1 \cdot 2^1 + 1 \cdot 2^0 \\ = \text{pattern 19} \end{array}$$

Figure 1.4: Example of calculation of excitation pattern

Shells empty and doubly occupied vanish in the evaluation of the pattern, shells singly occupied in both configurations result in a bit set to one, shells of changing occupation result in a bit set to zero. Thereby, all excitation patterns can be uniquely identified. Expression of the Hamiltonian in terms of excitation operators \hat{E}_i^j enables the reformulation of matrix elements between states as products of integrals and η -coefficients.

A detailed illustration of this approach including a derivation of terms over the Hamiltonian is presented in [156].

Algorithm: η -Pattern: spin-dependent

The algorithm of Wetmore and Segal is particularly suited for a configuration selecting algorithm as the main focus is the reduction in computational effort in the comparison and evaluation of pairs of configurations. The Grimme/Waletzke DFT/MRCI applies this scheme on the level of the spin-free operator. In the framework of an implementation of spin-orbit interaction employing DFT/MRCI states, Kleinschmidt and Marian [3] developed an extension of the algorithm to the case of the spin-orbit operator in its formulation as an effective one-electron interaction [122]. The one-electron spin-orbit operator in second quantization is introduced according to Kleinschmidt and Marian as:

$$\begin{aligned}\hat{\mathcal{H}}_{SO}^{eff} &= \sum_{m,n} \sum_{\mu,\nu} \langle m \mu | l \cdot s | n \nu \rangle a_{m\mu}^\dagger a_{n\nu} \\ &= \sum_{m,n} \sum_{\mu,\nu} \langle m | l | n \rangle \langle \mu | s | \nu \rangle a_{m\mu}^\dagger a_{n\nu} \\ &= \sum_{m,n} l_{mn} \left(\sum_{\mu,\nu} s_{\mu\nu} a_{m\mu}^\dagger a_{n\nu} \right)\end{aligned}\quad (1.32)$$

denoting spatial functions m , n and spin μ , ν , furthermore omitting the index in M_S as the program operates internally with wave functions for which $S = M_S$. The second step illustrates the possible decomposition of spatial and spin contributions in that the angular momentum operator can be grouped referring to the spatial part of the wavefunction only and the spin operator equivalently to the spin part.

The matrix element between two CSFs $|S, \omega, w\rangle$, $|S', \omega', w'\rangle$ which differ by a single excitation $b \rightarrow a$ thus formulates as:

$$\begin{aligned}\langle S', \omega', w' | \sum_{m,n} l_{mn} \sum_{\mu,\nu} s_{\mu\nu} a_{m\mu}^\dagger a_{n\nu} | S, \omega, w \rangle \\ = l_{ab} \langle S', \omega', w' | \sum_{\mu,\nu} s_{\mu\nu} a_{a\mu}^\dagger a_{b\nu} | S, \omega, w \rangle \\ \equiv l_{ab} \cdot \eta(S', \omega', w'; S, \omega, w).\end{aligned}\quad (1.33)$$

The matrix element between two CSFs is therefore reduced to the product of an angular momentum integral l_{ab} and a spin- η -coefficient which, in contrast to the spin-free η -coefficient, involves a dependence on the spin operator \hat{s}^{+1} , \hat{s}^0 , \hat{s}^{-1} .³ In the subsequent work, the term “ η -coefficient” shall denote implicitly the spin-dependent construct and

³Note that in Eq. (1.33) I chose a notation which differs slightly from the original one of Kleinschmidt and Marian in [3], again referring in my notation with the left-hand side of indices to the bra, the right-hand side to the ket, while separating these two quantities by a semicolon.

I will refer to the spin-free η -coefficient explicitly when necessary.

The consideration of spin operators introduces additional coupling terms as nonvanishing matrix elements may occur now between states for which $\Delta S = 0, \pm 1$. Consequently, the number of η -coefficients is noticeably higher in the spin-dependent than in the spin-free case. As in the spin-free case, the η -coefficient depends solely on number and positions of open shell electrons but not on individual occupation indices. This considerably limits the number of distinct *excitation patterns* and therefore coefficients and allows for a precalculation of the η -coefficients and storage in memory during the actual program run. Out of completeness, it should be mentioned that with each pattern and spin operator, four subcases are associated which are partly related to one another. Only an independent subset of the cases are precalculated and the individual one accounted for during the program run. As a description on this level of detail goes beyond the scope of this work, the reader is once again referred to [2–4, 153].

1.6 Experimental Formulation

The experimentally assessed observable corresponding to electron spin-spin coupling is the effect of “zero-field splitting” (ZFS), as was described at the end of Ch. 1.1.1. The possibly partial lifting of degeneracies between the M_S components of a state with spin S can be caused by spin-orbit and/or spin-spin coupling effects. The terms in the Breit-Pauli Hamiltonian giving rise to second-order SOC and first-order SSC exhibit an identical phenomenological structure, causing these effects to be experimentally indistinguishable. The effective spin Hamiltonian describing zero-field splittings is formulated in the case of a system with $S = 1$ as [24]:

$$\hat{\mathcal{H}}_{ZFS} = \hat{\mathbf{S}} \cdot \hat{\mathbf{D}} \cdot \hat{\mathbf{S}}. \quad (1.34)$$

$\hat{\mathbf{S}}$ denotes the spin operator $\hat{\mathbf{S}} = (\hat{S}_x, \hat{S}_y, \hat{S}_z)$ while the so-called zero-field tensor $\hat{\mathbf{D}}$ encapsulates the spatial dependence. As a Hermitian operator, $\hat{\mathbf{D}}$ can be diagonalized by a unitary transformation, yielding the eigenvalues D_{xx} , D_{yy} , D_{zz} and thereby simplifying the above spin Hamiltonian expression to:

$$\hat{\mathcal{H}}_{SS} = D_{xx}\hat{S}_x^2 + D_{yy}\hat{S}_y^2 + D_{zz}\hat{S}_z^2. \quad (1.35)$$

Furthermore, tracelessness follows from $\hat{\mathbf{D}}$ being a tensor of rank two, imposing additionally the condition $D_{xx} + D_{yy} + D_{zz} = 0$. Consequently, we obtain two independent values which quantify zero-field splittings and are commonly designated as D and E , obeying the following definition:

$$D = \frac{3}{2}D_{zz} \quad (1.36)$$

$$E = \frac{1}{2}(D_{xx} - D_{yy}). \quad (1.37)$$

Within an experimental context, the values of D and E depend on the choice of principal axis system and it is customary to choose the axis system so as to satisfy the condition:

$$|E| \leq |D/3|. \quad (1.38)$$

In a theoretical context, one frequently further imposes $E/D \geq 0$.

The experimentally observed zero-field splittings D/E have to be related to theoretically obtained values. The above discussion based on the general form of \mathcal{H}_{ZFS} was valid in the description of SOC as well as SSC. In the following, we will turn specifically to the assessment of the latter. In order to establish a connection between experimental and theoretical formulations, Eq. (1.34) has to be compared with the Breit-Pauli Hamiltonian describing electron spin-spin coupling, see Eq. (1.2). After regrouping of terms, we can identify operator expressions and thereby relate the phenomenological construct to the theoretical description. We arrive at the definition of D_{SS} already introduced in Eq. (1.8), associated with the operator formulation in Eq. (1.7) (see Ch. 1.5.1). The eigenvalues obtained by diagonalization of \mathcal{H}_{SS} directly correspond to the components D_{xx} , D_{yy} and D_{zz} of the phenomenological Hamiltonian (Eq. (1.34)) and can be assembled according to Eqs. (1.36)/(1.37) to compare with experimentally determined couplings D and E .

Systems with $S > 1$

The case $S = 1$ is the most common one in organic systems. Phenomenological terms describing higher spin symmetries have been discussed by Weltner [24] as well as by Abragam and Bleaney [25]. In general, the zero-field splitting is expressed therein as a summation over higher powers of \hat{S}_x , \hat{S}_y , \hat{S}_z and the coefficients parametrized accordingly. For further details, I refer in particular to [24].

Tracelessness of \hat{D}

In principle, \hat{D} does not necessarily exhibit tracelessness in the phenomenological description of $\hat{\mathcal{H}}_{ZFS}$, as was noted by Neese [119]. Since Eq. (1.34) is employed in the experimental context to parametrize observable zero-field splittings in general, other possible coupling effects which would necessitate a more complicated theoretical consideration are included alongside second-order spin-orbit and first-order spin-spin interactions. These further coupling effects do not necessarily have to comply with a traceless tensorial operator structure. This aspect is not relevant in the present context since we restrict our discussion primarily to spin-spin effects to first order as described by the Breit-Pauli Hamiltonian, but it is mentioned as this is a common misconception encountered in the literature.

Identification of the Axis System

The experiment allows the correlation of zero-field splitting levels with the principal axis system, as defined by the three components \mathcal{X} , \mathcal{Y} , \mathcal{Z} . This can be accomplished by aligning the molecule successively along external magnetic fields of different orientation and registering the dependence of energy transitions on the field strength. In the approximation of the weak-field regime, an orientation along a principal axis \mathcal{Z} distinguishes the corresponding eigenstate. Its energy can be observed to be independent of the external magnetic field $\mathbf{H}_{\mathcal{Z}}$ while the remaining two components \mathcal{X} , \mathcal{Y} exhibit a dependence on the field strength as their degree of mixing varies with the applied field (see description of $S = 1$ systems in Wertz and Bolton [28] as well as Weltner [24]). In the experimental context, it is therefore possible to establish a connection between energy levels and the molecular orientation and thereby interpret spin-spin couplings with respect to particular molecular axes. In the theoretical consideration, electron spin-spin coupling is calculated at zero magnetic field, yielding the eigenvalues of the system. The additional information of the dependence of spin splittings on the field strength is absent, and the correspondence of spin levels to the molecular geometry can therefore not be deduced. However, comparison with experiment can allow for an identification of the theoretical splittings. Furthermore, in systems of higher symmetry, the recognition of the principal axis system may be deducible from inspection of the molecular geometry. Nonetheless, it has to be recognized that in the theoretical context, assignment of spin splittings to specific molecular axes is generally not possible *a priori*.

1.7 Final Remarks

In the customary approach of evaluating electron spin-spin coupling and possibly furthermore spin-orbit coupling, implicit assumptions are frequently present. In the current first implementation of SPOCK.SISTR, I bring these to attention as possible issues.

Evaluation of $\mathcal{H}_{SO}/\mathcal{H}_{SS}$

In particular if it is to be expected that spin-orbit and spin-spin effects are of comparable magnitude, an assessment of both is desirable. The present program version allows the execution of the spin-spin parallel to the spin-orbit branch, thereby evaluating either \mathcal{H}_{SO} or \mathcal{H}_{SS} subsequent to a consideration of the purely electrostatic Hamiltonian \mathcal{H}_{el} within the MRCI program run. As both couplings are small compared to the Coulomb contribution in most systems, the implicit assumption of the effect of spin-orbit coupling on the wave function being negligible with respect to its impact on the magnitude of SSC (and vice versa) is usually legitimate. Nonetheless, a subtle aspect can manifest itself in an alternative consecutive assessment of the operators: Spin-orbit coupling can cause a splitting of initially degenerate levels and reduce the symmetry of the system. Upon subsequent evaluation of spin-spin coupling, this introduces the possibility of observing previously symmetry-forbidden SSC.

Calculation of D_{SO}/D_{SS}

In theoretical assessments, second-order spin-orbit and first-order spin-spin effects are frequently evaluated separately. It is important to note that in the general case, the unitary transformation diagonalizing the entire zero-field splitting tensor \hat{D} (see Eq. (1.34)) in the basis of the states of the system is not necessarily identical to the unitary transformation that diagonalizes the individual coupling matrices $\hat{D}_{SO}/\hat{D}_{SS}$. In general, the spin-coupling constants D_{SO} and D_{SS} are therefore *not* additive, which is crucial to recognize if theoretical values are to be compared with experiment. Only if an identical unitary transformation diagonalizes both coupling matrices is the simple relation $D = D_{SO} + D_{SS}$ valid. This is the case if the coupling matrices themselves commute which can occur accidentally if higher-symmetry systems result in sparse coupling matrices.

Fermi-Contact Term

In Eq. (1.1), the full Breit-Pauli spin-spin Hamiltonian was introduced. This operator can be decomposed into a sum of a tensor of rank zero (Fermi-contact term) and a tensor of rank two. Customarily, it is only the second-rank tensor \hat{D} that is evaluated in calculations of spin-spin coupling effects as the scalar term does not contribute to the magnitude of the splitting. The Fermi-contact term causes solely an identical energetic shift of all components of a specific spin state and the omission of this term does therefore not affect the evaluation of expectation values. In principle, an error can be introduced in the calculation of matrix elements between different states, though, as the Fermi-contact term does not necessarily account for identical shifts of *different* spin states. To the best of my knowledge, the possible magnitude of this error has not been assessed so far. In general, a δ function operator imposes a considerable demand on the computational description of short-range distances and is therefore very difficult to calculate. Considerations of the electron-nuclear Fermi-contact term of the hyperfine coupling tensor exist (e.g. [157, 158]) and the experience gained in this context may assist in future assessments of the electron-electron Fermi-contact term of the spin-spin operator.

Chapter 2

Computational Structure

The spin-spin branch SPOCK.SISTR developed within my PhD is embedded in the programming package SPOCK which in turn is conceptually based on the Grimme/Waletzke MRCI. In Ch. 1.4, I have introduced the basic connections between these programs on a general level (see Fig. 1.3) and outlined major aspects. Naturally, the programming decisions made in the context of the MRCI program and subsequently SPOCK guide the program structure and thereby set the scene for the spin-spin implementation.

In its outer framework as well as the constructs it depends on, the spin-spin implementation is based on the spin-orbit code. In the development of SPOCK itself, the basic structure of retrieving, comparing and processing configurations was ported from the MRCI program, the actual evaluation of configuration pairs was extended to the treatment of the spin-dependent one-electron operator $\hat{\mathcal{H}}_{SO}$ which necessitated the introduction of new structures and concepts, the details of which were illustrated in Ch. 1.5.2, p. 35ff. Adopting the spin-orbit implementation as a reference point, two major adaptations had to be considered in the case of the spin-spin operator. First, and predominantly reflected on a higher level in the outer routines, different selection rules have to be obeyed with respect to the spatial as well as the spin part. Second, the algorithm of η -coefficients and *pattern* evaluation had to be extended from the case of a one-electron to a two-electron operator (see Ch. 2.2); this point as the more crucial one concerns the concrete evaluation of the contribution of pairs of configurations.

In Ch. 2.1, I will illustrate the general program flow of the spin-spin implementation, which is structurally similar to the spin-orbit QDPT branch SPOCK.QDPT. I will start out on the outer level of SPOCK.SISTR and move towards the inner processing, reaching pictorially the step of calculating contributions of pairs of configurations. The subsequent chapter, Ch. 2.2, will be concerned with the detailed mathematical evaluation of the individual terms.

2.1 Program Structure

The principal program structure is illustrated in Fig. 2.1: At the begin of the code execution, information about molecular system and states is established by evaluation of the previous MRCI-run(s) and program variables of SPOCK are initialized. Subsequently, the spin-spin branch is entered if requested.

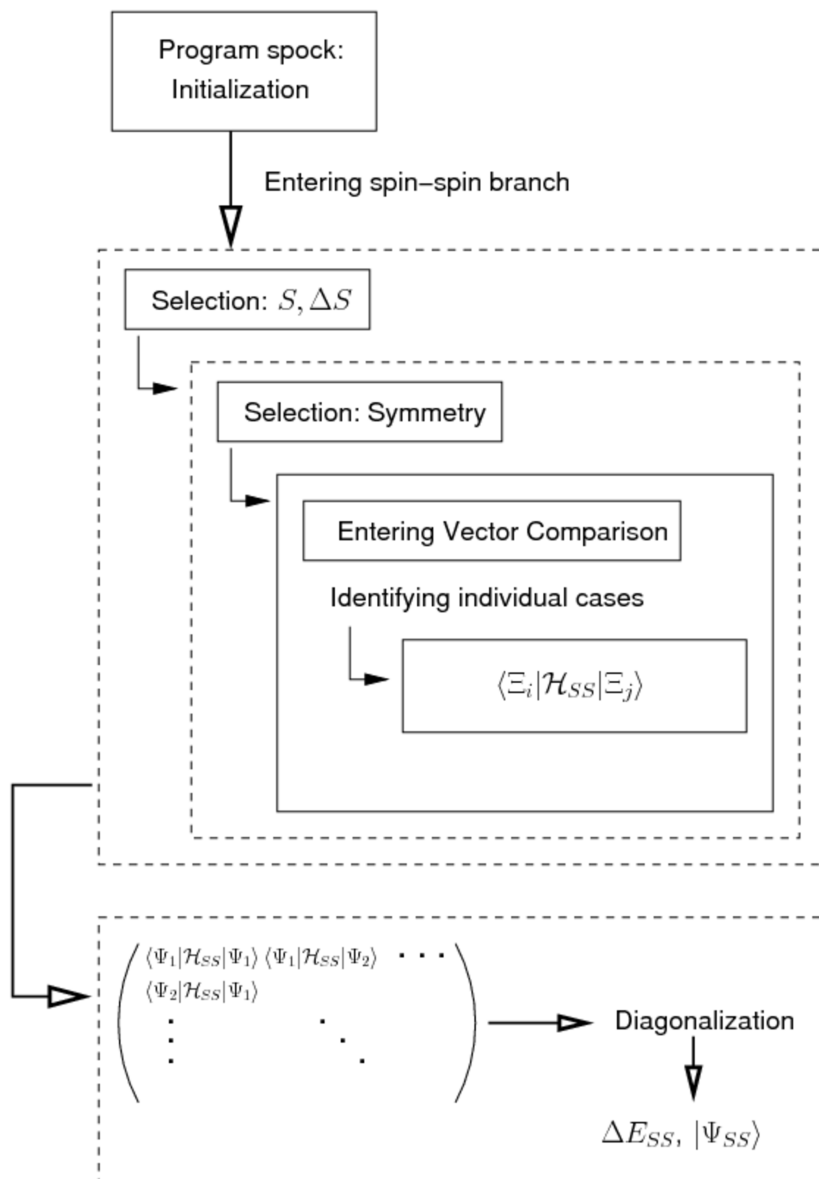


Figure 2.1: Program structure of SPOCK.SISTR

The outermost loop assesses the information concerning the spin and evaluates if spin-spin coupling is possible and with which states, based on the selection rule $\Delta S = 0, \pm 1, \pm 2$. The next loop evaluates the spatial symmetry of the states in question and determines the coupling component(s) of the operator, based on the point group of the molecule and the symmetry of the individual spin-spin terms. Subsequently, the routine of the actual vector comparison is entered and the contribution of pairs of configurations $|\Xi_i\rangle, |\Xi_j\rangle$ evaluated, the details of which will be illustrated below. After calculation of all matrix elements between $M_S = S$ wave functions, the interaction matrix in the basis of states of all M_S -values is constructed employing the Wigner-

Eckart theorem (see p. 30ff in Ch. 1.5.1). Diagonalization of this matrix yields the perturbation energy to second order as well as the first-order wave functions as linear combinations of the unperturbed states.

In the subsequent illustration of vector processing and configuration comparison, I introduce $|\Upsilon\rangle$ to denote CSFs while $|\Xi\rangle$ refers to configurations. A wave function $|\Psi_k\rangle$ can be expressed as a linear combination of CSFs, the coefficients c_i^k of which have been determined in the previous MRCI calculation:

$$|\Psi_k\rangle = \sum_i c_i^k |\Upsilon_i\rangle. \quad (2.1)$$

Storage of Wave Function

Internally, wave functions $|\Psi_k\rangle, |\Psi_l\rangle$ are stored as vectors of CSFs, while in turn CSFs belonging to an identical configuration are grouped consecutively.

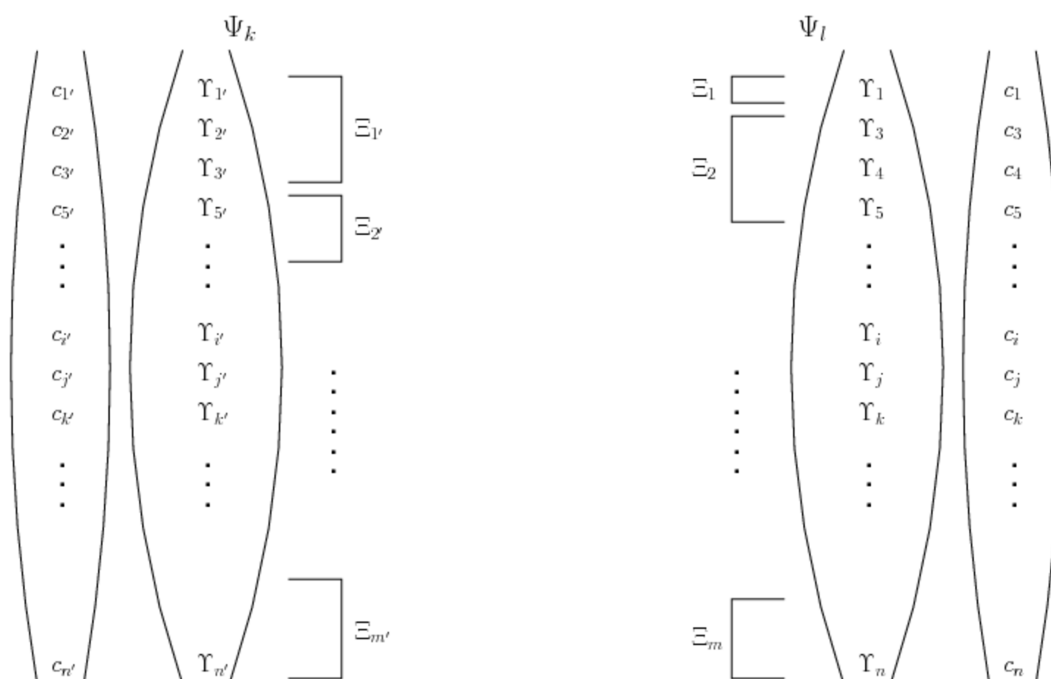


Figure 2.2: Alignment of configurations $|\Xi\rangle$, CSFs $|\Upsilon\rangle$

Note that I explicitly introduced primed subindices in the left vector while employing unprimed ones in the right vector. If $|\Psi_k\rangle, |\Psi_l\rangle$ fall into different symmetries, the configuration spaces of these two states differ, and we observe $|\Xi_{j'}\rangle \neq |\Xi_j\rangle$. A clear distinction between the two configuration spaces is therefore required if we display entire vectors. When discussing individual matrix elements

in subsequent sections, I will return to the simpler notation of employing different letters for configurations/CSFs of bra and ket.

The grouping of CSFs on the basis of configurations is advantageous in the framework of the algorithm, which operates on the higher level of configurations instead of CSFs.

Comparison of Configurations

The matrix element $\langle \Psi_k | \mathcal{H}_{SS} | \Psi_l \rangle$ is calculated by progressing through the vector of bra and ket. Individual configurations are compared pairwise and their difference in excitation *idiff* established as a branching criterion, yielding nonvanishing matrix elements and therefore further execution for $idiff = 0, 1, 2$. Subsequently, the excitation pattern for the pair of configurations $|\Xi_{i'}\rangle, |\Xi_j\rangle$ is determined and the corresponding set of η -coefficients retrieved from memory.

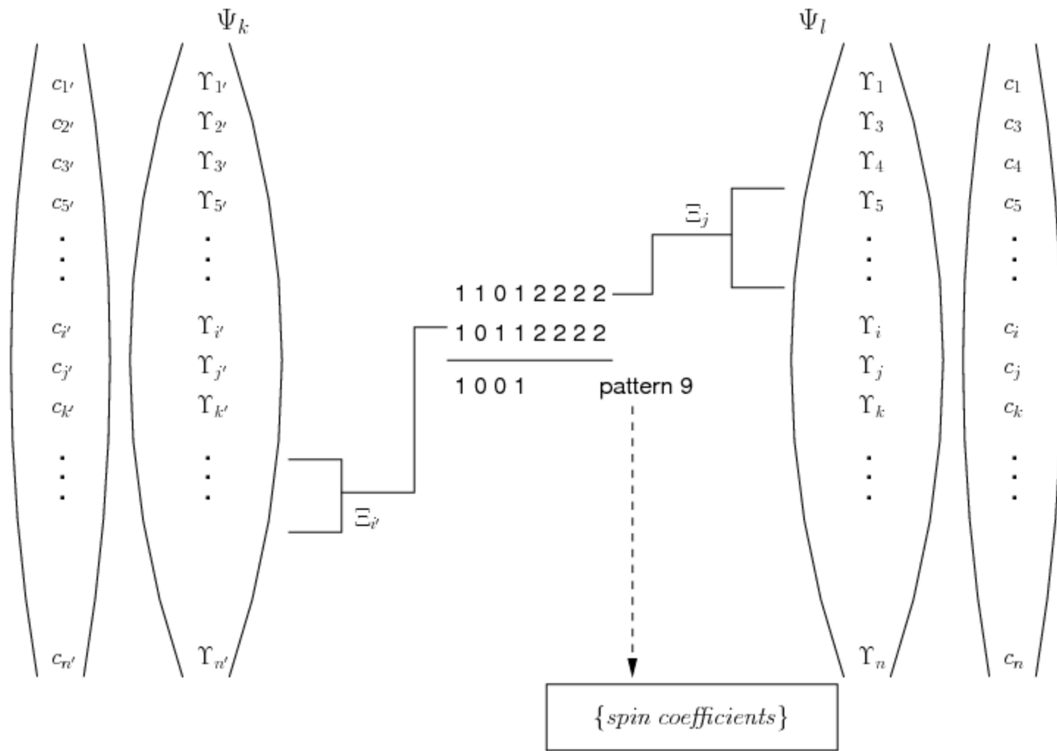


Figure 2.3: Comparison of configurations

Evaluation of Matrix Element

In the last step of a configuration comparison, the vectors of coefficients of the CSFs belonging to configurations $|\Xi_{i'}\rangle, |\Xi_j\rangle$ are accessed and assembled with spatial integrals and spin coefficients to calculate the contribution of $\langle \Xi_{i'} | \mathcal{H}_{SS} | \Xi_j \rangle$ to the matrix element $\langle \Psi_k | \mathcal{H}_{SS} | \Psi_l \rangle$.

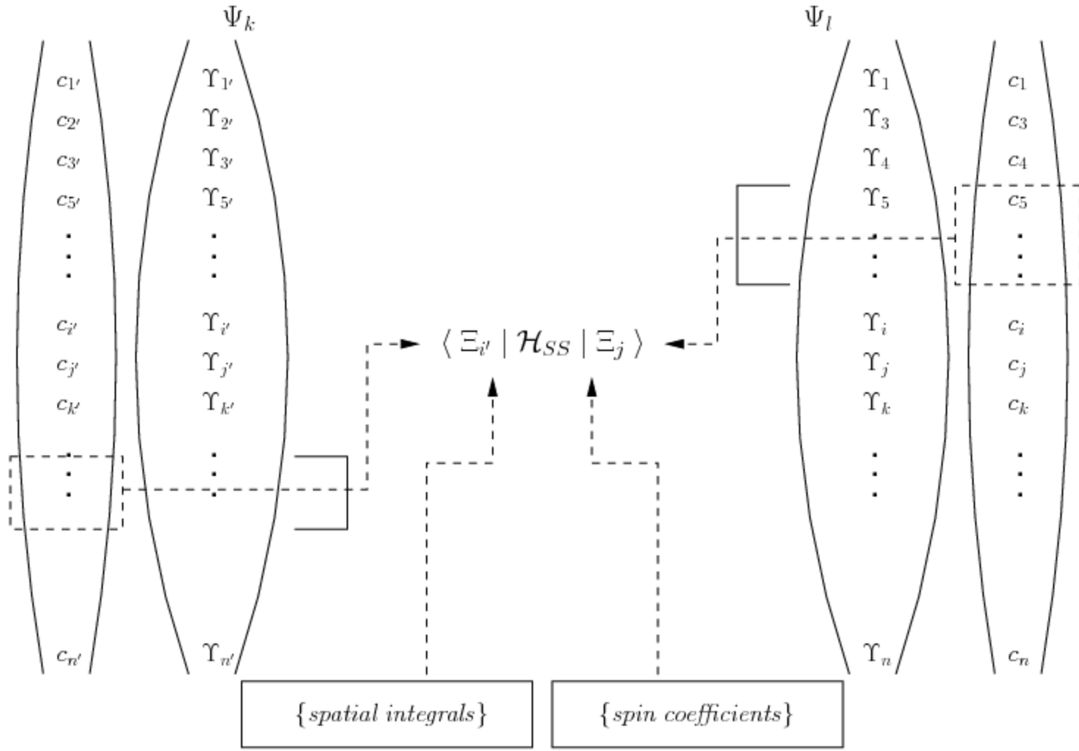


Figure 2.4: Calculation of contributions

It should be emphasized at this point that the comparison step involves solely configurations and does not descend to the level of CSFs, which constitutes a distinctive point of saving in the computational effort. After determination of associated patterns of the pair of configurations in question, the coefficients of CSFs are accessed directly and processed with spatial spin-spin integrals and spin coefficients to yield $\langle \Xi_{i'} | \mathcal{H}_{SS} | \Xi_j \rangle$. The evaluation of this term is derived in the following.

2.2 Calculation of Matrix Elements

In principle, a general matrix element $\langle \Xi_k | O | \Xi_l \rangle$ between two configurations $|\Xi_k\rangle$, $|\Xi_l\rangle$ entails a summation over CSFs $|\Upsilon'\rangle$ affiliated with $|\Xi_k\rangle$ and CSFs $|\Upsilon\rangle$ affiliated with $|\Xi_l\rangle$:

$$\langle \Xi_k | O | \Xi_l \rangle = \sum_{\Upsilon'} \sum_{\Upsilon} \langle \Upsilon' | O | \Upsilon \rangle. \quad (2.2)$$

It has to be remembered that the introduction of $|\Upsilon\rangle$ constitutes a compact notation for a particular spin eigenfunction with definite values of spin S , spin component M_S , space occupation vector w and and spin vector ω : $|S, M_S, \omega, w\rangle = |\Upsilon\rangle$.

As an element in a CI wave function, Eq. (2.2) has to be weighted by the CI coefficients $\{c^i\}$, $\{c^j\}$ that specify the contribution of individual CSFs to the electronic states $|\Psi_i\rangle$,

$|\Psi_j\rangle$. We therefore obtain in the evaluation of spin-spin coupling for the contribution of $\langle \Xi_k | \mathcal{H}_{SS} | \Xi_l \rangle$ to $\langle \Psi_i | \mathcal{H}_{SS} | \Psi_j \rangle$:

$$\langle \Xi_k | \mathcal{H}_{SS} | \Xi_l \rangle = \sum_{\Upsilon'} \sum_{\Upsilon} c^i(\Upsilon') c^j(\Upsilon) \langle \Upsilon' | \mathcal{H}_{SS} | \Upsilon \rangle \quad (2.3)$$

with the definition of $\hat{\mathcal{H}}_{SS}$ given in Eq. (1.2). We introduce at this point a simplified notation for the spin-spin Hamiltonian by referring with a general label \hat{S} to a component of the spin tensor $\hat{T}_i^{(2)}$ while the accompanying spatial part is denoted \hat{R} . Using this abbreviated notation, the spin-spin operator reads:

$$\hat{\mathcal{H}}_{SS} = k \sum_m \sum_{i \neq j}^N \hat{R}^{(m)} \cdot \hat{S}^{(m)} \quad (2.4)$$

with the compound prefactor $k = -g_e^2 \mu_B^2 \alpha^2$. It is legitimate to decompose the CSFs into spatial and spin information and evaluate these contributions as a product expression over the corresponding operators, thereby allowing to write in an abstract sense:

$$\langle \Xi_k | \mathcal{H}_{SS} | \Xi_l \rangle = k \sum_{\Upsilon'} \sum_{\Upsilon} c^i(\Upsilon') c^j(\Upsilon) \sum_m \langle w' | R^{(m)} | w \rangle \langle S', M_S', \omega' | S^{(m)} | S, M_S, \omega \rangle. \quad (2.5)$$

At this point, we recognize the product of CI coefficients, spatial integrals over \hat{R} and spin coupling over \hat{S} which is assembled to the corresponding matrix element. The spatial spin-spin integrals depend solely on the excitation between the two configurations and are therefore common to the set of CSFs associated with $|\Xi_{i'}\rangle$, $|\Xi_j\rangle$. The spin contribution on the other hand depends on the spin eigenfunctions as well as the spin operator in question and thereby incorporates the entire spin information of the term.

The factorization of spatial and spin information is reflected on the level of the derivation as well as the implementation. The labour in the derivation of expressions describing electron spin-spin coupling in the framework of SPOCK constitutes therefore of two parts. The first is concerned with the development of the concrete spatial coupling expressions over \hat{R} under consideration of selection rules and permutational properties of the spin-spin operator. The second concerns the evaluation of spin coupling expressions over \hat{S} , again employing operator relations while resorting to individual spin operator components in order to simplify the expressions that arise.

In the case of the one-electron spin-orbit operator, the spin contribution is given by a single η -coefficient (see Ch. 1.5.2, Eq. (1.33)). The question in the context of the present thesis was if the concept of spin-dependent η -coefficients could be extended from a one- to a two-electron operator, and in particular if this could be done efficiently within the framework of the existing program. Following the idea of Wetmore and Segal, the decomposition of a two-electron to a product of two one-electron operators by insertion of the resolution of identity is in principle straightforward (see p. 33ff

in Ch. 1.5.2). As so often with ideas, the actual realization is more intricate in the case of the spin-spin operator than it may seem at first sight, however. The majority of this chapter is devoted to the stepwise derivation of the implemented formulas. At the end of it stands a construct which indeed allows the calculation of matrix elements over the spin-spin operator consistent with the structures employed within SPOCK, and it is shown specifically that the spin term can be evaluated as a scalar product of η vectors. It should be pointed out that this decomposition was crucial for the realizability of the implementation of the spin-spin operator as the alternative would have been the introduction of a compound two-electron construct depending on two CSFs and four spin indices. This would have been distinctly more demanding in terms of memory requirement.¹

The route I am about to commence is as follows:

Spin-Spin Operator: I will start out with the introduction of the spin-spin operator in second quantization. After specification of the three possible cases of spatial excitation ($idiff = 0, 1, 2$), I will introduce the expressions associated with each case (Ch. 2.2.1).

Derivation (I): The first part of my derivation refers to the spatial contribution. Under consideration of spatial excitations, I will establish selection rules and matrix element expressions which follow from the mathematical properties of the spin-spin operator. It consists of the steps:

- Derivation of the *selection rules* associated with each case of excitation.
- Showing that the *contribution of closed shells* is vanishing in the calculation.
- Introduction of a *permutational relation* between spin indices which is necessary for further reformulations.

I will finish this section giving compact expressions for the evaluation of spin-spin coupling on a general background, e.g., without further resolution of the spin coupling contribution (Ch. 2.2.2).

Derivation (II): The second part of the derivation is concerned with the evaluation of the spin coupling information within the existing program environment. In particular, it is here that the decomposition of two-electron spin-spin terms into a product of one-electron spin- η -coefficients will be accomplished. The second aspect of major relevance that has to be accounted for in derivation and implementation is the imposition of an algorithm based on wave functions with $M_S = S$, as will be shown herein (Ch. 2.2.3).

Implemented Formulas: At the end of the derivation, I will present the formulas for the evaluation of the spin coupling terms as they are implemented in SPOCK.SISTR, casewise dependent on the excitation and the difference in multiplicity (Ch. 2.2.4).

¹Considering as an example the excitation between two triplets with ten open shells, the storage demand would increase approximately (based on a simplified assessment) by a factor of 15.

Spatial Integrals: The previous steps were related to the program structure and the evaluation of the spin-coupling contribution. For the evaluation of the entire matrix element, the spatial spin-spin integrals have to be furthermore incorporated. I will therefore describe the calculation of exact spatial integrals, obtained by modification of the program DALTON (Ch. 2.2.5).

2.2.1 Spin-Spin Operator

The starting point of my derivation is the spin-spin operator as introduced in the abbreviated notation of Eq. (2.4). The MRCI as well as SPOCK code evaluate configurations based on their difference in excitation. This processing is related conceptually to the formalism of second quantization, and it therefore constitutes a compact notation that I adapt for the subsequent derivation (the most important relationships were introduced in Ch. 1.5.1, p. 31ff). The reader more familiar with first quantization may find some of the reformulations less intuitive which may make some steps appear hasty and others more elaborate.

Introducing now the spin-spin operator in second quantization, we obtain:

$$\begin{aligned}
 \hat{\mathcal{H}}_{SS} &= k \frac{1}{2} \sum_m \sum_{rstu} \sum_{\rho\sigma\tau\nu} \langle r\rho\ s\sigma | R^{(m)} \cdot S^{(m)} | t\tau\ u\nu \rangle a_{r\rho}^\dagger a_{s\sigma}^\dagger a_{uv} a_{t\tau} \\
 &= k \frac{1}{2} \sum_m \sum_{rstu} \sum_{\rho\sigma\tau\nu} \langle rs | R^{(m)} | tu \rangle \langle \rho\sigma | S^{(m)} | \tau\nu \rangle a_{r\rho}^\dagger a_{s\sigma}^\dagger a_{uv} a_{t\tau} \\
 &= k \frac{1}{2} \sum_m \sum_{rstu} \sum_{\rho\sigma\tau\nu} R_{rstu}^{(m)} S_{\rho\sigma\tau\nu}^{(m)} a_{r\rho}^\dagger a_{s\sigma}^\dagger a_{uv} a_{t\tau}, \tag{2.6}
 \end{aligned}$$

with the spatial orbitals r, s, t, u and spin indices ρ, σ, τ, ν ; the factor of $\frac{1}{2}$ is conventional (see [7], Eq. (1.4.15) and encompassing exposition). Note that indices $r, t/\rho, \tau$ refer to electron 1, indices $s, u/\sigma, \nu$ to electron 2. This translates in the case of the spin-spin operator, illustrated with one component, into: $\langle \rho\sigma | T_{+2}^{(2)} | \tau\nu \rangle = \langle \rho\sigma | s_1^{+1} s_2^{+1} | \tau\nu \rangle = \langle \rho | s_1^{+1} | \tau \rangle \cdot \langle \sigma | s_2^{+1} | \nu \rangle$. In the further evaluation, the first spin operator in a product will implicitly refer to electron one, the second to electron two, and I will therefore omit the explicit electron indices $1/2$.

Comparing an arbitrary pair of configurations, the cases that have to be distinguished with respect to a spatial occupation w, w' of ket and bra are:

- i. no excitation: $w' = w$
- ii. single excitation: $w' = a_b^\dagger a_a w$
- iii. double excitation: $w' = a_c^\dagger a_d^\dagger a_b a_a w$.

I start out from the general expression for a matrix element between two CSFs $|S', M'_S, \omega', w'\rangle, |S, M_S, \omega, w\rangle$:

$$\langle S', M'_S, \omega', w' | \mathcal{H}_{SS} | S, M_S, \omega, w \rangle = \frac{k}{2} \sum_m \sum_{rstu} \sum_{\rho\sigma\tau\nu} R_{rstu}^{(m)} S_{\rho\sigma\tau\nu}^{(m)} \langle \Upsilon' | a_{r\rho}^\dagger a_{s\sigma}^\dagger a_{uv} a_{t\tau} | \Upsilon \rangle, \tag{2.7}$$

introducing $|S', M'_S, \omega', w'\rangle \equiv |\Upsilon'\rangle$, $|S, M_S, \omega, w\rangle \equiv |\Upsilon\rangle$ for compactness.

i. $w' = w$

The CSFs $|\Upsilon\rangle$, $|\Upsilon'\rangle$ do not differ in their spatial occupation, nonvanishing contributions can therefore occur only if the combined application of creation and annihilation operators does not alter the occupation vector:

$$\langle \Upsilon' | a_r^\dagger a_s^\dagger a_u a_t | \Upsilon \rangle = \pm \langle \Upsilon' | \Upsilon \rangle \quad (2.8)$$

which is fulfilled for the two possible cases:

$$\begin{aligned} u = r & \quad \wedge \quad t = s \\ u = s & \quad \wedge \quad t = r. \end{aligned} \quad (2.9)$$

Thereby, the summation reduces to:

$$\langle \Upsilon' | \mathcal{H}_{SS} | \Upsilon \rangle = \frac{k}{2} \sum_m \sum_{r \neq s} \sum_{\rho\sigma\tau\nu} \left\{ R_{rsrs}^{(m)} S_{\rho\sigma\tau\nu}^{(m)} \langle \Upsilon' | a_{r\rho}^\dagger a_{s\sigma}^\dagger a_{s\nu} a_{r\tau} | \Upsilon \rangle + R_{rssr}^{(m)} S_{\rho\sigma\tau\nu}^{(m)} \langle \Upsilon' | a_{r\rho}^\dagger a_{s\sigma}^\dagger a_{r\nu} a_{s\tau} | \Upsilon \rangle \right\}. \quad (2.10)$$

It should be mentioned that the selection rule $r \neq s$ was already introduced at this point for clearness, the proof of it will follow in the next section (*Selection Rules*, p. 52).

ii. $w' = a_b^\dagger a_a w$

The CSFs $|\Upsilon\rangle$, $|\Upsilon'\rangle$ differ in their spatial occupation by a single excitation $a \rightarrow b$, thereby resulting in nonvanishing contributions only if:

$$\langle \Upsilon' | a_r^\dagger a_s^\dagger a_u a_t | \Upsilon \rangle = \pm \langle \Upsilon' | a_b^\dagger a_a | \Upsilon \rangle. \quad (2.11)$$

The four possible cases that have to be considered are therefore:

$$\begin{aligned} r = b, \quad u = a & \quad \wedge \quad s = t \\ r = b, \quad t = a & \quad \wedge \quad s = u \\ s = b, \quad u = a & \quad \wedge \quad r = t \\ s = b, \quad t = a & \quad \wedge \quad r = u, \end{aligned} \quad (2.12)$$

resulting in a reduction of the summation to:

$$\langle \Upsilon' | \mathcal{H}_{SS} | \Upsilon \rangle = \frac{k}{2} \sum_m \sum_{r \neq a, b} \sum_{\rho\sigma\tau\nu} \left\{ R_{brar}^{(m)} S_{\rho\sigma\tau\nu}^{(m)} \langle \Upsilon' | a_{b\rho}^\dagger a_{r\sigma}^\dagger a_{r\nu} a_{a\tau} | \Upsilon \rangle + R_{brra}^{(m)} S_{\rho\sigma\tau\nu}^{(m)} \langle \Upsilon' | a_{b\rho}^\dagger a_{r\sigma}^\dagger a_{a\nu} a_{r\tau} | \Upsilon \rangle + R_{rbar}^{(m)} S_{\rho\sigma\tau\nu}^{(m)} \langle \Upsilon' | a_{r\rho}^\dagger a_{b\sigma}^\dagger a_{r\nu} a_{a\tau} | \Upsilon \rangle + R_{rbra}^{(m)} S_{\rho\sigma\tau\nu}^{(m)} \langle \Upsilon' | a_{r\rho}^\dagger a_{b\sigma}^\dagger a_{a\nu} a_{r\tau} | \Upsilon \rangle \right\}. \quad (2.13)$$

This expression can be further simplified as it can be shown that term (1) is equivalent to term (4), and term (2) is equivalent to term (3). The proof will

be illustrated in detail for the case of term (1)–term (4). Starting out with the expression for term (1), we can rewrite:

$$\begin{aligned} & \sum_{\rho\sigma\tau\nu} \left\{ R_{brar}^{(m)} S_{\rho\sigma\tau\nu}^{(m)} \langle \Upsilon' | a_{b\rho}^\dagger a_{r\sigma}^\dagger a_{r\nu} a_{a\tau} | \Upsilon \rangle \right\} \\ &= \sum_{\rho\sigma\tau\nu} \left\{ R_{brar}^{(m)} S_{\rho\sigma\tau\nu}^{(m)} \langle \Upsilon' | a_{r\sigma}^\dagger a_{b\rho}^\dagger a_{a\tau} a_{r\nu} | \Upsilon \rangle \right\} \end{aligned} \quad (2.14)$$

$$= \sum_{\rho\sigma\tau\nu} \left\{ R_{brra}^{(m)} S_{\rho\sigma\tau\nu}^{(m)} \langle \Upsilon' | a_{r\sigma}^\dagger a_{b\rho}^\dagger a_{a\tau} a_{r\nu} | \Upsilon \rangle \right\} \quad (2.15)$$

$$= \sum_{\rho\sigma\tau\nu} \left\{ R_{brra}^{(m)} S_{\sigma\rho\nu\tau}^{(m)} \langle \Upsilon' | a_{r\rho}^\dagger a_{b\sigma}^\dagger a_{a\nu} a_{r\tau} | \Upsilon \rangle \right\}. \quad (2.16)$$

The first step consisted of an application of the anticommutation rule $\{a_{s\sigma}^\dagger, a_{t\tau}^\dagger\} = \{a_{s\sigma}, a_{t\tau}\} = 0$, in the next step the permutational symmetry in the spatial integrals: $R_{rstu} = R_{srut}$ was employed, and in the last step a relabeling of the dummy summation indices was performed. The final step of the derivation of above stated equivalence constitutes of employing the permutational symmetry in the spin indices: $S_{\rho\sigma\tau\nu} = S_{\sigma\rho\nu\tau}$. This permutational symmetry shall be illustrated for the component $\hat{T}_{+1}^{(+2)} = \frac{1}{\sqrt{2}} \{\hat{s}_i^0 \hat{s}_j^{+1} + \hat{s}_i^{+1} \hat{s}_j^0\}$ for which it translates into:

$$\begin{aligned} & \langle \rho | s_i^0 | \tau \rangle \langle \sigma | s_j^{+1} | \nu \rangle + \langle \rho | s_i^{+1} | \tau \rangle \langle \sigma | s_j^0 | \nu \rangle \\ &= \langle \sigma | s_i^0 | \nu \rangle \langle \rho | s_j^{+1} | \tau \rangle + \langle \sigma | s_i^{+1} | \nu \rangle \langle \rho | s_j^0 | \tau \rangle \end{aligned} \quad (2.17)$$

which holds upon permutation of the electron indices i, j in one of the terms. The permutational relationship in the spin indices is evidently a direct consequence of the symmetrical appearance of the electron indices in the spin terms. We can thereby perform the last step in the derivation and conclude:

$$\begin{aligned} & \sum_{\rho\sigma\tau\nu} \left\{ R_{brar}^{(m)} S_{\rho\sigma\tau\nu}^{(m)} \langle \Upsilon' | a_{b\rho}^\dagger a_{r\sigma}^\dagger a_{r\nu} a_{a\tau} | \Upsilon \rangle \right\} \\ &= \sum_{\rho\sigma\tau\nu} \left\{ R_{rbra}^{(m)} S_{\rho\sigma\tau\nu}^{(m)} \langle \Upsilon' | a_{r\rho}^\dagger a_{b\sigma}^\dagger a_{a\nu} a_{r\tau} | \Upsilon \rangle \right\}. \end{aligned} \quad (2.18)$$

Identifying the right-hand side with term (4) in Eq. (2.13), the above stated equivalence between term (1) and term (4) was therefore proved. Employing an analogous line of argument, one may show equivalently for term (2)–term (3):

$$\begin{aligned} & \sum_{\rho\sigma\tau\nu} \left\{ R_{brra}^{(m)} S_{\rho\sigma\tau\nu}^{(m)} \langle \Upsilon' | a_{b\rho}^\dagger a_{r\sigma}^\dagger a_{a\nu} a_{r\tau} | \Upsilon \rangle \right\} \\ &= \sum_{\rho\sigma\tau\nu} \left\{ R_{brra}^{(m)} S_{\rho\sigma\tau\nu}^{(m)} \langle \Upsilon' | a_{r\sigma}^\dagger a_{b\rho}^\dagger a_{r\tau} a_{a\nu} | \Upsilon \rangle \right\} \end{aligned} \quad (2.19)$$

$$= \sum_{\rho\sigma\tau\nu} \left\{ R_{rbar}^{(m)} S_{\rho\sigma\tau\nu}^{(m)} \langle \Upsilon' | a_{r\sigma}^\dagger a_{b\rho}^\dagger a_{r\tau} a_{a\nu} | \Upsilon \rangle \right\} \quad (2.20)$$

$$= \sum_{\rho\sigma\tau\nu} \left\{ R_{rbar}^{(m)} S_{\sigma\rho\nu\tau}^{(m)} \langle \Upsilon' | a_{r\rho}^\dagger a_{b\sigma}^\dagger a_{r\nu} a_{a\tau} | \Upsilon \rangle \right\} \quad (2.21)$$

$$= \sum_{\rho\sigma\tau\nu} \left\{ R_{rbar}^{(m)} S_{\rho\sigma\tau\nu}^{(m)} \langle \Upsilon' | a_{r\rho}^\dagger a_{b\sigma}^\dagger a_{r\nu} a_{a\tau} | \Upsilon \rangle \right\}. \quad (2.22)$$

We can therefore combine identical terms and reformulate Eq. (2.13) as:

$$\langle \Upsilon' | \mathcal{H}_{SS} | \Upsilon \rangle = k \sum_m \sum_{r \neq a, b} \sum_{\rho\sigma\tau\nu} \left\{ R_{brar}^{(m)} S_{\rho\sigma\tau\nu}^{(m)} \langle \Upsilon' | a_{b\rho}^\dagger a_{r\sigma}^\dagger a_{r\nu} a_{a\tau} | \Upsilon \rangle + R_{brra}^{(m)} S_{\rho\sigma\tau\nu}^{(m)} \langle \Upsilon' | a_{b\rho}^\dagger a_{r\sigma}^\dagger a_{a\nu} a_{r\tau} | \Upsilon \rangle \right\}. \quad (2.23)$$

Again, it should be mentioned that the indicated selection rule ($r \neq a, b$) will be proved in the following section *Selection Rules* (p. 52).

iii. $w' = a_c^\dagger a_d^\dagger a_b a_a w$

The CSFs $|\Upsilon\rangle$, $|\Upsilon'\rangle$ differ in their spatial occupation by a double excitation $a, b \rightarrow c, d$. Nonvanishing contributions in the summation do therefore only result if the indices t, u of the annihilation operators are identified with a, b while at the same time the indices r, s of the creation operators have to agree with c, d . This restricts the possible cases to the following permutations:

$$\begin{aligned} r = c, \quad s = d, \quad u = a, \quad t = b \\ r = c, \quad s = d, \quad u = b, \quad t = a \\ r = d, \quad s = c, \quad u = a, \quad t = b \\ r = d, \quad s = c, \quad u = b, \quad t = a, \end{aligned} \quad (2.24)$$

thereby yielding for the matrix element expression:

$$\begin{aligned} \langle \Upsilon' | \mathcal{H}_{SS} | \Upsilon \rangle = \frac{k}{2} \sum_m \sum_{\rho\sigma\tau\nu} \left\{ R_{cdba}^{(m)} S_{\rho\sigma\tau\nu}^{(m)} \langle \Upsilon' | a_{c\rho}^\dagger a_{d\sigma}^\dagger a_{a\nu} a_{b\tau} | \Upsilon \rangle \right. \\ + R_{cdab}^{(m)} S_{\rho\sigma\tau\nu}^{(m)} \langle \Upsilon' | a_{c\rho}^\dagger a_{d\sigma}^\dagger a_{b\nu} a_{a\tau} | \Upsilon \rangle \\ + R_{dcba}^{(m)} S_{\rho\sigma\tau\nu}^{(m)} \langle \Upsilon' | a_{d\rho}^\dagger a_{c\sigma}^\dagger a_{a\nu} a_{b\tau} | \Upsilon \rangle \\ \left. + R_{dcab}^{(m)} S_{\rho\sigma\tau\nu}^{(m)} \langle \Upsilon' | a_{d\rho}^\dagger a_{c\sigma}^\dagger a_{b\nu} a_{a\tau} | \Upsilon \rangle \right\}. \end{aligned} \quad (2.25)$$

Employing an analogous line of argument as in (ii.), we can establish equivalence of term (1)–term (4):

$$\begin{aligned} & \sum_{\rho\sigma\tau\nu} \left\{ R_{cdba}^{(m)} S_{\rho\sigma\tau\nu}^{(m)} \langle \Upsilon' | a_{c\rho}^\dagger a_{d\sigma}^\dagger a_{a\nu} a_{b\tau} | \Upsilon \rangle \right\} \\ = & \sum_{\rho\sigma\tau\nu} \left\{ R_{dcab}^{(m)} S_{\rho\sigma\tau\nu}^{(m)} \langle \Upsilon' | a_{d\sigma}^\dagger a_{c\rho}^\dagger a_{b\tau} a_{a\nu} | \Upsilon \rangle \right\} \end{aligned} \quad (2.26)$$

$$= \sum_{\rho\sigma\tau\nu} \left\{ R_{dcab}^{(m)} S_{\rho\sigma\tau\nu}^{(m)} \langle \Upsilon' | a_{d\rho}^\dagger a_{c\sigma}^\dagger a_{b\nu} a_{a\tau} | \Upsilon \rangle \right\} \quad (2.27)$$

and term (2)–term (3):

$$\begin{aligned} & \sum_{\rho\sigma\tau\nu} \left\{ R_{cdab}^{(m)} S_{\rho\sigma\tau\nu}^{(m)} \langle \Upsilon' | a_{c\rho}^\dagger a_{d\sigma}^\dagger a_{b\nu} a_{a\tau} | \Upsilon \rangle \right\} \\ &= \sum_{\rho\sigma\tau\nu} \left\{ R_{dcba}^{(m)} S_{\rho\sigma\tau\nu}^{(m)} \langle \Upsilon' | a_{d\sigma}^\dagger a_{c\rho}^\dagger a_{a\tau} a_{b\nu} | \Upsilon \rangle \right\} \end{aligned} \quad (2.28)$$

$$= \sum_{\rho\sigma\tau\nu} \left\{ R_{dcba}^{(m)} S_{\rho\sigma\tau\nu}^{(m)} \langle \Upsilon' | a_{d\rho}^\dagger a_{c\sigma}^\dagger a_{a\nu} a_{b\tau} | \Upsilon \rangle \right\}, \quad (2.29)$$

thereby leading to the simpler expression:

$$\begin{aligned} \langle \Upsilon' | \mathcal{H}_{SS} | \Upsilon \rangle &= k \sum_m \sum_{\rho\sigma\tau\nu} \left\{ R_{cdba}^{(m)} S_{\rho\sigma\tau\nu}^{(m)} \langle \Upsilon' | a_{c\rho}^\dagger a_{d\sigma}^\dagger a_{a\nu} a_{b\tau} | \Upsilon \rangle \right. \\ &\quad \left. + R_{cdab}^{(m)} S_{\rho\sigma\tau\nu}^{(m)} \langle \Upsilon' | a_{c\rho}^\dagger a_{d\sigma}^\dagger a_{b\nu} a_{a\tau} | \Upsilon \rangle \right\}. \end{aligned} \quad (2.30)$$

At this point, we have introduced in Eqs. (2.10)/(2.23)/(2.30) formulas for the three types of nonvanishing excitations in the calculation of spin-spin coupling. This constitutes our starting point for the introduction of further relevant relationships, and, following from there, the derivation of the concrete terms implemented in SPOCK.SISTR.

2.2.2 Derivation – Part (I)

Selection Rules

As already partly indicated in Eqs. (2.10)–(2.30), the cases obey the following selection rules:

- i. $w' = w$: $r \neq s$, see Eq. (2.10)
- ii. $w' = a_b^\dagger a_a w$: $a \neq r$, $b \neq r$, see Eq. (2.23)
- iii. $w' = a_c^\dagger a_d^\dagger a_b a_a w$: $a \neq b$, $c \neq d$

These selection rules are an application of the more general statement that nonvanishing contributions for a term $\sum_{\rho\sigma\tau\nu} R_{rstu}^{(m)} S_{\rho\sigma\tau\nu}^{(m)} \langle \Upsilon' | a_{r\rho}^\dagger a_{s\sigma}^\dagger a_{u\nu} a_{t\tau} | \Upsilon \rangle$ occur solely for $r \neq s$, $u \neq t$. The proof consisting of two parts follows.

- (I). Assume $u = t$. We therefore operate in succession with two annihilation operators, both of which refer to an identical spatial orbital, onto an occupation vector and can formulate this as the general case: $a_{j\rho} a_{j\sigma} | \Upsilon \rangle$. A nonvanishing contribution can only result if $\rho \neq \sigma$ and the occupation vector contains both j_α , j_β . The restriction on the spin states limits the possible nonvanishing contributions for the individual spin tensor components $\hat{T}_i^{(2)}$ to:

$$\begin{aligned} \hat{T}_{+2}^{(2)} &: \text{no contribution} \\ \hat{T}_{+1}^{(2)} &: R_{rstt}^{(m)} \frac{1}{\sqrt{2}} \langle \alpha | s^0 | \alpha \rangle \langle \alpha | s^{+1} | \beta \rangle \langle \Upsilon' | a_{r\alpha}^\dagger a_{s\alpha}^\dagger a_{t\beta} a_{t\alpha} | \Upsilon \rangle \end{aligned}$$

$$+ R_{rstt}^{(m)} \frac{1}{\sqrt{2}} \langle \alpha | s^{+1} | \beta \rangle \langle \alpha | s^0 | \alpha \rangle \langle \Upsilon' | a_{r\alpha}^\dagger a_{s\alpha}^\dagger a_{t\alpha} a_{t\beta} | \Upsilon \rangle \quad (2.31)$$

$$= R_{rstt}^{(m)} \frac{1}{4} \left\{ -\langle \Upsilon' | a_{r\alpha}^\dagger a_{s\alpha}^\dagger a_{t\beta} a_{t\alpha} | \Upsilon \rangle - \langle \Upsilon' | a_{r\alpha}^\dagger a_{s\alpha}^\dagger a_{t\alpha} a_{t\beta} | \Upsilon \rangle \right\} \quad (2.32)$$

$$= R_{rstt}^{(m)} \frac{1}{4} \left\{ -\langle \Upsilon' | a_{r\alpha}^\dagger a_{s\alpha}^\dagger a_{t\beta} a_{t\alpha} | \Upsilon \rangle + \langle \Upsilon' | a_{r\alpha}^\dagger a_{s\alpha}^\dagger a_{t\beta} a_{t\alpha} | \Upsilon \rangle \right\} \quad (2.33)$$

$$= 0$$

$$\hat{T}_0^{(2)} : R_{rstt}^{(m)} \frac{1}{\sqrt{6}} \left\{ 2 \langle \alpha | s^0 | \alpha \rangle \langle \beta | s^0 | \beta \rangle \langle \Upsilon' | a_{r\alpha}^\dagger a_{s\beta}^\dagger a_{t\beta} a_{t\alpha} | \Upsilon \rangle \right. \\ \left. + 2 \langle \beta | s^0 | \beta \rangle \langle \alpha | s^0 | \alpha \rangle \langle \Upsilon' | a_{r\beta}^\dagger a_{s\alpha}^\dagger a_{t\alpha} a_{t\beta} | \Upsilon \rangle \right. \\ \left. + \langle \beta | s^{-1} | \alpha \rangle \langle \alpha | s^{+1} | \beta \rangle \langle \Upsilon' | a_{r\beta}^\dagger a_{s\alpha}^\dagger a_{t\beta} a_{t\alpha} | \Upsilon \rangle \right. \\ \left. + \langle \alpha | s^{+1} | \beta \rangle \langle \beta | s^{-1} | \alpha \rangle \langle \Upsilon' | a_{r\alpha}^\dagger a_{s\beta}^\dagger a_{t\alpha} a_{t\beta} | \Upsilon \rangle \right\} \quad (2.34)$$

$$= R_{rstt}^{(m)} \frac{1}{\sqrt{6}} \left\{ -\frac{1}{2} \langle \Upsilon' | a_{r\alpha}^\dagger a_{s\beta}^\dagger a_{t\beta} a_{t\alpha} | \Upsilon \rangle - \frac{1}{2} \langle \Upsilon' | a_{r\beta}^\dagger a_{s\alpha}^\dagger a_{t\alpha} a_{t\beta} | \Upsilon \rangle \right. \\ \left. - \frac{1}{2} \langle \Upsilon' | a_{r\beta}^\dagger a_{s\alpha}^\dagger a_{t\beta} a_{t\alpha} | \Upsilon \rangle - \frac{1}{2} \langle \Upsilon' | a_{r\alpha}^\dagger a_{s\beta}^\dagger a_{t\alpha} a_{t\beta} | \Upsilon \rangle \right\} \quad (2.35)$$

$$= R_{rstt}^{(m)} \frac{1}{2\sqrt{6}} \left\{ \langle \Upsilon' | a_{r\alpha}^\dagger a_{s\beta}^\dagger a_{t\alpha} a_{t\beta} | \Upsilon \rangle + \langle \Upsilon' | a_{r\beta}^\dagger a_{s\alpha}^\dagger a_{t\beta} a_{t\alpha} | \Upsilon \rangle \right. \\ \left. - \langle \Upsilon' | a_{r\beta}^\dagger a_{s\alpha}^\dagger a_{t\beta} a_{t\alpha} | \Upsilon \rangle - \langle \Upsilon' | a_{r\alpha}^\dagger a_{s\beta}^\dagger a_{t\alpha} a_{t\beta} | \Upsilon \rangle \right\} \quad (2.36)$$

$$= 0$$

$$\hat{T}_{-1}^{(2)} : R_{rstt}^{(m)} \frac{1}{\sqrt{2}} \langle \beta | s^0 | \beta \rangle \langle \beta | s^{-1} | \alpha \rangle \langle \Upsilon' | a_{r\beta}^\dagger a_{s\beta}^\dagger a_{t\alpha} a_{t\beta} | \Upsilon \rangle \\ + R_{rstt}^{(m)} \frac{1}{\sqrt{2}} \langle \beta | s^{-1} | \alpha \rangle \langle \beta | s^0 | \beta \rangle \langle \Upsilon' | a_{r\beta}^\dagger a_{s\beta}^\dagger a_{t\beta} a_{t\alpha} | \Upsilon \rangle \quad (2.37)$$

$$= R_{rstt}^{(m)} \frac{1}{4} \left\{ -\langle \Upsilon' | a_{r\beta}^\dagger a_{s\beta}^\dagger a_{t\alpha} a_{t\beta} | \Upsilon \rangle - \langle \Upsilon' | a_{r\beta}^\dagger a_{s\beta}^\dagger a_{t\beta} a_{t\alpha} | \Upsilon \rangle \right\} \quad (2.38)$$

$$= R_{rstt}^{(m)} \frac{1}{4} \left\{ -\langle \Upsilon' | a_{r\beta}^\dagger a_{s\beta}^\dagger a_{t\alpha} a_{t\beta} | \Upsilon \rangle + \langle \Upsilon' | a_{r\beta}^\dagger a_{s\beta}^\dagger a_{t\alpha} a_{t\beta} | \Upsilon \rangle \right\} \quad (2.39)$$

$$= 0$$

$$\hat{T}_{-2}^{(2)} : \text{no contribution.}$$

The individual reformulations consisted of applications of the anticommutation relation between annihilation operators, to be precise employing $a_{r\alpha} a_{r\beta} | \Upsilon \rangle = -a_{r\beta} a_{r\alpha} | \Upsilon \rangle$.

The proof regarding the selection rule $r \neq s$ is performed analogously as follows.

- (II). Assume $r = s$. We operate now with two creation operators with reference to an identical spatial orbital onto an occupation vector and consider thereby the general case: $a_{j\rho}^\dagger a_{j\sigma}^\dagger | \Upsilon \rangle$. Therefore, orbital j has to be vacant in the occupation vector and again $\rho \neq \sigma$. Examining now individual spin tensor components yields under the restriction in spin values:

$$\hat{T}_{+2}^{(2)} : \text{no contribution}$$

$$\begin{aligned} \hat{T}_{+1}^{(2)} : R_{sstu}^{(m)} \frac{1}{\sqrt{2}} \langle \beta | s^0 | \beta \rangle \langle \alpha | s^{+1} | \beta \rangle \langle \Upsilon' | a_{s\beta}^\dagger a_{s\alpha}^\dagger a_{u\beta} a_{t\beta} | \Upsilon \rangle \\ + R_{sstu}^{(m)} \frac{1}{\sqrt{2}} \langle \alpha | s^{+1} | \beta \rangle \langle \beta | s^0 | \beta \rangle \langle \Upsilon' | a_{s\alpha}^\dagger a_{s\beta}^\dagger a_{u\beta} a_{t\beta} | \Upsilon \rangle \end{aligned} \quad (2.40)$$

$$\begin{aligned} &= R_{sstu}^{(m)} \frac{1}{4} \{ \langle \Upsilon' | a_{s\beta}^\dagger a_{s\alpha}^\dagger a_{u\beta} a_{t\beta} | \Upsilon \rangle + \langle \Upsilon' | a_{s\alpha}^\dagger a_{s\beta}^\dagger a_{u\beta} a_{t\beta} | \Upsilon \rangle \} \\ &= 0 \end{aligned} \quad (2.41)$$

$$\begin{aligned} \hat{T}_0^{(2)} : R_{sstu}^{(m)} \frac{1}{\sqrt{6}} \{ 2 \langle \alpha | s^0 | \alpha \rangle \langle \beta | s^0 | \beta \rangle \langle \Upsilon' | a_{s\alpha}^\dagger a_{s\beta}^\dagger a_{u\beta} a_{t\alpha} | \Upsilon \rangle \\ + 2 \langle \beta | s^0 | \beta \rangle \langle \alpha | s^0 | \alpha \rangle \langle \Upsilon' | a_{s\beta}^\dagger a_{s\alpha}^\dagger a_{u\alpha} a_{t\beta} | \Upsilon \rangle \\ + \langle \beta | s^{-1} | \alpha \rangle \langle \alpha | s^{+1} | \beta \rangle \langle \Upsilon' | a_{s\beta}^\dagger a_{s\alpha}^\dagger a_{u\beta} a_{t\alpha} | \Upsilon \rangle \\ + \langle \alpha | s^{+1} | \beta \rangle \langle \beta | s^{-1} | \alpha \rangle \langle \Upsilon' | a_{s\alpha}^\dagger a_{s\beta}^\dagger a_{u\alpha} a_{t\beta} | \Upsilon \rangle \} \end{aligned} \quad (2.42)$$

$$\begin{aligned} &= R_{sstu}^{(m)} \frac{1}{2\sqrt{6}} \{ \langle \Upsilon' | a_{s\alpha}^\dagger a_{s\beta}^\dagger a_{u\alpha} a_{t\beta} | \Upsilon \rangle + \langle \Upsilon' | a_{s\beta}^\dagger a_{s\alpha}^\dagger a_{u\beta} a_{t\alpha} | \Upsilon \rangle \\ &\quad - \langle \Upsilon' | a_{s\beta}^\dagger a_{s\alpha}^\dagger a_{u\beta} a_{t\alpha} | \Upsilon \rangle - \langle \Upsilon' | a_{s\alpha}^\dagger a_{s\beta}^\dagger a_{u\alpha} a_{t\beta} | \Upsilon \rangle \} \\ &= 0 \end{aligned} \quad (2.43)$$

$$\begin{aligned} \hat{T}_{-1}^{(2)} : R_{sstu}^{(m)} \frac{1}{\sqrt{2}} \langle \alpha | s^0 | \alpha \rangle \langle \beta | s^{-1} | \alpha \rangle \langle \Upsilon' | a_{s\alpha}^\dagger a_{s\beta}^\dagger a_{u\alpha} a_{t\alpha} | \Upsilon \rangle \\ + R_{sstu}^{(m)} \frac{1}{\sqrt{2}} \langle \beta | s^{-1} | \alpha \rangle \langle \alpha | s^0 | \alpha \rangle \langle \Upsilon' | a_{s\beta}^\dagger a_{s\alpha}^\dagger a_{u\alpha} a_{t\alpha} | \Upsilon \rangle \end{aligned} \quad (2.44)$$

$$\begin{aligned} &= R_{sstu}^{(m)} \frac{1}{4} \{ \langle \Upsilon' | a_{s\alpha}^\dagger a_{s\beta}^\dagger a_{u\alpha} a_{t\alpha} | \Upsilon \rangle + \langle \Upsilon' | a_{s\beta}^\dagger a_{s\alpha}^\dagger a_{u\alpha} a_{t\alpha} | \Upsilon \rangle \} \\ &= 0 \end{aligned} \quad (2.45)$$

$$\hat{T}_{-2}^{(2)} : \text{no contribution.}$$

We have thereby proved in general that the contributions from terms vanish in which either the indices of the creation operators and/or the indices of the annihilation operators coincide. We can therefore exclude from our calculation terms with identical indices in the creation operators and identical indices in the annihilation operators. Returning to the three cases of excitation upon consideration, we can from inspection of the matrix element expressions (Eqs. (2.10)/(2.23)/(2.30)) identify operator indices and establish our selection rules:

- i. $w' = w$
Terms: $\langle \Upsilon' | a_{r\rho}^\dagger a_{s\sigma}^\dagger a_{sv} a_{r\tau} | \Upsilon \rangle / \langle \Upsilon' | a_{r\rho}^\dagger a_{s\sigma}^\dagger a_{rv} a_{s\tau} | \Upsilon \rangle$
Selection rule: $r \neq s$
- ii. $w' = a_b^\dagger a_a w$
Terms: $\langle \Upsilon' | a_{b\rho}^\dagger a_{r\sigma}^\dagger a_{rv} a_{a\tau} | \Upsilon \rangle / \langle \Upsilon' | a_{b\rho}^\dagger a_{r\sigma}^\dagger a_{av} a_{r\tau} | \Upsilon \rangle$
Selection rule: $a \neq r, b \neq r$
- iii. $w' = a_c^\dagger a_d^\dagger a_b a_a w$
Terms: $\langle \Upsilon' | a_{c\rho}^\dagger a_{d\sigma}^\dagger a_{av} a_{b\tau} | \Upsilon \rangle / \langle \Upsilon' | a_{c\rho}^\dagger a_{d\sigma}^\dagger a_{bv} a_{a\tau} | \Upsilon \rangle$
Selection rule: $a \neq b, c \neq d$.

Contribution of Closed Shells

Contrary to the spin-free Coulomb operator, the summation does not involve closed shells in the case of the spin-spin operator. This can be shown in general, considering the three possible excitations solely as special cases, as follows: Assume that the summation index r refers to a closed shell while indices i/j refer to the creation/annihilation of an electron in an arbitrary orbital i/j without further restriction. The possible permutations of $i/j/r$ in the indices of creation/annihilation operators can be reduced to two distinct cases which I treat individually:

$$(I). \sum_{\rho\sigma\tau\nu} R_{irrj}^{(m)} S_{\rho\sigma\tau\nu}^{(m)} \langle \Upsilon' | a_{i\rho}^\dagger a_{r\sigma}^\dagger a_{j\nu} a_{r\tau} | \Upsilon \rangle$$

$$(II). \sum_{\rho\sigma\tau\nu} R_{irjr}^{(m)} S_{\rho\sigma\tau\nu}^{(m)} \langle \Upsilon' | a_{i\rho}^\dagger a_{r\sigma}^\dagger a_{r\nu} a_{j\tau} | \Upsilon \rangle .$$

From the derivations in the previous section, we know furthermore that $i \neq r$, $j \neq r$. Therefore, the creation and annihilation in the doubly occupied orbital r has to refer to identical spin indices: $a_{r\sigma}^\dagger a_{r\nu} | r_\alpha r_\beta \rangle = \delta_{\sigma\nu} | r_\alpha r_\beta \rangle$. The summation in ρ, σ, τ, ν thereby reduces to:

$$(I). R_{irrj}^{(m)} S_{\rho\alpha\nu}^{(m)} \langle \Upsilon' | a_{i\rho}^\dagger a_{r\alpha}^\dagger a_{j\nu} a_{r\alpha} | \Upsilon \rangle + R_{irrj}^{(m)} S_{\rho\beta\nu}^{(m)} \langle \Upsilon' | a_{i\rho}^\dagger a_{r\beta}^\dagger a_{j\nu} a_{r\beta} | \Upsilon \rangle$$

$$(II). R_{irjr}^{(m)} S_{\rho\alpha\tau\alpha}^{(m)} \langle \Upsilon' | a_{i\rho}^\dagger a_{r\alpha}^\dagger a_{r\alpha} a_{j\tau} | \Upsilon \rangle + R_{irjr}^{(m)} S_{\rho\beta\tau\beta}^{(m)} \langle \Upsilon' | a_{i\rho}^\dagger a_{r\beta}^\dagger a_{r\beta} a_{j\tau} | \Upsilon \rangle .$$

Having established the nonvanishing terms for a summation over closed shells r , I turn now to the specific tensor components $\hat{T}_i^{(2)}$ and examine the contributions originating from each component individually.

(I). considering spin terms $\langle \rho | s | \alpha \rangle \langle \alpha | s | \nu \rangle / \langle \rho | s | \beta \rangle \langle \beta | s | \nu \rangle$

$$\hat{T}_{+2}^{(2)} : \text{no contribution}$$

$$\hat{T}_{+1}^{(2)} : R_{irrj}^{(m)} \frac{1}{\sqrt{2}} \langle \alpha | s^0 | \alpha \rangle \langle \alpha | s^{+1} | \beta \rangle \langle \Upsilon' | a_{i\alpha}^\dagger a_{r\alpha}^\dagger a_{j\beta} a_{r\alpha} | \Upsilon \rangle$$

$$+ R_{irrj}^{(m)} \frac{1}{\sqrt{2}} \langle \alpha | s^{+1} | \beta \rangle \langle \beta | s^0 | \beta \rangle \langle \Upsilon' | a_{i\alpha}^\dagger a_{r\beta}^\dagger a_{j\beta} a_{r\beta} | \Upsilon \rangle \quad (2.46)$$

$$= R_{irrj}^{(m)} \left\{ -\frac{1}{4} \langle \Upsilon' | a_{i\alpha}^\dagger a_{j\beta} | \Upsilon \rangle + \frac{1}{4} \langle \Upsilon' | a_{i\alpha}^\dagger a_{j\beta} | \Upsilon \rangle \right\} \quad (2.47)$$

$$= 0$$

$$\hat{T}_0^{(2)} : R_{irrj}^{(m)} \frac{1}{\sqrt{6}} \left\{ 2 \langle \alpha | s^0 | \alpha \rangle \langle \alpha | s^0 | \alpha \rangle \langle \Upsilon' | a_{i\alpha}^\dagger a_{r\alpha}^\dagger a_{j\alpha} a_{r\alpha} | \Upsilon \rangle \right.$$

$$\left. + \langle \beta | s^{-1} | \alpha \rangle \langle \alpha | s^{+1} | \beta \rangle \langle \Upsilon' | a_{i\beta}^\dagger a_{r\alpha}^\dagger a_{j\beta} a_{r\alpha} | \Upsilon \rangle \right\}$$

$$+ R_{irrj}^{(m)} \frac{1}{\sqrt{6}} \left\{ 2 \langle \beta | s^0 | \beta \rangle \langle \beta | s^0 | \beta \rangle \langle \Upsilon' | a_{i\beta}^\dagger a_{r\beta}^\dagger a_{j\beta} a_{r\beta} | \Upsilon \rangle \right.$$

$$\left. + \langle \alpha | s^{+1} | \beta \rangle \langle \beta | s^{-1} | \alpha \rangle \langle \Upsilon' | a_{i\alpha}^\dagger a_{r\beta}^\dagger a_{j\alpha} a_{r\beta} | \Upsilon \rangle \right\} \quad (2.48)$$

$$= R_{irrj}^{(m)} \frac{1}{\sqrt{6}} \left\{ \frac{1}{2} \langle \Upsilon' | a_{i\alpha}^\dagger a_{j\alpha} | \Upsilon \rangle - \frac{1}{2} \langle \Upsilon' | a_{i\beta}^\dagger a_{j\beta} | \Upsilon \rangle \right\}$$

$$+ \frac{1}{2} \langle \Upsilon' | a_{i\beta}^\dagger a_{j\beta} | \Upsilon \rangle - \frac{1}{2} \langle \Upsilon' | a_{i\alpha}^\dagger a_{j\alpha} | \Upsilon \rangle \} \quad (2.49)$$

$$= 0$$

$$\begin{aligned} \hat{T}_{-1}^{(2)} : & R_{irrj}^{(m)} \frac{1}{\sqrt{2}} \langle \beta | s^{-1} | \alpha \rangle \langle \alpha | s^0 | \alpha \rangle \langle \Upsilon' | a_{i\beta}^\dagger a_{r\alpha}^\dagger a_{j\alpha} a_{r\alpha} | \Upsilon \rangle \\ & + R_{irrj}^{(m)} \frac{1}{\sqrt{2}} \langle \beta | s^0 | \beta \rangle \langle \beta | s^{-1} | \alpha \rangle \langle \Upsilon' | a_{i\beta}^\dagger a_{r\beta}^\dagger a_{j\alpha} a_{r\beta} | \Upsilon \rangle \end{aligned} \quad (2.50)$$

$$= R_{irrj}^{(m)} \left\{ \frac{1}{4} \langle \Upsilon' | a_{i\beta}^\dagger a_{j\alpha} | \Upsilon \rangle - \frac{1}{4} \langle \Upsilon' | a_{i\beta}^\dagger a_{j\alpha} | \Upsilon \rangle \right\} \quad (2.51)$$

$$= 0$$

$$\hat{T}_{-2}^{(2)} : \text{no contribution}$$

(II). considering spin terms $\langle \rho | s | \tau \rangle \langle \alpha | s | \alpha \rangle / \langle \rho | s | \tau \rangle \langle \beta | s | \beta \rangle$

$$\hat{T}_{+2}^{(2)} : \text{no contribution}$$

$$\begin{aligned} \hat{T}_{+1}^{(2)} : & R_{irjr}^{(m)} \frac{1}{\sqrt{2}} \langle \alpha | s^{+1} | \beta \rangle \langle \alpha | s^0 | \alpha \rangle \langle \Upsilon' | a_{i\alpha}^\dagger a_{r\alpha}^\dagger a_{r\alpha} a_{j\beta} | \Upsilon \rangle \\ & + R_{irjr}^{(m)} \frac{1}{\sqrt{2}} \langle \alpha | s^{+1} | \beta \rangle \langle \beta | s^0 | \beta \rangle \langle \Upsilon' | a_{i\alpha}^\dagger a_{r\beta}^\dagger a_{r\beta} a_{j\beta} | \Upsilon \rangle \end{aligned} \quad (2.52)$$

$$= R_{irjr}^{(m)} \left\{ -\frac{1}{4} \langle \Upsilon' | a_{i\alpha}^\dagger a_{j\beta} | \Upsilon \rangle + \frac{1}{4} \langle \Upsilon' | a_{i\alpha}^\dagger a_{j\beta} | \Upsilon \rangle \right\} \quad (2.53)$$

$$= 0$$

$$\begin{aligned} \hat{T}_0^{(2)} : & R_{irjr}^{(m)} \frac{1}{\sqrt{6}} \left\{ 2 \langle \alpha | s^0 | \alpha \rangle \langle \alpha | s^0 | \alpha \rangle \langle \Upsilon' | a_{i\alpha}^\dagger a_{r\alpha}^\dagger a_{r\alpha} a_{j\alpha} | \Upsilon \rangle \right. \\ & \quad \left. + 2 \langle \beta | s^0 | \beta \rangle \langle \alpha | s^0 | \alpha \rangle \langle \Upsilon' | a_{i\beta}^\dagger a_{r\alpha}^\dagger a_{r\alpha} a_{j\beta} | \Upsilon \rangle \right\} \\ & + R_{irjr}^{(m)} \frac{1}{\sqrt{6}} \left\{ 2 \langle \alpha | s^0 | \alpha \rangle \langle \beta | s^0 | \beta \rangle \langle \Upsilon' | a_{i\alpha}^\dagger a_{r\beta}^\dagger a_{r\beta} a_{j\alpha} | \Upsilon \rangle \right. \\ & \quad \left. + 2 \langle \beta | s^0 | \beta \rangle \langle \beta | s^0 | \beta \rangle \langle \Upsilon' | a_{i\beta}^\dagger a_{r\beta}^\dagger a_{r\beta} a_{j\beta} | \Upsilon \rangle \right\} \end{aligned} \quad (2.54)$$

$$= R_{irjr}^{(m)} \frac{1}{\sqrt{6}} \left\{ \frac{1}{2} \langle \Upsilon' | a_{i\alpha}^\dagger a_{j\alpha} | \Upsilon \rangle - \frac{1}{2} \langle \Upsilon' | a_{i\beta}^\dagger a_{j\beta} | \Upsilon \rangle \right. \\ \left. - \frac{1}{2} \langle \Upsilon' | a_{i\alpha}^\dagger a_{j\alpha} | \Upsilon \rangle + \frac{1}{2} \langle \Upsilon' | a_{i\beta}^\dagger a_{j\beta} | \Upsilon \rangle \right\} \quad (2.55)$$

$$= 0$$

$$\begin{aligned} \hat{T}_{-1}^{(2)} : & R_{irjr}^{(m)} \frac{1}{\sqrt{2}} \langle \beta | s^{-1} | \alpha \rangle \langle \alpha | s^0 | \alpha \rangle \langle \Upsilon' | a_{i\beta}^\dagger a_{r\alpha}^\dagger a_{r\alpha} a_{j\alpha} | \Upsilon \rangle \\ & + R_{irjr}^{(m)} \frac{1}{\sqrt{2}} \langle \beta | s^{-1} | \alpha \rangle \langle \beta | s^0 | \beta \rangle \langle \Upsilon' | a_{i\beta}^\dagger a_{r\beta}^\dagger a_{r\beta} a_{j\alpha} | \Upsilon \rangle \end{aligned} \quad (2.56)$$

$$= R_{irjr}^{(m)} \left\{ \frac{1}{4} \langle \Upsilon' | a_{i\alpha}^\dagger a_{j\beta} | \Upsilon \rangle - \frac{1}{4} \langle \Upsilon' | a_{i\alpha}^\dagger a_{j\beta} | \Upsilon \rangle \right\} \quad (2.57)$$

$$= 0$$

$$\hat{T}_{-2}^{(2)} : \text{no contribution.}$$

I have established now that shells which are doubly occupied in bra as well as ket do not contribute to spin-spin coupling. Therefore, only shells singly or variably occupied have to be considered in calculations, a fact which is well-known in the evaluation of zero-field splitting. The obvious consequence is a saving in the computational cost, a further consequence which is usually not reflected on is the strong dependence of the magnitude of spin-spin coupling on the description of open-shell occupation. Since closed shells do not enter the expression, there is no “weighting” effect associated with the occupation of closed shells which in turn renders a reliable open shell treatment to be of crucial relevance. This point will be illustrated with the example of O_2 in the context of application calculations (Ch. 3.1).

Permutational Relation

A further permutational relation which is employed in my subsequent derivation and should therefore be proved here is:

$$\sum_{\rho\sigma\tau\nu} S_{\rho\sigma\tau\nu}^{(m)} \langle \Upsilon' | a_{r\rho}^\dagger a_{s\sigma}^\dagger a_{uv} a_{t\tau} | \Upsilon \rangle = \sum_{\rho\sigma\tau\nu} S_{\rho\sigma\tau\nu}^{(m)} \langle \Upsilon' | a_{r\rho}^\dagger a_{s\sigma}^\dagger a_{u\tau} a_{tv} | \Upsilon \rangle, \quad (2.58)$$

or, equivalently:

$$\sum_{\rho\sigma\tau\nu} S_{\rho\sigma\tau\nu}^{(m)} \langle \Upsilon' | a_{r\rho}^\dagger a_{s\sigma}^\dagger a_{uv} a_{t\tau} | \Upsilon \rangle = \sum_{\rho\sigma\nu\tau} S_{\rho\sigma\nu\tau}^{(m)} \langle \Upsilon' | a_{r\rho}^\dagger a_{s\sigma}^\dagger a_{uv} a_{t\tau} | \Upsilon \rangle. \quad (2.59)$$

I stress at this point that this entails a permutational symmetry between one index of electron 1 and electron 2, namely: $\langle \rho | s | \tau \rangle \langle \sigma | s | \nu \rangle \rightarrow \langle \rho | s | \nu \rangle \langle \sigma | s | \tau \rangle$. This permutational symmetry is a consequence of the full summation over spin indices in combination with the symmetrical structure of the tensor components and the symmetry in electron indices. It may be shown for the individual tensor components straightforwardly:

$$\hat{T}_{+2}^{(2)}$$

The only nonvanishing spin term is: $\langle \alpha | s^{+1} | \beta \rangle \langle \alpha | s^{+1} | \beta \rangle$. The permutational symmetry in the second index is therefore trivial.

$$\hat{T}_{+1}^{(2)}$$

It has to be shown that:

$$\begin{aligned} & \sum_{\rho\sigma\tau\nu} \{ \langle \rho | s^{+1} | \tau \rangle \langle \sigma | s^0 | \nu \rangle + \langle \rho | s^0 | \tau \rangle \langle \sigma | s^{+1} | \nu \rangle \} \langle \Upsilon' | a_{r\rho}^\dagger a_{s\sigma}^\dagger a_{uv} a_{t\tau} | \Upsilon \rangle \\ &= \sum_{\rho\sigma\tau\nu} \{ \langle \rho | s^{+1} | \tau \rangle \langle \sigma | s^0 | \nu \rangle + \langle \rho | s^0 | \tau \rangle \langle \sigma | s^{+1} | \nu \rangle \} \langle \Upsilon' | a_{r\rho}^\dagger a_{s\sigma}^\dagger a_{u\tau} a_{tv} | \Upsilon \rangle. \end{aligned} \quad (2.60)$$

Considering nonvanishing terms in the spin summation, we obtain for the left-hand side:

$$\sum_{\rho\sigma\tau\nu} \{ \langle \rho | s^{+1} | \tau \rangle \langle \sigma | s^0 | \nu \rangle + \langle \rho | s^0 | \tau \rangle \langle \sigma | s^{+1} | \nu \rangle \} \langle \Upsilon' | a_{r\rho}^\dagger a_{s\sigma}^\dagger a_{uv} a_{t\tau} | \Upsilon \rangle$$

$$\begin{aligned}
&= \langle \alpha | s^{+1} | \beta \rangle \langle \alpha | s^0 | \alpha \rangle \langle \Upsilon' | a_{r\alpha}^\dagger a_{s\alpha}^\dagger a_{u\alpha} a_{t\beta} | \Upsilon \rangle \\
&\quad + \langle \alpha | s^{+1} | \beta \rangle \langle \beta | s^0 | \beta \rangle \langle \Upsilon' | a_{r\alpha}^\dagger a_{s\beta}^\dagger a_{u\beta} a_{t\beta} | \Upsilon \rangle \\
&\quad + \langle \alpha | s^0 | \alpha \rangle \langle \alpha | s^{+1} | \beta \rangle \langle \Upsilon' | a_{r\alpha}^\dagger a_{s\alpha}^\dagger a_{u\beta} a_{t\alpha} | \Upsilon \rangle \\
&\quad + \langle \beta | s^0 | \beta \rangle \langle \alpha | s^{+1} | \beta \rangle \langle \Upsilon' | a_{r\beta}^\dagger a_{s\alpha}^\dagger a_{u\beta} a_{t\beta} | \Upsilon \rangle.
\end{aligned} \tag{2.61}$$

The right-hand side reduces to:

$$\begin{aligned}
&\sum_{\rho\sigma\tau\nu} \{ \langle \rho | s^{+1} | \tau \rangle \langle \sigma | s^0 | \nu \rangle + \langle \rho | s^0 | \tau \rangle \langle \sigma | s^{+1} | \nu \rangle \} \langle \Upsilon' | a_{r\rho}^\dagger a_{s\sigma}^\dagger a_{u\tau} a_{t\nu} | \Upsilon \rangle \\
&= \langle \alpha | s^{+1} | \beta \rangle \langle \alpha | s^0 | \alpha \rangle \langle \Upsilon' | a_{r\alpha}^\dagger a_{s\alpha}^\dagger a_{u\beta} a_{t\alpha} | \Upsilon \rangle \\
&\quad + \langle \alpha | s^{+1} | \beta \rangle \langle \beta | s^0 | \beta \rangle \langle \Upsilon' | a_{r\alpha}^\dagger a_{s\beta}^\dagger a_{u\beta} a_{t\beta} | \Upsilon \rangle \\
&\quad + \langle \alpha | s^0 | \alpha \rangle \langle \alpha | s^{+1} | \beta \rangle \langle \Upsilon' | a_{r\alpha}^\dagger a_{s\alpha}^\dagger a_{u\alpha} a_{t\beta} | \Upsilon \rangle \\
&\quad + \langle \beta | s^0 | \beta \rangle \langle \alpha | s^{+1} | \beta \rangle \langle \Upsilon' | a_{r\beta}^\dagger a_{s\alpha}^\dagger a_{u\beta} a_{t\beta} | \Upsilon \rangle.
\end{aligned} \tag{2.62}$$

Since $\langle \alpha | s^{+1} | \beta \rangle \langle \alpha | s^0 | \alpha \rangle = \langle \alpha | s^0 | \alpha \rangle \langle \alpha | s^{+1} | \beta \rangle = -\frac{1}{2\sqrt{2}}$ and $\langle \alpha | s^{+1} | \beta \rangle \langle \beta | s^0 | \beta \rangle = \langle \beta | s^0 | \beta \rangle \langle \alpha | s^{+1} | \beta \rangle = \frac{1}{2\sqrt{2}}$, both expressions are identical.

$\hat{T}_0^{(2)}$

Stating:

$$\begin{aligned}
&\sum_{\rho\sigma\tau\nu} \{ 2\langle \rho | s^0 | \tau \rangle \langle \sigma | s^0 | \nu \rangle + \langle \rho | s^{+1} | \tau \rangle \langle \sigma | s^{-1} | \nu \rangle \\
&\quad + \langle \rho | s^{-1} | \tau \rangle \langle \sigma | s^{+1} | \nu \rangle \} \langle \Upsilon' | a_{r\rho}^\dagger a_{s\sigma}^\dagger a_{u\tau} a_{t\nu} | \Upsilon \rangle \\
&= \sum_{\rho\sigma\tau\nu} \{ 2\langle \rho | s^0 | \tau \rangle \langle \sigma | s^0 | \nu \rangle + \langle \rho | s^{+1} | \tau \rangle \langle \sigma | s^{-1} | \nu \rangle \\
&\quad + \langle \rho | s^{-1} | \tau \rangle \langle \sigma | s^{+1} | \nu \rangle \} \langle \Upsilon' | a_{r\rho}^\dagger a_{s\sigma}^\dagger a_{u\tau} a_{t\nu} | \Upsilon \rangle
\end{aligned} \tag{2.63}$$

and examining again independently left-hand side:

$$\begin{aligned}
&\sum_{\rho\sigma\tau\nu} \{ 2\langle \rho | s^0 | \tau \rangle \langle \sigma | s^0 | \nu \rangle + \langle \rho | s^{+1} | \tau \rangle \langle \sigma | s^{-1} | \nu \rangle + \langle \rho | s^{-1} | \tau \rangle \langle \sigma | s^{+1} | \nu \rangle \} \langle \Upsilon' | a_{r\rho}^\dagger a_{s\sigma}^\dagger a_{u\tau} a_{t\nu} | \Upsilon \rangle \\
&= 2\langle \alpha | s^0 | \alpha \rangle \langle \alpha | s^0 | \alpha \rangle \langle \Upsilon' | a_{r\alpha}^\dagger a_{s\alpha}^\dagger a_{u\alpha} a_{t\alpha} | \Upsilon \rangle \\
&\quad + 2\langle \alpha | s^0 | \alpha \rangle \langle \beta | s^0 | \beta \rangle \langle \Upsilon' | a_{r\alpha}^\dagger a_{s\beta}^\dagger a_{u\beta} a_{t\alpha} | \Upsilon \rangle \\
&\quad + 2\langle \beta | s^0 | \beta \rangle \langle \alpha | s^0 | \alpha \rangle \langle \Upsilon' | a_{r\beta}^\dagger a_{s\alpha}^\dagger a_{u\alpha} a_{t\beta} | \Upsilon \rangle \\
&\quad + 2\langle \beta | s^0 | \beta \rangle \langle \beta | s^0 | \beta \rangle \langle \Upsilon' | a_{r\beta}^\dagger a_{s\beta}^\dagger a_{u\beta} a_{t\beta} | \Upsilon \rangle \\
&\quad + \langle \alpha | s^{+1} | \beta \rangle \langle \beta | s^{-1} | \alpha \rangle \langle \Upsilon' | a_{r\alpha}^\dagger a_{s\beta}^\dagger a_{u\alpha} a_{t\beta} | \Upsilon \rangle \\
&\quad + \langle \beta | s^{-1} | \alpha \rangle \langle \alpha | s^{+1} | \beta \rangle \langle \Upsilon' | a_{r\beta}^\dagger a_{s\alpha}^\dagger a_{u\beta} a_{t\alpha} | \Upsilon \rangle
\end{aligned} \tag{2.64}$$

and right-hand side:

$$\begin{aligned}
&\sum_{\rho\sigma\tau\nu} \{ 2\langle \rho | s^0 | \tau \rangle \langle \sigma | s^0 | \nu \rangle + \langle \rho | s^{+1} | \tau \rangle \langle \sigma | s^{-1} | \nu \rangle + \langle \rho | s^{-1} | \tau \rangle \langle \sigma | s^{+1} | \nu \rangle \} \langle \Upsilon' | a_{r\rho}^\dagger a_{s\sigma}^\dagger a_{u\tau} a_{t\nu} | \Upsilon \rangle \\
&= 2\langle \alpha | s^0 | \alpha \rangle \langle \alpha | s^0 | \alpha \rangle \langle \Upsilon' | a_{r\alpha}^\dagger a_{s\alpha}^\dagger a_{u\alpha} a_{t\alpha} | \Upsilon \rangle
\end{aligned}$$

$$\begin{aligned}
& + 2\langle\alpha|s^0|\alpha\rangle\langle\beta|s^0|\beta\rangle\langle\Upsilon'|a_{r\alpha}^\dagger a_{s\beta}^\dagger a_{u\alpha} a_{t\beta}|\Upsilon\rangle \\
& + 2\langle\beta|s^0|\beta\rangle\langle\alpha|s^0|\alpha\rangle\langle\Upsilon'|a_{r\beta}^\dagger a_{s\alpha}^\dagger a_{u\beta} a_{t\alpha}|\Upsilon\rangle \\
& + 2\langle\beta|s^0|\beta\rangle\langle\beta|s^0|\beta\rangle\langle\Upsilon'|a_{r\beta}^\dagger a_{s\beta}^\dagger a_{u\beta} a_{t\beta}|\Upsilon\rangle \\
& + \langle\alpha|s^+|\beta\rangle\langle\beta|s^-|\alpha\rangle\langle\Upsilon'|a_{r\alpha}^\dagger a_{s\beta}^\dagger a_{u\beta} a_{t\alpha}|\Upsilon\rangle \\
& + \langle\beta|s^-|\alpha\rangle\langle\alpha|s^+|\beta\rangle\langle\Upsilon'|a_{r\beta}^\dagger a_{s\alpha}^\dagger a_{u\alpha} a_{t\beta}|\Upsilon\rangle,
\end{aligned} \tag{2.65}$$

we recognize again that with $2\langle\alpha|s^0|\alpha\rangle\langle\beta|s^0|\beta\rangle = 2\langle\beta|s^0|\beta\rangle\langle\alpha|s^0|\alpha\rangle = \langle\alpha|s^+|\beta\rangle\langle\beta|s^-|\alpha\rangle = \langle\beta|s^-|\alpha\rangle\langle\alpha|s^+|\beta\rangle = -\frac{1}{2}$, left- and right-hand side are equal.

$\hat{T}_{-1}^{(2)}$

Analogously to the $\{+1\}$ -component, we start out from the expression:

$$\begin{aligned}
& \sum_{\rho\sigma\tau\nu} \{ \langle\rho|s^-|\tau\rangle\langle\sigma|s^0|\nu\rangle + \langle\rho|s^0|\tau\rangle\langle\sigma|s^-|\nu\rangle \} \langle\Upsilon'|a_{r\rho}^\dagger a_{s\sigma}^\dagger a_{u\nu} a_{t\tau}|\Upsilon\rangle \\
& = \sum_{\rho\sigma\tau\nu} \{ \langle\rho|s^-|\tau\rangle\langle\sigma|s^0|\nu\rangle + \langle\rho|s^0|\tau\rangle\langle\sigma|s^-|\nu\rangle \} \langle\Upsilon'|a_{r\rho}^\dagger a_{s\sigma}^\dagger a_{u\tau} a_{t\nu}|\Upsilon\rangle
\end{aligned} \tag{2.66}$$

and consider the left-hand side:

$$\begin{aligned}
& \sum_{\rho\sigma\tau\nu} \{ \langle\rho|s^-|\tau\rangle\langle\sigma|s^0|\nu\rangle + \langle\rho|s^0|\tau\rangle\langle\sigma|s^-|\nu\rangle \} \langle\Upsilon'|a_{r\rho}^\dagger a_{s\sigma}^\dagger a_{u\nu} a_{t\tau}|\Upsilon\rangle \\
& = \langle\beta|s^-|\alpha\rangle\langle\alpha|s^0|\alpha\rangle\langle\Upsilon'|a_{r\beta}^\dagger a_{s\alpha}^\dagger a_{u\alpha} a_{t\alpha}|\Upsilon\rangle \\
& \quad + \langle\beta|s^-|\alpha\rangle\langle\beta|s^0|\beta\rangle\langle\Upsilon'|a_{r\beta}^\dagger a_{s\beta}^\dagger a_{u\beta} a_{t\alpha}|\Upsilon\rangle \\
& \quad + \langle\alpha|s^0|\alpha\rangle\langle\beta|s^-|\alpha\rangle\langle\Upsilon'|a_{r\alpha}^\dagger a_{s\beta}^\dagger a_{u\alpha} a_{t\alpha}|\Upsilon\rangle \\
& \quad + \langle\beta|s^0|\beta\rangle\langle\beta|s^-|\alpha\rangle\langle\Upsilon'|a_{r\beta}^\dagger a_{s\beta}^\dagger a_{u\alpha} a_{t\beta}|\Upsilon\rangle.
\end{aligned} \tag{2.67}$$

and right-hand side:

$$\begin{aligned}
& \sum_{\rho\sigma\tau\nu} \{ \langle\rho|s^-|\tau\rangle\langle\sigma|s^0|\nu\rangle + \langle\rho|s^0|\tau\rangle\langle\sigma|s^-|\nu\rangle \} \langle\Upsilon'|a_{r\rho}^\dagger a_{s\sigma}^\dagger a_{u\tau} a_{t\nu}|\Upsilon\rangle \\
& = \langle\beta|s^-|\alpha\rangle\langle\alpha|s^0|\alpha\rangle\langle\Upsilon'|a_{r\beta}^\dagger a_{s\alpha}^\dagger a_{u\alpha} a_{t\alpha}|\Upsilon\rangle \\
& \quad + \langle\beta|s^-|\alpha\rangle\langle\beta|s^0|\beta\rangle\langle\Upsilon'|a_{r\beta}^\dagger a_{s\beta}^\dagger a_{u\alpha} a_{t\beta}|\Upsilon\rangle \\
& \quad + \langle\alpha|s^0|\alpha\rangle\langle\beta|s^-|\alpha\rangle\langle\Upsilon'|a_{r\alpha}^\dagger a_{s\beta}^\dagger a_{u\alpha} a_{t\alpha}|\Upsilon\rangle \\
& \quad + \langle\beta|s^0|\beta\rangle\langle\beta|s^-|\alpha\rangle\langle\Upsilon'|a_{r\beta}^\dagger a_{s\beta}^\dagger a_{u\beta} a_{t\alpha}|\Upsilon\rangle,
\end{aligned} \tag{2.68}$$

and using $\langle\beta|s^-|\alpha\rangle\langle\alpha|s^0|\alpha\rangle = \langle\alpha|s^0|\alpha\rangle\langle\beta|s^-|\alpha\rangle = \frac{1}{2\sqrt{2}}$, $\langle\beta|s^-|\alpha\rangle\langle\beta|s^0|\beta\rangle = \langle\beta|s^0|\beta\rangle\langle\beta|s^-|\alpha\rangle = -\frac{1}{2\sqrt{2}}$, obtain identical terms.

$\hat{T}_{-2}^{(2)}$

The only nonvanishing spin term is: $\langle\beta|s^-|\alpha\rangle\langle\beta|s^-|\alpha\rangle$. As in the case of the $\{+2\}$ -component, the permutational symmetry in the second index is trivial.

Having established this relation, we can now employ it to further simplify the three expressions for the calculation of spin-spin coupling (terms (2.10)/(2.23)/(2.30)) as follows:

i. $w' = w$

$$\langle \Upsilon' | \mathcal{H}_{SS} | \Upsilon \rangle = \frac{k}{2} \sum_m \sum_{r \neq s} \sum_{\rho\sigma\tau\nu} \left\{ R_{rsrs}^{(m)} S_{\rho\sigma\tau\nu}^{(m)} \langle \Upsilon' | a_{r\rho}^\dagger a_{s\sigma}^\dagger a_{s\nu} a_{r\tau} | \Upsilon \rangle \right. \\ \left. + R_{rssi}^{(m)} S_{\rho\sigma\tau\nu}^{(m)} \langle \Upsilon' | a_{r\rho}^\dagger a_{s\sigma}^\dagger a_{r\nu} a_{s\tau} | \Upsilon \rangle \right\} \quad (2.69)$$

$$= \frac{k}{2} \sum_m \sum_{r \neq s} \sum_{\rho\sigma\tau\nu} \left\{ R_{rsrs}^{(m)} S_{\rho\sigma\tau\nu}^{(m)} \langle \Upsilon' | a_{r\rho}^\dagger a_{s\sigma}^\dagger a_{s\nu} a_{r\tau} | \Upsilon \rangle \right. \\ \left. + R_{rssi}^{(m)} S_{\rho\sigma\tau\nu}^{(m)} \langle \Upsilon' | a_{r\rho}^\dagger a_{s\sigma}^\dagger a_{r\tau} a_{s\nu} | \Upsilon \rangle \right\} \quad (2.70)$$

$$= \frac{k}{2} \sum_m \sum_{r \neq s} \sum_{\rho\sigma\tau\nu} \left\{ R_{rsrs}^{(m)} S_{\rho\sigma\tau\nu}^{(m)} \langle \Upsilon' | a_{r\rho}^\dagger a_{s\sigma}^\dagger a_{s\nu} a_{r\tau} | \Upsilon \rangle \right. \\ \left. - R_{rssi}^{(m)} S_{\rho\sigma\tau\nu}^{(m)} \langle \Upsilon' | a_{r\rho}^\dagger a_{s\sigma}^\dagger a_{s\nu} a_{r\tau} | \Upsilon \rangle \right\} \quad (2.71)$$

$$= \frac{k}{2} \sum_m \sum_{r \neq s} \sum_{\rho\sigma\tau\nu} \left\{ R_{rsrs}^{(m)} - R_{rssi}^{(m)} \right\} S_{\rho\sigma\tau\nu}^{(m)} \langle \Upsilon' | a_{r\rho}^\dagger a_{s\sigma}^\dagger a_{s\nu} a_{r\tau} | \Upsilon \rangle \quad (2.72)$$

ii. $w' = a_b^\dagger a_a w$

$$\langle \Upsilon' | \mathcal{H}_{SS} | \Upsilon \rangle = k \sum_m \sum_{r \neq a, b} \sum_{\rho\sigma\tau\nu} \left\{ R_{brar}^{(m)} S_{\rho\sigma\tau\nu}^{(m)} \langle \Upsilon' | a_{b\rho}^\dagger a_{r\sigma}^\dagger a_{r\nu} a_{a\tau} | \Upsilon \rangle \right. \\ \left. + R_{brra}^{(m)} S_{\rho\sigma\tau\nu}^{(m)} \langle \Upsilon' | a_{b\rho}^\dagger a_{r\sigma}^\dagger a_{a\nu} a_{r\tau} | \Upsilon \rangle \right\} \quad (2.73)$$

$$= k \sum_m \sum_{r \neq a, b} \sum_{\rho\sigma\tau\nu} \left\{ R_{brar}^{(m)} S_{\rho\sigma\tau\nu}^{(m)} \langle \Upsilon' | a_{b\rho}^\dagger a_{r\sigma}^\dagger a_{r\nu} a_{a\tau} | \Upsilon \rangle \right. \\ \left. + R_{brra}^{(m)} S_{\rho\sigma\tau\nu}^{(m)} \langle \Upsilon' | a_{b\rho}^\dagger a_{r\sigma}^\dagger a_{a\tau} a_{r\nu} | \Upsilon \rangle \right\} \quad (2.74)$$

$$= k \sum_m \sum_{r \neq a, b} \sum_{\rho\sigma\tau\nu} \left\{ R_{brar}^{(m)} S_{\rho\sigma\tau\nu}^{(m)} \langle \Upsilon' | a_{b\rho}^\dagger a_{r\sigma}^\dagger a_{r\nu} a_{a\tau} | \Upsilon \rangle \right. \\ \left. - R_{brra}^{(m)} S_{\rho\sigma\tau\nu}^{(m)} \langle \Upsilon' | a_{b\rho}^\dagger a_{r\sigma}^\dagger a_{r\nu} a_{a\tau} | \Upsilon \rangle \right\} \quad (2.75)$$

$$= k \sum_m \sum_{r \neq a, b} \sum_{\rho\sigma\tau\nu} \left\{ R_{brar}^{(m)} - R_{brra}^{(m)} \right\} S_{\rho\sigma\tau\nu}^{(m)} \langle \Upsilon' | a_{b\rho}^\dagger a_{r\sigma}^\dagger a_{r\nu} a_{a\tau} | \Upsilon \rangle \quad (2.76)$$

iii. $w' = a_c^\dagger a_d^\dagger a_b a_a w$

$$\langle \Upsilon' | \mathcal{H}_{SS} | \Upsilon \rangle = k \sum_m \sum_{\rho\sigma\tau\nu} \left\{ R_{cdba}^{(m)} S_{\rho\sigma\tau\nu}^{(m)} \langle \Upsilon' | a_{c\rho}^\dagger a_{d\sigma}^\dagger a_{a\nu} a_{b\tau} | \Upsilon \rangle \right. \\ \left. + R_{cdab}^{(m)} S_{\rho\sigma\tau\nu}^{(m)} \langle \Upsilon' | a_{c\rho}^\dagger a_{d\sigma}^\dagger a_{b\nu} a_{a\tau} | \Upsilon \rangle \right\} \quad (2.77)$$

$$= k \sum_m \sum_{\rho\sigma\tau\nu} \left\{ R_{cdba}^{(m)} S_{\rho\sigma\tau\nu}^{(m)} \langle \Upsilon' | a_{c\rho}^\dagger a_{d\sigma}^\dagger a_{a\nu} a_{b\tau} | \Upsilon \rangle \right. \\ \left. + R_{cdab}^{(m)} S_{\rho\sigma\tau\nu}^{(m)} \langle \Upsilon' | a_{c\rho}^\dagger a_{d\sigma}^\dagger a_{b\tau} a_{a\nu} | \Upsilon \rangle \right\} \quad (2.78)$$

$$= k \sum_m \sum_{\rho\sigma\tau\nu} \left\{ R_{cdba}^{(m)} S_{\rho\sigma\tau\nu}^{(m)} \langle \Upsilon' | a_{c\rho}^\dagger a_{d\sigma}^\dagger a_{a\nu} a_{b\tau} | \Upsilon \rangle \right. \\ \left. - R_{cdab}^{(m)} S_{\rho\sigma\tau\nu}^{(m)} \langle \Upsilon' | a_{c\rho}^\dagger a_{d\sigma}^\dagger a_{a\nu} a_{b\tau} | \Upsilon \rangle \right\} \quad (2.79)$$

$$= k \sum_m \sum_{\rho\sigma\tau\nu} \left\{ R_{cdba}^{(m)} - R_{cdab}^{(m)} \right\} S_{\rho\sigma\tau\nu}^{(m)} \langle \Upsilon' | a_{c\rho}^\dagger a_{d\sigma}^\dagger a_{a\nu} a_{b\tau} | \Upsilon \rangle \quad (2.80)$$

We thereby arrive at the intermediate formulation of the implemented terms. This part of the derivation concerned simplifications in the spatial contribution, yielding expressions of general relevance in a possible calculation of spin-spin coupling. The main incentive was a reduction in the number of terms, employing the mathematical properties of the operators.

The second part of the derivation will consider the spin contribution, ultimately introducing the η -coefficient scheme. The reformulations reflect a level closer to the actual implementation, as they are governed by computational constructs present in the program. At the end of this derivation, we will arrive at a form of the expressions which resembles as closely as possible the actual realization within SPOCK.SISTR.

2.2.3 Derivation – Part (II)

SPOCK operates internally with wave functions for which $M_S = S$. Within the spin-orbit branches SPOCK.QDPT/SPOCK.CI, nonvanishing matrix elements occur for $\Delta S = 0, \pm 1$. The spin contribution of pairs of states for which $\Delta S = 0$ is obtained by evaluating the matrix elements $\langle S, M_S = S | s^0 | S, M_S = S \rangle$; matrix elements $\langle S, M_S \neq S | s^0 | S, M_S \neq S \rangle$ are derived from these by application of the WET (see p. 30ff in Ch. 1.5.1). Analogously, spin contributions of pairs for which $\Delta S = \pm 1$ are obtained by evaluating the element $\langle S+1, M_S = S+1 | s^{+1} | S, M_S = S \rangle$, from which again all elements of differing M_S values are derived. Furthermore, the relationship $(\hat{s}^{+1})^\dagger = -\hat{s}^{-1}$ is employed, thereby restricting the calculation entirely to the evaluation of matrix elements over the spin operator components \hat{s}^0, \hat{s}^{+1} .

In the evaluation of spin-spin contributions, the selection rule $\Delta S = 0, \pm 1, \pm 2$ applies. As in the spin-orbit case, relationships between operator components facilitate a reduction in the amount of work. In particular, employing that:

$$\left(\hat{T}_{+2}^{(2)}\right)^\dagger = \left(\hat{s}_i^{+1}\hat{s}_j^{+1}\right)^\dagger = \hat{s}_j^{-1}\hat{s}_i^{-1} = \hat{T}_{-2}^{(2)} \quad (2.81)$$

$$\left(\hat{T}_{+1}^{(2)}\right)^\dagger = \left(\frac{1}{\sqrt{2}}\{\hat{s}_i^0\hat{s}_j^{+1} + \hat{s}_i^{+1}\hat{s}_j^0\}\right)^\dagger = \frac{1}{\sqrt{2}}\{-\hat{s}_j^{-1}\hat{s}_i^0 - \hat{s}_j^0\hat{s}_i^{-1}\} = -\hat{T}_{-1}^{(2)}, \quad (2.82)$$

with $(\hat{s}^{+1})^\dagger = -\hat{s}^{-1}$, $(\hat{s}^0)^\dagger = \hat{s}^0$, $(\hat{s}_i\hat{s}_j)^\dagger = \hat{s}_j^\dagger\hat{s}_i^\dagger$, limits the computational labour to the calculation of matrix elements over $\hat{T}_{+2}^{(2)}, \hat{T}_{+1}^{(2)}, \hat{T}_0^{(2)}$.

Considering now the concrete evaluation of the spin components, the most important aspect in the further derivation constitutes the adaptation of the η -pattern formalism to the spin-spin-operator case. The crucial step herein consists of the insertion of the resolution of identity $1 = \sum_{\Upsilon''} |\Upsilon''\rangle\langle\Upsilon''|$, represented here as a summation over an infinite number of states $|\Upsilon''\rangle = |S'', M_S'', \omega'', w''\rangle$ with all possible occupations of spin and space. Terms (2.72)/(2.76)/(2.80) have to be reformulated in the context of this insertion to account for the constructs that are imposed by the surrounding program environment.

So far, I have been operating with compound expressions of space and spin $R^{(m)}/S^{(m)}$ and have directed my derivation by the three possible cases of excitation. I will turn now successively to the individual spin tensor components $\hat{T}_{+2}^{(2)}$, $\hat{T}_{+1}^{(2)}$, $\hat{T}_0^{(2)}$, resolving the compound expression in $S_{\rho\sigma\tau\nu}^{(m)}$. After discussing important individual steps in detail, I will perform the derivation for general orbital indices r , s , t , u as it is common to all three possible cases of excitation. Following the derivation itself, I will then give the concrete formulas for the three cases of excitation for the three tensor operators, thereby listing the expressions that are directly implemented in SPOCK.SISTR.²

Anticommutation

For an adaption of the η -scheme to spin-spin coupling, the two-electron expression has to be decomposed into effectively a product of two one-electron expressions. This entails a reordering of creation and annihilation operators and grouping together with the respective spin integral. Inspecting a general term

$$\sum_{\rho\sigma\tau\nu} \langle \rho|s|\tau \rangle \langle \sigma|s|v \rangle \langle \Upsilon' | a_{r\rho}^\dagger a_{s\sigma}^\dagger a_{uv} a_{t\tau} | \Upsilon \rangle,$$

we recognize that the operators $a_{r\rho}^\dagger/a_{t\tau}$ are associated with spin integral $\langle \rho|s|\tau \rangle$ while the operators $a_{s\sigma}^\dagger/a_{uv}$ refer to spin integral $\langle \sigma|s|v \rangle$. Prior to the insertion of the resolution of identity, the operators have to be anticommutated correspondingly, either as

$$a_{r\rho}^\dagger a_{s\sigma}^\dagger a_{uv} a_{t\tau} = a_{r\rho}^\dagger a_{t\tau} a_{s\sigma}^\dagger a_{uv}$$

or

$$a_{r\rho}^\dagger a_{s\sigma}^\dagger a_{uv} a_{t\tau} = a_{s\sigma}^\dagger a_{uv} a_{r\rho}^\dagger a_{t\tau}.$$

Reflecting on the anticommutation relations of creation and annihilation operators (see p. 31ff in Ch. 1.5.1), this can be performed accompanied solely by a change of sign if the indices of the operators are disjoint. If the indices of the operators coincide, an additional term is introduced in the anticommutation of creation with annihilation operator. Returning briefly to the terms under consideration (see Eqs. (2.72)/(2.76)/(2.80)), we recognize that the ordering of the operators in combination with the selection rules that were established previously indeed ensures disjoint indices in the anticommutations that we accomplish. To be precise, this particular ordering of the operators was of course achieved in the knowledge of the subsequent reformulations in order to avoid the introduction of additional terms as this would constitute a substantial disadvantage in the computational treatment.

²Note that the numerical prefactors of $\frac{1}{\sqrt{2}}/\frac{1}{\sqrt{6}}$ in the components $\hat{T}_{+1}^{(2)}/\hat{T}_0^{(2)}$ are evaluated separately in the program and will be omitted in the derivation as well as in the concrete form of the equations.

Insertion of Resolution of Identity

The insertion of the resolution of identity is equivalent to the insertion of an infinite number of all possible occupations of spin and space, considering all possible quantum states in S , M_S . Fortunately, of course, the number of nonvanishing terms originating in this step is rather modest as the individual creation and annihilation operators acting on the configuration of bra and ket constitute a definite selection in the quantum state. Considering the insertion:

$$\begin{aligned} & \sum_{\rho\sigma\tau\nu} \langle \rho|s|\tau \rangle \langle \sigma|s|\nu \rangle \langle \Upsilon' | a_{r\rho}^\dagger a_{t\tau} a_{s\sigma}^\dagger a_{\nu\nu} | \Upsilon \rangle \\ &= \sum_{\rho\sigma\tau\nu} \langle \rho|s|\tau \rangle \langle \sigma|s|\nu \rangle \sum_{\Upsilon''} [\langle \Upsilon' | a_{r\rho}^\dagger a_{t\tau} | \Upsilon'' \rangle \langle \Upsilon'' | a_{s\sigma}^\dagger a_{\nu\nu} | \Upsilon \rangle] \end{aligned} \quad (2.83)$$

$$\begin{aligned} &= \sum_{\rho\sigma\tau\nu} \langle \rho|s|\tau \rangle \langle \sigma|s|\nu \rangle \sum_{S''} \sum_{M_S''} \sum_{\omega''} \sum_{w''} [\langle S', M_S', \omega', w' | a_{r\rho}^\dagger a_{t\tau} | S'', M_S'', \omega'', w'' \rangle \\ & \quad \times \langle S'', M_S'', \omega'', w'' | a_{s\sigma}^\dagger a_{\nu\nu} | S, M_S, \omega, w \rangle] , \end{aligned} \quad (2.84)$$

we recognize that the operation of $a_{s\sigma}^\dagger a_{\nu\nu}$ on the configuration of $|\Upsilon\rangle$ with spatial occupation w reduces the summation over the spatial occupation w'' of $|\Upsilon''\rangle$ to one case, to be precise to the case which results from the application of a single excitation $u \rightarrow s$ on w : $w'' = a_s^\dagger a_u w$. It should be noted that this is identical to the excitation $r \rightarrow t$ with respect to the spatial occupation of $|\Upsilon'\rangle$: $w'' = a_t^\dagger a_r w'$. In addition, we recapitulate at this point that we imposed on $|\Upsilon'\rangle$, $|\Upsilon\rangle$ that $M_S' = S'$, $M_S = S$ by operating solely with spin functions within SPOCK which were generated under this restriction. We may therefore rewrite:

$$\begin{aligned} & \sum_{\rho\sigma\tau\nu} \langle \rho|s|\tau \rangle \langle \sigma|s|\nu \rangle \sum_{S''} \sum_{M_S''} \sum_{\omega''} \sum_{w''} [\langle S', M_S', \omega', w' | a_{r\rho}^\dagger a_{t\tau} | S'', M_S'', \omega'', w'' \rangle \\ & \quad \times \langle S'', M_S'', \omega'', w'' | a_{s\sigma}^\dagger a_{\nu\nu} | S, M_S, \omega, w \rangle] \\ &= \sum_{\rho\sigma\tau\nu} \langle \rho|s|\tau \rangle \langle \sigma|s|\nu \rangle \sum_{S''} \sum_{M_S''} \sum_{\omega''} [\langle S', M_S' = S', \omega', w' | a_{r\rho}^\dagger a_{t\tau} | S'', M_S'' = S'', \omega'', w'' \rangle \\ & \quad \times \langle S'', M_S'' = S'', \omega'', w'' | a_{s\sigma}^\dagger a_{\nu\nu} | S, M_S = S, \omega, w \rangle] . \end{aligned} \quad (2.85)$$

Furthermore, we recognize that the projection of bra and ket onto the state manifold $|\Upsilon''\rangle$, in combination with the selection rules associated with the spin operators $\hat{s} = \hat{s}^{-1}$, \hat{s}^0 , \hat{s}^{+1} , constitutes a restriction to a limited number of elements in the summation in S'' , M_S'' . The form of the resulting expression depends on the concrete spin operator and has therefore to be examined for each spin tensor component individually.

Sequence of Spin Terms

The programming decision of basing the entire algorithm on spin functions with $M_S = S$ has a subtle but substantial impact on the details of the spin-spin implementation. As a consequence, careful consideration is demanded in the derivation of the expressions

to be evaluated.

I will illustrate this issue with the term $\sum_{\rho\sigma\tau\nu}\langle\rho|s^{+1}|\tau\rangle\langle\sigma|s^0|\nu\rangle\langle\Upsilon'|a_{r\rho}^\dagger a_{t\tau}^\dagger a_{s\sigma}^\dagger a_{\nu\nu}|\Upsilon\rangle$ which constitutes one part of the $\hat{T}_{+1}^{(2)}$ component.

In general, the \hat{s}^{+1} operator restricts the coupling state to possess quantum number $\Delta M_S = +1$, analogously does the \hat{s}^{-1} component operate with the selection of $\Delta M_S = -1$, while the \hat{s}^0 component couples states for which $\Delta M_S = 0$. Furthermore, all of the spin operators allow for coupling of $\Delta S = 0, \pm 1$. These selection rules have a direct consequence for the evaluation of terms within the specific framework of the program which will be shown as follows. I start out with the insertion of the resolution of identity in above term:

$$\begin{aligned} & \sum_{\rho\sigma\tau\nu}\langle\rho|s^{+1}|\tau\rangle\langle\sigma|s^0|\nu\rangle\langle\Upsilon'|a_{r\rho}^\dagger a_{t\tau}^\dagger a_{s\sigma}^\dagger a_{\nu\nu}|\Upsilon\rangle \\ &= \sum_{\rho\sigma\tau\nu}\langle\rho|s^{+1}|\tau\rangle\langle\sigma|s^0|\nu\rangle\sum_{\Upsilon''}[\langle\Upsilon'|a_{r\rho}^\dagger a_{t\tau}^\dagger|\Upsilon''\rangle\langle\Upsilon''|a_{s\sigma}^\dagger a_{\nu\nu}|\Upsilon\rangle]. \end{aligned} \quad (2.86)$$

The selection rules of the individual spin operators translate into the restriction of $M'_S = M_S + 1$, furthermore $M''_S = M_S$, $M'_S = M''_S + 1$. Noticing additionally the program constraint of $M'_S = S'$, $M_S = S$, we obtain:

$$\begin{aligned} & \sum_{\rho\sigma\tau\nu}\langle\rho|s^{+1}|\tau\rangle\langle\sigma|s^0|\nu\rangle\sum_{\Upsilon''}[\langle\Upsilon'|a_{r\rho}^\dagger a_{t\tau}^\dagger|\Upsilon''\rangle\langle\Upsilon''|a_{s\sigma}^\dagger a_{\nu\nu}|\Upsilon\rangle] \\ &= \sum_{\rho\sigma\tau\nu}\langle\rho|s^{+1}|\tau\rangle\langle\sigma|s^0|\nu\rangle\sum_{S''}\sum_{\omega''}[\langle S+1, M'_S = S+1, \omega', w'|a_{r\rho}^\dagger a_{t\tau}^\dagger|S'', M''_S = S, \omega'', w''\rangle \\ & \quad \times \langle S'', M''_S = S, \omega'', w''|a_{s\sigma}^\dagger a_{\nu\nu}|S, M_S, \omega, w\rangle]. \end{aligned} \quad (2.87)$$

We observe that the projection of states $|\Upsilon\rangle$, $|\Upsilon'\rangle$ onto the manifold $|\Upsilon''\rangle$ constitutes a selection criterion in spin and spatial states. The limited number of nonvanishing terms associated with the summation in S'' depends on the action of \hat{s}^0 , \hat{s}^{+1} onto $|\Upsilon\rangle$, $|\Upsilon'\rangle$. I mention at this point that the remaining summation over the spin vector ω'' which represents individual CSFs associated with the state $|S'', M''_S, \omega''\rangle$ will be incorporated into the η -coefficient expression in the later part of the derivation.

Further considering the possible quantum numbers of the inserted state $|\Upsilon''\rangle$, we have to reflect that although we selected states $|\Upsilon\rangle$, $|\Upsilon'\rangle$ with $M'_S = S'$, $M_S = S$ by the program choice of spin function and algorithm, on the other hand the insertion of the resolution of identity does not impose any such restriction on $|\Upsilon''\rangle$. To be precise: In order for this step of the derivation to be formally valid, we have to allow a summation over all possible spin functions, with all possible values of M''_S , S'' , including of course $M''_S \neq S''$. In this particular case, remembering that both spin operators \hat{s}^0 , \hat{s}^{+1} permit coupling for states of $\Delta S = \pm 1$ as well as $\Delta S = 0$, we obtain the following nonvanishing terms:

$$\sum_{\rho\sigma\tau\nu}\langle\rho|s^{+1}|\tau\rangle\langle\sigma|s^0|\nu\rangle\sum_{S''}\sum_{\omega''}[\langle S+1, M'_S = S+1, \omega', w'|a_{r\rho}^\dagger a_{t\tau}^\dagger|S'', M''_S = S, \omega'', w''\rangle$$

$$\begin{aligned}
& \times \langle S'', M_S'' = S, \omega'', w'' | a_{s\sigma}^\dagger a_{uv} | S, M_S, \omega, w \rangle] \\
= & \sum_{\rho\sigma\tau\nu} \langle \rho | s^{+1} | \tau \rangle \langle \sigma | s^0 | \nu \rangle \sum_{\omega''} [\langle S+1, M_S' = S+1, \omega', w' | a_{r\rho}^\dagger a_{t\tau} | S+1, M_S'' = S, \omega'', w'' \rangle \\
& \times \langle S+1, M_S'' = S, \omega'', w'' | a_{s\sigma}^\dagger a_{uv} | S, M_S, \omega, w \rangle] \\
+ & \sum_{\rho\sigma\tau\nu} \langle \rho | s^{+1} | \tau \rangle \langle \sigma | s^0 | \nu \rangle \sum_{\omega''} [\langle S+1, M_S' = S+1, \omega', w' | a_{r\rho}^\dagger a_{t\tau} | S, M_S'' = S, \omega'', w'' \rangle \\
& \times \langle S, M_S'' = S, \omega'', w'' | a_{s\sigma}^\dagger a_{uv} | S, M_S, \omega, w \rangle] . \quad (2.88)
\end{aligned}$$

The elementary point to recognize is that the operation of \hat{s}^0 onto $|\Upsilon\rangle$ permits states $|\Upsilon''\rangle$ exhibiting quantum numbers $S'' = S + 1$ as well as $S'' = S$. The further operation of \hat{s}^{+1} onto the intermediate $|\Upsilon''\rangle$ state may yield in both cases the quantum state $|\Upsilon'\rangle$ of the bra. The difference is that in the one case, an increase in the spin quantum number S to $S + 1$ is associated with the operation of \hat{s}^0 , while in the other case, it is associated with the operation of \hat{s}^{+1} . We note in passing that the state $S'' = S - 1$ cannot occur since although in principle the operator \hat{s}^0 could couple to a state with $\Delta S = -1$, it would imply in this particular case the appearance of a state with $S'' = S - 1$, $M_S'' = S$, i.e., $M_S'' > S''$, which is of course forbidden.

I arrive now at an observation that is crucial in the framework of the program: The derivation, as it was performed in this section, results in the necessity of a wave function with $M_S'' \neq S''$, to be precise, in the chosen case $M_S'' = S'' - 1$. This would pose a substantial problem in the spin-spin implementation as the program environment as well as the η -coefficients are constructed solely for wave functions with $M_S = S$. If possible, it would be advantageous to circumvent this issue as the introduction of functions with $M_S \neq S$ would permeate through the entire program construct and the necessary changes would constitute a nontrivial effort. As it is, I present a detailed exposition to illustrate this subtle but significant point and motivate a crucial step in the derivation which might otherwise not appear to be of obvious necessity. It is indeed by careful reordering of operators and integral expressions possible to circumvent the issue of the appearance of states with $M_S \neq S$.

Reflecting on the present case, we recognize that the operation of first \hat{s}^0 onto $|\Upsilon\rangle$, followed by the operation of \hat{s}^{+1} onto the intermediate state $|\Upsilon''\rangle$, resulted in the problematic appearance of states with $M_S'' \neq S''$. On the other hand, evaluating the second term of the component $\hat{T}_{+1}^{(2)} = \frac{1}{\sqrt{2}} \{ \hat{s}^{+1} \hat{s}^0 + \hat{s}^0 \hat{s}^{+1} \}$, we note that this case is not problematic. In operating first with \hat{s}^{+1} onto $|\Upsilon\rangle$, the selection rule $\Delta M_S = +1$ demands a raising to $M_S'' = M_S + 1$ and therefore imposes necessarily $S'' = S + 1$. The subsequent operation of \hat{s}^0 onto $|\Upsilon''\rangle$ can in principle alter the spin quantum number S'' , but in the projection of $|\Upsilon'\rangle$ onto the resulting state, we restrict the selection of states with $S'' = S + 1$. This consideration points to the resolution of the complication: We should aim at formally recasting the first term $\hat{s}^{+1} \hat{s}^0 \rightarrow \hat{s}^0 \hat{s}^{+1}$. This is indeed possible by careful permutation of operators and indices as follows:

$$\sum_{\rho\sigma\tau\nu} \langle \rho | s^{+1} | \tau \rangle \langle \sigma | s^0 | \nu \rangle \langle \Upsilon' | a_{r\rho}^\dagger a_{s\sigma}^\dagger a_{uv} a_{t\tau} | \Upsilon \rangle$$

$$= \sum_{\rho\sigma\tau\nu} \langle \sigma | s^0 | \nu \rangle \langle \rho | s^{+1} | \tau \rangle \langle \Upsilon' | a_{s\sigma}^\dagger a_{uv} a_{r\rho}^\dagger a_{t\tau} | \Upsilon \rangle \quad (2.89)$$

$$= \sum_{\rho\sigma\tau\nu} \langle \sigma | s^0 | \nu \rangle \langle \rho | s^{+1} | \tau \rangle \sum_{\Upsilon''} [\langle \Upsilon' | a_{s\sigma}^\dagger a_{uv} | \Upsilon'' \rangle \langle \Upsilon'' | a_{r\rho}^\dagger a_{t\tau} | \Upsilon \rangle] \quad (2.90)$$

$$= \sum_{\rho\sigma\tau\nu} \langle \sigma | s^0 | \nu \rangle \langle \rho | s^{+1} | \tau \rangle \sum_{\omega''} [\langle S+1, M'_S = S+1, \omega', w' | a_{s\sigma}^\dagger a_{uv} | S+1, M''_S = S, \omega'', w'' \rangle \times \langle S+1, M''_S = S, \omega'', w'' | a_{r\rho}^\dagger a_{t\tau} | S, M_S, \omega, w \rangle]. \quad (2.91)$$

Note the difference to the second term of the $\hat{T}_{+1}^{(2)}$ component:

$$\begin{aligned} & \sum_{\rho\sigma\tau\nu} \langle \rho | s^0 | \tau \rangle \langle \sigma | s^{+1} | \nu \rangle \langle \Upsilon' | a_{r\rho}^\dagger a_{s\sigma}^\dagger a_{uv} a_{t\tau} | \Upsilon \rangle \\ &= \sum_{\rho\sigma\tau\nu} \langle \rho | s^0 | \tau \rangle \langle \sigma | s^{+1} | \nu \rangle \sum_{\omega''} [\langle S+1, M'_S = S+1, \omega', w' | a_{r\rho}^\dagger a_{t\tau} | S+1, M''_S = S, \omega'', w'' \rangle \\ & \quad \times \langle S+1, M''_S = S, \omega'', w'' | a_{s\sigma}^\dagger a_{uv} | S, M_S, \omega, w \rangle]. \quad (2.92) \end{aligned}$$

In Eq. (2.91), we are considering a state $|\Upsilon''\rangle$ with the spatial occupation $w'' = a_r^\dagger a_t w$ while on the other hand in Eq. (2.92), the spatial occupation is reflected as $w'' = a_s^\dagger a_u w$. Therefore, these terms are not identical and have to be calculated independently.

I will now present the concise derivation for the three cases $\Delta S = 2$, $\Delta S = 1$, $\Delta S = 0$ for general orbital indices. The individual steps involve mainly anticommutation of operators and insertion of the resolution of identity and should be comprehensible from the previous exposition. I will distinguish the η -coefficients of the \hat{s}^{+1} operator by reference as $\eta^{(+1)}$ while the η -coefficients of the \hat{s}^0 operator will be denoted $\eta^{(0)}$.

$\Delta S = 2$

$$\begin{aligned} & \sum_{\rho\sigma\tau\nu} S_{\rho\sigma\tau\nu}^{(m)} \langle \Upsilon' | a_{r\rho}^\dagger a_{s\sigma}^\dagger a_{uv} a_{t\tau} | \Upsilon \rangle \\ &= \sum_{\rho\sigma\tau\nu} \langle \rho | s^{+1} | \tau \rangle \langle \sigma | s^{+1} | \nu \rangle \langle \Upsilon' | a_{r\rho}^\dagger a_{s\sigma}^\dagger a_{uv} a_{t\tau} | \Upsilon \rangle \quad (2.93) \end{aligned}$$

$$= \sum_{\rho\sigma\tau\nu} \langle \rho | s^{+1} | \tau \rangle \langle \sigma | s^{+1} | \nu \rangle \langle \Upsilon' | a_{r\rho}^\dagger a_{t\tau} a_{s\sigma}^\dagger a_{uv} | \Upsilon \rangle \quad (2.94)$$

$$= \sum_{\rho\sigma\tau\nu} \langle \rho | s^{+1} | \tau \rangle \langle \sigma | s^{+1} | \nu \rangle \sum_{\Upsilon''} [\langle \Upsilon' | a_{r\rho}^\dagger a_{t\tau} | \Upsilon'' \rangle \langle \Upsilon'' | a_{s\sigma}^\dagger a_{uv} | \Upsilon \rangle] \quad (2.95)$$

$$= \sum_{\Upsilon''} \left[\sum_{\rho\tau} \langle \rho | s^{+1} | \tau \rangle \langle \Upsilon' | a_{r\rho}^\dagger a_{t\tau} | \Upsilon'' \rangle \right] \left[\sum_{\sigma\nu} \langle \sigma | s^{+1} | \nu \rangle \langle \Upsilon'' | a_{s\sigma}^\dagger a_{uv} | \Upsilon \rangle \right] \quad (2.96)$$

$$\begin{aligned} &= \sum_{\omega''} \left[\sum_{\rho\tau} \langle \rho | s^{+1} | \tau \rangle \langle S+2, M_S = S+2, \omega', w' | a_{r\rho}^\dagger a_{t\tau} | S+1, M_S = S+1, \omega'', w'' \rangle \right] \\ & \quad \times \left[\sum_{\sigma\nu} \langle \sigma | s^{+1} | \nu \rangle \langle S+1, M_S = S+1, \omega'', w'' | a_{s\sigma}^\dagger a_{uv} | S, M_S = S, \omega, w \rangle \right] \quad (2.97) \end{aligned}$$

$$= \boldsymbol{\eta}^{(+1)}(\omega', w'; w'')_{\omega''} \cdot \boldsymbol{\eta}^{(+1)}(w''; \omega, w)_{\omega''} \quad (2.98)$$

The first step consists of a permutation of creation and annihilation operators so as to obtain a grouping of operators referring to identical electrons (Eq. (2.94)). This can be performed without introduction of additional terms due to disjoint indices, as discussed in the section *Anticommutation* (p. 62). After insertion of the resolution of identity $1 = \sum_{\Upsilon''} |\Upsilon''\rangle \langle \Upsilon''|$ (Eq. (2.95)), summations are interchanged grouping now spin integrals with the associated creation/annihilation operators and thereby succeeding in generating a product of two independent expressions (Eq. (2.96)). Substitution of the compound index Υ'' by $S'', M''_S, \omega'', w''$ and retention of nonvanishing terms yields the final expression involving a summation over individual CSFs ω'' (Eq. (2.97)). The individual bracketed factors correspond to spin- η -coefficients, the entire summation can therefore be conveniently formulated as the vector product of two η -vectors $\boldsymbol{\eta}$ with ω'' as the contracted dimension, as denoted by subindexation (Eq. (2.98)).

$$\Delta S = 1$$

$$\begin{aligned} & \sum_{\rho\sigma\tau\nu} S_{\rho\sigma\tau\nu}^{(m)} \langle \Upsilon' | a_{r\rho}^\dagger a_{s\sigma}^\dagger a_{uv} a_{t\tau} | \Upsilon \rangle \\ &= \sum_{\rho\sigma\tau\nu} \left\{ \langle \rho | s^{+1} | \tau \rangle \langle \sigma | s^0 | \nu \rangle + \langle \rho | s^0 | \tau \rangle \langle \sigma | s^{+1} | \nu \rangle \right\} \langle \Upsilon' | a_{r\rho}^\dagger a_{s\sigma}^\dagger a_{uv} a_{t\tau} | \Upsilon \rangle \end{aligned} \quad (2.99)$$

$$\begin{aligned} &= \sum_{\rho\sigma\tau\nu} \langle \rho | s^{+1} | \tau \rangle \langle \sigma | s^0 | \nu \rangle \langle \Upsilon' | a_{r\rho}^\dagger a_{s\sigma}^\dagger a_{uv} a_{t\tau} | \Upsilon \rangle \\ &+ \sum_{\rho\sigma\tau\nu} \langle \rho | s^0 | \tau \rangle \langle \sigma | s^{+1} | \nu \rangle \langle \Upsilon' | a_{r\rho}^\dagger a_{s\sigma}^\dagger a_{uv} a_{t\tau} | \Upsilon \rangle \end{aligned} \quad (2.100)$$

$$\begin{aligned} &= \sum_{\rho\sigma\tau\nu} \langle \sigma | s^0 | \nu \rangle \langle \rho | s^{+1} | \tau \rangle \langle \Upsilon' | a_{s\sigma}^\dagger a_{uv} a_{r\rho}^\dagger a_{t\tau} | \Upsilon \rangle \\ &+ \sum_{\rho\sigma\tau\nu} \langle \rho | s^0 | \tau \rangle \langle \sigma | s^{+1} | \nu \rangle \langle \Upsilon' | a_{r\rho}^\dagger a_{t\tau} a_{s\sigma}^\dagger a_{uv} | \Upsilon \rangle \end{aligned} \quad (2.101)$$

$$\begin{aligned} &= \sum_{\rho\sigma\tau\nu} \langle \sigma | s^0 | \nu \rangle \langle \rho | s^{+1} | \tau \rangle \sum_{\Upsilon''} [\langle \Upsilon' | a_{s\sigma}^\dagger a_{uv} | \Upsilon'' \rangle \langle \Upsilon'' | a_{r\rho}^\dagger a_{t\tau} | \Upsilon \rangle] \\ &+ \sum_{\rho\sigma\tau\nu} \langle \rho | s^0 | \tau \rangle \langle \sigma | s^{+1} | \nu \rangle \sum_{\Upsilon''} [\langle \Upsilon' | a_{r\rho}^\dagger a_{t\tau} | \Upsilon'' \rangle \langle \Upsilon'' | a_{s\sigma}^\dagger a_{uv} | \Upsilon \rangle] \end{aligned} \quad (2.102)$$

$$\begin{aligned} &= \sum_{\Upsilon''} \left[\sum_{\sigma\nu} \langle \sigma | s^0 | \nu \rangle \langle \Upsilon' | a_{s\sigma}^\dagger a_{uv} | \Upsilon'' \rangle \right] \left[\sum_{\rho\tau} \langle \rho | s^{+1} | \tau \rangle \langle \Upsilon'' | a_{r\rho}^\dagger a_{t\tau} | \Upsilon \rangle \right] \\ &+ \sum_{\Upsilon''} \left[\sum_{\rho\tau} \langle \rho | s^0 | \tau \rangle \langle \Upsilon' | a_{r\rho}^\dagger a_{t\tau} | \Upsilon'' \rangle \right] \left[\sum_{\sigma\nu} \langle \sigma | s^{+1} | \nu \rangle \langle \Upsilon'' | a_{s\sigma}^\dagger a_{uv} | \Upsilon \rangle \right] \end{aligned} \quad (2.103)$$

$$= \sum_{\omega''} \left[\sum_{\sigma\nu} \langle \sigma | s^0 | \nu \rangle \langle S+1, M_S = S+1, \omega', w' | a_{s\sigma}^\dagger a_{uv} | S+1, M_S = S+1, \omega'', w'' \rangle \right]$$

$$\begin{aligned}
& \times \left[\sum_{\rho\tau} \langle \rho | s^{+1} | \tau \rangle \langle S+1, M_S = S+1, \omega'', w'' | a_{r\rho}^\dagger a_{t\tau} | S, M_S = S, \omega, w \rangle \right] \\
& + \sum_{\omega''} \left[\sum_{\rho\tau} \langle \rho | s^0 | \tau \rangle \langle S+1, M_S = S+1, \omega', w' | a_{r\rho}^\dagger a_{t\tau} | S+1, M_S = S+1, \omega'', w'' \rangle \right] \\
& \times \left[\sum_{\sigma\nu} \langle \sigma | s^{+1} | \nu \rangle \langle S+1, M_S = S+1, \omega'', w''' | a_{s\sigma}^\dagger a_{\nu\nu} | S, M_S = S, \omega, w \rangle \right] \quad (2.104) \\
& = \boldsymbol{\eta}^{(0)}(\omega', w'; w'')_{\omega''} \cdot \boldsymbol{\eta}^{(+1)}(w''; \omega, w)_{\omega''} \\
& \quad + \boldsymbol{\eta}^{(0)}(\omega', w'; w''')_{\omega''} \cdot \boldsymbol{\eta}^{(+1)}(w'''; \omega, w)_{\omega''} \quad (2.105)
\end{aligned}$$

Note that I introduced w''' vs. w'' to distinguish between the differing spatial occupations and therefore differing η -coefficients associated with the first and second term.

The individual steps follow an analogous sequence as for $\Delta S = 2$: Permutation of operators (Eq. (2.101)), in this case with the additional consideration of an exchange of the position of \hat{s}^0 and \hat{s}^{+1} in the first term, insertion of the resolution of identity (Eq. (2.102)), interchange of summations accompanied by a separation into independent terms (Eq. (2.103)), resolution of the compound index Υ'' under consideration of nonvanishing terms (Eq. (2.104)), and finally a compact reexpression employing η -vectors $\boldsymbol{\eta}^{(0)}$, $\boldsymbol{\eta}^{(+1)}$.

$\Delta S = 0$

The consideration of this case is slightly more intricate. After the first steps, I will therefore split up the terms and will evaluate the expression over $\{\hat{s}^0 \cdot \hat{s}^0\}$ on the one hand and $\{\hat{s}^{-1} \cdot \hat{s}^{+1} + \hat{s}^{+1} \cdot \hat{s}^{-1}\}$ on the other hand separately.

$$\begin{aligned}
& \sum_{\rho\sigma\tau\nu} S_{\rho\sigma\tau\nu}^{(m)} \langle \Upsilon' | a_{r\rho}^\dagger a_{s\sigma}^\dagger a_{\nu\nu} a_{t\tau} | \Upsilon \rangle \\
& = \sum_{\rho\sigma\tau\nu} \left\{ 2 \langle \rho | s^0 | \tau \rangle \langle \sigma | s^0 | \nu \rangle + \langle \rho | s^{+1} | \tau \rangle \langle \sigma | s^{-1} | \nu \rangle \right. \\
& \quad \left. + \langle \rho | s^{-1} | \tau \rangle \langle \sigma | s^{+1} | \nu \rangle \right\} \langle \Upsilon' | a_{r\rho}^\dagger a_{s\sigma}^\dagger a_{\nu\nu} a_{t\tau} | \Upsilon \rangle \quad (2.106)
\end{aligned}$$

$$\begin{aligned}
& = \sum_{\rho\sigma\tau\nu} 2 \langle \rho | s^0 | \tau \rangle \langle \sigma | s^0 | \nu \rangle \langle \Upsilon' | a_{r\rho}^\dagger a_{s\sigma}^\dagger a_{\nu\nu} a_{t\tau} | \Upsilon \rangle \\
& \quad + \sum_{\rho\sigma\tau\nu} \langle \rho | s^{+1} | \tau \rangle \langle \sigma | s^{-1} | \nu \rangle \langle \Upsilon' | a_{r\rho}^\dagger a_{s\sigma}^\dagger a_{\nu\nu} a_{t\tau} | \Upsilon \rangle \\
& \quad + \sum_{\rho\sigma\tau\nu} \langle \rho | s^{-1} | \tau \rangle \langle \sigma | s^{+1} | \nu \rangle \langle \Upsilon' | a_{r\rho}^\dagger a_{s\sigma}^\dagger a_{\nu\nu} a_{t\tau} | \Upsilon \rangle \quad (2.107) \\
& = \sum_{\rho\sigma\tau\nu} 2 \langle \rho | s^0 | \tau \rangle \langle \sigma | s^0 | \nu \rangle \langle \Upsilon' | a_{r\rho}^\dagger a_{t\tau} a_{s\sigma}^\dagger a_{\nu\nu} | \Upsilon \rangle \\
& \quad + \sum_{\rho\sigma\tau\nu} \langle \sigma | s^{-1} | \nu \rangle \langle \rho | s^{+1} | \tau \rangle \langle \Upsilon' | a_{s\sigma}^\dagger a_{\nu\nu} a_{r\rho}^\dagger a_{t\tau} | \Upsilon \rangle
\end{aligned}$$

$$+ \sum_{\rho\sigma\tau\nu} \langle \rho | s^{-1} | \tau \rangle \langle \sigma | s^{+1} | \nu \rangle \langle \Upsilon' | a_{r\rho}^\dagger a_{t\tau} a_{s\sigma}^\dagger a_{uv} | \Upsilon \rangle \quad (2.108)$$

$$\begin{aligned} &= \sum_{\rho\sigma\tau\nu} 2 \langle \rho | s^0 | \tau \rangle \langle \sigma | s^0 | \nu \rangle \sum_{\Upsilon''} [\langle \Upsilon' | a_{r\rho}^\dagger a_{t\tau} | \Upsilon'' \rangle \langle \Upsilon'' | a_{s\sigma}^\dagger a_{uv} | \Upsilon \rangle] \\ &+ \sum_{\rho\sigma\tau\nu} \langle \sigma | s^{-1} | \nu \rangle \langle \rho | s^{+1} | \tau \rangle \sum_{\Upsilon''} [\langle \Upsilon' | a_{s\sigma}^\dagger a_{uv} | \Upsilon'' \rangle \langle \Upsilon'' | a_{r\rho}^\dagger a_{t\tau} | \Upsilon \rangle] \\ &+ \sum_{\rho\sigma\tau\nu} \langle \rho | s^{-1} | \tau \rangle \langle \sigma | s^{+1} | \nu \rangle \sum_{\Upsilon''} [\langle \Upsilon' | a_{r\rho}^\dagger a_{t\tau} | \Upsilon'' \rangle \langle \Upsilon'' | a_{s\sigma}^\dagger a_{uv} | \Upsilon \rangle] \end{aligned} \quad (2.109)$$

$$\begin{aligned} &= 2 \sum_{\Upsilon''} \left[\sum_{\rho\tau} \langle \rho | s^0 | \tau \rangle \langle \Upsilon' | a_{r\rho}^\dagger a_{t\tau} | \Upsilon'' \rangle \right] \left[\sum_{\sigma\nu} \langle \sigma | s^0 | \nu \rangle \langle \Upsilon'' | a_{s\sigma}^\dagger a_{uv} | \Upsilon \rangle \right] \\ &+ \sum_{\Upsilon''} \left[\sum_{\sigma\nu} \langle \sigma | s^{-1} | \nu \rangle \langle \Upsilon' | a_{s\sigma}^\dagger a_{uv} | \Upsilon'' \rangle \right] \left[\sum_{\rho\tau} \langle \rho | s^{+1} | \tau \rangle \langle \Upsilon'' | a_{r\rho}^\dagger a_{t\tau} | \Upsilon \rangle \right] \\ &+ \sum_{\Upsilon''} \left[\sum_{\rho\tau} \langle \rho | s^{-1} | \tau \rangle \langle \Upsilon' | a_{r\rho}^\dagger a_{t\tau} | \Upsilon'' \rangle \right] \left[\sum_{\sigma\nu} \langle \sigma | s^{+1} | \nu \rangle \langle \Upsilon'' | a_{s\sigma}^\dagger a_{uv} | \Upsilon \rangle \right] \end{aligned} \quad (2.110)$$

At this point, I turn to the individual operator expressions.

$$\{ \hat{s}^0 \cdot \hat{s}^0 \}$$

$$\begin{aligned} &2 \sum_{\Upsilon''} \left[\sum_{\rho\tau} \langle \rho | s^0 | \tau \rangle \langle \Upsilon' | a_{r\rho}^\dagger a_{t\tau} | \Upsilon'' \rangle \right] \left[\sum_{\sigma\nu} \langle \sigma | s^0 | \nu \rangle \langle \Upsilon'' | a_{s\sigma}^\dagger a_{uv} | \Upsilon \rangle \right] \\ &= 2 \sum_{\omega''} \left[\sum_{\rho\tau} \langle \rho | s^0 | \tau \rangle \langle S, M'_S = S, \omega', w' | a_{r\rho}^\dagger a_{t\tau} | S, M''_S = S, \omega'', w'' \rangle \right] \\ &\quad \times \left[\sum_{\sigma\nu} \langle \sigma | s^0 | \nu \rangle \langle S, M''_S = S, \omega'', w'' | a_{s\sigma}^\dagger a_{uv} | S, M_S = S, \omega, w \rangle \right] \\ &+ 2 \sum_{\omega''} \left[\sum_{\rho\tau} \langle \rho | s^0 | \tau \rangle \langle S, M'_S = S, \omega', w' | a_{r\rho}^\dagger a_{t\tau} | S+1, M''_S = S, \omega'', w'' \rangle \right] \\ &\quad \times \left[\sum_{\sigma\nu} \langle \sigma | s^0 | \nu \rangle \langle S+1, M''_S = S, \omega'', w'' | a_{s\sigma}^\dagger a_{uv} | S, M_S = S, \omega, w \rangle \right] \end{aligned} \quad (2.111)$$

After insertion of the resolution of identity and retention of nonvanishing terms, we encounter again in the second term the problematic appearance of a wave function with $M''_S \neq S''$. Recollecting the introduction of the WET (see p. 30ff in Ch. 1.5.1), in particular Eq. (1.15), we recognize that this expression can be reformulated employing the operators \hat{s}^{+1} , \hat{s}^{-1} and wave functions $M''_S = S''$ instead.

I repeat for clarity Eq. (1.15):

$$\langle \alpha', j' m''' | T_{q'}^{(k)} | \alpha, j m'' \rangle = \frac{\langle jk; m'' q' | jk; j' m''' \rangle}{\langle jk; m q | jk; j' m' \rangle} \langle \alpha', j' m' | T_q^{(k)} | \alpha, j m \rangle.$$

In compliance with this notation (and omitting for the present purpose irrelevant indices in ω, w as well as the summation over spin indices ρ, σ, τ, ν), the term we have to reformulate is written as:

$$\langle S, M'_S = S | s^0 | S+1, M''_S = S \rangle \cdot \langle S+1, M''_S = S | s^0 | S, M_S = S \rangle. \quad (2.112)$$

For the sequence of the application of the WET, I will remain in the notation of first quantization as it is more suitable for this purpose, resulting in more compact an evaluation. Subsequently, I will return to the notation of second quantization which is preferable in the context of the implemented equations.

In the consideration of the first factor I insert $T_{q'}^{(k)} = T_0^{(1)} = s^0$, $T_q^{(k)} = T_{-1}^{(1)} = s^{-1}$, $j' = S$, $j = S+1$, $m''' = S$, $m'' = S$, $m' = S$, $m = S+1$ and obtain:

$$\begin{aligned} & \langle S, M'_S = S | s^0 | S+1, M''_S = S \rangle \\ &= \frac{\langle S+1 \ 1; S \ 0 | S+1 \ 1; S \ S \rangle}{\langle S+1 \ 1; S+1 \ -1 | S+1 \ 1; S \ S \rangle} \langle S, M'_S = S | s^{-1} | S+1, M''_S = S+1 \rangle. \end{aligned} \quad (2.113)$$

Correspondingly, the second factor is formulated by insertion of $T_{q'}^{(k)} = T_0^{(1)} = s^0$, $T_q^{(k)} = T_{+1}^{(1)} = s^{+1}$, $j' = S+1$, $j = S$, $m''' = S$, $m'' = S$, $m' = S+1$, $m = S$ as:

$$\begin{aligned} & \langle S+1, M''_S = S | s^0 | S, M_S = S \rangle \\ &= \frac{\langle S \ 1; S \ 0 | S \ 1; S+1 \ S \rangle}{\langle S \ 1; S \ +1 | S \ 1; S+1 \ S+1 \rangle} \langle S+1, M''_S = S+1 | s^{+1} | S, M_S = S \rangle. \end{aligned} \quad (2.114)$$

The Clebsch-Gordan coefficients appearing in above quotient expressions are tabulated in literature [154] and we therefore obtain by insertion of the appropriate factors:

$$\langle S, M'_S = S | s^0 | S+1, M''_S = S \rangle = -\frac{1}{\sqrt{S+1}} \langle S, M'_S = S | s^{-1} | S+1, M''_S = S+1 \rangle \quad (2.115)$$

$$\langle S+1, M''_S = S | s^0 | S, M_S = S \rangle = \frac{1}{\sqrt{S+1}} \langle S+1, M''_S = S+1 | s^{+1} | S, M_S = S \rangle. \quad (2.116)$$

Combining these terms yields:

$$\begin{aligned} & \langle S, M'_S = S | s^0 | S+1, M''_S = S \rangle \cdot \langle S+1, M''_S = S | s^0 | S, M_S = S \rangle \\ &= -\frac{1}{S+1} \langle S, M'_S = S | s^{-1} | S+1, M''_S = S+1 \rangle \\ & \quad \cdot \langle S+1, M''_S = S+1 | s^{+1} | S, M_S = S \rangle \end{aligned} \quad (2.117)$$

$$\begin{aligned} &= -\frac{1}{S+1} \sum_{\omega''} \left[\sum_{\rho\tau} \langle \rho | s^{-1} | \tau \rangle \langle S, M'_S = S, \omega', w' | a_{r\rho}^\dagger a_{t\tau} | S+1, M''_S = S+1, \omega'', w'' \rangle \right] \\ & \quad \times \left[\sum_{\sigma\nu} \langle \sigma | s^{+1} | \nu \rangle \langle S+1, M''_S = S+1, \omega'', w'' | a_{s\sigma}^\dagger a_{u\nu} | S, M_S = S, \omega, w \rangle \right], \end{aligned} \quad (2.118)$$

returning in the last step to the notation of second quantization in compliance with the indexation of Eq. (2.111).

We recollect at this point furthermore that the program implements η -coefficients for the operators \hat{s}^{+1} , \hat{s}^0 while the operator \hat{s}^{-1} is recast employing the relationship $\hat{s}^{-1} = -(\hat{s}^{+1})^\dagger$. We therefore have to convert the matrix element appearing in Eq. (2.118) accordingly:

$$\begin{aligned} & \langle \rho | s^{-1} | \tau \rangle \langle S, M'_S = S, \omega', w' | a_{r\rho}^\dagger a_{t\tau} | S+1, M''_S = S+1, \omega'', w'' \rangle \\ &= -\langle \rho | (s^{+1})^\dagger | \tau \rangle \langle S, M'_S = S, \omega', w' | a_{r\rho}^\dagger a_{t\tau} | S+1, M''_S = S+1, \omega'', w'' \rangle \end{aligned} \quad (2.119)$$

$$= -\left(\langle \tau | s^{+1} | \rho \rangle \right)^\dagger \left(\langle S+1, M''_S = S+1, \omega'', w'' | a_{t\tau}^\dagger a_{r\rho} | S, M'_S = S, \omega', w' \rangle \right)^\dagger \quad (2.120)$$

$$= -\langle \tau | s^{+1} | \rho \rangle \langle S+1, M''_S = S+1, \omega'', w'' | a_{t\tau}^\dagger a_{r\rho} | S, M'_S = S, \omega', w' \rangle. \quad (2.121)$$

In the last step we employ that the matrix element $\langle \tau | s^{+1} | \rho \rangle$ constitutes a real number, furthermore that the program operates with real wave functions, thereby yielding a real matrix element $\langle S+1, M''_S = S+1, \omega'', w'' | a_{t\tau}^\dagger a_{r\rho} | S, M'_S = S, \omega', w' \rangle$ the adjoint of which is solely its transpose.

Combining the individual steps while returning now to Eq. (2.111), we obtain:

$$\begin{aligned} & 2 \sum_{\omega''} \left[\sum_{\rho\tau} \langle \rho | s^0 | \tau \rangle \langle S, M'_S = S, \omega', w' | a_{r\rho}^\dagger a_{t\tau} | S, M''_S = S, \omega'', w'' \rangle \right] \\ & \quad \times \left[\sum_{\sigma v} \langle \sigma | s^0 | v \rangle \langle S, M''_S = S, \omega'', w'' | a_{s\sigma}^\dagger a_{uv} | S, M_S = S, \omega, w \rangle \right] \\ & + 2 \sum_{\omega''} \left[\sum_{\rho\tau} \langle \rho | s^0 | \tau \rangle \langle S, M'_S = S, \omega', w' | a_{r\rho}^\dagger a_{t\tau} | S+1, M''_S = S, \omega'', w'' \rangle \right] \\ & \quad \times \left[\sum_{\sigma v} \langle \sigma | s^0 | v \rangle \langle S+1, M''_S = S, \omega'', w'' | a_{s\sigma}^\dagger a_{uv} | S, M_S = S, \omega, w \rangle \right] \\ & = 2 \sum_{\omega''} \left[\sum_{\rho\tau} \langle \rho | s^0 | \tau \rangle \langle S, M'_S = S, \omega', w' | a_{r\rho}^\dagger a_{t\tau} | S, M''_S = S, \omega'', w'' \rangle \right] \\ & \quad \times \left[\sum_{\sigma v} \langle \sigma | s^0 | v \rangle \langle S, M''_S = S, \omega'', w'' | a_{s\sigma}^\dagger a_{uv} | S, M_S = S, \omega, w \rangle \right] \\ & - \frac{2}{S+1} \sum_{\omega''} \left[\sum_{\rho\tau} \langle \rho | s^{-1} | \tau \rangle \langle S, M'_S = S, \omega', w' | a_{r\rho}^\dagger a_{t\tau} | S+1, M''_S = S+1, \omega'', w'' \rangle \right] \\ & \quad \times \left[\sum_{\sigma v} \langle \sigma | s^{+1} | v \rangle \langle S+1, M''_S = S+1, \omega'', w'' | a_{s\sigma}^\dagger a_{uv} | S, M_S = S, \omega, w \rangle \right] \quad (2.122) \\ & = 2 \sum_{\omega''} \left[\sum_{\rho\tau} \langle \rho | s^0 | \tau \rangle \langle S, M'_S = S, \omega', w' | a_{r\rho}^\dagger a_{t\tau} | S, M''_S = S, \omega'', w'' \rangle \right] \end{aligned}$$

$$\begin{aligned}
& \times \left[\sum_{\sigma v} \langle \sigma | s^0 | v \rangle \langle S, M_S'' = S, \omega'', w'' | a_{s\sigma}^\dagger a_{uv} | S, M_S = S, \omega, w \rangle \right] \\
& + \frac{2}{S+1} \sum_{\omega''} \left[\sum_{\rho\tau} \langle \tau | s^{+1} | \rho \rangle \langle S+1, M_S'' = S+1, \omega'', w'' | a_{t\tau}^\dagger a_{r\rho} | S, M_S' = S, \omega', w' \rangle \right] \\
& \times \left[\sum_{\sigma v} \langle \sigma | s^{+1} | v \rangle \langle S+1, M_S'' = S+1, \omega'', w'' | a_{s\sigma}^\dagger a_{uv} | S, M_S = S, \omega, w \rangle \right]. \quad (2.123)
\end{aligned}$$

To summarize the sequence of reformulations of the first term for the case of $\Delta S = 0$: After insertion of the resolution of identity we obtain two terms, the first of which is unproblematic to calculate in the context of the program environment while the second contains wave functions which are not provided in the program. Employing the Wigner-Eckart Theorem, the second term is first recast in an expression over the operator product $\{\hat{s}^{-1} \cdot \hat{s}^{+1}\}$ instead of $\{\hat{s}^0 \cdot \hat{s}^0\}$. In a second step, we obtain formally an expression over $\{\hat{s}^{+1} \cdot \hat{s}^{+1}\}$, in compliance with the η -coefficients present within the program environment.

I turn now to the consideration of the remaining terms of the case $\Delta S = 0$.

$$\left\{ \hat{s}^{-1} \cdot \hat{s}^{+1} + \hat{s}^{+1} \cdot \hat{s}^{-1} \right\}$$

For the reformulation of the second and third term of the $\hat{T}_0^{(2)}$ component, we start out from Eq. (2.110). After insertion of the resolution of identity, the matrix element expression over \hat{s}^{-1} is recast over the \hat{s}^{+1} operator in accordance with the implemented η -coefficients.

$$\begin{aligned}
& \sum_{\Upsilon''} \left[\sum_{\sigma v} \langle \sigma | s^{-1} | v \rangle \langle \Upsilon' | a_{s\sigma}^\dagger a_{uv} | \Upsilon'' \rangle \right] \left[\sum_{\rho\tau} \langle \rho | s^{+1} | \tau \rangle \langle \Upsilon'' | a_{r\rho}^\dagger a_{t\tau} | \Upsilon \rangle \right] \\
& + \sum_{\Upsilon''} \left[\sum_{\rho\tau} \langle \rho | s^{-1} | \tau \rangle \langle \Upsilon' | a_{r\rho}^\dagger a_{t\tau} | \Upsilon'' \rangle \right] \left[\sum_{\sigma v} \langle \sigma | s^{+1} | v \rangle \langle \Upsilon'' | a_{s\sigma}^\dagger a_{uv} | \Upsilon \rangle \right] \\
& = \sum_{\omega''} \left[\sum_{\sigma v} \langle \sigma | s^{-1} | v \rangle \langle S, M_S' = S, \omega', w' | a_{s\sigma}^\dagger a_{uv} | S+1, M_S'' = S, \omega'', w'' \rangle \right] \\
& \quad \times \left[\sum_{\rho\tau} \langle \rho | s^{+1} | \tau \rangle \langle S+1, M_S'' = S, \omega'', w'' | a_{r\rho}^\dagger a_{t\tau} | S, M_S = S, \omega, w \rangle \right] \\
& + \sum_{\omega''} \left[\sum_{\rho\tau} \langle \rho | s^{-1} | \tau \rangle \langle S, M_S' = S, \omega', w' | a_{r\rho}^\dagger a_{t\tau} | S+1, M_S'' = S, \omega'', w'' \rangle \right] \\
& \quad \times \left[\sum_{\sigma v} \langle \sigma | s^{+1} | v \rangle \langle S+1, M_S'' = S, \omega'', w'' | a_{s\sigma}^\dagger a_{uv} | S, M_S = S, \omega, w \rangle \right] \quad (2.124)
\end{aligned}$$

$$\begin{aligned}
&= - \sum_{\omega''} \left[\sum_{\sigma v} \langle v | s^{+1} | \sigma \rangle \langle S+1, M_S'' = S, \omega'', w'' | a_{uv}^\dagger a_{s\sigma} | S, M_S' = S, \omega', w' \rangle \right] \\
&\quad \times \left[\sum_{\rho\tau} \langle \rho | s^{+1} | \tau \rangle \langle S+1, M_S'' = S, \omega'', w'' | a_{r\rho}^\dagger a_{t\tau} | S, M_S = S, \omega, w \rangle \right] \\
&- \sum_{\omega''} \left[\sum_{\rho\tau} \langle \tau | s^{+1} | \rho \rangle \langle S+1, M_S'' = S, \omega'', w'' | a_{t\tau}^\dagger a_{r\rho} | S, M_S' = S, \omega', w' \rangle \right] \\
&\quad \times \left[\sum_{\sigma v} \langle \sigma | s^{+1} | v \rangle \langle S+1, M_S'' = S, \omega'', w'' | a_{s\sigma}^\dagger a_{uv} | S, M_S = S, \omega, w \rangle \right] \quad (2.125)
\end{aligned}$$

At this point, we can combine the individual terms associated with the $\hat{T}_0^{(2)}$ component, namely Eqs. (2.123) and (2.125), to obtain the compound expression for this component.

$$\begin{aligned}
&\left\{ \hat{s}^0 \cdot \hat{s}^0 \right\} + \left\{ \hat{s}^{-1} \cdot \hat{s}^{+1} + \hat{s}^{+1} \cdot \hat{s}^{-1} \right\} \\
&2 \sum_{\omega''} \left[\sum_{\rho\tau} \langle \rho | s^0 | \tau \rangle \langle S, M_S' = S, \omega', w' | a_{r\rho}^\dagger a_{t\tau} | S, M_S'' = S, \omega'', w'' \rangle \right] \\
&\quad \times \left[\sum_{\sigma v} \langle \sigma | s^0 | v \rangle \langle S, M_S'' = S, \omega'', w'' | a_{s\sigma}^\dagger a_{uv} | S, M_S = S, \omega, w \rangle \right] \\
&+ \frac{2}{S+1} \sum_{\omega''} \left[\sum_{\rho\tau} \langle \tau | s^{+1} | \rho \rangle \langle S+1, M_S'' = S+1, \omega'', w'' | a_{t\tau}^\dagger a_{r\rho} | S, M_S' = S, \omega', w' \rangle \right] \\
&\quad \times \left[\sum_{\sigma v} \langle \sigma | s^{+1} | v \rangle \langle S+1, M_S'' = S+1, \omega'', w'' | a_{s\sigma}^\dagger a_{uv} | S, M_S = S, \omega, w \rangle \right] \\
&- \sum_{\omega''} \left[\sum_{\sigma v} \langle v | s^{+1} | \sigma \rangle \langle S+1, M_S'' = S, \omega'', w'' | a_{uv}^\dagger a_{s\sigma} | S, M_S' = S, \omega', w' \rangle \right] \\
&\quad \times \left[\sum_{\rho\tau} \langle \rho | s^{+1} | \tau \rangle \langle S+1, M_S'' = S, \omega'', w'' | a_{r\rho}^\dagger a_{t\tau} | S, M_S = S, \omega, w \rangle \right] \\
&- \sum_{\omega''} \left[\sum_{\rho\tau} \langle \tau | s^{+1} | \rho \rangle \langle S+1, M_S'' = S, \omega'', w'' | a_{t\tau}^\dagger a_{r\rho} | S, M_S' = S, \omega', w' \rangle \right] \\
&\quad \times \left[\sum_{\sigma v} \langle \sigma | s^{+1} | v \rangle \langle S+1, M_S'' = S, \omega'', w'' | a_{s\sigma}^\dagger a_{uv} | S, M_S = S, \omega, w \rangle \right] \quad (2.126) \\
&= 2 \sum_{\omega''} \left[\sum_{\rho\tau} \langle \rho | s^0 | \tau \rangle \langle S, M_S' = S, \omega', w' | a_{r\rho}^\dagger a_{t\tau} | S, M_S'' = S, \omega'', w'' \rangle \right]
\end{aligned}$$

$$\begin{aligned}
& \times \left[\sum_{\sigma v} \langle \sigma | s^0 | v \rangle \langle S, M_S'' = S, \omega'', w'' | a_{s\sigma}^\dagger a_{uv} | S, M_S = S, \omega, w \rangle \right] \\
& - \left(\frac{S-1}{S+1} \right) \sum_{\omega''} \left[\sum_{\rho\tau} \langle \tau | s^{+1} | \rho \rangle \langle S+1, M_S'' = S+1, \omega'', w'' | a_{t\rho}^\dagger a_{r\rho} | S, M_S' = S, \omega', w' \rangle \right] \\
& \quad \times \left[\sum_{\sigma v} \langle \sigma | s^{+1} | v \rangle \langle S+1, M_S'' = S+1, \omega'', w'' | a_{s\sigma}^\dagger a_{uv} | S, M_S = S, \omega, w \rangle \right] \\
& - \sum_{\omega''} \left[\sum_{\sigma v} \langle v | s^{+1} | \sigma \rangle \langle S+1, M_S'' = S, \omega'', w'' | a_{uv}^\dagger a_{s\sigma} | S, M_S' = S, \omega', w' \rangle \right] \\
& \quad \times \left[\sum_{\rho\tau} \langle \rho | s^{+1} | \tau \rangle \langle S+1, M_S'' = S, \omega'', w'' | a_{r\rho}^\dagger a_{t\tau} | S, M_S = S, \omega, w \rangle \right] \quad (2.127) \\
& = 2 \boldsymbol{\eta}^{(0)}(\omega', w'; w'')_{\omega''} \cdot \boldsymbol{\eta}^{(0)}(w''; \omega, w)_{\omega''} \\
& \quad - \left(\frac{S-1}{S+1} \right) \boldsymbol{\eta}^{(+1)}(w''; \omega', w')_{\omega''} \cdot \boldsymbol{\eta}^{(+1)}(w''; \omega, w)_{\omega''} \\
& \quad \quad - \boldsymbol{\eta}^{(+1)}(w'''; \omega', w')_{\omega''} \cdot \boldsymbol{\eta}^{(+1)}(w'''; \omega, w)_{\omega''} \quad (2.128)
\end{aligned}$$

As the second term originating from the operator product $\{\hat{s}^0 \cdot \hat{s}^0\}$ is identical to the second term of $\{\hat{s}^{-1} \cdot \hat{s}^{+1} + \hat{s}^{+1} \cdot \hat{s}^{-1}\}$, these two expressions were combined in Eq. (2.127) with the prefactor $\left(\frac{2}{S+1} - 1\right) = -\left(\frac{S-1}{S+1}\right)$.

I have now presented the derivation of the formulas for the calculation of spin-spin coupling for general orbital indices r, s, t, u for the three cases $\Delta S = 2$ (Eqs. (2.97), (2.98)), $\Delta S = 1$ (Eqs. (2.104), (2.105)), $\Delta S = 0$ (Eqs. (2.127), (2.128)). This part of the derivation was strongly directed by two elements imposed within the environment of SPOCK: First, the construct of one-electron spin- η -coefficients, and second, the program framework based on wave functions of $M_S = S$. Employing one-electron spin- η -coefficients necessitated the decomposition of two-electron spin-spin terms into a product of two one-electron quantities by insertion of the resolution of identity and appropriate grouping of expressions. The implementation being based on $M_S = S$ functions necessitated a careful reordering of terms as well as the application of the WET and transposition of elements so as to obtain formulas which can be efficiently evaluated within the existing program structure.

I will now list the individual equations as implemented in SPOCK.SISTR for the three possible cases of excitation $w' = w$, $w' = a_b^\dagger a_a w$, $w' = a_c^\dagger a_d^\dagger a_b a_a w$, for the three different cases of spin coupling $\Delta S = 2$, $\Delta S = 1$, $\Delta S = 0$.

2.2.4 Implemented Formulas

$$w' = w$$

$$\Delta S = 2$$

$$\begin{aligned} & \sum_{\omega''} \left[\sum_{\rho\tau} \langle \rho | s^{+1} | \tau \rangle \langle S+2, M_S = S+2, \omega', w | a_{r\rho}^\dagger a_{r\tau} | S+1, M_S = S+1, \omega'', w \rangle \right] \\ & \quad \times \left[\sum_{\sigma v} \langle \sigma | s^{+1} | v \rangle \langle S+1, M_S = S+1, \omega'', w | a_{s\sigma}^\dagger a_{sv} | S, M_S = S, \omega, w \rangle \right] \end{aligned} \quad (2.129)$$

$$\Delta S = 1$$

$$\begin{aligned} & \sum_{\omega''} \left[\sum_{\sigma v} \langle \sigma | s^0 | v \rangle \langle S+1, M_S = S+1, \omega', w | a_{s\sigma}^\dagger a_{sv} | S+1, M_S = S+1, \omega'', w \rangle \right] \\ & \quad \times \left[\sum_{\rho\tau} \langle \rho | s^{+1} | \tau \rangle \langle S+1, M_S = S+1, \omega'', w | a_{r\rho}^\dagger a_{r\tau} | S, M_S = S, \omega, w \rangle \right] \\ & + \sum_{\omega''} \left[\sum_{\rho\tau} \langle \rho | s^0 | \tau \rangle \langle S+1, M_S = S+1, \omega', w | a_{r\rho}^\dagger a_{r\tau} | S+1, M_S = S+1, \omega'', w \rangle \right] \\ & \quad \times \left[\sum_{\sigma v} \langle \sigma | s^{+1} | v \rangle \langle S+1, M_S = S+1, \omega'', w | a_{s\sigma}^\dagger a_{sv} | S, M_S = S, \omega, w \rangle \right] \end{aligned} \quad (2.130)$$

$$\Delta S = 0$$

$$\begin{aligned} & 2 \sum_{\omega''} \left[\sum_{\rho\tau} \langle \rho | s^0 | \tau \rangle \langle S, M'_S = S, \omega', w | a_{r\rho}^\dagger a_{r\tau} | S, M''_S = S, \omega'', w \rangle \right] \\ & \quad \times \left[\sum_{\sigma v} \langle \sigma | s^0 | v \rangle \langle S, M''_S = S, \omega'', w | a_{s\sigma}^\dagger a_{sv} | S, M_S = S, \omega, w \rangle \right] \\ & - \left(\frac{S-1}{S+1} \right) \sum_{\omega''} \left[\sum_{\rho\tau} \langle \tau | s^{+1} | \rho \rangle \langle S+1, M''_S = S+1, \omega'', w | a_{r\tau}^\dagger a_{r\rho} | S, M'_S = S, \omega', w \rangle \right] \\ & \quad \times \left[\sum_{\sigma v} \langle \sigma | s^{+1} | v \rangle \langle S+1, M''_S = S+1, \omega'', w | a_{s\sigma}^\dagger a_{sv} | S, M_S = S, \omega, w \rangle \right] \\ & - \sum_{\omega''} \left[\sum_{\sigma v} \langle v | s^{+1} | \sigma \rangle \langle S+1, M''_S = S, \omega'', w | a_{sv}^\dagger a_{s\sigma} | S, M'_S = S, \omega', w \rangle \right] \\ & \quad \times \left[\sum_{\rho\tau} \langle \rho | s^{+1} | \tau \rangle \langle S+1, M''_S = S, \omega'', w | a_{r\rho}^\dagger a_{r\tau} | S, M_S = S, \omega, w \rangle \right] \end{aligned} \quad (2.131)$$

$$w' = a_b^\dagger a_a w$$

$$\Delta S = 2$$

$$\begin{aligned} & \sum_{\omega''} \left[\sum_{\rho\tau} \langle \rho | s^{+1} | \tau \rangle \langle S+2, M_S = S+2, \omega', w' | a_{b\rho}^\dagger a_{a\tau} | S+1, M_S = S+1, \omega'', w \rangle \right] \\ & \quad \times \left[\sum_{\sigma v} \langle \sigma | s^{+1} | v \rangle \langle S+1, M_S = S+1, \omega'', w | a_{r\sigma}^\dagger a_{rv} | S, M_S = S, \omega, w \rangle \right] \end{aligned} \quad (2.132)$$

$$\Delta S = 1$$

$$\begin{aligned} & \sum_{\omega''} \left[\sum_{\sigma v} \langle \sigma | s^0 | v \rangle \langle S+1, M_S = S+1, \omega', w' | a_{r\sigma}^\dagger a_{rv} | S+1, M_S = S+1, \omega'', w' \rangle \right] \\ & \quad \times \left[\sum_{\rho\tau} \langle \rho | s^{+1} | \tau \rangle \langle S+1, M_S = S+1, \omega'', w' | a_{b\rho}^\dagger a_{a\tau} | S, M_S = S, \omega, w \rangle \right] \\ & + \sum_{\omega''} \left[\sum_{\rho\tau} \langle \rho | s^0 | \tau \rangle \langle S+1, M_S = S+1, \omega', w' | a_{b\rho}^\dagger a_{a\tau} | S+1, M_S = S+1, \omega'', w \rangle \right] \\ & \quad \times \left[\sum_{\sigma v} \langle \sigma | s^{+1} | v \rangle \langle S+1, M_S = S+1, \omega'', w | a_{r\sigma}^\dagger a_{rv} | S, M_S = S, \omega, w \rangle \right] \end{aligned} \quad (2.133)$$

$$\Delta S = 0$$

$$\begin{aligned} & 2 \sum_{\omega''} \left[\sum_{\rho\tau} \langle \rho | s^0 | \tau \rangle \langle S, M'_S = S, \omega', w' | a_{b\rho}^\dagger a_{a\tau} | S, M''_S = S, \omega'', w \rangle \right] \\ & \quad \times \left[\sum_{\sigma v} \langle \sigma | s^0 | v \rangle \langle S, M''_S = S, \omega'', w | a_{r\sigma}^\dagger a_{rv} | S, M_S = S, \omega, w \rangle \right] \\ & - \left(\frac{S-1}{S+1} \right) \sum_{\omega''} \left[\sum_{\rho\tau} \langle \tau | s^{+1} | \rho \rangle \langle S+1, M''_S = S+1, \omega'', w | a_{a\tau}^\dagger a_{b\rho} | S, M'_S = S, \omega', w' \rangle \right] \\ & \quad \times \left[\sum_{\sigma v} \langle \sigma | s^{+1} | v \rangle \langle S+1, M''_S = S+1, \omega'', w | a_{r\sigma}^\dagger a_{rv} | S, M_S = S, \omega, w \rangle \right] \\ & - \sum_{\omega''} \left[\sum_{\sigma v} \langle v | s^{+1} | \sigma \rangle \langle S+1, M''_S = S, \omega'', w' | a_{rv}^\dagger a_{r\sigma} | S, M'_S = S, \omega', w' \rangle \right] \\ & \quad \times \left[\sum_{\rho\tau} \langle \rho | s^{+1} | \tau \rangle \langle S+1, M''_S = S, \omega'', w' | a_{b\rho}^\dagger a_{a\tau} | S, M_S = S, \omega, w \rangle \right] \end{aligned} \quad (2.134)$$

$$w' = a_c^\dagger a_d^\dagger a_b a_a w$$

$$\Delta S = 2$$

$$\begin{aligned} & \sum_{\omega''} \left[\sum_{\rho\tau} \langle \rho | s^{+1} | \tau \rangle \langle S+2, M_S = S+2, \omega', w' | a_{c\rho}^\dagger a_{b\tau} | S+1, M_S = S+1, \omega'', w'' \rangle \right] \\ & \quad \times \left[\sum_{\sigma v} \langle \sigma | s^{+1} | v \rangle \langle S+1, M_S = S+1, \omega'', w'' | a_{d\sigma}^\dagger a_{av} | S, M_S = S, \omega, w \rangle \right] \end{aligned} \quad (2.135)$$

$$\Delta S = 1$$

$$\begin{aligned} & \sum_{\omega''} \left[\sum_{\sigma v} \langle \sigma | s^0 | v \rangle \langle S+1, M_S = S+1, \omega', w' | a_{d\sigma}^\dagger a_{av} | S+1, M_S = S+1, \omega'', w'' \rangle \right] \\ & \quad \times \left[\sum_{\rho\tau} \langle \rho | s^{+1} | \tau \rangle \langle S+1, M_S = S+1, \omega'', w'' | a_{c\rho}^\dagger a_{b\tau} | S, M_S = S, \omega, w \rangle \right] \\ & + \sum_{\omega''} \left[\sum_{\rho\tau} \langle \rho | s^0 | \tau \rangle \langle S+1, M_S = S+1, \omega', w' | a_{c\rho}^\dagger a_{b\tau} | S+1, M_S = S+1, \omega'', w'' \rangle \right] \\ & \quad \times \left[\sum_{\sigma v} \langle \sigma | s^{+1} | v \rangle \langle S+1, M_S = S+1, \omega'', w'' | a_{d\sigma}^\dagger a_{av} | S, M_S = S, \omega, w \rangle \right] \end{aligned} \quad (2.136)$$

$$\Delta S = 0$$

$$\begin{aligned} & 2 \sum_{\omega''} \left[\sum_{\rho\tau} \langle \rho | s^0 | \tau \rangle \langle S, M_S' = S, \omega', w' | a_{c\rho}^\dagger a_{b\tau} | S, M_S'' = S, \omega'', w'' \rangle \right] \\ & \quad \times \left[\sum_{\sigma v} \langle \sigma | s^0 | v \rangle \langle S, M_S'' = S, \omega'', w'' | a_{d\sigma}^\dagger a_{av} | S, M_S = S, \omega, w \rangle \right] \\ & - \left(\frac{S-1}{S+1} \right) \sum_{\omega''} \left[\sum_{\rho\tau} \langle \tau | s^{+1} | \rho \rangle \langle S+1, M_S'' = S+1, \omega'', w'' | a_{b\tau}^\dagger a_{c\rho} | S, M_S' = S, \omega', w' \rangle \right] \\ & \quad \times \left[\sum_{\sigma v} \langle \sigma | s^{+1} | v \rangle \langle S+1, M_S'' = S+1, \omega'', w'' | a_{d\sigma}^\dagger a_{av} | S, M_S = S, \omega, w \rangle \right] \\ & - \sum_{\omega''} \left[\sum_{\sigma v} \langle v | s^{+1} | \sigma \rangle \langle S+1, M_S'' = S, \omega'', w'' | a_{av}^\dagger a_{d\sigma} | S, M_S' = S, \omega', w' \rangle \right] \\ & \quad \times \left[\sum_{\rho\tau} \langle \rho | s^{+1} | \tau \rangle \langle S+1, M_S'' = S, \omega'', w'' | a_{c\rho}^\dagger a_{b\tau} | S, M_S = S, \omega, w \rangle \right] \end{aligned} \quad (2.137)$$

The individual position of the spatial indices r, s, a, b, c, d in Eqs. (2.129)–(2.137) is determined by the reformulations in the first part of the derivation (Ch. 2.2.2), see in

particular Eqs. (2.72)/(2.76)/(2.80).

On an implementational level, the case of $\Delta S = 2$ is obviously the most straightforward one. Additional complexity beyond an increase in the number of terms is introduced in the further spin coupling cases due to the intricate steps in the derivation. The transposition necessitated by the reexpression of the \hat{s}^{-1} operator manifests itself in permuted spatial indices, as can most clearly be observed for the case of $w' = a_c^\dagger a_d^\dagger a_b a_a w$. For $\Delta S = 0$ (Eq. (2.137)), we note for example that the first factor in term 2 exhibits a permutation of indices $b\tau/c\rho$ as compared to the first factor in term 1. On the other hand, the altered sequence of spin terms as necessitated by the construct of $M_S = S$ wave functions is reflected in the permuted appearance of the spin terms themselves, as can for example be observed in the comparison of term 2 and term 3 in Eq. (2.137) concerning the excitation $av/d\sigma$ which appears in term 2 within the second factor while being present in the first factor of term 3. As a consequence, we consider different configurations and therefore different CSFs in the two cases and have to determine the individual excitation patterns of these terms independently.

Concluding Examination

Comparing with the spin-orbit implementation, it has to be recognized that the extension of the η scheme to the case of the spin-spin operator increases the degree of complexity distinctly. While in the spin-orbit case, the spin element between two CSFs is expressed as a single η -coefficient:

$$\langle S', \omega', w' | \sum_{\rho\sigma} s_{\rho\sigma} a_{a\rho}^\dagger a_{b\sigma} | S, \omega, w \rangle = \eta(S', \omega', w'; S, \omega, w)$$

(see Eq. (1.33) and accompanying text), the corresponding evaluation in the spin-spin case entails the consideration of two (case $\Delta S = 2$) to six (case $\Delta S = 0$) η vectors, the length of which is given by the number of inserted CSFs $|\Upsilon''$). This can be most straightforwardly seen by inspection of Eqs. (2.98)/(2.105)/(2.128).

2.2.5 Spatial Integrals

The exposition so far covered the illustration of the program framework as well as the derivation of the spin-coupling expressions. The spin contribution is assembled together with the CI coefficients and the spatial integrals into the final matrix element (see Eq. (2.5)). The coefficients are present from a previous MRCI program run, while the two-electron spatial spin-spin integrals, denoted in this work in general as R_{rstu} (see Eqs. (2.10)/(2.23)/(2.30) for the concrete case dependent expressions, Eq. (1.2) for the individual operator components), had to be obtained in the course of the PhD project. The program DALTON already implements the calculation of spin-spin integrals over non-symmetry-adapted atomic orbitals and constituted therefore a suitable starting point for the present purpose. In the course of my PhD, I modified DALTON so as to

implement the calculation of integrals over symmetrized atomic orbitals which are now obtained in a preparatory program run. In the subsequent execution of SPOCK.SISTR, these integrals are present on corresponding integral files, read in at the beginning, and at the innermost level multiplied together with CI- and η -coefficients into the final matrix element.

Principal scheme

In order to obtain spatial spin-spin integrals, the DALTON code was extended to calculate integral derivatives over symmetry-adapted orbitals. In principle, the entire program operates with symmetry-adapted atomic orbitals F_{aA}^α (SOs) which constitute linear combinations of atomic orbitals f_{aA} (AOs) over symmetry-equivalent nuclear centers:

$$F_{aA}^\alpha = g^{-1} \sum_G \chi^\alpha(G) G f_{aA}, \quad (2.138)$$

with A referring to the symmetry equivalent nuclear centers, a to the type of orbital (s, p, d, \dots), α denoting the irreducible representation of the molecular point group \mathcal{G} , g its order, and $\chi^\alpha(G)$ referring to the characters associated with irrep α and symmetry operation G . The implementation of symmetry in a quantum chemistry program has in general the distinct advantage of possibly considerable savings in the size of the calculation related to the application of symmetry selection rules. With respect to the size of integral expressions in particular, the savings are on the order of g (at most $g = 8$ in the case of the point group D_{2h}). This is especially crucial for the case of the two-electron spin-spin integrals as the integral expressions consist of the six operator components $\frac{x_{ij}^2}{r_{ij}^5}$, $\frac{x_{ij}y_{ij}}{r_{ij}^5}$, $\frac{x_{ij}z_{ij}}{r_{ij}^5}$, $\frac{y_{ij}^2}{r_{ij}^5}$, $\frac{y_{ij}z_{ij}}{r_{ij}^5}$, $\frac{z_{ij}^2}{r_{ij}^5}$ which have to be transferred between DALTON and SPOCK.SISTR.

The spatial components of the two-electron spin-spin operator exhibit a close resemblance to second derivatives of the Coulomb operator [159]. This can be illustrated trivially by inspecting the example of a derivation of the Coulomb operator with respect to coordinate y of electron 1 and coordinate z of electron 2:

$$\frac{\partial^2}{\partial y_1 \partial z_2} \left(\frac{1}{r_{12}} \right) = \frac{\partial}{\partial y_1} \left(-\frac{z_{12}}{r_{12}^3} \right) = -\frac{3y_{12}z_{12}}{r_{12}^3}. \quad (2.139)$$

The most straightforward way to calculate two-electron spin-spin integrals constitutes therefore of calculating the second derivative of the integral expressions over the Coulomb operator with respect to electron 1/2:

$$\begin{aligned} & (\nabla_1 \nabla_1 + \nabla_2 \nabla_2 + \nabla_1 \nabla_2 + \nabla_1 \nabla_2) \left\langle \frac{1}{r_{12}} \right\rangle \rightarrow \\ & \left\langle \frac{x_{12}^2}{r_{12}^5} \right\rangle \left\langle \frac{3x_{12}y_{12}}{r_{12}^5} \right\rangle \left\langle \frac{3x_{12}z_{12}}{r_{12}^5} \right\rangle \left\langle \frac{y_{12}^2}{r_{12}^5} \right\rangle \left\langle \frac{3y_{12}z_{12}}{r_{12}^5} \right\rangle \left\langle \frac{z_{12}^2}{r_{12}^5} \right\rangle \end{aligned} \quad (2.140)$$

employing the notation $\langle \mathcal{O} \rangle = \langle rs | \mathcal{O} | tu \rangle$. Construction of the corresponding spin-spin integrals entails a summation of the second derivatives under appropriate consideration of sign changes and resulting prefactors. The advantage of an evaluation over

the second derivatives lies in the observation that most quantum chemistry codes already possess an implementation of integral derivatives, a necessity in the calculation of molecular properties. Therefore, the code modification required to obtain spin-spin integrals is in principle very modest. The step of calculating spin-spin integrals and the combination into integral expressions over AOs was already present in DALTON, the next step, the symmetrization of these integrals in order to obtain integral expressions over SOs, was not.

The theoretical foundations for the symmetrization of integral derivatives were laid in 1986 by Taylor [160]. The symmetrization of integrals is based on employing *double coset decomposition* (DCD), the details of the principal scheme can be found in [161]. The basic idea lies in introducing DCD to obtain a subset of operators R of \mathcal{G} , so-called *double coset representatives* (DCR). The set \mathcal{R} (with $R \in \mathcal{R}$) constitutes the minimum set of operators which generate all symmetry-distinct pairs $A-B$ (with nuclear centers A, B) by application of R onto B . Thereby, the number of transformations to obtain all unique two-center contributions is reduced to the absolute minimum. The extension to the four-center case holds analogously. For further details, the reader is referred to [160, 161]. I would like to illustrate though the most important consequences in the symmetrization of two-electron integrals by comparison of the resulting expressions as obtained through a direct straightforward approach versus the introduction of DCD.

A general operator belonging to the symmetry ε is denoted as \mathcal{O}^ε . Directly resolving the SOs according to Eq. (2.138), a general two-electron integral $\langle F_{aA}^\alpha F_{bB}^\beta | \mathcal{O}^\varepsilon | F_{cC}^\gamma F_{dD}^\delta \rangle$ is evaluated as:

$$\begin{aligned} \langle F_{aA}^\alpha F_{bB}^\beta | \mathcal{O}^\varepsilon | F_{cC}^\gamma F_{dD}^\delta \rangle &= g^{-4} \sum_G \sum_H \sum_I \sum_J \chi^\alpha(G) \chi^\beta(H) \chi^\gamma(I) \chi^\delta(J) \\ &\quad \times \langle G f_{aA} H f_{bB} | \mathcal{O}^\varepsilon | I f_{cC} J f_{dD} \rangle. \end{aligned} \quad (2.141)$$

Application of DCD in reexpressing symmetry operators G, H, I, J employing DCRs yields instead after some intricate derivation:

$$\begin{aligned} \langle F_{aA}^\alpha F_{bB}^\beta | \mathcal{O}^\varepsilon | F_{cC}^\gamma F_{dD}^\delta \rangle &= g^{-4} uvwx \lambda_T^{-1} I_{\alpha\beta\gamma\delta\varepsilon} \sum_R \sum_S \sum_T \chi^\beta(R) \chi^\gamma(T) \chi^\delta(TS) \\ &\quad \times p_b(R) p_c(T) p_d(TS) \langle f_{aA} f_{bR(B)} | \mathcal{O}^\varepsilon | f_{cT(C)} f_{dTS(D)} \rangle. \end{aligned} \quad (2.142)$$

This at first sight more complicated expression is evaluated straightforwardly, as most of the appearing quantities constitute simple factors. The prefactor $g^{-4} uvwx \lambda_T^{-1}$ is composed of orders of (sub)groups and the individual elements therefore attain values between 1 and 8, $I_{\alpha\beta\gamma\delta\varepsilon}$ represents the selection rule as the direct product of the involved irreps has to belong to the totally symmetric one ($\alpha \otimes \beta \otimes \gamma \otimes \delta \otimes \varepsilon = A_1$), R, S, T refer to DCRs and therefore denote a (sub)set of the operations G of \mathcal{G} , and $p_b(R), p_c(T), p_d(TS)$ represent parity factors of ± 1 .

In comparison of Eq. (2.141) with Eq. (2.142), we neglect the prefactors in both expressions as they are trivially evaluated. The most apparent difference and point of saving

lies in the summation: First, a reduction from a quadruple to a triple summation was achieved. Second, the triple summation only extends over the DCRs R, S, T , thereby covering a subset of \mathcal{G} . This observation is directly related to the beforehand mentioned properties of DCRs: We have selected the minimum subset of operators with which we can generate all symmetry-distinct integral expressions. In a summation over all elements G, H, I, J as in Eq. (2.141), possibly identical integrals are evaluated multiple times. In the introduction of double coset decomposition, we are able to eliminate these redundancies.

Existing Approach in Dalton

Although DALTON in principle operates with SOs, this is not the case in the calculation of electron spin-spin coupling which is implemented employing AOs. This apparent inconsistency is directly related to the evaluation of zero-field splitting solely as an expectation value within DALTON and will be clarified in the following.

The calculation of an expectation value over an arbitrary operator \mathcal{O}^ε can in principle be evaluated as a trace operation according to:

$$\sum_{\alpha\beta\gamma\delta} \sum_{aA bB cC dD} P_{aA bB cC dD}^{\alpha\beta\gamma\delta} \langle F_{aA}^\alpha F_{bB}^\beta | \mathcal{O}^\varepsilon | F_{cC}^\gamma F_{dD}^\delta \rangle \quad (2.143)$$

with P referring to the second-order reduced density matrix, incorporating the information concerning molecular orbitals. The above integral is formulated over SOs and thereby encapsulates the symmetry information of the molecular system. Alternatively, expressing the SO integrals according to Eq. (2.142) and exchanging summations while rearranging factors, we can reformulate:

$$\begin{aligned} & \sum_{aA bB cC dD} \sum_{\alpha\beta\gamma\delta} P_{aA bB cC dD}^{\alpha\beta\gamma\delta} \langle F_{aA}^\alpha F_{bB}^\beta | \mathcal{O}^\varepsilon | F_{cC}^\gamma F_{dD}^\delta \rangle \\ = & \sum_{aA bB cC dD} \sum_{RST} \sum_{\alpha\beta\gamma\delta} P_{aA bB cC dD}^{\alpha\beta\gamma\delta} g^{-4} uvwx \lambda_T^{-1} I_{\alpha\beta\gamma\delta\varepsilon} \chi^\beta(R) \chi^\gamma(T) \chi^\delta(TS) \\ & \times p_b(R) p_c(T) p_d(TS) \langle f_{aA} f_{bR(B)} | \mathcal{O}^\varepsilon | f_{cT(C)} f_{dTS(D)} \rangle \end{aligned} \quad (2.144)$$

$$= \sum_{aA bB cC dD} \sum_{RST} P_{aA bB cC dD}^{RST} \langle f_{aA} f_{bR(B)} | \mathcal{O}^\varepsilon | f_{cT(C)} f_{dTS(D)} \rangle \quad (2.145)$$

with

$$\begin{aligned} P_{aA bB cC dD}^{RST} = & \sum_{\alpha\beta\gamma\delta} g^{-4} uvwx \lambda_T^{-1} I_{\alpha\beta\gamma\delta\varepsilon} \chi^\beta(R) \chi^\gamma(T) \chi^\delta(TS) \\ & \times p_b(R) p_c(T) p_d(TS) P_{aA bB cC dD}^{\alpha\beta\gamma\delta}. \end{aligned} \quad (2.146)$$

Comparing Eq. (2.143) with Eq. (2.145), we recognize that the symmetrization information was transferred from the integrals to the second-order reduced density matrix.

In the actual program execution, Eq. (2.145) is evaluated by first symmetrizing the density matrix (e.g., calculating $P_{aA bB cC dD}^{RST}$) and subsequently employing the existing symmetry loop structure over R, S, T to assemble the trace expression. The integrals over AOs can be calculated within each loop anew and immediately discarded after folding together with the corresponding density expression. In the case of the present example, there is no distinct advantage associated with either choosing to symmetrize the AOs (Eq. (2.143)) or symmetrizing the reduced density matrix (Eq. (2.145)) instead. If we are considering on the other hand the evaluation of ZFS where we introduce 21 second order derivatives instead of the single integral expression appearing in Eqs. (2.143)/(2.145), it is obvious that the single symmetrization of the reduced density matrix is more efficient than symmetrizing 21 AO-integral expressions. Therefore, within DALTON, it was chosen to calculate the ZFS as a trace operation employing AO integrals and a symmetrized second-order reduced density matrix (Eq. (2.145)). The choice between these two transformations is only possible in the evaluation of an expectation value since the reformulation in Eq. (2.144) is based on the possibility of associating the symmetry loop structure either with the second-order reduced density matrix or the integral expression. This is permitted as the presence of complete summation indices allows for an arbitrary permutation of the appearing factors. If we are not evaluating trace expressions, a formulation according to Eq. (2.143) employing the second-order reduced density matrix does obviously not occur. In the calculation of matrix elements between different states, as is implemented within SPOCK.SISTR, we therefore have to resolve to incorporating the symmetry information in the integral expression and thereby employ SO integrals if we want to take advantage of the computational savings associated with the consideration of symmetry.

Interlude

At this point, I have illustrated the principal program structure and outlined the processing based on configuration comparison. Formulas for the calculation of the spin contribution were derived and the concrete expressions implemented in SPOCK.SISTR explicitly stated. The mechanism of obtaining the spatial contribution to the matrix element expression was introduced.

The presentation on this abstract conceptual/mathematical level has now to be set into the context of the program implementation. In the remaining part of the chapter, I will parallel structural aspects of the evaluation with the level of program routines and internal processing. After outlining briefly the overall connection of the spin-spin routines, I will consider each of these routines individually and describe the position in the calculation of spin-spin matrix elements.

2.3 Implementation

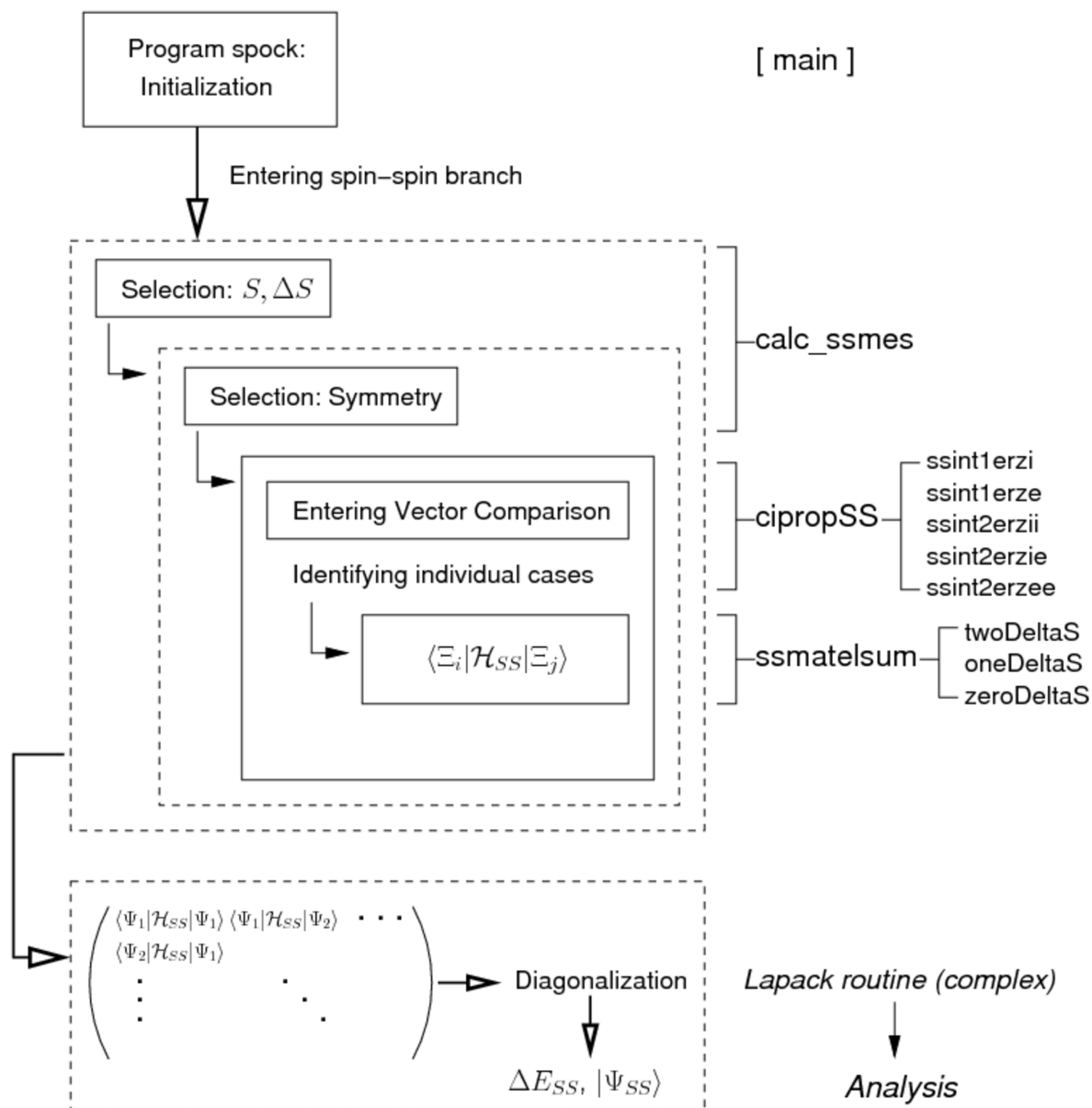


Figure 2.5: Contrasting: Structure/Major routines of SPOCK.SISTR

In Fig. 2.5, I display the program structure of SPOCK.SISTR as introduced abstractly in Fig. 2.1, facing additionally on the right-hand side the implementational level with reference to program routines. The initialization process driven by the routine `main` employs the program logic previously implemented in SPOCK. It is concerned with reading of input parameters passed into the program and establishing information of molecular states provided by a previous MRCI calculation. After return to `main`, different branches of the program can be called from the driving routine as specified in the input file, one of it being the evaluation of the spin-spin contribution. The

execution of SPOCK.SISTR is initialized by call to `calc_ssmes`, the driving routine of the spin-spin branch which in turn controls the entire calculation of spin-spin matrix elements.

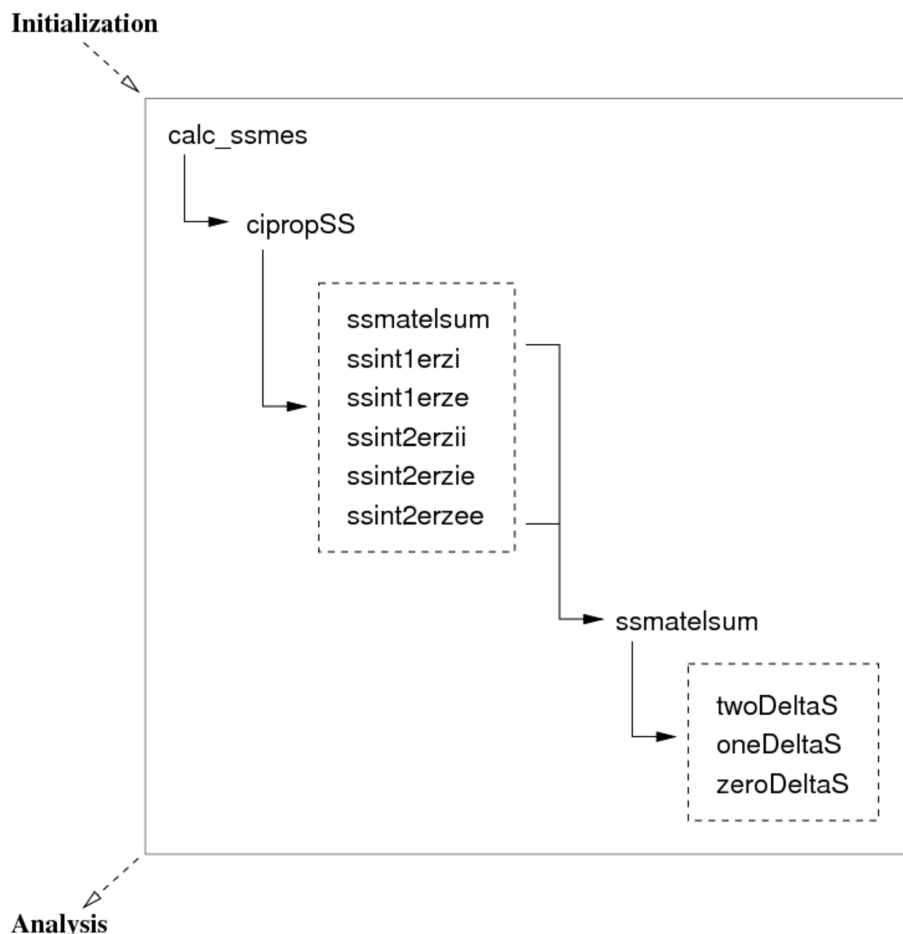


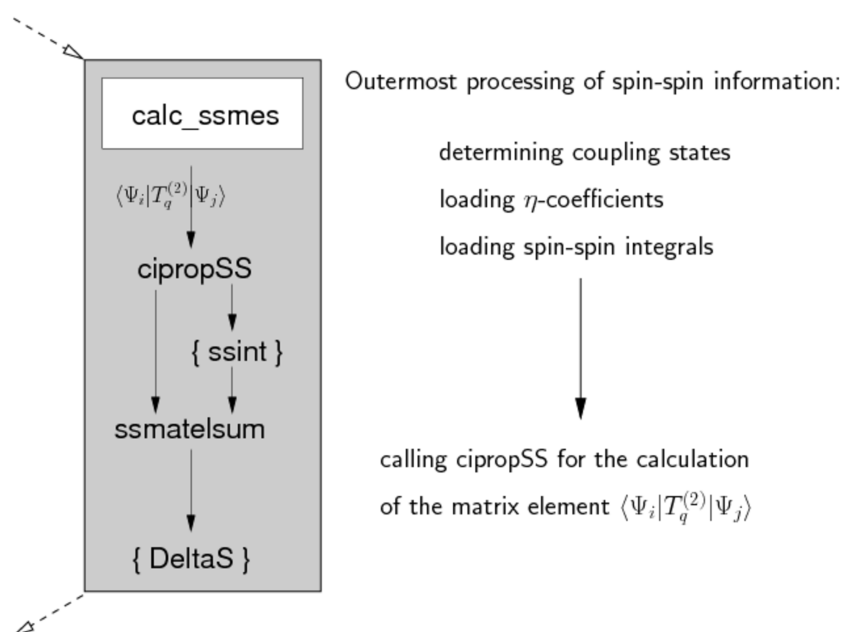
Figure 2.6: Hierarchy of spin-spin routines in SPOCK.SISTR

Fig. 2.5 depicts the correspondence of program routines to the structure of the computational evaluation of spin-spin matrix elements; Fig. 2.6 indicates in turn the hierarchy among these routines. Dashed boxes encompass a set of related routines one of which is actually called in an individual loop execution, a case decision determined by the information of individual configurations (set `{ssint}`) and by the difference in spin ΔS (set `{deltaS}`).

Each of the intermediate routines is dedicated to the stepwise processing of configuration information before passing its results downwards until the lowest level of the actual multiplication of CI coefficients and η -values is reached in `{deltaS}`. After having now set the spin-spin branch into the program context and outlined the hierarchy between the program routines involved, I will at this point turn to the individual components and step in detail through the algorithm of the spin-spin calculation.

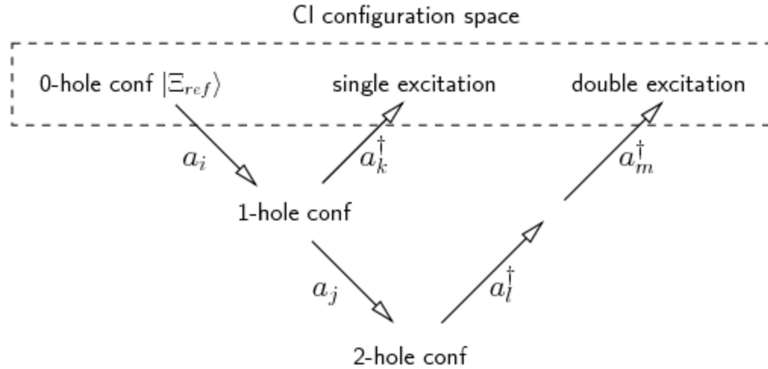
(I). `calc_ssmes`

The driving routine of the spin-spin branch evaluates the information about spin and spatial symmetry of states passed in from `main` on the basis of the selection rules for spin-spin coupling. After establishing the knowledge about coupling states over operator components for the entire program run, η -coefficients for a particular pair of coupling multiplicities are loaded as determined by the spin of the individual states and their difference ΔS . Spatial spin-spin integrals are read into memory based on the spatial symmetry of the two states (which determines the spatial symmetry of the coupling operator component). The subsequent program structure is executed for each operator component $\hat{T}_q^{(2)}$ and pair of states $|\Psi_i\rangle, |\Psi_j\rangle$ successively, thereby passing on the evaluation of the single matrix element $\langle \Psi_i | T_q^{(2)} | \Psi_j \rangle$ to `cipropSS`.

Figure 2.7: `calc_ssmes`(II). `cipropSS`

Upon entry of `cipropSS`, detailed information on the states $|\Psi_i\rangle, |\Psi_j\rangle$ is established by reading configuration information and associated CI coefficients $\{c^i\}, \{c^j\}$ from file. The configuration space itself is structured based on the algorithm of configuration generation and processing of the preceding MRCI calculation [153, 162]: The set of reference configurations $|\Xi_{ref}\rangle$ is specified by the user and constitutes the core from which the full CI space is generated by application of single and double excitations. The information about the full configurational space is stored relative to the configurations of the reference space. Associated with individual reference configurations are 1-hole and 2-hole configurations

which are obtained by application of one or two annihilation operators a_i . The final CI configurations are generated by subsequent application of the appropriate number of creation operators a_k^\dagger .



We therefore have a division of the configuration space into 0-hole, 1-hole and 2-hole configurations. A classification of the applied excitation is introduced by the categorization of the MO space into internal and external, distinguishing thereby between MOs which are occupied in at least one reference configuration and MOs which are not occupied in any reference. Originating from an n -hole configuration ($n = 1, 2$), an excitation within the internal or into the external MO space is possible.

The classification scheme of the configuration space mirrors the conceptual relation of MRCI as well SPOCK to the notion of second quantization. It further strongly influences the subsequent configuration processing, the principles of which are common to the spin-free, spin-orbit and, derived from those, the spin-spin code: Within **ciproSS**, the configurations of bra $\langle\Psi_i|$ and ket $|\Psi_j\rangle$ are processed successively in groups of n -hole configurations ($n = 0, 1, 2$). We therefore identify the following six batches corresponding to the possible distinct pairings of bra and ket:

- (1). 0-hole configuration – 0-hole configuration
- (2). 0-hole configuration – 1-hole configuration
- (3). 1-hole configuration – 1-hole configuration
- (4). 0-hole configuration – 2-hole configuration
- (5). 1-hole configuration – 2-hole configuration
- (6). 2-hole configuration – 2-hole configuration.

I note for completeness that in the case of differing configuration spaces for $\langle\Psi_i|$ vs. $|\Psi_j\rangle$, the processing of a pair of the kind m -hole – n -hole with $n \neq m$ (cases 2,4,5) necessitates two executions, namely the group of elements $\langle(m)\Psi_i|T_q^{(2)}|(n)\Psi_j\rangle$ and $\langle(n)\Psi_i|T_q^{(2)}|(m)\Psi_j\rangle$. Internally, this is executed by treatment of the second combination as a transposed matrix element, the details of which will be omitted

as they are intricate and not relevant for the understanding of the algorithm.

Within a particular group $\langle m\text{-hole} | - | n\text{-hole} \rangle$, the processing performed in `cipropSS` consists of the application of n creation operator(s) onto the n -hole-configuration $|\Xi_l\rangle$ of the ket and assessment of the difference in spatial occupation to the m -hole configuration $\langle \Xi_k |$ of the bra. The further evaluation of the matrix element is passed downwards by call to one of the routines out of the set denoted $\{\text{ssint}\}$ or possibly the routine `ssmatelsum` itself in the case of the batch 0-hole – 0-hole configuration.

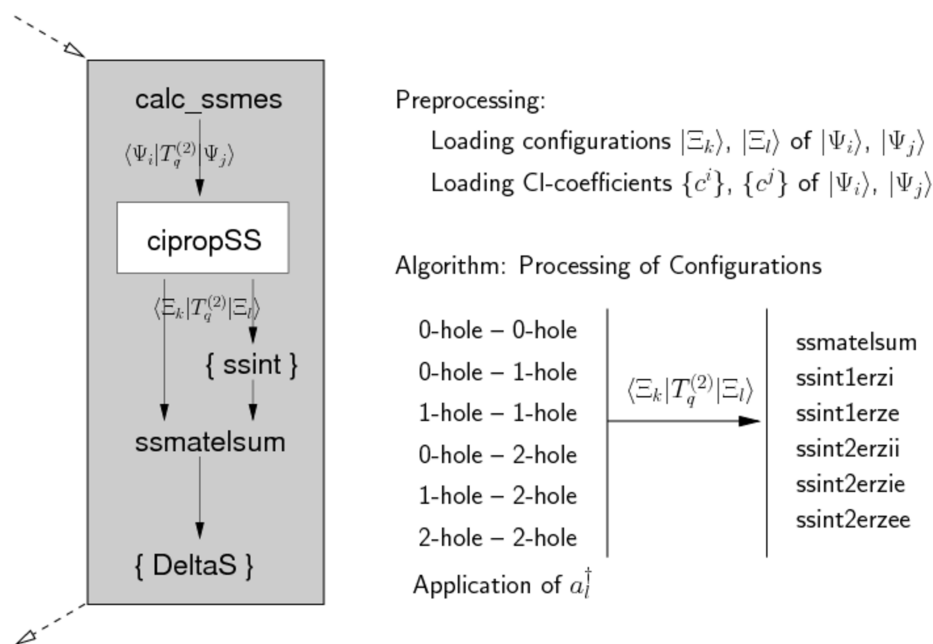


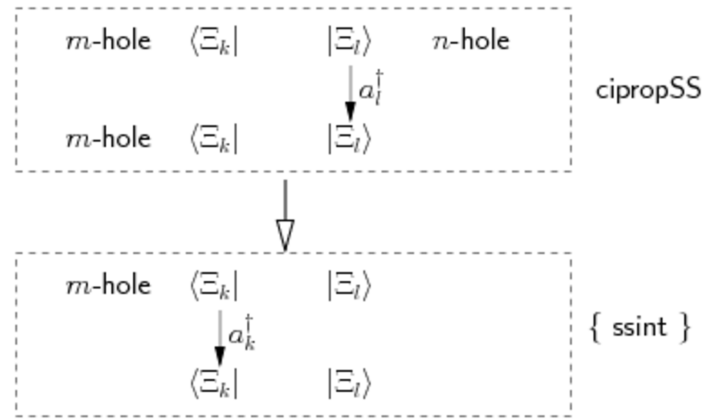
Figure 2.8: `cipropSS`

(III). $\{\text{ssint}\}$

The individual names of the routines $\{\text{ssint}\} = \text{ssint1erzi}, \text{ssint1erze}, \text{ssint2erzii}, \text{ssint2erzie}, \text{ssint2erzee}$ reflect the previous configuration processing of the ket $|\Psi_j\rangle$. The number denotes the origin in a 1- or 2-hole configuration while the trailing letters or letter combinations of i/e refer to the creation operator(s) and indicate an excitation into the internal/external space of molecular orbitals.

Upon entry of an $\{\text{ssint}\}$ routine, the configuration $|\Xi_l\rangle$ constitutes a single or double excitation with respect to a reference configuration $|\Xi_{ref}\rangle$ while the configuration $\langle \Xi_k |$ represents at this stage an m -hole configuration ($m = 0, 1, 2$). The processing of the n -hole configuration of the ket was performed in `cipropSS`. The corresponding treatment of the m -hole configuration of the bra in terms of the application of the creation operator(s) a_k^\dagger is realized within the $\{\text{ssint}\}$ rou-

tine. The accompanying processing entails a synchronization of the information about creation and annihilation operators of bra and ket, accounting for redundant (de)excitations.



This step generates thereby finally two valid configurations $|\Xi_k\rangle, |\Xi_l\rangle$ of the CI calculation space. Their difference in spatial occupation is stored as the number of creation/annihilation operators ($idiff = 0, 1, 2$) and the individual values of a, a^\dagger which connect $\langle \Xi_k |$ with $|\Xi_l\rangle$. Together with the CI coefficients read previously in `cipropSS`, this information is passed downwards for the evaluation of the particular matrix element $\langle \Xi_k | T_q^{(2)} | \Xi_l \rangle$ by `ssmatelsum`.

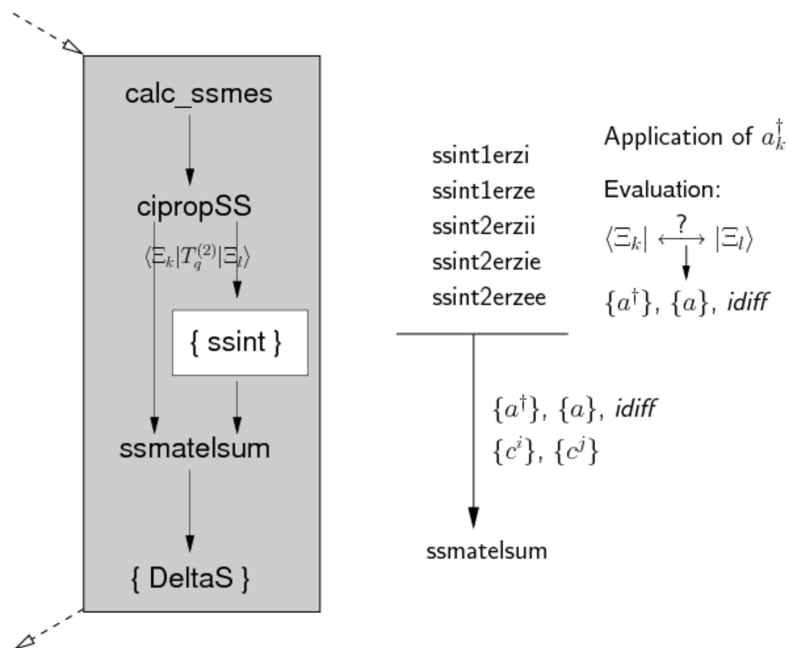


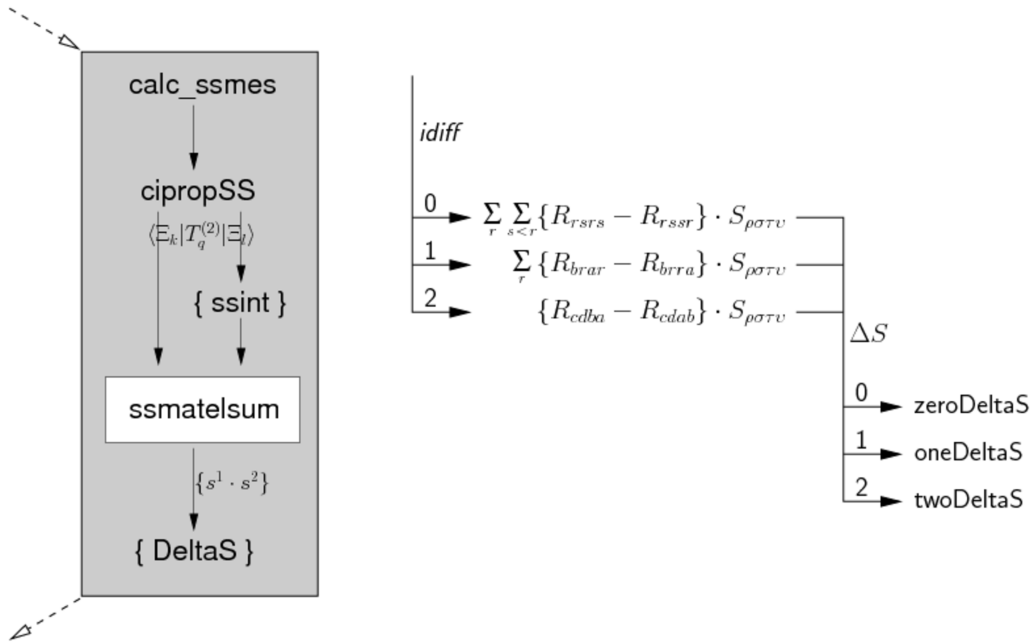
Figure 2.9: `{ssint}`

(IV). `ssmatelsum`

The routine `ssmatelsum` is called by `cipropSS` in the case of the 0-hole – 0-hole branch and by an `{ssint}` routine in the case of the execution of any other batches.

The first branching decision is governed by the difference in excitation $idiff$, as this impacts the further execution in the possible summation over open shells common to the configurations $|\Xi_k\rangle, |\Xi_l\rangle$. For $idiff = 2$ and thereby evaluation of the element $\langle \Xi_k | a_c^\dagger a_d^\dagger a_b a_a | \Xi_l \rangle$, the spatial contribution is entirely determined by the creation and annihilation operators that connect $\langle \Xi_k |$ with $|\Xi_l\rangle$, the case $idiff = 1$ entails a single summation over open shells r common to the two configurations, while for $idiff = 0$, a double summation over common shells r, s is initiated within `ssmatelsum` (see Eqs. (2.72)/(2.76)/(2.80)).

For a particular quadruplet of orbital indices, the spatial contribution is calculated as the difference of two integrals and the evaluation of the spin part deferred to one of the `{DeltaS}` routines.

Figure 2.10: `ssmatelsum`(V). `{DeltaS}`

Until this point, the at most double excitation between $\langle \Xi_k |$ and $|\Xi_l\rangle$ was passed on as a set of creation and annihilation operators. It is in the `{DeltaS}` routine that this compound expression is resolved into the product of two single excitations according to the insertion of the resolution of identity. The two resulting individual expressions are treated independently for the determination of

patterns and subcases. It is in the subsequent step that finally the information concerning the spin part is evaluated and incorporated into the calculation: The required set of η -coefficients as determined by excitation pattern and the case of the called routine is requested from memory. Thereby, the association of a particular excitation with the \hat{s}^0 or \hat{s}^{+1} operator is established.

The computational labour differs in this respect for the routines `twoDeltaS`/`oneDeltaS`/`zeroDeltaS` in that `twoDeltaS` entails the calculation of a single product expression, while `oneDeltaS` necessitates a sum of two product expression and in the case of `zeroDeltaS`, we are faced with three terms (see Eqs. (2.129)–(2.137)). This affects not only the arithmetic workload but impacts the number of pattern expressions that have to be determined and evaluated, which is between two (`twoDeltaS`) and six (`zeroDeltaS`).

Remembering that the entire matrix element is assembled as a product of spatial integrals, spin contribution and CI coefficients (see Eq. (2.5) and accompanying text in Ch. 2.2), we recognize that on the previous level in `ssmatelsum`, the spatial part associated with the element $\langle \Xi_k | T_q^{(2)} | \Xi_l \rangle$ is considered. It is in the last step of the processing in `{DeltaS}` that the further information of CI- and spin coupling is incorporated. We therefore obtain for the contribution of $\langle \Xi_k | T_q^{(2)} | \Xi_l \rangle$ to $\langle \Psi_i | T_q^{(2)} | \Psi_j \rangle$:

$$\langle \Xi_k | T_q^{(2)} | \Xi_l \rangle = \sum_{\Upsilon'} \sum_{\Upsilon} c^i(\Upsilon') c^j(\Upsilon) \langle \Upsilon' | T_q^{(2)} | \Upsilon \rangle \quad (2.147)$$

$$= \sum_{\Upsilon'} \sum_{\Upsilon} c^i(\Upsilon') c^j(\Upsilon) \sum_{\Upsilon''} \{ \langle \Upsilon' | s^1 | \Upsilon'' \rangle \langle \Upsilon'' | s^2 | \Upsilon \rangle \}, \quad (2.148)$$

resolving in the last step the operator component $T_q^{(2)}$ as $T_q^{(2)} = \{s^1 \cdot s^2\}$ for the general case, which may entail more than one term in the individual case, and obtaining the familiar product of two spin operator expressions under insertion of the resolution of identity $1 = \sum_{\Upsilon''} |\Upsilon''\rangle \langle \Upsilon''|$.

The spin expression $\{ \langle \Upsilon' | s^1 | \Upsilon'' \rangle \langle \Upsilon'' | s^2 | \Upsilon \rangle \}$ denotes the matrix element between two CSFs $|\Upsilon'\rangle$, $|\Upsilon\rangle$ over a general spin operator component $T_q^{(2)}$ and corresponds thereby to the spin- η -coefficient expressions that were derived for the specific cases (see Eqs. (2.97)/(2.98) for $\Delta S = 2$, Eqs. (2.104)/(2.105) for $\Delta S = 1$, Eqs. (2.127)/(2.128) for $\Delta S = 0$). Continuing with the compound notation of a CSF as $|\Upsilon\rangle$ instead of the resolution into $|\Upsilon\rangle = |S, M_S, \omega, w\rangle$ which was chosen in respective equations, the above matrix element can be formulated employing η -coefficients as:

$$\langle \Xi_k | T_q^{(2)} | \Xi_l \rangle = \sum_{\Upsilon'} \sum_{\Upsilon} c^i(\Upsilon') c^j(\Upsilon) \sum_{\Upsilon''} \{ \eta(\Upsilon'; \Upsilon'')^{(1)} \cdot \eta(\Upsilon''; \Upsilon)^{(2)} \}. \quad (2.149)$$

We recognize that calculation of the matrix element $\langle \Xi_k | T_q^{(2)} | \Xi_l \rangle$ entails the multiplication of two matrices, the dimensions of which are determined by the number of CSFs that are affiliated with the configurations $|\Xi_k\rangle$, $|\Xi_l\rangle$ and $|\Xi''\rangle$.

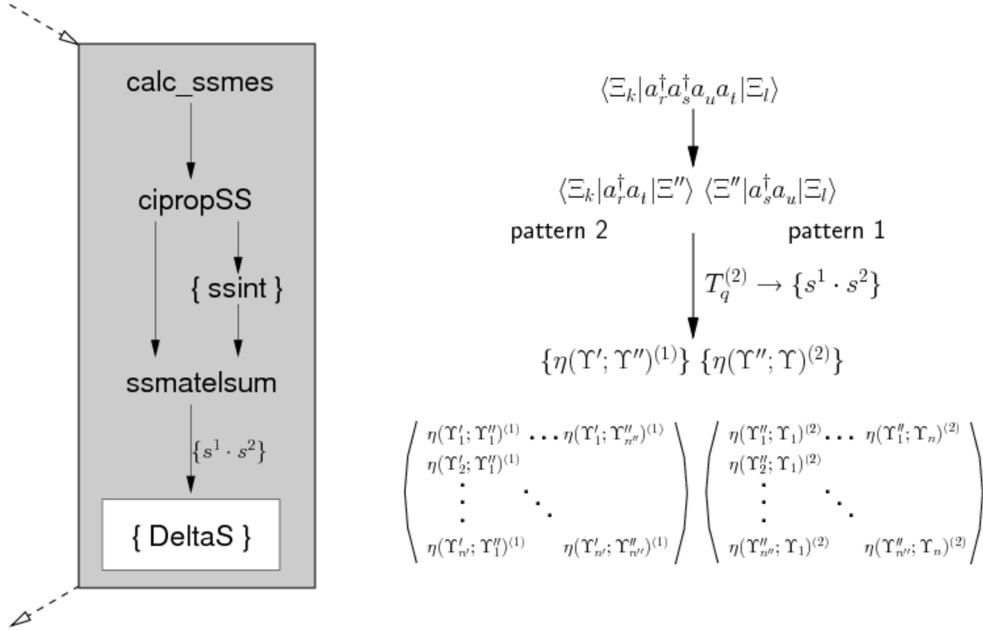


Figure 2.11: { DeltaS }

In summary, the principle of the calculation of the spin-spin contribution for CI wave functions is based on the evaluation of the matrix element $\langle \Psi_i | T_q^{(2)} | \Psi_j \rangle$ between wave functions $|\Psi_i\rangle$, $|\Psi_j\rangle$ in terms of the contributions of elements $\langle \Xi_k | T_q^{(2)} | \Xi_l \rangle$ between configurations $|\Xi_k\rangle$, $|\Xi_l\rangle$. It is not until the very last step in this process that the information about individual CSFs is assessed through CI- and η -coefficients.

The above algorithm is executed for the calculation of matrix elements between $M_S = S$ wave functions. Subsequent application of the WET (see p. 30 ff in Ch. 1.5.1) enables the construction of the entire interaction matrix over the spin-spin operator, as indicated in Fig. 2.5. Diagonalization is performed by call to the Lapack-routine ZHEEVD which is suitable for the calculation of eigenvalues and eigenvectors of a complex Hermitian matrix. We obtain the spin-spin eigenvalues and the eigenvectors as linear combinations of the unperturbed MRCI states. In the case of a triplet state, the eigenvalues are further processed for a calculation of the zero-field splitting values D and E of the triplet manifold.

2.3.1 Program Execution

On the level of program execution, the preparatory step for SPOCK.SISTR consists of obtaining the spin-spin integrals by running a local version of DALTON in which the sym-

metrization of second derivative integrals was implemented according to Eq. (2.142). The spin-spin integrals are written to six files, a subsequent transformation from the SO to the MO basis is performed employing the program FLASH [163]. The DFT/MRCI code is executed unaltered, yielding the multireference wave function(s) in the appropriate scratch directories. The spin-spin integral files are read into memory at the beginning of the SPOCK.SISTR program run. During code execution, the two-electron spin-spin interaction between pairs of configurations $|\Xi_k\rangle, |\Xi_l\rangle$ is evaluated based on Eq. (2.3), with the resolution of the matrix element expression between pairs of CSFs as given in Eqs. (2.72)/(2.76)/(2.80). The spin-coupling contribution is resolved according to Eqs. (2.129) – (2.137), at which point the appropriate η -coefficients, spin-spin integrals and CI coefficients are loaded from memory and assembled as the contribution of $\langle \Xi_k | \mathcal{H}_{SS} | \Xi_l \rangle$ to the matrix element $\langle \Psi_i | \mathcal{H}_{SS} | \Psi_j \rangle$ between the MRCI-wave functions $|\Psi_i\rangle, |\Psi_j\rangle$.

2.4 Conclusion

In the present chapter, I have presented the inner workings of the program SPOCK.SISTR: The equations employed in the calculation of electron spin-spin coupling were derived in detail, the principle of the implementation in terms of processing of configurations and assembling of individual matrix elements was outlined. In the following chapter, I will illustrate the program operation with suitable test cases.

Chapter 3

Calculations

I turn now to the actual program execution which I illustrate with sample calculations. The initial test phase encompassed di- and triatomic systems, the advantage of which lay in the high symmetry of these molecules. In this phase, useful insight was obtained with respect to the general behaviour and convergence of electron spin-spin coupling. The choice of subsequent molecules was strongly influenced by the interests of the group of Theoretical and Computational Chemistry at the University of Düsseldorf. In the context of this thesis, I present the following calculations:

1. The ZFS of the triplet ground state of O₂ is a common test case for the evaluation of electron spin-spin coupling and comparison calculations from different groups are accessible. In the implementation of SPOCK.SISTR, the execution involves a test of the $\Delta S = 0$ branch, corresponding to Eqs. (2.131)/(2.134)/(2.137). The relevance of ionic and covalent contributions and their balanced description in this system is a salient point which has not been discussed so far. Furthermore, I investigated on this system the convergence behaviour of electron spin-spin coupling with the size of the CI space, gaining insights of general relevance in the calculation of this effect.
2. An off-diagonal spin-coupling element of SPOCK.SISTR was assessed with calculations of the singlet–quintet coupling in NH, corresponding to an execution of the $\Delta S = 2$ branch (Eqs. (2.129)/(2.132)/(2.135)). This choice was motivated by the increasing spin-spin coupling between $c^1\Pi$ and $1^5\Sigma^-$ at larger bond distances, as discussed in the context of predissociation of the $c^1\Pi$ state by Bohn et al. [164,165].
3. Conjugated hydrocarbons possess the possibility for delocalization of uncoupled electrons, allowing for a stabilization of excited states. The mechanism of excitation and de-excitation of photoactive substances belonging to this class, such as carotenoids, is not understood in detail so far. Electron spin-spin coupling as a means of assessing the average interelectronic distance between unpaired electrons is a promising instrument in this context. In this work, I present calculations on the triplet states of the smaller all-*trans* polyenes. Investigation of these systems constitutes a first step towards understanding electron distributions in structurally related larger compounds. These calculations involve application of the DFT branch of the DFT/MRCI program.

3.1 O₂

The triplet ground state of O₂ constitutes the first test case of SPOCK.SISTR. High-level correlation calculations on this system were previously reported by Vahtras et al. [48] as well as Sinnecker and Neese [124]. Vahtras et al. performed CASSCF calculations employing DALTON, choosing an active space of 10 electrons in 12 active orbitals (the three lowest orbitals $1\sigma_g$, $1\sigma_u$, $2\sigma_g$ were kept inactive) and the aug-cc-pCVTZ [166,167] basis set. Sinnecker and Neese [124] performed calculations with the ORCA [168] electronic structure program. Spin-spin coupling was evaluated from a CASSCF wave function (active space of 12 electrons in 8 orbitals), applying their approximate SSC implementation based on the product decomposition of the two-electron density. Furthermore, calculations with restricted and unrestricted DFT (B3LYP) were carried out. Basis sets under consideration were EPR-II, EPR-III [169] and QZVP [170].

Single-point calculations on O₂ were performed at an internuclear distance of $r_e = 1.207$ Å, consistent with Vahtras et al. [48] and Sinnecker and Neese [124]. Second-order spin-orbit (D_{SO}) and first-order spin-spin effects (D_{SS}) are of similar magnitude in this system. The exact contribution of D_{SO} vs. D_{SS} has been a point of argument over a period of several decades, as was discussed by Vahtras et al. as well as by Langhoff [58] and by Langhoff and Kern [27]. The experimental value of D ($= D_{SO} + D_{SS}$) is well established to be 3.965 cm⁻¹ [171,172], and it is agreed meanwhile from computational investigations that SOC contributes to a larger extent than SSC. Spin-orbit CI calculations with SPOCK were performed to provide a value for D_{SO} and thereby assess D .

Vahtras et al. determined a D_{SS} value of 1.44 cm⁻¹. Sinnecker and Neese reported calculations with BP, B3LYP and CASSCF in the range of 1.52 to 1.59 cm⁻¹, with smaller values ($1.52 - 1.55$ cm⁻¹) in the EPR-II basis, and slightly larger ones in EPR-III and QZVP ($1.57 - 1.58$ cm⁻¹). The difference in the methodological treatment amounted to at most 0.02 cm⁻¹. In general, little is established about SSC with respect to basis-set dependencies and convergence behaviour. In this context, Havlas et al. [79] investigated CH₂ with basis sets ranging in quality from STO-3G to aug-cc-pVTZ employing different methods and found that most basis sets (except for the clearly deficient STO-3G basis) provide D and E values in the right range, although fully converged results were not obtained yet.

The present investigation encompassed basis sets cc-pVDZ, cc-pVTZ, cc-pVQZ, aug-cc-pVDZ, aug-cc-pVTZ, and aug-cc-pVQZ [166,173]. Molecular orbitals were obtained from an ROHF TURBOMOLE-DSCF [148,149,174]-calculation of the triplet state. The orbitals $1\sigma_g$ and $1\sigma_u$ were kept frozen throughout. In the MRCI calculations, reference spaces of various sizes were chosen, constructing wave functions from the reference configurations only and from all single and double excitations (SD) out of the chosen reference space — no configuration selection was applied so as to exclude a further variable from the investigation. All calculations utilized the RI-integral approximation [150,151] and energies given include Davidson correction unless otherwise stated.

Throughout the discussion, I provided values for D_{SS} including four decimal places for the illustration of trends. The final value for D is provided with two decimal places as a more realistic reflection of the intrinsic precision.

3.1.1 One- vs. Two-Center Contributions

In the first part of my investigation, I operated with a strongly simplified space with no excitations out of the references. The most important basis-set independent finding relates to a one-configuration vs. a two-configuration description of O₂. Table 3.1 lists D_{SS} for the HF ground state reference Ψ_0 (valence occupation: $\sigma_g^2 \pi_u^4 \pi_g^2$), and for a calculation including Ψ_0 and the $\pi_u^2 \rightarrow \pi_g^2$ doubly excited configuration with the valence occupation $\sigma_g^2 \pi_u^2 \pi_g^4$ denoted Ψ_1 .

	Ψ_0	$\Psi_0 + \Psi_1$
cc-pVDZ	1.5094	0.7244
cc-pVTZ	1.5197	0.7421
cc-pVQZ	1.5223	0.7434
aug-cc-pVDZ	1.5054	0.7280
aug-cc-pVTZ	1.5192	0.7420
aug-cc-pVQZ	1.5222	0.7430

Table 3.1: Values for $D_{SS}[\text{cm}^{-1}]$ in O₂: The one- and two-configuration case (no further excitations)

The CI coefficients in the two-configuration case range between 0.9730 and 0.9733 for Ψ_0 and -0.2296 and -0.2309 for Ψ_1 . The substantial decrease in D_{SS} upon inclusion of Ψ_1 is easily understood when interpreting the wave function with respect to covalent versus ionic contributions. In this argument, only the occupation of π_u and π_g is of relevance, and we will omit further occupied and empty shells. The configuration Ψ_0 corresponds therefore to the occupation $\pi_u^4 \pi_g^2$, but we can equally well treat it as a two-hole instead of a six-electron configuration, that is, it is equivalent to π_g^2 . With the same argument, Ψ_1 corresponds to π_u^2 . The wave function Ψ composed of $\Psi_0 + \Psi_1$ can therefore be written as:

$$\Psi = c_1 |\pi_{gx} \pi_{gy}| + c_2 |\pi_{ux} \pi_{uy}| \quad (3.1)$$

with the spatial orbitals:

$$\begin{aligned} \pi_{gx} &= p_x^A - p_x^B & \pi_{gy} &= p_y^A - p_y^B \\ \pi_{ux} &= p_x^A + p_x^B & \pi_{uy} &= p_y^A + p_y^B \end{aligned}$$

at the centers A and B. Decomposing Ψ accordingly, we obtain:

$$\Psi = c_1 |\pi_{gx} \pi_{gy}| + c_2 |\pi_{ux} \pi_{uy}| \quad (3.2)$$

$$= c_1|(p_x^A - p_x^B)(p_y^A - p_y^B)| + c_2|(p_x^A + p_x^B)(p_y^A + p_y^B)| \quad (3.3)$$

$$= c_1 \{ |p_x^A p_y^A| - |p_x^A p_y^B| - |p_x^B p_y^A| + |p_x^B p_y^B| \} \\ + c_2 \{ |p_x^A p_y^A| + |p_x^A p_y^B| + |p_x^B p_y^A| + |p_x^B p_y^B| \} \quad (3.4)$$

$$= (c_1 + c_2)|p_x^A p_y^A| + (c_1 + c_2)|p_x^B p_y^B| - (c_1 - c_2)|p_x^A p_y^B| - (c_1 - c_2)|p_x^B p_y^A|. \quad (3.5)$$

Terms 1 and 2 in Eq. (3.5) correspond to ionic contributions, with both electrons located on one center, while terms 3 and 4 can be classified as covalent contributions. Electron spin-spin coupling is described by a strongly singular operator, one-center contributions are therefore expected to be of distinctly higher magnitude than two-center contributions. For $c_2 = 0$ (only Ψ_0), Eq. (3.5) yields the well-known result that the wave function consists of an equal mixture of covalent and ionic states. Inclusion of Ψ_1 results in a reduction of one-center contributions and an increase of two-center contributions. As to be expected, this causes the D -value to decrease considerably. The relevance of this observation for a CI calculation lies in the recognition that the relative contribution of Ψ_0 vs. Ψ_1 has immediate impact on the magnitude of D_{SS} in the case of O_2 .

In a second set of calculations, I considered all SD excitations of Ψ_0 and of $\Psi_0 + \Psi_1$. In Table 3.2, the energy and electron spin-spin coupling obtained in these calculations is presented.

	$E[E_h]$		$D_{SS}[\text{cm}^{-1}]$	
	Ψ_0	$\Psi_0 + \Psi_1$	Ψ_0	$\Psi_0 + \Psi_1$
cc-pVDZ	-149.976157	-149.982223	1.5618	1.3601
cc-pVTZ	-150.112903	-150.119932	1.6092	1.3699
cc-pVQZ	-150.155785	-150.163060	1.5960	1.3481
aug-cc-pVDZ	-150.009054	-150.015539	1.5664	1.3641
aug-cc-pVTZ	-150.123754	-150.130934	1.6095	1.3702
aug-cc-pVQZ	-150.160026	-150.167349	1.5971	1.3487

Table 3.2: O_2 : The one- and two-configuration case + SD excitations: Energies and spin-spin coupling

Comparing the one-reference with the two-reference case, we note that the bias present from the choice of reference configurations has an impact on D_{SS} , but less so on the energy, causing at most a difference of $\Delta E = 7.3 \text{ mE}_h$. The relevance of the present calculation lies in the observation that the correlation energy and electron spin-spin coupling *do not behave in the same way*. Even a slight improvement in the correlation energy causes here a distinct change in the spin-spin coupling, which contraindicates an immediate, direct relation between these two quantities. It is to be expected that in general, an improvement in the correlation treatment results in an improvement in the description of electron spin-spin coupling. With respect to concrete trends though,

it is not necessarily the case that both quantities exhibit a comparable behaviour, a point that will further be illustrated in Ch. 3.1.2 and Ch. 3.1.4.

3.1.2 Augmented vs. Non-Augmented Basis Sets

The question of a balanced description of Ψ_1 vs. Ψ_0 is of distinct relevance in O₂ as this aspects manifests itself to some extent in subsequent calculations. Having established one of the underlying issues in the calculation of SSC in O₂, a further question of interest arising in an assessment of D_{SS} concerns basis-set effects.

In the first part of this investigation, I operated again only with the reference configurations and applied no SD excitation. I chose a limited reference space of 8 electrons in 6 orbitals ($3\sigma_g, 1\pi_u, 1\pi_g, 3\sigma_u$) which resulted in 14 CSFs. The configuration space therefore consisted of Ψ_0, Ψ_1 , and configurations with occupations of the virtual orbital σ_u . Table 3.3 lists values for D_{SS} . In the comparison of the 8 in 6 reference space calculation with the two-configuration calculation (see Table 3.1), we observe that the values for the augmented basis sets hardly change while there is an increase in the magnitude of D_{SS} in the case of non-augmented basis sets. Inspection of the CI space shows that Ψ_0 and Ψ_1 constitute the largest contribution. In the non-augmented basis sets, we observe furthermore noticeable admixture of configurations with occupation in the σ_u ; the CI coefficient of the next CSF ranges between 0.0502 and 0.0581 (with the smallest value in cc-pVQZ and the largest in cc-pVDZ). In the augmented basis sets, the third largest CI coefficient ranges between 0.0028 and 0.0063 (analogously observing the smallest value in aug-cc-pVQZ and the largest in aug-cc-pVDZ), thereby being an order of magnitude smaller. Careful inspection of the MOs reveals that the only virtual HF orbital in this space, the σ_u , is of course of substantially diffuse character in the augmented basis sets. This orbital is obviously of less relevance in the correlation treatment in the augmented basis sets than in the non-augmented ones, in which the σ_u , not surprisingly, is more compact due to the lack of diffuse functions. Therefore, the reference space D_{SS} value in the augmented basis sets is almost entirely defined by the two-configuration case.

	$D_{SS}[\text{cm}^{-1}]$
cc-pVDZ	0.8873
cc-pVTZ	0.8269
cc-pVQZ	0.7683
aug-cc-pVDZ	0.7286
aug-cc-pVTZ	0.7422
aug-cc-pVQZ	0.7430

Table 3.3: Values for D_{SS} in O₂: 8 in 6 reference space (no further excitations)

In the second part of this investigation, an MRCI correlation treatment based on the 8 in 6 references was performed. This represents the attempt of a direct comparison

of basis sets in a full dynamical multireference correlation treatment (Table 3.4). I remark that this approach is deficient in that especially the σ_u orbital exhibits a different character in the non-augmented vs. the augmented basis sets but expect that the observations nonetheless represent general trends. In particular, it can be inferred that the alternative approach of employing reference configuration spaces based on the contribution of configurations to the wave function will improve results by introducing an additional degree of flexibility to compensate for basis set inadequacies but complicate a direct comparison of basis set effects. Table 3.4 shows that augmented basis sets result in this calculation in lower values for D_{SS} than non-augmented sets. Inclusion of the augmented shell is of minor relevance with respect to the energy: For the case cc-pVTZ vs. aug-cc-pVTZ, the correlation energy (comparing here variational MRCI energies) is 443.989 mE_h vs. 446.551 mE_h. The effect on D_{SS} is clearly more pronounced. The explanation for this trend lies in the description of the HF virtual orbitals. Inclusion of contributions from diffuse orbitals has less of an effect on the correlation energy, but due to the strong dependence of D_{SS} on the distance of electrons, e.g., on the electron distribution, a more diffuse description has a stronger effect on the magnitude of electron spin-spin coupling. We therefore observe in our calculations that the use of an augmented basis is problematic: The more diffuse character of the wave function represents its relevance for electron correlation but is overestimated with respect to a description of electron spin-spin coupling. We speculate that for a satisfactory calculation of D_{SS} , a compact basis which is better able to describe the electron cusp and therefore model the behaviour at short interelectronic distances reliably is advisable.

	$D_{SS}[\text{cm}^{-1}]$
cc-pVDZ	1.4227
cc-pVTZ	1.4219
cc-pVQZ	1.3807
aug-cc-pVDZ	1.3793
aug-cc-pVTZ	1.3881
aug-cc-pVQZ	1.3663

Table 3.4: Values for D_{SS} in O₂: 8 in 6 reference space + SD excitation

3.1.3 Effect of Selected Reference Configurations

In the previous sections, I operated with a generic reference space by specification of the number of electrons and the associated occupied and virtual orbitals. This is not a customary approach in a multireference calculation as it is well-established that a choice of references based on their relevance for the wave function constitutes a more appropriate description of the system. To investigate the effect of the generic 8 in 6 versus a selected reference space, I performed calculations considering a limited number of reference configurations based on their contribution to the wave function. Based on an 8 in 6-MRCI calculation, configurations with a value of $c^2 > 0.001$ were chosen for

the reference space. Depending on the basis set, between 8 – 13 configurations were obtained (20 – 33 CSFs). Table 3.5 lists D_{SS} obtained for the references only while Table 3.6 includes single and double excitations out of the reference space.

Comparison of Table 3.3 with 3.5 reflects the fact that in employing a selected reference space, configurations which are of higher relevance to the description of the state and contribute with larger CI coefficients to the wave function are included. This reduces the contribution of Ψ_1 and has immediate effect on the magnitude of D_{SS} , causing it to increase (see discussion in Ch. 3.1.1). Again, the values in the augmented basis are smaller than in the non-augmented.

	$D_{SS}[\text{cm}^{-1}]$
cc-pVDZ	1.2841
cc-pVTZ	1.1754
cc-pVQZ	1.0766
aug-cc-pVDZ	1.2296
aug-cc-pVTZ	1.1151
aug-cc-pVQZ	1.0433

Table 3.5: Values for D_{SS} in O₂: n ($n = 8 - 13$) reference configurations (no further excitations)

Comparison of Table 3.4 with 3.6 shows that in a fully correlated calculation, the effect of augmentation is distinctly less pronounced in the tailored reference space than in a calculation based on a general 8 in 6 consideration: The flexibility of choosing relevant configurations in combination with a configuration interaction treatment is able to compensate partly for problems associated with augmented basis sets.

	$D_{SS}[\text{cm}^{-1}]$
cc-pVDZ	1.4846
cc-pVTZ	1.5008
cc-pVQZ	1.4606
aug-cc-pVDZ	1.4817
aug-cc-pVTZ	1.4855
aug-cc-pVQZ	1.4525

Table 3.6: Values for D_{SS} in O₂: n ($n = 8 - 13$) reference configurations + SD excitation

The question of employing an augmented basis or not in a calculation based on HF MOs has ultimately to be answered in the context of balancing the improvement of electron correlation with the impact on the description of SSC. Out of the present experience, the difficulties introduced by employing an augmented basis for the calculation

of D_{SS} are sometimes substantial but could possibly be strongly system dependent. Unless necessitated by an ionic electron distribution in the system, the choice of a non-augmented set appears to be advisable if the calculation is based on HF MOs. It is suggestive that employing more compact molecular orbitals, such as those obtained with a CASSCF or a DFT treatment, leads to an improvement in the behaviour of the calculation.

3.1.4 Convergence with Reference Space

To investigate the convergence of D_{SS} with the size of the MRCI, a series of calculations with increasing size of the reference space under inclusion of MRCI excitations employing the cc-pVTZ basis was performed. Fig. 3.1 displays the dependence of D_{SS} on the number of reference configurations, Fig. 3.2 presents this dependence for the variational CI energy $E_{MRCI(V)}$.

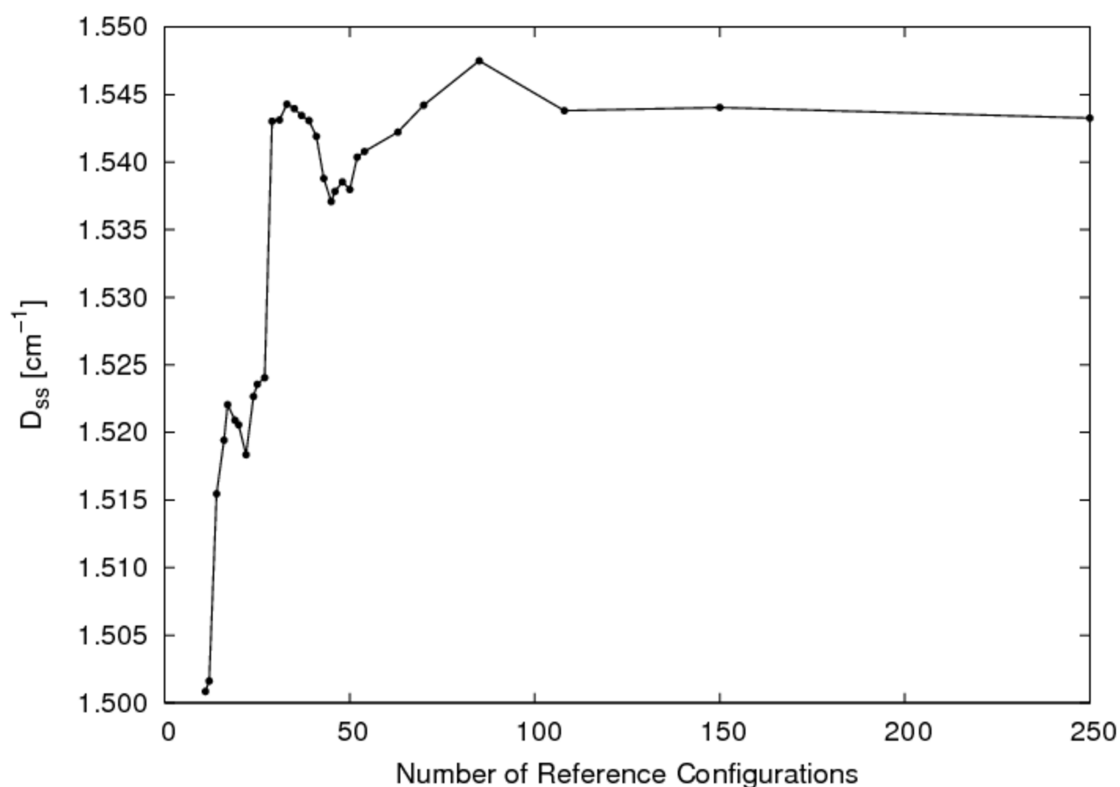


Figure 3.1: Dependence of D_{SS} (O_2) on the size of the reference space

The most important points are: First, as a qualitative trend, D_{SS} does exhibit asymptotic convergence with the size of the calculation. Second, although $E_{MRCI(V)}$ converges smoothly, this does not hold for D_{SS} . This is consistent with previous observations that energy and electron spin-spin coupling exhibit different behaviour. In particular, inconsistencies in the region of 16 – 24 configurations and in the region of 29 – 50 configurations are observed. Employing reference spaces selected based on the

contribution of configurations to the wave function frequently results in introduction of particular “shells” upon extension of the reference space. Closer investigation of the problematic regions reveals indeed the connection to the occupation of specific orbitals. In the first region, we note a maximum of $D_{SS} = 1.5221 \text{ cm}^{-1}$ at a space of 17 configurations which drops to 1.5184 cm^{-1} at 22 configurations. Inspection of the additional five configurations shows that particularly occupations in the orbitals $2 b_{2g}$, $2 b_{3g}$ and $3 b_{1u}$ are introduced. All of these orbitals exhibit a nodal plane between the bonding oxygen atoms. It is therefore tempting to speculate that the separation of electrons is increased upon introduction of these additional references, causing a slight decrease in D_{SS} . In the second region, an almost constant value of D_{SS} occurs for a reference space of 29 to 41 configurations, with a maximum of $D_{SS} = 1.5443 \text{ cm}^{-1}$ at 33. A sudden decrease is observable, with a minimum of 1.5371 cm^{-1} at a space of 45 references. The additional configurations introduced going from 29 to 41 reflect excitations into the orbitals $2 b_{2u}$, $2 b_{3u}$, as well as the high-lying $1 b_{1g}$ and $6 a_g$, none of which exhibit nodes in the xy plane perpendicular to the bonding z direction. In the configurations 42 – 48, again configurations with an occupation of the $2 b_{2g}$, $2 b_{3g}$ and $3 b_{1u}$ are introduced and we observe a decrease in D_{SS} , as was noted in the discussion of the first region. Overall, we conclude that additional configurations are introduced on the basis of an improved description of electron correlation but do not reflect their relevance for electron spin-spin effects adequately.

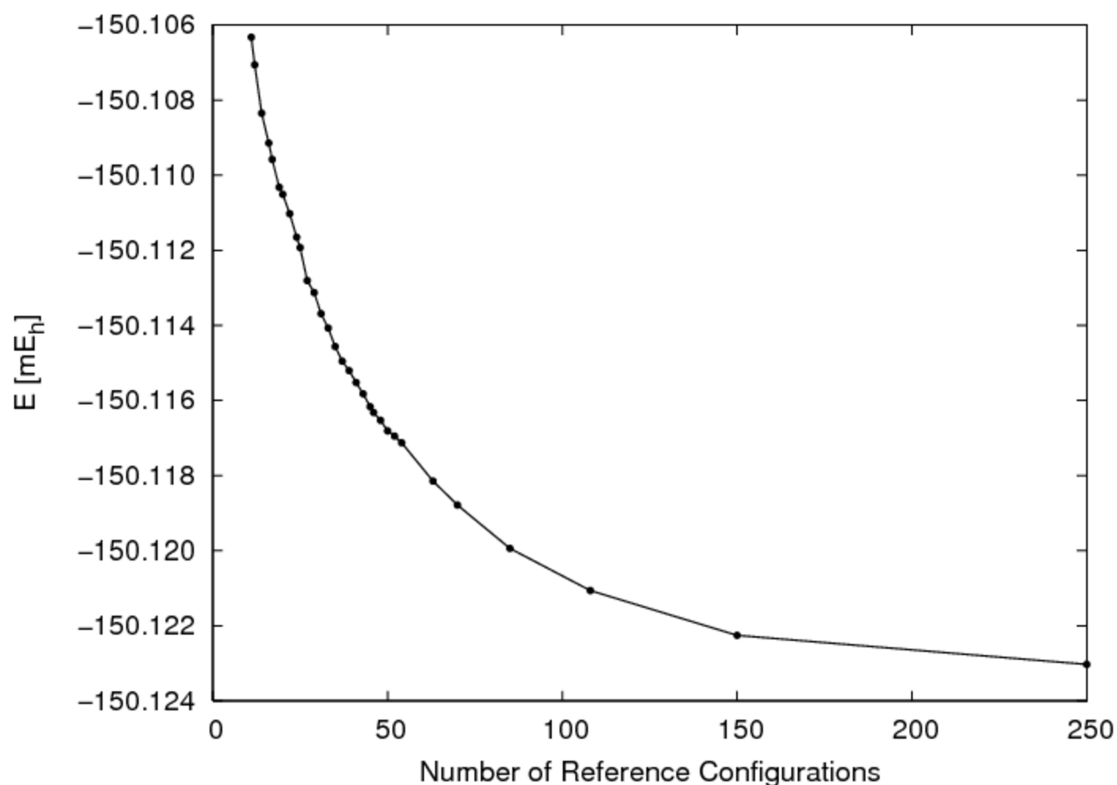


Figure 3.2: Dependence of $E_{MRCI(V)}$ (O₂) on the size of the reference space

3.1.5 Evaluation of Results for O₂

To summarize the findings from the calculation of electron spin-spin coupling in O₂:

- We observe a direct impact of the contribution of the doubly excited configuration Ψ_1 (valence occupation $\sigma_g^2 \pi_u^2 \pi_g^4$) on the value of D_{SS} (see Ch. 3.1.1). It is therefore mandatory to obtain a balanced description of the ground state, particularly with respect to a realistic assessment of the contribution of this configuration.
- Employing augmented basis sets is problematic in highly correlated calculations of electron spin-spin coupling based on HF orbitals (see Ch. 3.1.2 as well as conclusions in Ch. 3.1.3). We speculate that these basis sets introduce too diffuse a bias for the description of the short-range operator $\hat{\mathcal{H}}_{SS}$ in the context of HF virtuals. It is suggestive that more compact MOs would lead to a reduction in the observed difficulties.
- In the extension of the MRCI configuration space, we observe qualitatively a comparable trend of convergence for correlation energy and spin-spin coupling. The convergence of D_{SS} is distinctly discontinuous, however, as this property exhibits a different dependence on changes in the wave function than the energy.

The last two points can be summarized to the important observation: Correlation energy and electron spin-spin coupling exhibit different behaviour. It cannot be expected that an improvement in the correlation, either by improving the basis or improving the method, directly relates to an improvement in the value of D_{SS} .

I finish by stating the value for D_{SS} of 1.54 cm⁻¹ obtained with an MRCI calculation based on a reference space of 250 configurations in the cc-pVTZ basis. A value of $D_{SO} = 2.27$ cm⁻¹ in the spin-orbit CI treatment was calculated in the same basis, no configuration selection was applied here either. The established rapid convergence of spin-orbit coupling elements with the size of the expansion and number of roots [4] allowed for a smaller reference space of 68 configurations in the triplet and 85 in the singlet symmetry. Two roots in ¹A_g were calculated with the second root representing the $b^1\Sigma_g^+$ which accounts almost entirely for the spin-orbit splitting of the ground state. One root each was calculated in all other gerade symmetries, thereby sufficiently spanning the calculation space.

The results for spin-spin and spin-orbit splittings can be combined to $D = 3.81$ cm⁻¹, in error by 4 % compared to the experimental value of $D = 3.965$ cm⁻¹ [171,172]. The principal focus of this study was the investigation of SSC trends and without further comprehensive analysis, the deviation cannot be attributed conclusively to D_{SO} or D_{SS} . As further possible causes of error, the neglect of vibrational averaging as well as the application of the spin-orbit mean-field approximation can be mentioned. It is commonly known that the former may amount for uncertainties on the order of 5 % while investigations of the latter indicate similar magnitudes of error [175]. Considering these aspects, the present agreement with experiment can be noted as very satisfactory.

3.2 NH

The spin-spin coupling between the states $c^1\Pi$ and $1^5\Sigma^-$ of NH was calculated at various bond distances in the cc-pVTZ basis as a test of the off-diagonal spin-coupling branch of SPOCK.SISTR. This is motivated by the reported role of singlet–quintet coupling in predissociation of the $c^1\Pi$ state, as investigated by Bohn et al. [164]. We will compare with their calculation but will refrain from further analysis. In particular, it is not attempted to discuss the correlation description of the calculated states. Recent investigation of the higher-lying states of NH by Owono et al. [176] indicate a distinct Rydberg character in the $1^5\Sigma^-$ at equilibrium and seem to necessitate a considerably diffuse basis; we note in this context that the character of this state is presumably more well-defined in the crossing region, furthermore, a bias towards Rydberg states is undoubtedly introduced by their inclusion of Rydberg MOs in their CASSCF active space. A detailed investigation of this issue is not the purpose of the present calculations, and we will confine ourselves to reporting spin-spin couplings.

Bohn et al. employed a $(8s\ 6p\ 4d\ 1f)$ basis on nitrogen (including two diffuse s and one diffuse p) and a $(5s\ 4p)$ basis on hydrogen (including one diffuse s), based on the scheme by Manz et al. [177]. Their CI wave function was constructed from molecular orbitals obtained from a state-averaged MCSCF reference [165, 178, 179] while keeping the 1σ frozen. This resulted in an expansion size on the order of 170 000 CSFs for each state.

The present calculation in the C_{2v} symmetry in the cc-pVTZ basis employed for the 1B_1 and 1B_2 states a reference space of 44 – 52 configurations, spanning a CI space of 65 000 – 86 000 CSFs in each of the two irreps. The 5A_2 was described by 19 – 27 reference configurations (65 000 – 84 000 CSFs), the 1σ orbital was kept frozen throughout. Calculations were performed at the five bond distances $1.975\ a_0$, $2.475\ a_0$, $2.775\ a_0$, $3.075\ a_0$, and $3.675\ a_0$. At a distance of $1.975\ a_0$, close to the equilibrium bond distance of NH, the $1^5\Sigma^-$ is a high-lying state (8.65 eV above the ground state [176]) but drops rapidly in energy with increasing bond distance, crossing $c^1\Pi$ at $2.685\ a_0$ at an energy of 5.878 eV [176] which at this bond distance is only 0.13 eV below its dissociation threshold. The observation of the crossing region is consistent with the calculations in this work, where we find the $1^5\Sigma^-$ to be 0.712 eV above the $c^1\Pi$ at $2.475\ a_0$ and 0.525 eV below at $2.775\ a_0$. Simplifying to a linear dependence on the bond distance we would estimate a crossing at approximately $2.65\ a_0$.

Bohn et al. reported first-order spin-spin matrix elements $\langle c^1\Pi_1 | \mathcal{H}_{SS} | 1^5\Sigma_1^- \rangle$ in the Breit-Pauli approximation. The subindex in the states refers to the Ω -quantum number and has therefore to be related to the calculation of the SPOCK.SISTR matrix elements $\langle c^1\Pi_x | \mathcal{H}_{SS} | 1^5\Sigma^- \rangle / \langle c^1\Pi_y | \mathcal{H}_{SS} | 1^5\Sigma^- \rangle$ as:

$$\langle c^1\Pi_{\pm 1} | \mathcal{H}_{SS} | 1^5\Sigma_{\pm 1}^- \rangle = \mp \frac{1}{\sqrt{2}} (\langle c^1\Pi_x | \mathcal{H}_{SS}(yz) | 1^5\Sigma^- \rangle \pm i \langle c^1\Pi_y | \mathcal{H}_{SS}(xz) | 1^5\Sigma^- \rangle) \quad (3.6)$$

with $|\Pi_{\pm 1}\rangle = \mp \frac{1}{\sqrt{2}} (|\Pi_x\rangle \pm i|\Pi_y\rangle)$. The yz component of the spin-spin operator is imag-

inary while the xz component is real, yielding overall an imaginary coupling element. Table 3.7 reports the spin-spin coupling elements $\langle c^1\Pi_{\pm 1}|\mathcal{H}_{SS}|1^5\Sigma_1^- \rangle$ of Bohn et al. as well as the results of this work. Their values are reproduced very satisfactorily, deviating at most by 0.05 cm^{-1} . Especially in the context of the difficulties encountered in the calculations of O_2 , we note that NH is expected to represent a distinctly better behaved system as the electron spin-spin coupling is predominantly located on the N atom and the question of ionic and covalent contributions and their balanced description is not of relevance here.

	$\langle c^1\Pi_{\pm 1} \mathcal{H}_{SS} 1^5\Sigma_{\pm 1}^- \rangle [\text{cm}^{-1}]$	
r (a_0)	Bohn et al. [164]	this work
1.975	0.30	0.35
2.475	0.70	0.72
2.775	0.88	0.91
3.075	1.03	1.06
3.675	1.20	1.23

Table 3.7: NH: Spin-spin coupling elements between $c^1\Pi$ and $1^5\Sigma^-$ in dependence of the bond distance

3.3 All-trans Polyenes

Conjugated hydrocarbons of medium size have been a particular focus of experimental and theoretical studies since they are obvious model systems for polymer compounds as well as for biologically relevant molecules. The linear (all-*trans*) polyene docosaundecaene ($\text{C}_{22}\text{H}_{24}$) can be regarded as a simplified relative of β -carotene as these two substances share an identical single–double bond sequence. Investigating trends in the smaller polyenes is therefore a promising approach towards understanding structural aspects and reaction behaviour of related, more complex compounds.

Excited triplet states of conjugated hydrocarbons are frequently described as a superposition of several resonant structures. This picture captures the main characteristics of this class of substances, namely the capability of delocalization of unpaired electrons along the chain. It is the explanation for their stability as well as their reactivity in a multitude of possible pathways, as the redistribution of reactive centers of the molecule opens the possibility for various processes of de-excitation. At the same time, it poses the question of the structural characteristics of the excited states and a possible localization of the unpaired electrons at particular carbon atoms.

Takahashi et al. [180, 181] investigated the bond alternation in the T_1 state of all-*trans* polyenes, motivated by computational disagreement regarding the underlying pattern. Previous studies by Kuki et al. [182] based on semiempirical Pariser-Parr-Pople single and double CI (SDCI) calculations observed a loss of bond alternation in the central part of the polyene chain; this geometry effect was interpreted as a “triplet-excited

region". Takahashi et al. employed single-excitation CI (SCI) to study the series of polyenes from C_8H_{18} to $C_{22}H_{46}$, obtaining geometries in agreement with Kuki et al. However, comparison calculations with CASSCF on octatetraene gave a considerably different bond alternation pattern (see next but one paragraph for a detailed description of this pattern in linear polyenes of different sizes). Takahashi et al. concluded the appearance of a "triplet-excited region" to be artifactual in SCI and SDCI calculations, related to the use of RHF MOs in combination with limitations on the excitations in the CI space. Consideration of the higher polyenes employing this method was not feasible, however. Geometry optimizations by Ma et al. [183,184] focussing on an assessment of the semiempirical Pariser-Parr-Pople model as well as providing results obtained with the UB3LYP method supported the observed trend of bond alternation in the longer polyenes.

The study of extended π -systems employing sophisticated methods is computationally demanding and therefore limited. Recent work by Marian [185] investigates the applicability of the DFT/MRCI approach to polyenes as well as polyacenes, evaluating low-lying singlet and triplet states. In particular the consideration of excited singlet states in these systems is complicated due to their multireference character and the distinct contribution of double excitations. The DFT/MRCI method combines molecular orbitals obtained with a restricted closed-shell Kohn-Sham determinant with a subsequent multireference calculation. The idea of this approach is to incorporate dynamical correlation already partly at the level of the molecular orbitals while the multireference treatment accounts for non-dynamical correlation effects. The effective DFT/MRCI Hamiltonian includes five empirical scaling factors, the parametrization of which only depends on the multiplicity of the state, the number of open shells and the type of density functional; no information on specific atoms or molecules is incorporated. Double-counting of dynamical correlation in the multireference treatment is prevented by extensive configuration selection. High-lying configurations which account for dynamical effects in regular CI expansions are excluded by specification of an energy cutoff with respect to the highest root of the reference space. Application of configuration selection has furthermore the advantage of considerably reducing the CI space, thereby providing the basis for a fast evaluation. The DFT/MRCI method has been shown to yield reliable results in the calculation of excitation energies and transition moments [1, 4, 186–188]. The thorough study of Marian establishes its reliability in benchmark calculations on polyacenes, diphenylpolyenes, and on the smaller all-*trans* polyenes hexatriene, octatetraene and decapentaene, with an emphasis on the latter group. For these systems, experimental data as well as previous theoretical results were available for comparison. Furthermore, Marian investigated basis set effects on geometrical parameters, vertical absorptions and adiabatic excitation energies and found satisfactory agreement already in the SV(P) basis at the SV(P)-optimized geometry. Energy spectra as well as effects of geometry relaxation were studied in the larger homologues, including systems of the size of $C_{26}H_{54}$.

The geometry of the T_1 state of all-*trans* polyenes were investigated by Marian based on unrestricted B3LYP geometry optimizations with the TURBOMOLE program [148,

189–191] in the SV(P) basis [170] (and additionally TZVP on the smaller systems). Her findings are qualitatively consistent with previous work on these molecules. Upon excitation to the T_1 state in the smaller polyenes, an inversion of the bond alternation pattern as compared to the S_0 ground state is observed. Consideration of the larger homologues reveals the entire pattern: The strong bond alternation in the center of the molecule diminishes on progression towards the ends of the chain. Located symmetrically away from the center, we observe two regions exhibiting a minimum in the bond alternation, with adjacent C–C bonds of similar length. Strong bond alternation resumes at the terminating C-atoms. Fig. 3.3 depicts this behaviour for docosaundecaene, taken from the calculations by Marian.

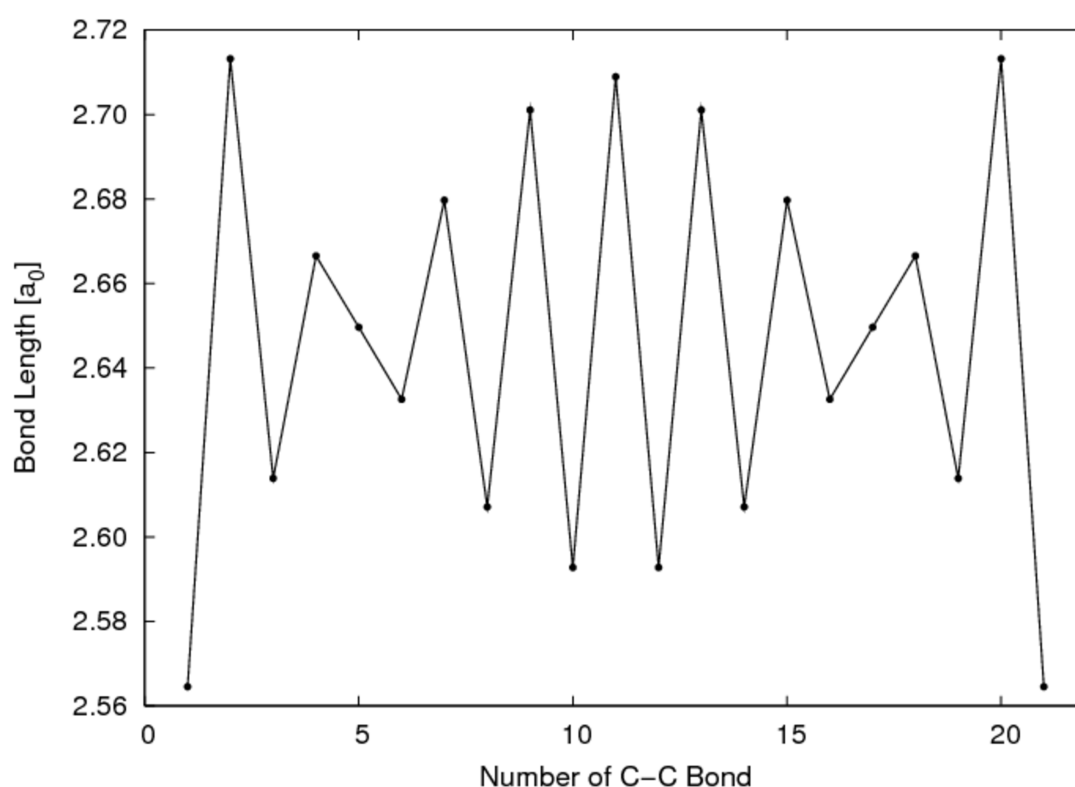


Figure 3.3: Variation of C–C bond distance in docosaundecaene ($C_{22}H_{24}$)

According to the geometry optimizations of Marian, this effect will start to be observable around a length of 14–16 carbon atoms, corresponding to the compounds tetradecaheptaene ($C_{14}H_{16}$)/hexadecaoctaene ($C_{16}H_{18}$).

Inspection of this geometry pattern poses the immediate question of a possible localization of electrons. Kuki et al. related their computationally observed domain of diminishing bond alternation (which was erroneously established at the central carbon atoms) to bond orders and postulated a “triplet-excited” region. Takahashi et al. as well as Ma et al. refrained from speculations in this respect in their later work, confining themselves to an observation of geometrical effects.

Different scenarios are possible with respect to a localization, which can be listed in a reduction to their asymptotic behaviour as:

- The electrons are evenly distributed along the carbon atom chain.
- The electrons are localized in the central part.
- The electrons are localized strongly towards the terminating atoms.

It is here that calculations of electron spin-spin coupling can assist in a clarification. As was discussed in detail (see the applications in the experimental context in Ch. 1.1.2 as well as the reflections on the operator structure in Ch. 1.3), SSC can be interpreted in a simple model as assessing the mean distance between unpaired electrons. In general, we would therefore expect a decrease in D_{SS} with increasing chain length; the concrete behaviour would strongly depend on the characteristics in the electron distribution, however. In the case of a consistent delocalization, we would presumably expect a gradual decrease in the magnitude of electron spin-spin coupling with increasing chain length. A strong localization at the center of the molecule relates to a near-constant value of D_{SS} , although this speculation has to be viewed on the background of the strong distance dependence of the operator which can cause a noticeable decrease in the spin-spin coupling magnitude even in the case of minor changes in the electron distribution. A specific localization of unpaired electrons at the end of the polyene chain would manifest itself in overall very small values of D_{SS} , further decreasing with increasing chain length. In the longer polyenes, another possibility is introduced in a localization at carbon atoms either side of the central region, similar to the manifestation of the geometry pattern described earlier. Establishing this region accurately necessitates a deeper understanding of behaviour and dependencies of electron spin-spin coupling.

This introduction was designed to provide the background and motivate the interest in an evaluation of spin-spin coupling effects in all-*trans* polyenes. In this study, we will restrict ourselves to the consideration of the smaller homologues. It is essential to establish the methodological foundation by investigation of smaller systems and verification that our assumptions are consistent with our observations given that so little is known. The main question is therefore what behaviour we note in the magnitude of electron spin-spin coupling and if we can support this with other data that can explain the trend. Inspection of the molecular orbitals will be a particularly useful means as the MOs provide a direct interpretation of the distribution of electrons. Of special interest is the use of the DFT branch of the Grimme/Waletzke DFT/MRCI program. As was discussed in detail in the context of O₂ (Ch. 3.1, see in particular Ch. 3.1.2 and 3.1.3), HF virtual orbitals exhibit a rather diffuse character which imposes a strong demand on the evaluation of electron spin-spin coupling. Alternative approaches which would presumably suffer less from this shortcoming could be based on molecular orbitals obtained through CASSCF or DFT.

The DFT/MRCI calculations included in this work are based on the calculations of Marian [185]. The geometry was obtained through UB3LYP optimizations of the planar

T_1 state in C_{2h} symmetry, thereby corresponding to the state 3B_u . Molecular orbitals employed in the subsequent multireference treatment constitute BHLYP-ground state MOs, consistent with the DFT branch of the DFT/MRCI program being parametrized for this particular functional. The configuration space was established in a preparatory DFT/MRCI calculation of either three roots in A_g and three roots in B_u or six roots in A_g and six roots in B_u , depending on molecule and basis. *Ab initio* calculations employed the UB3LYP-optimized geometry, molecular orbitals were obtained in an ROHF calculation of the triplet. MOs composed from the $1s$ atomic orbital of the carbon atoms were kept frozen throughout in the multireference treatment. Visualization of molecular orbitals was accomplished using the program MOLDEEN [192].

3.3.1 Discussion of MOs

The character of the molecular orbitals employed in the correlation treatment obviously strongly influences the description of the wave function. In general, there is a fundamental difference between the virtual molecular orbitals calculated with DFT as compared to HF. HF virtual MOs represent one-electron functions which experience an N -electron potential, with N being the number of electrons in the molecular system. The approximate physical interpretation that is usually connected with these molecular orbitals, based on Koopman's theorem, is the energy associated with binding a *further* electron and thereby form an $(N + 1)$ -electron system. HF virtual MOs are therefore in general distinctly more diffuse than their occupied counterparts as they basically correspond to molecular orbitals of the anion. Out of this reason, it is critical to base the subsequent correlation treatment of an excited state on HF MOs obtained through a calculation of exactly this state. In contrast, in the limit of the exact functional, DFT virtual MOs are evaluated as one-electron functions experiencing an $(N - 1)$ -electron potential [193, 194]. The energy differences between virtual and occupied orbitals are better related to excitation energies,¹ and virtual MOs obtained through DFT calculations are consequently more compact by construction. A calculation of excited states based on DFT MOs is not ideal, but presumably suffers from less shortcomings than a calculation based on HF MOs. Considering the experiences in the assessment of O_2 based on the *ab initio* approach of the MRCI program (Ch. 3.1), diffuse functions/molecular orbitals constitute a particular difficulty in the computation of electron spin-spin coupling.

These general issues may of course manifest themselves to a greater or lesser extent in specific calculations, strongly dependent on the actual evaluation. Basis sets with diffuse functions will presumably bias the character of the HF virtual MOs towards a more diffuse description; molecular systems which exhibit bound anionic states might on the other hand provide more compact virtual orbitals.

¹However, the authors in [194] note the insufficient accuracy of popular approximate density functionals, such as the local density approximation (LDA) as well as various general gradient approximations (GGA), in this respect.

Hexatriene

In the calculation of small linear polyenes, a further issue of particular relevance for the evaluation of electron spin-spin coupling was encountered in the comparison of the DFT with the HF assessment. This will be discussed in the context of calculations of hexatriene in the SV(P) basis. I emphasize that the calculations in this section are entirely based on the *ab initio* branch of the MRCI program and do not employ the effective DFT/MRCI Hamiltonian. The only difference in the DFT vs. the HF execution lies in the choice of MOs. This was done on the background of a direct comparison of the effect introduced by the molecular orbitals themselves.

Figs. 3.4/3.5 depict the molecular orbital $2a_u$. This orbital is doubly occupied in the ground state S_0 and singly occupied in the first excited triplet state T_1 of hexatriene. Figs. 3.6/3.7 show the orbital $2b_g$ which is unoccupied in the ground state and singly occupied in T_1 . An identical contour surface value of 0.02 was chosen throughout. DFT MOs were obtained through a restricted closed-shell BHLYP evaluation while HF calculations correspond to a restricted open shell treatment of T_1 .

First singly occupied MO ($2a_u$) of the T_1 state

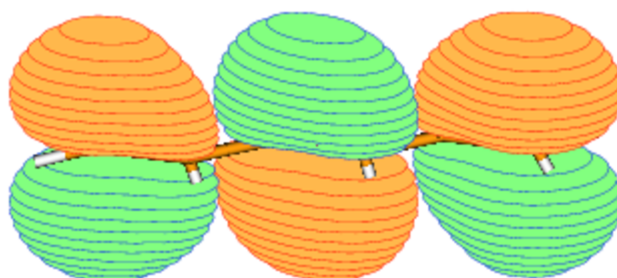


Figure 3.4: DFT (BHLYP) calculation

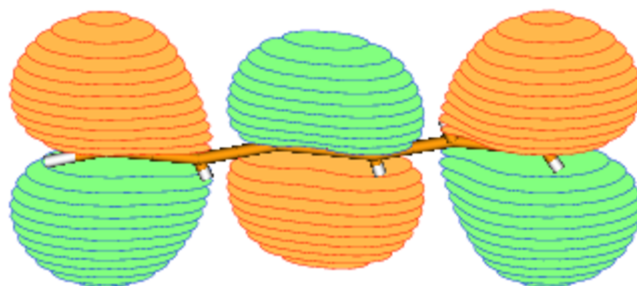


Figure 3.5: ROHF calculation

Second singly occupied MO ($2b_g$) of the T_1 state

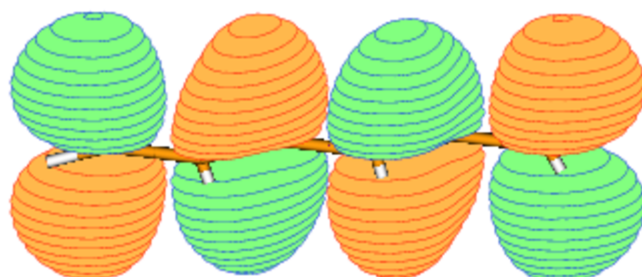


Figure 3.6: DFT (BHLYP) calculation

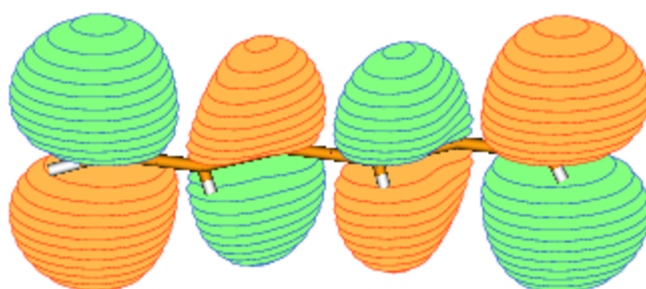


Figure 3.7: ROHF calculation

The main aspect of interest in these figures is the slightly different shape of the molecular orbitals: In the case of DFT, the electron density, represented by the size of the lobes, appears to be fairly evenly distributed along the carbon atom chain. In the HF MOs, we observe instead larger contributions at the end of the chain and smaller ones on the central atoms. This effect can be rationalized as a tendency in the ROHF calculation to separate the open-shell electrons. The impact on the magnitude of electron spin-spin coupling is immediate: Table 3.8 shows the values for D_{SS} and E_{SS} , calculated only for the open-shell reference of the T_1 state, without considering any further configurations.

	$D_{SS}[\text{cm}^{-1}]$	$E_{SS}[\text{cm}^{-1}]$
DFT MOs	0.1218	0.0021
HF MOs	0.0454	0.0015

Table 3.8: SSC in hexatriene, calculated with DFT or HF MOs: Single-reference case (no further excitations)

The difference between DFT and HF seems to be dramatic. On the other hand, it has to be recognized that we are inspecting a single-reference case which magnifies the bias from the molecular orbitals and is not representative for a fully correlated calculation. The overall MO space is orthogonal, and related to the reduced electron density at the central carbon atoms in $2a_u$ and $2b_g$ in HF, we observe an increased electron density at the same atoms in the next two orbitals of this symmetry, $3a_u$

and $3b_g$. For a calculation based on six electrons in six π -orbitals (1–3 a_u , 1–3 b_g), that is, just considering the references for a simplified comparison, we obtain the SSC contributions listed in Table 3.9.

	$D_{SS}[\text{cm}^{-1}]$	$E_{SS}[\text{cm}^{-1}]$
DFT MOs	0.1189	0.0034
HF MOs	0.1038	0.0032

Table 3.9: SSC in hexatriene, calculated with DFT or HF MOs: 6 in 6 reference space (no further excitations)

In this calculation the HF values for D_{SS} (and E_{SS}) approach the DFT results. We may speculate that the artefact introduced in employing ROHF MOs can partly be compensated in the subsequent correlation treatment, nonetheless, it would be preferable not to introduce this bias in the first place.

3.3.2 Hexatriene: Comparison of DFT/MRCI, HF/MRCI, and CASSCF

The DFT/MRCI calculations in this section are based on the approach by Marian. The reference space consisted of 30 configurations, generated in a preliminary DFT/MRCI calculation as described at the end of the introduction in Ch. 3.3. The *ab initio* study employed ROHF MOs and an iteratively determined reference space of 11 configurations, with consideration of different selection thresholds in the construction of the CI space. The CASSCF calculation with DALTON [84] comprised six electrons in six π -orbitals (1–3 a_u , 1–3 b_g). All of the calculations evaluated the lowest triplet state 3B_u in the SV(P) basis, with the orbitals 1–3 a_g , 1–3 b_u kept frozen.

Table 3.10 lists electron spin-spin coupling parameters for the T_1 state of hexatriene as evaluated with DFT/MRCI, HF/MRCI with no configuration selection, and CASSCF.

	$D_{SS}[\text{cm}^{-1}]$	$E_{SS}[\text{cm}^{-1}]$
DFT/MRCI	0.1172	0.0023
HF/MRCI	0.1002	0.0018
CASSCF	0.1230	0.0042

Table 3.10: SSC in hexatriene (SV(P) basis): Comparison of different approaches

Values for CASSCF and DFT/MRCI are in reasonable agreement, indicating the suitability of these methods for the evaluation of spin-spin coupling effects. The results for HF/MRCI deviate slightly, yielding lower coupling parameters than either of the other two methods. Critical for a consideration of the feasibility of the individual approaches is the timing though: The CASSCF calculation required less than one minute, DFT/MRCI + SISTR only a few seconds since extensive selection of configurations accounts for a substantial reduction in the CI space, as discussed in the introduction at

the beginning of Ch. 3.3. The HF/MRCI + SISTR evaluation on the other hand occupied a week. This is directly related to performing this calculation with no selection threshold enabled, thereby considering all single and double excitations out of the given reference space. Table 3.11 provides for comparison a series of HF/MRCI evaluations with increasing selection, listing furthermore the timing of the calculations. The selection threshold E_{sel} determines the selection of configurations for the CI space based on their contribution in perturbation theory to the 3B_u state considering only their interaction with the reference configurations [162].² A value of $E_{sel} = 0$ corresponds to no selection, thereby considering all single and double excitations out of the chosen reference space, while the specification of $E_{sel} = \infty$ results in a configuration space spanned by the references only.

$E_{sel}/\mu E_h$	$D_{SS}[\text{cm}^{-1}]$	$E_{SS}[\text{cm}^{-1}]$	CPU (MRCI)	CPU (SISTR)
0.0	0.1002	0.0018	2 d 11 h 02 m	5 d 10 h 34 m
0.0001	0.1003	0.0019	2 d 04 h 07 m	4 d 15 h 29 m
0.0005	0.1003	0.0019	1 d 15 h 06 m	3 d 11 h 54 m
0.001	0.1003	0.0019	1 d 07 h 01 m	2 d 17 h 27 m
0.005	0.0990	0.0020	13 h 56 m	18 h 35 m
0.01	0.0962	0.0019	6 h 58 m	13 h 07 m
0.05	0.0814	0.0011	1 h 41 m	3 h 41 m
0.1	0.0744	0.0006	1 h 05 m	2 h 38 m
0.5	0.0647	0.0001	27 m	1 h 13 m
1.0	0.0627	0.0006	15 m	42 m
5.0	0.0650	0.0012	1 m	5 m
10.0	0.0709	0.0017	< 1 m	1 m
50.0	0.0898	0.0052	\ll 1 m	\ll 1 m
∞	0.0837	0.0027	\ll 1 m	\ll 1 m

Table 3.11: SSC with HF/MRCI in hexatriene (SV(P) basis): Assessment of selection thresholds

Most important, we note a very slow convergence of D_{SS} with the selection threshold. The bias introduced in the molecular orbitals can partly be compensated by consideration of a sufficient number of configurations, albeit only gradually so. As a further observation, we note a rise in D_{SS} at very high selection thresholds. This can be directly explained by the structure of the MO space: As already discussed, the singly occupied $2a_u$, $2b_g$ exhibit an increased electron probability at the terminating carbon atoms while the $3a_u$, $3b_g$ are characterized by higher AO contributions at the central atoms. Extension of the single-configuration to the 6 in 6 case correlates with an immediate increase in D_{SS} (corresponding to a comparison of Table 3.8 with Table 3.9). Addition of contributions from higher-lying orbitals by allowing excitations out of the 6 in 6 configuration space corresponds to an excitation into molecular orbitals which

²Note that this differs from the selection in the DFT/MRCI branch where the criterion constitutes the specification of an energy *cutoff*.

possess a less centrally-localized character, therefore causing at first a decrease in D_{SS} .

The HF/MRCI ($E_{sel} = 0.0 \mu E_h$) spin-spin coupling values being slightly lower than the CASSCF and DFT/MRCI results can be understood by comparison with a HF/MRCI calculation based on a smaller reference space of six configurations instead of eleven, again considering all single and double excitations. This calculation yields values of $D_{SS} = 0.0720 \text{ cm}^{-1}$ and $E_{SS} = 0.0008 \text{ cm}^{-1}$. We therefore recognize that with respect to the size of the reference space, the HF/MRCI calculation is not converged yet. Increasing the reference space would conceivably lead to a convergence of the HF/MRCI results towards the DFT/MRCI and CASSCF values but imposes significant demands on the computational resources.

3.3.3 DFT/MRCI: Basis Set Comparison for Hexatriene, Octatetraene, Decapentaene

The results in this section comprise DFT/MRCI calculations at the UB3LYP-optimized geometry of the lowest triplet state 3B_u . The reference spaces generated as described previously consisted of 30–70 configurations in the case of the smaller polyenes hexatriene, octatetraene, decapentaene. Table 3.12 lists spin-spin-coupling parameters for these systems in the SV(P) basis while Table 3.13 provides values in the TZVP basis.

	$D_{SS}[\text{cm}^{-1}]$	$E_{SS}[\text{cm}^{-1}]$
Hexatriene	0.1172	0.0023
Octatetraene	0.0862	0.0010
Decapentaene	0.0771	0.0002

Table 3.12: SSC in small all-*trans* polyenes, evaluated with DFT/MRCI in the SV(P) basis

	$D_{SS}[\text{cm}^{-1}]$	$E_{SS}[\text{cm}^{-1}]$
Hexatriene	0.1245	0.0032
Octatetraene	0.0911	0.0011
Decapentaene	0.0648	0.0016

Table 3.13: SSC in small all-*trans* polyenes, evaluated with DFT/MRCI in the TZVP basis

The basis set effect in this calculation is not very pronounced, and we observe in both bases an agreement with respect to the general expectation of a decreasing value for D_{SS} with increasing chain length. Values for E_{SS} are on the order of 10^{-3} cm^{-1} , and it is therefore difficult to attach significance to the observed fluctuations in the magnitude. On average, we note slightly higher couplings in the TZVP than the SV(P) basis which an inspection of the molecular orbitals explains. The main observation can be illustrated with octatetraene, considering the highest π -orbital of the π -MO system

formed by the $2p_z$ AOs of the carbon atoms ($4b_g$). This molecular orbital is sufficiently high-lying and diffuse to exhibit the relevant features to which I would like to draw attention. Equivalent findings were obtained for the corresponding MOs in hexatriene ($3b_g$) and decapentaene ($5b_g$).

Fig. 3.8 displays the $4b_g$ of octatetraene, in the SV(P) basis on the left, in the TZVP basis on the right; both plots were taken with an identical contour surface value of 0.03. As was already discussed at the end of Ch. 1.6, it is not possible in principle to correlate values of zero-field splittings to particular molecular axes in the theoretical context. So far, we have postulated that the considerable magnitude of D_{SS} is related to an assessment of electron spin-spin coupling along the C-C-chain and interpreted decreasing values as information about the increase in the mean distance between the unpaired electrons along this chain. This assumption seems legitimate considering the geometry of the molecule but it has to be recognized that this information cannot be derived from the theoretical evaluation itself. An interpretation of E_{SS} is less straightforward. It seems suggestive, though, based on observations in CH_2 of a vanishing E_{SS} upon straightening the molecule to a linear shape, as well as considering the spatial operator components that contribute to E_{SS} in the case of polyenes ($x^2 - y^2$ and xy), to relate the magnitude of this coupling to the electron distribution in the directions orthogonal to the carbon chain.

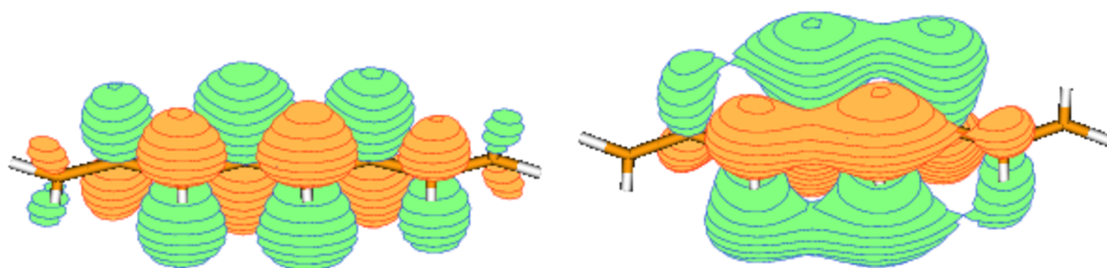


Figure 3.8: Orbital $4b_g$ of octatetraene: SV(P) (left) vs. TZVP (right)

In Fig. 3.8, we observe a well-defined shape of the MO in the SV(P) basis, identifying individual AOs separately. The diffuseness of the TZVP basis manifests itself in an expansion of the MO towards and away from the observer. Furthermore, we note a decreased contribution of the terminating carbon atoms. On the basis of our more intuitive interpretation with respect to E_{SS} , we may relate its consistently higher magnitude in the TZVP basis to a stronger distribution of the molecular orbital *away* from the carbon atom chain. Higher values of D_{SS} in the TZVP basis correlate with a more compact shape of the MO in the direction of the carbon atom chain. The exception of decapentaene in the trend of D_{SS} is noted in this context but will not be discussed further as it is obvious that the present analysis constitutes a substantially simplified picture and undoubtedly neglects further effects.

In summary, an inspection of the molecular orbitals seems indeed to establish a correspondence between the electron distribution and calculated values of electron spin-spin

coupling.

3.3.4 DFT/MRCI: Results for C_6H_8 – $C_{16}H_{34}$

The calculations in this section employ the SV(P) basis and were consistent with the study described earlier, spanning reference spaces of 89 – 99 configurations in the case of the systems dodecahexaene to hexadecaoctaene. As usual, the MOs composed from the 1s AO of the carbon atoms were kept frozen throughout.

		$D_{SS}[\text{cm}^{-1}]$	$E_{SS}[\text{cm}^{-1}]$
Hexatriene	C_6H_{14}	0.1172	0.0023
Octatetraene	C_8H_{18}	0.0862	0.0010
Decapentaene	$C_{10}H_{22}$	0.0771	0.0002
Dodecahexaene	$C_{12}H_{26}$	0.0574	0.0001
Tetradecaheptaene	$C_{14}H_{30}$	0.0488	0.0003
Hexadecaoctaene	$C_{16}H_{34}$	0.0407	0.0003

Table 3.14: SSC: Values for C_6H_{14} to $C_{16}H_{34}$ (SV(P) basis)

Table 3.14 displays the values for D_{SS} and E_{SS} in the series of all-*trans* polyenes from hexatriene (C_6H_{14}) to hexadecaoctaene ($C_{16}H_{34}$). The result for E_{SS} converges rapidly to a magnitude of 10^{-3} cm^{-1} , its further discussion will be omitted on the ground of its small absolute value. D_{SS} decreases in a crude first approximation linearly with the chain length, see Fig. 3.9.

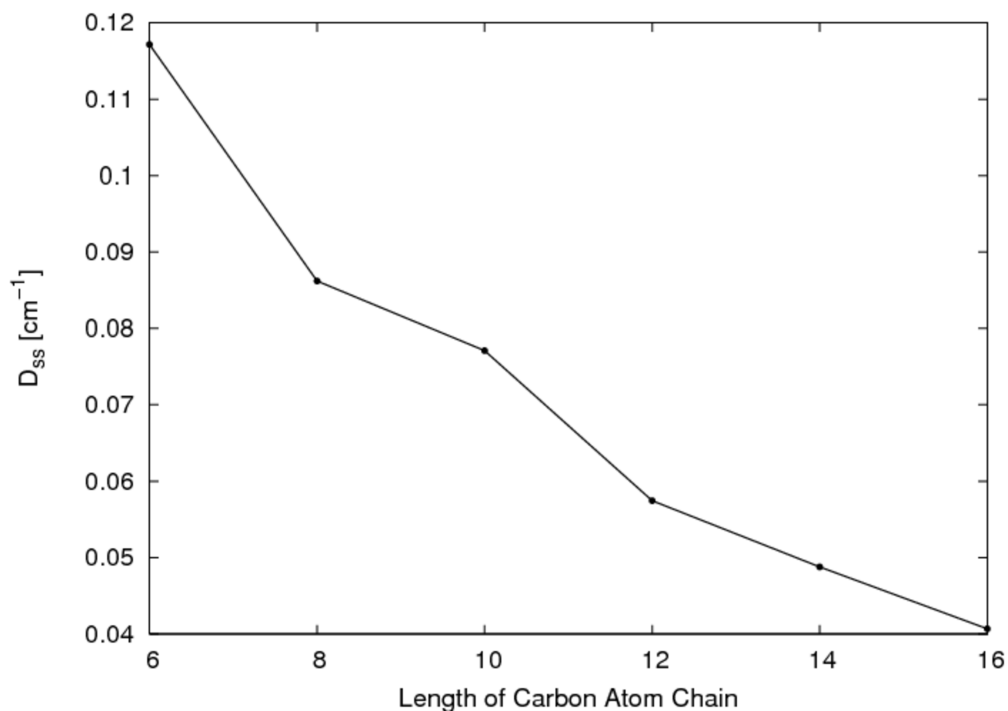


Figure 3.9: Dependence of D_{SS} on the chain length in all-*trans* polyenes

In the examination of these results, we note as a further issue the possibility that polyenes with an even number of double bonds exhibit a different behaviour than polyenes with an odd number of double bonds, in which case Fig. 3.9 would constitute a superposition of two trends. The pattern of a noticeable C-C-bond alternation in the terminating atoms is expected to establish itself gradually starting with the compounds $C_{14}H_{30}/C_{16}H_{34}$. In the present set of molecules, this aspect should therefore not be of considerable influence.

We return to our speculations regarding the possible localization of unpaired electrons in linear polyenes. Considering the strong distance dependence of the spin-spin operator, an exclusive localization of the unpaired electrons at the terminating carbon atoms appears to be unlikely, especially in view of the still noticeable coupling in hexadecaoctaene. A localization predominantly in the central part of the polyenes on the other hand would presumably result in a more constant value of D_{SS} . From the present calculations, we may therefore exclude these two possibilities and speculate on an even electron distribution or possibly a localization at intermediate carbon atoms. Comparison with further theoretical data, such as for example values of spin distributions, could assist in a more definite evaluation.

3.3.5 All-trans Polyenes: Conclusions

Calculations of electron spin-spin coupling in the first excited triplet state T_1 of all-*trans* polyenes C_6H_{14} to $C_{16}H_{34}$ were presented, focussing in particular on application and evaluation of SPOCK.SISTR with the DFT/MRCI program. Spin-spin-coupling parameters obtained with CASSCF and HF/MRCI on hexatriene support the validity of this method. Discussion of differences in the HF/MRCI as compared to DFT/MRCI, arising on the level of molecular orbitals and in the subsequent correlation treatment, indicate advantages of DFT/MRCI over HF/MRCI with respect to the description of spin-spin coupling effects as well as the computational demand. However, the basis of this comparison is confined to calculations of hexatriene in the SV(P) basis, and further investigations are undoubtedly necessary to verify these observations.

In the group of polyenes hexatriene, octatetraene, and decapentaene basis set effects in the DFT/MRCI approach are noticeable but of minor magnitude in a comparison of SV(P) with TZVP calculations. The differences arising can be partly related to changes in the shape of molecular orbitals, indicating the direct connection of a description of the electron distribution with calculated values of spin-spin coupling. Further investigations of the basis set dependence of spin-spin-coupling interactions for different basis sets and molecular systems, in particular focussing on the clarification of contributing and possibly partly compensating effects, would extend our understanding.

Investigation of the series hexatriene, octatetraene, decapentaene, dodecahexaene, tetradecaheptaene, and hexadecaoctaene provides first conclusions on the localization of unpaired electrons in the T_1 state, as decreasing values of D_{SS} indicate an increasing mean distance between the excited electrons. Further calculations as well as evaluation

of other computed properties will facilitate a more precise interpretation. Establishing a relation between the electron distribution and magnitudes of electron spin-spin coupling is a promising starting point for the investigation of more complicated systems where geometrical information is more difficult to analyze and spin-spin coupling calculations will assist in providing information on the electron distribution in excited states.

3.4 Conclusion

In this last chapter of my thesis, I presented calculations of electron spin-spin coupling on small and medium-sized systems, with emphasis on the validation of the SPOCK.SISTR implementation. Diagonal as well as off-diagonal spin-coupling elements were evaluated in the high-symmetry systems O_2 and NH , based on the HF/MRCI approach. First observations concerning basis set effects as well as the dependence of calculated values on molecular orbitals and CI spaces were established. Applicability of the DFT/MRCI branch in small polyenes was illustrated and its advantages discussed in comparison to the HF/MRCI execution. The calculation of spin-spin-coupling effects in a series of all-*trans* polyenes provided information on electron localization in the first excited triplet state T_1 .

The motivation for the calculations presented here was to study trends and establish the behaviour of computed values of electron spin-spin coupling. Work is still to be done in improving our understanding of this quantity, but the first steps in the calculation of electron spin-spin interactions based on a sophisticated evaluation of dynamical and non-dynamical correlation effects have been taken. They confirm the applicability of spin-spin coupling to gaining insight into systems of chemical interest, and thus provide a firm foundation for further activities in this area.

Summary and Outlook

This work presents the methodological development of the calculation of electron spin-spin interactions within a high-level correlation treatment, based on an evaluation of the Breit-Pauli spin-spin Hamiltonian in quasi-degenerate perturbation theory (QDPT). This task encompassed two main aspects — the derivation of sets of equations describing electron spin-spin effects, and the implementation of these equations into the existing program SPOCK, thereby creating SPOCK.SISTR. SPOCK calculates one-electron spin-orbit mean-field interactions of multireference CI wave functions and SPOCK.SISTR extends the capabilities of SPOCK by consideration of two-electron spin-spin coupling effects.

The crucial aspect in the derivation of the implemented equations lay in the extension of the efficient computation of the spin part as implemented within SPOCK from a one- to a two-electron spin operator. Issues had to be resolved in the theoretical reformulation as well as additional cases considered in the concrete implementation which necessitated a substantial extension of the code design. At the end, the development of the two-electron spin-coupling scheme as well as the adaptation to the existing program environment was successfully accomplished.

SPOCK.SISTR permits the calculation of expectation values, corresponding to a consideration of the spin-spin contribution to zero-field splittings, as well as coupling elements between different spin and spatial symmetries. The evaluation employs a multireference CI wave function calculated in a previous MRCI program run, and it is therefore one of the first implementations that realizes a consideration of dynamical as well as non-dynamical correlation effects on an equal basis. The multireference approach permits a reliable description of excited states while an execution with the efficient DFT/MRCI treatment provides the additional capability of investigating systems of larger size. It is the combination of these aspects that represents the power of this approach. The present work builds on the existing correlation treatment, creating a means of studying the characteristics of excited states through the high-level computation of spin-spin coupling effects.

The program operation of SPOCK.SISTR combined with the *ab initio* MRCI branch has been illustrated in calculations of diagonal and off-diagonal spin-coupling elements in diatomic systems; the applicability with the DFT/MRCI approach was investigated on a series of conjugated hydrocarbons. A first understanding of the issues specific to the computation of this effect was established and insight into questions of chemical interest obtained.

The present work has provided the theoretical and computational basis for the calculation of electron spin-spin coupling effects in ground and excited states of systems of chemical and biochemical relevance. From here, our understanding of this quantity, of its behaviour as well as its dependence on computational and molecular circumstances, has to be improved. The comparison with experimental data as well as other theoretical information will establish the foundation. Going further, electron spin-spin coupling enables us to study characteristics of electronic structure from an entirely new angle. What it is that we can learn from a computation of this effect, what it will tell us about the molecular state in question, will come from investigations on individual systems. Since electron spin-spin coupling constitutes a different means of analyzing the electron distribution of excited states, it will undoubtedly extend our knowledge in this respect. This work, then, opens the way to a multitude of exciting problems and questions.

List of Tables

3.1	Values for $D_{SS}[\text{cm}^{-1}]$ in O_2 : The one- and two-configuration case (no further excitations)	95
3.2	O_2 : The one- and two-configuration case + SD excitations: Energies and spin-spin coupling	96
3.3	Values for D_{SS} in O_2 : 8 in 6 reference space (no further excitations) . .	97
3.4	Values for D_{SS} in O_2 : 8 in 6 reference space + SD excitation	98
3.5	Values for D_{SS} in O_2 : n ($n = 8 - 13$) reference configurations (no further excitations)	99
3.6	Values for D_{SS} in O_2 : n ($n = 8 - 13$) reference configurations + SD excitation	99
3.7	NH: Spin-spin coupling elements between $c^1\Pi$ and $1^5\Sigma^-$ in dependence of the bond distance	104
3.8	SSC in hexatriene, calculated with DFT or HF MOs: Single-reference case (no further excitations)	110
3.9	SSC in hexatriene, calculated with DFT or HF MOs: 6 in 6 reference space (no further excitations)	111
3.10	SSC in hexatriene (SV(P) basis): Comparison of different approaches .	111
3.11	SSC with HF/MRCI in hexatriene (SV(P) basis): Assessment of selection thresholds	112
3.12	SSC in small all- <i>trans</i> polyenes, evaluated with DFT/MRCI in the SV(P) basis	113
3.13	SSC in small all- <i>trans</i> polyenes, evaluated with DFT/MRCI in the TZVP basis	113
3.14	SSC: Values for C_6H_{14} to $\text{C}_{16}\text{H}_{34}$ (SV(P) basis)	115

List of Figures

1.1	General picture of the splitting of a triplet state	6
1.2	Pairwise comparison of configurations	26
1.3	Connection of MRCI, SPOCK, SPOCK.SISTR	27
1.4	Example of calculation of excitation pattern	34
2.1	Program structure of SPOCK.SISTR	42
2.2	Alignment of configurations $ \Xi\rangle$, CSFs $ \Upsilon\rangle$	43
2.3	Comparison of configurations	44
2.4	Calculation of contributions	45
2.5	Contrasting: Structure/Major routines of SPOCK.SISTR	83
2.6	Hierarchy of spin-spin routines in SPOCK.SISTR	84
2.7	calc.ssmes	85
2.8	cipropSS	87
2.9	{ ssint }	88
2.10	ssmatelsum	89
2.11	{ DeltaS }	91
3.1	Dependence of D_{SS} (O_2) on the size of the reference space	100
3.2	Dependence of $E_{MRCI(V)}$ (O_2) on the size of the reference space	101
3.3	Variation of C–C bond distance in docosaundecaene ($C_{22}H_{24}$)	106
3.4	MO $2a_u$: DFT (BHLYP) calculation	109
3.5	MO $2a_u$: ROHF calculation	109
3.6	MO $2b_g$: DFT (BHLYP) calculation	110
3.7	MO $2b_g$: ROHF calculation	110
3.8	Orbital $4b_g$ of octatetraene: SV(P) vs. TZVP basis	114
3.9	Dependence of D_{SS} on the chain length in all- <i>trans</i> polyenes	115

Bibliography

- [1] S. Grimme and M. Waletzke. A combination of Kohn-Sham density functional theory and multi-reference configuration interaction methods. *J. Chem. Phys.* **111** (13), 5645–5655 (1999).
- [2] M. Kleinschmidt, J. Tatchen, and C. M. Marian. Spin-orbit coupling of DFT/MRCI wavefunctions: Method, test calculations, and application to thiophene. *J. Comput. Chem.* **23** (8), 824–833 (2002).
- [3] M. Kleinschmidt and C. M. Marian. Efficient generation of matrix elements for one-electron spin-orbit operators. *Chem. Phys.* **311** (1–2), 71–79 (2005).
- [4] M. Kleinschmidt, J. Tatchen, and C. M. Marian. SPOCK.CI: A multireference spin-orbit configuration interaction method for large molecules. *J. Chem. Phys.* **124** (12), 124101–1–124101–17 (2006).
- [5] A. Szabo and N. S. Ostlund. *Modern Quantum Chemistry*. Dover Publications, Mineola, New York, 1st ed., rev. New York, unabr. republ. edition, 1996.
- [6] J. J. Sakurai (Ed.: S. F. Tuan). *Modern Quantum Mechanics*. Addison-Wesley Publishing Company, Reading, Massachusetts [et al.], rev. edition, 1994.
- [7] T. Helgaker, P. Jørgensen, and J. Olsen. *Molecular Electronic-Structure Theory*. John Wiley & Sons, Ltd, Chichester [et al.], 2000.
- [8] P. A. M. Dirac. The quantum theory of the electron. *Proc. Roy. Soc. A* **117** (778), 610–624 (1928).
- [9] P. A. M. Dirac. The quantum theory of the electron. Part II. *Proc. Roy. Soc. A* **118** (779), 351–361 (1928).
- [10] R. E. Moss. *Advanced Molecular Quantum Mechanics*. Chapman and Hall, London, 1973.
- [11] K. G. Dyall and K. Fægri, Jr. *Introduction to Relativistic Quantum Chemistry*. Oxford University Press, New York [et. al], 2007.
- [12] W. Gerlach and O. Stern. Der experimentelle Nachweis des magnetischen Moments des Silberatoms. *Z. Phys.* **8** (1), 110–111 (1922).
- [13] W. Gerlach and O. Stern. Der experimentelle Nachweis der Richtungsquantelung im Magnetfeld. *Z. Phys.* **9** (1), 349–352 (1922).

- [14] W. Pauli. Über den Einfluß der Geschwindigkeitsabhängigkeit der Elektronenmasse auf den Zeemaneffekt. *Z. Phys.* **31** (1), 373–385 (1925).
- [15] G. E. Uhlenbeck and S. Goudsmit. Ersetzung der Hypothese vom unmechanischen Zwang durch eine Forderung bezüglich des inneren Verhaltens jedes einzelnen Elektrons. *Naturw.* **13** (47), 953–954 (1925).
- [16] G. E. Uhlenbeck and S. Goudsmit. Spinning electrons and the structure of spectra. *Nature* **117**, 264–265 (1926).
- [17] C. M. Marian. Spin-orbit coupling in molecules. In *Reviews in Computational Chemistry*, edited by K. Lipkowitz and D. Boyd, pages 99 – 204, Wiley-VCH, Weinheim, 2001.
- [18] P. A. M. Dirac. *The Principles of Quantum Mechanics*. Clarendon Press, Oxford, 1930.
- [19] G. Breit. The fine structure of He as a test of the spin interactions of two electrons. *Phys. Rev.* **36** (3), 383–397 (1930).
- [20] G. Breit. Dirac’s equation and the spin-spin interactions of two electrons. *Phys. Rev.* **39** (4), 616–624 (1932).
- [21] H. A. Bethe and E. E. Salpeter. *Quantum Mechanics of One- and Two-Electron Atoms*. Academic Press, New York, 1957.
- [22] M. Kaupp, M. Bühl, and V. G. Malkin, editors. *Calculation of NMR and EPR parameters*. Wiley-VCH, Weinheim, 2004.
- [23] R. McWeeny. *Spins in Chemistry*. Academic Press, New York and London, 1970.
- [24] W. Weltner, Jr. *Magnetic Atoms and Molecules*. Scientific and Academic Editions, New York, 1983.
- [25] A. Abragam and B. Bleaney. *Electron Paramagnetic Resonance of Transition Ions*. Clarendon Press, Oxford, 1970.
- [26] A. Carrington and A. D. McLachlan. *Introduction to Magnetic Resonance*. Harper & Row, John Weatherhill, New York, Tokyo, 1969.
- [27] S. R. Langhoff and C. W. Kern. Molecular fine structure. In *Applications of Electronic Structure Theory*, edited by H. F. Schaefer, III, volume 4, pages 381–437, Plenum Press, New York and London, 1977.
- [28] J. E. Wertz and J. R. Bolton. *Electron Spin Resonance – Elementary Theory and Practical Applications*. McGraw-Hill Series in Advanced Chemistry, McGraw-Hill Book Company, New York [et al.], 1972.
- [29] S. P. McGlynn, T. Azumi, and M. Kinoshita. *Molecular Spectroscopy of the Triplet State*. Prentice-Hall, Englewood Cliffs (New Jersey), 1969.

- [30] W. Gordy. *Theory and Applications of Electron Spin Resonance*, volume XV of *Techniques of Chemistry*. John Wiley & Sons, New York, 1980.
- [31] A. Bencini and D. Gatteschi. *EPR of Exchange Coupled Systems*. Springer-Verlag, Berlin [et al.], 1990.
- [32] W. Pauli, Jr. Zur Quantenmechanik des magnetischen Elektrons. *Z. Phys.* **43** (9-10), 601–623 (1927).
- [33] J. E. Harriman. *Theoretical Foundations of Electron Spin Resonance*. Academic Press, New York [et al.], 1978.
- [34] F. Neese and M. L. Munzarová. Historical aspects of EPR parameter calculations. In *Calculation of NMR and EPR parameters*, edited by M. Kaupp, M. Bühl, and V. G. Malkin, chapter 3, pages 21–32, Wiley-VCH, Weinheim, 2004.
- [35] A. Schweiger and G. Jeschke. *Principles of Pulse Electron Paramagnetic Resonance*. Oxford University Press, Oxford, 2001.
- [36] W. Lubitz, K. Möbius, and K.-P. Dinse. Guest Editors' Foreword: High-field EPR. *Magn. Reson. Chem.* **43** (S2–S3) (2005).
- [37] G. Jeschke. Determination of the nanostructure of polymer materials by electron paramagnetic resonance spectroscopy. *Macromol. Rapid Commun.* **23** (4), 227–246 (2002).
- [38] G. Jeschke and Y. Polyhach. Distance measurements on spin-labelled biomacromolecules by pulsed electron paramagnetic resonance. *Phys. Chem. Chem. Phys.* **9** (16), 1895–1910 (2007).
- [39] C. Calle, R.-A. Eichel, C. Finazzo, J. Forrer, J. Granwehr, I. Gromov, W. Groth, J. Harmer, M. Kälin, W. Lämmler, L. Liesum, Z. Mádi, S. Stoll, S. van Doorslaer, and A. Schweiger. Electron paramagnetic resonance spectroscopy. *Chimie* **55** (10), 763–766 (2001).
- [40] L. J. Berliner, S. S. Eaton, and G. R. Eaton, editors. *Biological Magnetic Resonance: Distance Measurements in Biological Systems by EPR*, volume 19. Kluwer Academic/Plenum Publishers, New York, 2000.
- [41] A. D. Milov, A. G. Maryasov, and Y. D. Tsvetkov. Pulsed electron double resonance (PELDOR) and its applications in free-radicals research. *Appl. Magn. Reson.* **15** (1), 107–143 (1998).
- [42] G. Jeschke. Distance measurements in the nanometer range by pulse EPR. *Chem. Phys. Chem.* **3** (11), 927–932 (2002).
- [43] Y. Polyhach, A. Godt, C. Bauer, and G. Jeschke. Spin pair geometry revealed by high-field DEER in the presence of conformational distributions. *J. Mag. Res.* **185** (1), 118–129 (2007).

- [44] A. Savitsky, A. A. Dubinskii, M. Flores, W. Lubitz, and K. Möbius. Orientation-resolving pulsed electron dipolar high-field EPR spectroscopy on disordered solids: I. Structure of spin-correlated radical pairs in bacterial photosynthetic reaction centers. *J. Phys. Chem. B* **111** (22), 6245–6262 (2007).
- [45] H. Hamerka. Theory of the electron spin resonance of benzene in the triplet state. *J. Chem. Phys.* **31** (2), 315–321 (1959).
- [46] C. A. Hutchison, Jr. and B. W. Mangum. Paramagnetic resonance absorption in naphthalene in its phosphorescent state. *J. Chem. Phys.* **29** (4), 952–953 (1958).
- [47] S. A. Boorstein and M. Gouterman. Theory for zero-field splittings in aromatic hydrocarbons. III. *J. Chem. Phys.* **39** (10), 2443–2452 (1963).
- [48] O. Vahtras, O. Loboda, B. Minaev, H. Ågren, and K. Ruud. Ab initio calculations of zero-field splitting parameters. *Chem. Phys.* **279** (2–3), 133–142 (2002).
- [49] K. Kayama. Spin dipole-dipole interaction in O₂. *J. Chem. Phys.* **42** (2), 622–630 (1965).
- [50] S. R. Langhoff and E. R. Davidson. An ab initio calculation of the spin dipole-dipole parameters for methylene. *Int. J. Quantum Chem.* **7** (4), 759–777 (1973).
- [51] M. Tinkham and M. W. P. Strandberg. Interaction of molecular oxygen with a magnetic field. *Phys. Rev.* **97** (4), 951–966 (1955).
- [52] K. Kayama and J. C. Baird. Spin-orbit effects and the fine structure in the $^3\Sigma_g^-$ ground state of O₂. *J. Chem. Phys.* **46** (7), 2604–2618 (1967).
- [53] R. H. Pritchard, M. L. Sink, J. D. Allen, and C. W. Kern. Theoretical studies of fine structure in the ground state of O₂. *Chem. Phys. Lett.* **17** (2), 157–159 (1972).
- [54] R. H. Pritchard, C. W. Kern, O. Zamani-Khamiri, and H. F. Hamerka. Further commentary on the oxygen spin-orbit problem. *J. Chem. Phys.* **58** (1), 411–412 (1973).
- [55] J. A. Hall. Comment on the spin-orbit contribution to the zero-field splitting of the oxygen molecule. *J. Chem. Phys.* **58** (1), 410–411 (1973).
- [56] L. Veseth and A. Lofthus. Fine structure and centrifugal distortion in the electronic and microwave spectra of O₂ and SO. *Mol. Phys.* **27** (2), 511–519 (1974).
- [57] F. D. Wayne. Origin of the variation with vibrational and rotational state of the fine-structure constants in O₂, SO and S₂. *Chem. Phys. Lett.* **31** (1), 97–101 (1975).
- [58] S. R. Langhoff. Ab initio evaluation of the fine structure of the oxygen molecule. *J. Chem. Phys.* **61** (5), 1708–1716 (1974).

- [59] F. D. Wayne and E. A. Colburn. Effective spin-spin interactions and singlet-triplet transition intensities in a class of open-shell diatomic molecules. *Mol. Phys.* **34** (4), 1141–1155 (1977).
- [60] M. L. Sink, H. Lefebvre-Brion, and J. A. Hall. Ab initio calculations of the effective spin-spin constants of the $^3\Sigma$ excited states of the N_2 and CO molecules. *J. Chem. Phys.* **62** (5), 1802–1805 (1975).
- [61] A. V. Luzanov and V. N. Poltavets. Calculation of the parameters of zero-field splitting for triplet states of conjugated systems. *J. Struct. Chem.* **15** (3), 457–460 (1974).
- [62] S. R. Langhoff. Spin-orbit contribution to the zero-field splitting in CH_2 . *J. Chem. Phys.* **61** (10), 3881–3885 (1974).
- [63] S. R. Langhoff, E. R. Davidson, and C. W. Kern. Ab initio study of the zero-field splitting parameters of $^3B_{1u}$ benzene. *J. Chem. Phys.* **63** (11), 4800–4807 (1975).
- [64] S. R. Langhoff. Comment on the zero-field splitting in the $b^3\Sigma_g^-$ state of C_2 . *J. Chem. Phys.* **64** (3), 1245–1246 (1976).
- [65] S. R. Langhoff and E. R. Davidson. Ab initio evaluation of the fine structure and radiative lifetime of the $^3A_2(n \rightarrow \pi^*)$ state of formaldehyde. *J. Chem. Phys.* **64** (11), 4699–4710 (1976).
- [66] E. R. Davidson, J. C. Ellenbogen, and S. R. Langhoff. An ab initio calculation of the zero-field splitting parameters of the $^3A''$ state of formaldehyde. *J. Chem. Phys.* **73** (2), 865–869 (1980).
- [67] J. C. Ellenbogen, D. Feller, and E. R. Davidson. Ab initio calculation of the properties and the geometry of the lowest triplet state of pyrazine. *J. Phys. Chem.* **86** (9), 1583–1588 (1982).
- [68] D. Feller, W. T. Borden, and E. R. Davidson. Ab initio calculation of the zero-field splitting parameters of vinylmethylene. *J. Phys. Chem.* **87** (24), 4833–4839 (1983).
- [69] H. F. Schaefer, III. *Applications of Electronic Structure Theory*. Modern Theoretical Chemistry, Plenum Press, New York and London, 1977.
- [70] J. S. Griffith. *The Theory of Transition Metal Ions*. Cambridge University Press, Cambridge, 1964.
- [71] J. Mählmann and M. Klessinger. Zero-field splitting calculations based on semiempirical MR–CI wave functions. *Int. J. Quantum Chem.* **77** (1), 446–453 (2000).
- [72] B. Bomfleur, M. Sironi, M. Raimondi, and J. Voitländer. Ab initio calculation of the zero-field splitting parameter D of benzene and naphthalene. *J. Chem. Phys.* **112** (3), 1066–1069 (2000).

- [73] B. Bomfleur, J. Voitländer, M. Sironi, and M. Raimondi. Spin correlation function of benzene and naphthalene from spin-coupled wave functions. *J. Chem. Phys.* **114** (4), 1505–1509 (2001).
- [74] A. O. Mitrushenkov, P. Palmieri, and R. Tarroni. Improved calculation of spin-dependent properties for internally contracted multireference configuration interaction wavefunctions. *Mol. Phys.* **101** (13), 2043–2046 (2003).
- [75] H.-J. Werner, P. J. Knowles, R. Lindh, F. R. Manby, M. Schütz, et al. MOLPRO, a package of ab initio programs.
- [76] A. Spielfiedel, P. Palmieri, and A. O. Mitrushenkov. Ab initio calculation of molecular hydrogen electronic states' properties: fine structure spin-spin constants. *Mol. Phys.* **102** (21–22), 2191–2200 (2004).
- [77] A. Spielfiedel, P. Palmieri, and A. O. Mitrushenkov. Ab initio calculation of molecular hydrogen electronic states' properties: transition matrix elements among triplet electronic states. *Mol. Phys.* **102** (21–22), 2249–2258 (2004).
- [78] J. Michl. Spin-orbit coupling in biradicals. 1. The 2-electrons-in-2-orbitals model revisited. *J. Am. Chem. Soc.* **118** (15), 3568–3579 (1996).
- [79] Z. Havlas, J. W. Downing, and J. Michl. Spin-orbit coupling in biradicals. 2. Ab initio methodology and application to 1,1-biradicals: Carbene and silylene. *J. Phys. Chem. A* **102** (28), 5681–5692 (1998).
- [80] Z. Havlas and J. Michl. Spin-orbit coupling in biradicals. 3. Heavy atom effects in carbenes. *Collect. Czech. Chem. C.* **63** (9), 1485–1497 (1998).
- [81] Z. Havlas and J. Michl. Ab initio calculation of zero-field splitting and spin-orbit coupling in ground and excited triplets of m-xylylene. *J. Chem. Soc., Perkin Trans. 2* (11), 2299–2303 (1999).
- [82] Z. Havlas, M. Kývala, and J. Michl. Spin-orbit coupling in biradicals. 4. Zero-field splitting in triplet nitrenes, phosphinidenes, and arsinidenes. *Collect. Czech. Chem. C.* **68** (12), 2335–2343 (2003).
- [83] Z. Havlas, M. Kývala, and J. Michl. Spin-orbit coupling in biradicals. 5. Zero-field splitting in triplet dimethylnitrenium, dimethylphosphenium and dimethylarsenium cations. *Mol. Phys.* **103** (2–3), 407–411 (2005).
- [84] DALTON, a molecular electronic structure program. See <http://www.kjemi.uio.no/software/dalton/dalton.html>.
- [85] O. Loboda, B. Minaev, O. Vahtras, B. Schimmelpfennig, H. Ågren, K. Ruud, and D. Jonsson. Ab initio calculations of zero-field splitting parameters in linear polyacenes. *Chem. Phys.* **286** (1), 127–137 (2003).

- [86] O. Loboda, B. Minaev, O. Vahtras, K. Ruud, and H. Ågren. Ab initio study of nonhomogeneous broadening of the zero-field splitting of triplet guest molecules in diluted glasses. *J. Chem. Phys.* **119** (6), 3120–3129 (2003).
- [87] B. Minaev, O. Loboda, Z. Rinkevicius, O. Vahtras, and H. Ågren. Fine and hyperfine structure in three low-lying $X^3\Sigma^+$ states of molecular hydrogen. *Mol. Phys.* **101** (15), 2335–2346 (2003).
- [88] B. Minaev. Fine structure and radiative lifetime of the low-lying triplet states of the helium excimer. *Phys. Chem. Chem. Phys.* **5** (11), 2314–2319 (2003).
- [89] Ó. Rubio-Pons, O. Loboda, B. Minaev, B. Schimmelpfennig, O. Vahtras, and H. Ågren. CASSCF calculations of triplet state properties: Applications to benzene derivatives. *Mol. Phys.* **101** (13), 2103–2114 (2003).
- [90] B. Minaev, I. Tunell, P. Salek, O. Loboda, O. Vahtras, and H. Ågren. Singlet-triplet transitions in three-atomic molecules studied by time-dependent MCSCF and density functional theory. *Mol. Phys.* **102** (13), 1391–1406 (2004).
- [91] B. Minaev, O. Loboda, O. Vahtras, K. Ruud, and H. Ågren. Solvent effects on optically detected magnetic resonance in triplet spin labels. *Theor. Chem. Acc.* **111** (2–6), 168–175 (2004).
- [92] B. Minaev, L. Yaschuk, and V. Kukueva. Calculation of the fine structure and intensity of the singlet-triplet transitions in the imidogen radical. *Spectrochim. Acta, Part A* **61** (6), 1105–1112 (2005).
- [93] B. Minaev. Ab initio study of low-lying triplet states of the lithium dimer. *Spectrochim. Acta, Part A* **62** (4–5), 790–799 (2005).
- [94] Ó. Rubio-Pons, B. Minaev, O. Loboda, and H. Ågren. Ab initio calculations of vibronic activity in phosphorescence microwave double resonance spectra of p-dichlorobenzene. *Theor. Chem. Acc.* **113** (1), 15–27 (2005).
- [95] O. Loboda, I. Tunell, B. Minaev, and H. Ågren. Theoretical study of triplet state properties of free-base porphin. *Chem. Phys.* **312** (1–3), 299–309 (2005).
- [96] T. T. Petrenko, T. L. Petrenko, and V. Y. Bratus. The carbon $\langle 100 \rangle$ split interstitial in SiC. *J. Phys.: Condens. Matter* **14** (47), 12433–12440 (2002).
- [97] P. A. M. Dirac. Note on exchange phenomena in the Thomas atom. *Proc. Cambridge Phil. Soc.* **26**, 376–385 (1930).
- [98] R. McWeeny. On the origin of spin-Hamiltonian parameters. *J. Chem. Phys.* **42** (5), 1717–1725 (1965).
- [99] M. Shoji, K. Koizumi, T. Hamamoto, T. Taniguchi, R. Takeda, Y. Kitagawa, T. Kawakami, M. Okumura, S. Yamanaka, and K. Yamaguchi. A theoretical study of zero-field splitting of organic biradicals. *Polyhedron* **24** (16–17), 2708–2715 (2005).

- [100] H. M. McConnell. A theorem on zero-field splittings. *Proc. Nat. Acad. Sci. USA* **45** (2), 172–174 (1959).
- [101] F. Neese and E. I. Solomon. Calculation of zero-field splittings, g-values, and the relativistic nephelauxetic effect in transition metal complexes. Application to high-spin ferric complexes. *Inorg. Chem.* **37** (26), 6568–6582 (1998).
- [102] F. Neese. Metal and ligand hyperfine couplings in transition metal complexes: The effect of spin-orbit coupling as studied by coupled perturbed Kohn-Sham theory. *J. Chem. Phys.* **118** (9), 3939–3948 (2003).
- [103] M. van Gastel, W. Lubitz, G. Lassmann, and F. Neese. Electronic structure of the cysteine thiy radical: A DFT and correlated ab initio study. *J. Am. Chem. Soc.* **126** (7), 2237–2246 (2004).
- [104] S. Sinnecker, F. Neese, L. Noodleman, and W. Lubitz. Calculating the electron paramagnetic resonance parameters of exchange coupled transition metal complexes using broken symmetry density functional theory: Application to a Mn^{III}/Mn^{IV} model compound. *J. Am. Chem. Soc.* **126** (8), 2613–2622 (2004).
- [105] S. Sinnecker, E. Reijerse, F. Neese, and W. Lubitz. Hydrogen bond geometries from electron paramagnetic resonance and electron-nuclear double resonance parameters: Density functional study of quinone radical anion-solvent interactions. *J. Am. Chem. Soc.* **126** (10), 3280–3290 (2004).
- [106] K. Ray, A. Begum, T. Weyhermüller, S. Piligkos, J. van Slageren, F. Neese, and K. Wieghardt. The electronic structure of the isoelectronic, square-planar complexes [Fe^{II}(L)₂]²⁻ and [Co^{III}(L^{Bu})₂]⁻ (L²⁻ and (L^{Bu})²⁻ = benzene-1,2-dithiolates): An experimental and density functional theoretical study. *J. Am. Chem. Soc.* **127** (12), 4403–4415 (2005).
- [107] S. Sinnecker, F. Neese, and W. Lubitz. Dimanganese catalase – spectroscopic parameters from broken-symmetry density functional theory of the superoxidized Mn^{III}/Mn^{IV} state. *J. Biol. Inorg. Chem.* **10** (2), 231–238 (2005).
- [108] F. Neese. Importance of direct spin-spin coupling and spin-flip excitations for the zero-field splittings of transition metal complexes: A case study. *J. Am. Chem. Soc.* **128** (31), 10213–10222 (2006).
- [109] F. Neese. A critical evaluation of DFT, including time-dependent DFT, applied to bioinorganic chemistry. *J. Biol. Inorg. Chem.* **11** (6), 702–711 (2006).
- [110] J. Chalupský, F. Neese, E. I. Solomon, U. Ryde, and L. Rulíšek. Multireference ab initio calculations on reaction intermediates of the multicopper oxidases. *Inorg. Chem.* **45** (26), 11051–11059 (2006).
- [111] C. Duboc, T. Phoeung, S. Zein, J. Pécaut, M.-N. Collomb, and F. Neese. Origin of the zero-field splitting in mononuclear octahedral dihalide Mn^{II} complexes: An

- investigation by multifrequency high-field electron paramagnetic resonance and density functional theory. *Inorg. Chem.* **46** (2), 4905–4916 (2007).
- [112] S. Sinnecker and F. Neese. QM/MM calculations with DFT for taking into account protein effects on the EPR and optical spectra of metalloproteins. Plastocyanin as a case study. *J. Comp. Chem.* **27** (12), 1463–1475 (2006).
- [113] J. C. Schöneboom, F. Neese, and W. Thiel. Toward identification of the compound I reactive intermediate in cytochrome P450 chemistry: A QM/MM study of its EPR and Mössbauer parameters. *J. Am. Chem. Soc.* **127** (16), 5840–5853 (2005).
- [114] F. Neese and E. I. Solomon. Interpretation and calculation of spin-Hamiltonian parameters in transition metal complexes. In *Magnetism: Molecules to Materials IV*, edited by J. S. Miller and M. Drillon, pages 345–466, Wiley-VCH, Weinheim, 2003.
- [115] F. Neese. Quantum chemical calculations of spectroscopic properties of metalloproteins and model compounds: EPR and Mössbauer properties. *Curr. Op. Chem. Biol.* **7** (1), 125–135 (2003).
- [116] F. Neese, T. Petrenko, D. Ganyushin, and G. Olbrich. Advanced aspects of ab initio theoretical optical spectroscopy of transition metal complexes: Multiplets, spin-orbit coupling and resonance Raman intensities. *Coord. Chem. Rev.* **251** (3–4), 288–327 (2007).
- [117] B. Kirchner, F. Wennmohs, S. Ye, and F. Neese. Theoretical bioinorganic chemistry: the electronic structure makes a difference. *Curr. Op. Chem. Biol.* **11** (2), 134–141 (2007).
- [118] S. Sinnecker and F. Neese. Theoretical bioinorganic spectroscopy. *Top. Curr. Chem.* **268**, 47–83 (2007).
- [119] F. Neese. Zero-field splitting. In *Calculation of NMR and EPR parameters*, edited by M. Kaupp, M. Bühl, and V. G. Malkin, chapter 34, pages 541–564, Wiley-VCH, Weinheim, 2004.
- [120] F. Neese. Applications to EPR in bioinorganic chemistry. In *Calculation of NMR and EPR parameters*, edited by M. Kaupp, M. Bühl, and V. G. Malkin, chapter 36, pages 581–591, Wiley-VCH, Weinheim, 2004.
- [121] F. Neese. Spin-Hamiltonian parameters from first principle calculations: Theory and application. In *Mag. Res. Biol.*, 2007. In press.
- [122] B. A. Heß, C. M. Marian, U. Wahlgren, and O. Gropen. A mean-field spin-orbit method applicable to correlated wavefunctions. *Chem. Phys. Lett.* **251** (5–6), 365–371 (1996).

- [123] B. A. Heß, C. M. Marian, and S. D. Peyerimhoff. Ab initio calculation of spin-orbit effects in molecules including electron correlation. In *Modern Electronic Structure Theory, Part I*, edited by D. R. Yarkony, volume 2, pages 152–278, World Scientific Publishing Co. Pte. Ltd., Singapore, 1995.
- [124] S. Sinnecker and F. Neese. Spin-spin contributions to the zero-field splitting tensor in organic triplets, carbenes and biradicals – a density functional and ab initio study. *J. Phys. Chem. A* **110** (44), 12267–12275 (2006).
- [125] D. Ganyushin and F. Neese. First-principles calculations of zero-field splitting parameters. *J. Chem. Phys.* **125** (2), 024103–1–024103–10 (2006).
- [126] K. Möbius, A. Savitsky, A. Schnegg, M. Plato, and M. Fuchs. High-field EPR spectroscopy applied to biological systems: characterization of molecular switches for electron and ion transfer. *Phys. Chem. Chem. Phys.* **7** (1), 19–42 (2005).
- [127] A. G. Agrawal, M. van Gastel, W. Gärtner, and W. Lubitz. Hydrogen bonding affects the [NiFe] active site of *desulfovibrio vulgaris* Miyazaki F hydrogenase: A hyperfine sublevel correlation spectroscopy and density functional theory study. *J. Phys. Chem. B* **110** (15), 8142–8150 (2006).
- [128] B. Epel, J. Niklas, S. Sinnecker, H. Zimmermann, and W. Lubitz. Phylloquinone and related radical anions studied by pulse electron nuclear double resonance spectroscopy at 34 GHz and density functional theory. *J. Phys. Chem. B* **110** (23), 11549–11560 (2006).
- [129] S. Sinnecker, M. Flores, and W. Lubitz. Protein-cofactor interactions in bacterial reaction centers from *rhodobacter sphaeroides* R-26: Effect of hydrogen bonding on the electronic and geometric structure of the primary quinone. A density functional study. *Phys. Chem. Chem. Phys.* **8** (48), 5659–5670 (2006).
- [130] R. Bittl, E. Schlodder, I. Geisenheimer, W. Lubitz, and R. J. Cogdell. Transient EPR and absorption studies of carotenoid triplet formation in purple bacterial antenna complexes. *J. Phys. Chem. B* **105** (23), 5525–5535 (2001).
- [131] W. Lubitz, F. Lendzian, and R. Bittl. Radicals, radical pairs and triplet states in photosynthesis. *Acc. Chem. Res.* **35** (5), 313–320 (2002).
- [132] W. Lubitz. Pulse EPR and ENDOR studies of light-induced radicals and triplet states in photosystem II of oxygenic photosynthesis. *Phys. Chem. Chem. Phys.* **4** (22), 5539–5545 (2002).
- [133] W. Lubitz. Photochemical processes in photosynthesis studied by advanced EPR techniques. *Pure Appl. Chem.* **75** (8), 1021–1030 (2003).
- [134] M. G. Müller, J. Niklas, W. Lubitz, and A. R. Holzwarth. Ultrafast transient absorption studies on photosystem I reaction centers from *chlamydomonas reinhardtii*. 1. A new interpretation of the energy trapping and early electron transfer steps in photosystem I. *Biophys. J.* **85** (6), 3899–3922 (2003).

- [135] C. Teutloff, R. Bittl, and W. Lubitz. Pulse ENDOR studies on the radical pair $P_{700}^+ A_1^-$ and the photoaccumulated quinone acceptor A_1^- of photosystem I. *Appl. Magn. Reson.* **26** (1–2), 5–21 (2004).
- [136] Y. N. Pushkar, D. Stehlik, M. van Gastel, and W. Lubitz. An EPR/ENDOR study of the asymmetric hydrogen bond between the quinone electron acceptor and the protein backbone in photosystem I. *J. Mol. Struct.* **700** (1–3), 233–241 (2004).
- [137] M. van Gastel, C. Fichtner, F. Neese, and W. Lubitz. EPR experiments to elucidate the structure of the ready and unready states of the [NiFe] hydrogenase of *desulfovibrio vulgaris* Miyazaki F. *Biochem. Soc. Trans.* **33** (Part 1), 7–11 (2005).
- [138] L. V. Kulik, W. Lubitz, and J. Messinger. Electron spin-lattice relaxation of the S_0 state of the oxygen-evolving complex in photosystem II and of dinuclear manganese model complexes. *Biochem.* **44** (26), 9368–9374 (2005).
- [139] L. V. Kulik, B. Epel, J. Messinger, and W. Lubitz. Pulse EPR, ^{55}Mn -ENDOR and ELDOR-detected NMR of the S_2 state of the oxygen evolving complex in photosystem II. *Photosynth. Res.* **84** (1–3), 347–353 (2005).
- [140] L. V. Kulik, B. Epel, W. Lubitz, and J. Messinger. ^{55}Mn pulse ENDOR at 34 GHz of the S_0 and S_2 states of the oxygen-evolving complex in photosystem II. *J. Am. Chem. Soc.* **127** (8), 2392–2393 (2005).
- [141] S. Foerster, M. van Gastel, M. Brecht, and W. Lubitz. An orientation-selected ENDOR and HYSORE study of the Ni-C active state of *desulfovibrio vulgaris* Miyazaki F hydrogenase. *J. Biol. Inorg. Chem.* **10** (1), 51–62 (2005).
- [142] B. Epel, J. Niklas, M. L. Antonkine, and W. Lubitz. Absolute signs of hyperfine coupling constants as determined by pulse ENDOR of polarized radical pairs. *Appl. Magn. Reson.* **30** (3–4), 311–327 (2006).
- [143] M. Flores, R. Isaacson, E. Abresch, R. Calvo, W. Lubitz, and G. Feher. Protein-cofactor interactions in bacterial reaction centers from *rhodobacter sphaeroides* R-26: I. Identification of the ENDOR lines associated with the hydrogen bonds to the primary quinone Q_A^- . *Biophys. J.* **90** (9), 3356–3362 (2006).
- [144] M. Flores, R. Isaacson, E. Abresch, R. Calvo, W. Lubitz, and G. Feher. Protein-cofactor interactions in bacterial reaction centers from *rhodobacter sphaeroides* R-26: II. Geometry of the hydrogen bonds to the primary quinone Q_A^- by ^1H and ^2H ENDOR spectroscopy. *Biophys. J.* **92** (2), 671–682 (2007).
- [145] A. Schnegg, A. A. Dubinskii, M. R. Fuchs, Y. A. Grishin, E. P. Kirilina, W. Lubitz, M. Plato, A. Savitsky, and K. Möbius. High-field EPR, ENDOR and ELDOR on bacterial photosynthetic reaction centers. *Appl. Magn Reson.* **31** (1–2), 59–98 (2007).

- [146] C. M. Marian. Relaxation pathways of electronically excited chromophores. Presentation at: SFB-Symposium, Bad Münstereifel, April 16–18 2007.
- [147] C. M. Marian. Personal Communication.
- [148] R. Ahlrichs, M. Bär, M. Häser, H. Horn, and C. Kölmel. Electronic structure calculations on workstation computers: The program system turbomole. *Chem. Phys. Lett.* **162** (3), 165–169 (1989).
- [149] M. Häser and R. Ahlrichs. Improvements on the direct SCF method. *J. Comput. Chem.* **10** (1), 104–111 (1989).
- [150] O. Vahtras, J. Almlöf, and M. W. Feyereisen. Integral approximations for LCAO-SCF calculations. *Chem. Phys. Lett.* **213** (5-6), 514–518 (1993).
- [151] F. Weigend and M. Häser. RI-MP2: First derivatives and global consistency. *Theor. Chem. Acc.* **97** (1–4), 331–340 (1997).
- [152] B. Schimmelpfennig. *Atomic spin-orbit Mean-Field Integral program AMFI*, 1996. Stockholms Universitet, Sweden.
- [153] M. Kleinschmidt. *Konfigurationswechselwirkung und Spin-Bahn-Kopplung: Neue Methoden zur Behandlung großer Moleküle*. PhD thesis, Universität Düsseldorf, 2006.
- [154] D. A. Varshalovich, A. N. Moskalev, and V. K. Khersonskii. *Quantum Theory of Angular Momentum*. World Scientific Publishing Co. Pte. Ltd., Singapore, 1988.
- [155] B. L. Silver. *Irreducible Tensor Methods*, volume 36 of *Physical Chemistry – A Series of Monographs*. Academic Press, New York, 1976.
- [156] R. W. Wetmore and G. A. Segal. Efficient generation of configuration interaction matrix elements. *Chem. Phys. Lett.* **36** (4), 478–483 (1975).
- [157] M. L. Munzarová. DFT calculations of EPR hyperfine coupling tensors. In *Calculation of NMR and EPR parameters*, edited by M. Kaupp, M. Bühl, and V. G. Malkin, chapter 29, pages 581–591, Wiley-VCH, Weinheim, 2004.
- [158] V. A. Rassolov and D. M. Chipman. Alternative Fermi contact operators for EPR and NMR. In *Calculation of NMR and EPR parameters*, edited by M. Kaupp, M. Bühl, and V. G. Malkin, chapter 31, pages 581–591, Wiley-VCH, Weinheim, 2004.
- [159] L. E. McMurchie and E. R. Davidson. One- and two-electron integrals over cartesian Gaussian functions. *J. Comp. Phys.* **26** (2), 218–231 (1978).
- [160] P. R. Taylor. Symmetry-adapted integral derivatives. *Theor. Chim. Acta* **69** (5–6), 447–460 (1986).

- [161] P. R. Taylor. Molecular symmetry and quantum chemistry. In *European Summerschool in Quantum Chemistry*, edited by B. O. Roos, volume 58 of *Lecture Notes in Chemistry*, Springer-Verlag, Berlin and Heidelberg, 1992.
- [162] M. Waletzke. *Implementation und Anwendung von Multireferenz-DFT und -ab initio Methoden für große Moleküle*. PhD thesis, Universität Bonn, 2001.
- [163] P. R. Taylor. FLASH, in-core symmetry-blocked 4-index transformation for any symmetry of 2-electron operators, 2007 (unpublished). University of Warwick, UK.
- [164] B. Bohn, F. Stuhl, G. Parlant, P. J. Dagdigian, and D. R. Yarkony. Predissociation of the NH/ND($c^1\Pi$, v' , J') states. *J. Chem. Phys.* **96** (7), 5059–5068 (1992).
- [165] G. Parlant, P. J. Dagdigian, and D. R. Yarkony. Predissociation of the $c^1\Pi$ state of NH (ND): The role of dipolar spin-spin coupling. *J. Chem. Phys.* **94** (3), 2364–2367 (1991).
- [166] T. H. Dunning, Jr. Gaussian basis sets for use in correlated molecular calculations. 1. The atoms boron through neon and hydrogen. *J. Chem. Phys.* **90** (2), 1007–1023 (1989).
- [167] D. E. Woon and T. H. Dunning, Jr. Gaussian basis sets for use in correlated molecular calculations. 5. Core-valence basis-sets for boron through neon. *J. Chem. Phys.* **103**, 4572–4585 (1995).
- [168] F. Neese. ORCA, an ab initio, DFT and semiempirical SCF-MO package. Universität Bonn, Germany.
- [169] V. Barone. Structure, magnetic properties and reactivities of open-shell species from density functional and self-consistent hybrid methods. In *Recent Advances in Density Functional Methods*, edited by D. P. Chong, volume I of *Recent Advances in Computational Chemistry*, pages 287–334, World Scientific, Singapore, 1995.
- [170] A. Schäfer, C. Huber, and R. Ahlrichs. Fully optimized contracted Gaussian basis sets of triple zeta valence quality for atoms Li to Kr. *J. Chem. Phys.* **100** (8), 5829–5835 (1994).
- [171] T. Amano and E. Hirota. Microwave spectrum of the molecular oxygen in the excited vibrational state. *J. Mol Spectrosc.* **53** (3), 346–363 (1974).
- [172] T. J. Cook, B. R. Zegarski, W. H. Breckenridge, and T. A. Miller. Gas phase EPR of vibrationally excited O₂. *J. Chem. Phys.* **58** (4), 1548–1552 (1973).
- [173] R. A. Kendall, T. H. Dunning, Jr, and R. J. Harrison. Electron affinities of the first-row atoms revisited - systematic basis-sets and wave functions. *J. Chem. Phys.* **96**, 6796–6806 (1992).

- [174] H. Horn, H. Weiss, M. Häser, M. Ehrig, and R. Ahlrichs. Prescreening of two-electron integral derivatives in SCF gradient and Hessian calculations. *J. Comput. Chem.* **12** (9), 1058–1064 (1991).
- [175] J. Tatchen and C. M. Marian. On the performance of approximate spin-orbit Hamiltonians in light conjugated molecules: The fine-structure splitting of HC_6H^+ , NC_5H^+ , and NC_4N^+ . *Chem. Phys. Lett.* **313** (1–2), 351–357 (1999).
- [176] L. C. Owono Owono, N. Jaidane, M. G. Kwato Njock, and Z. Ben Lakhdar. Theoretical investigation of excited and Rydberg states of imidogen radical NH: Potential energy curves, spectroscopic constants, and dipole moment functions. *J. Chem. Phys.* **126** (24), 244302–1 – 244302–13 (2007).
- [177] J. Manz, A. Zilch, P. Rosmus, and H.-J. Werner. MCSCF-CI calculations of infrared transition-probabilities in the CH^- and NH^- ions. *J. Chem. Phys.* **84** (9), 5037–5044 (1986).
- [178] D. Patel-Misra, G. Parlant, D. G. Sauder, D. R. Yarkony, and P. J. Dagdigian. Radiative and nonradiative decay of the NH (ND) $A^3\Pi$ electronic state: Predisociation induced by the $^5\Sigma^-$ state. *J. Chem. Phys.* **94** (3), 1913–1922 (1991).
- [179] D. R. Yarkony. On the electronic structure of the NH radical. The fine structure splitting of the $X^3\Sigma^-$ state and the spin-forbidden ($b^1\Sigma^+$, $a^1\Delta$) \rightarrow $X^3\Sigma^-$, and the spin-allowed $A^3\Pi \rightarrow X^3\Sigma^-$ and $c^1\Pi \rightarrow (b^1\Sigma^+, a^1\Delta)$, radiative transitions. *J. Chem. Phys.* **91** (8), 4745–4757 (1989).
- [180] O. Takahashi, M. Watanabe, and O. Kikuchi. The 'triplet-excited region' in linear polyenes: Real or artifactual? *Theochem-J. Mol. Struct.* **469**, 121–125 (1999).
- [181] O. Takahashi, M. Watanabe, and O. Kikuchi. Structure of the T_1 -state wave function of linear polyenes. *Int. J. Quantum Chem.* **67** (2), 101–106 (1998).
- [182] M. Kuki, Y. Koyama, and H. Nagae. Triplet-sensitized and thermal-isomerization of all-trans, 7-cis, 9-cis, 13-cis, and 15-cis isomers of β -carotene - configurational dependence of the quantum yield of isomerization via the T_1 state. *J. Phys. Chem.* **95** (19), 7171–7180 (1991).
- [183] H. Ma, C. Liu, and Y. Jiang. "Triplet-excited region" in polyene oligomers revisited: Pariser-Parr-Pople model studied with the density matrix renormalization group method. *J. Chem. Phys.* **120** (19), 9316–9320 (2004).
- [184] H. Ma, F. Cai, C. Liu, and Y. Jiang. Spin distribution in neutral polyene radicals: Pariser-Parr-Pople model studied with the density matrix renormalization group method. *J. Chem. Phys.* **122** (10), 104909–1–104909–7 (2005).
- [185] C. M. Marian. Performance of the combined density functional theory/-multireference configuration interaction method on electronic excitation of extended π -systems. To be published.

- [186] J. Tatchen and C. M. Marian. Vibronic absorption, fluorescence, and phosphorescence spectra of psoralen: A quantum chemical investigation. *Phys. Chem. Chem. Phys.* **8** (18), 2133–2144 (2006).
- [187] C. M. Marian. The guanine tautomer puzzle: Quantum chemical investigation of ground and excited states. *J. Phys. Chem. A* **111** (8), 1545–1553 (2007).
- [188] S. Perun, J. Tatchen, and C. M. Marian. Singlet and triplet excited states and intersystem crossing in free-base porphyrin: TDDFT and DFT/MRCI study. *ChemPhysChem* **9**, 282–292 (2008).
- [189] O. Treutler and R. Ahlrichs. Efficient molecular numerical integration schemes. *J. Chem. Phys.* **102** (1), 346–354 (1995).
- [190] K. Eichkorn, F. Weigend, O. Treutler, and R. Ahlrichs. Auxiliary basis sets for main row atoms and transition metals and their use to approximate Coulomb potentials. *Theor. Chem. Acc.* **97** (1–4), 119–124 (1997).
- [191] M. von Arnim and R. Ahlrichs. Geometry optimization in generalized natural internal coordinates. *J. Chem. Phys.* **111** (20), 9183–9190 (1999).
- [192] G. Schaftenaar and J. H. Noordik. MOLDEN: A pre- and post-processing program for molecular and electronic structures. *J. Comput.-Aid. Mol. Des.* **14** (2), 123–134 (2000).
- [193] S. Hirata, S. Ivanov, and R. J. Bartlett. Exact-exchange time-dependent density-functional theory for static and dynamic polarizabilities. *Phys. Rev. A* **71** (3), 032507–1–032507–7 (2005).
- [194] A. Savin, C. J. Umrigar, and X. Gonze. Relationship of Kohn-Sham eigenvalues to excitation energies. *Chem. Phys. Lett.* **288** (2–4), 391–395 (1998).

Acknowledgement

First of all, I would like to thank my advisor Christel M. Marian for endowing me with this intensely interesting and challenging project. She gave me the chance to pursue its depths in my own respect, to learn and improve in this process, and ultimately to contribute genuinely to the scientific field. I sincerely thank her for the confidence and judgment in assigning this task to me, for providing me with the freedom to investigate it, and for her support not only in a scientific respect.

The initiation by Martin Kleinschmidt into the existing program environment was undoubtedly an important aspect in obtaining an overview over this task, and his continuing responsiveness in particular in questions concerning the implementation and computational realization was of considerable support to me.

I would like to thank Jörg Tatchen for his open-mindedness, his knowledgeability, and for always being interested in and approachable for my questions. Engaging in scientific discussions with him was not only a joy, but constituted a crucial element in improving my understanding of issues arising.

The interaction with Karin Schuck as a person who constantly displays an enjoyable positiveness as well as providing ground for various interesting conversations certainly contributed to the realization of this project.

The tremendous support from Susanne Salzmänn extends beyond the scientific level. Thanks for all the smiles, the uncountable cups of tea, and for being a friend I very much value.

I would furthermore like to thank those persons at the Institute of Theoretical and Computational Chemistry at the University of Düsseldorf that I did not mention individually: I cannot say more than that I enjoyed very much being there.

Peter Taylor I could thank in multitudinous respects — I confine myself by thanking him, above all, for being so much more than just a friend. It is apparent that without him I would not be where I am.

I furthermore thank the Stipend-Fonds trust of the Verband der Chemischen Industrie e. V. for supporting this work through the Chemiefonds-scholarship. The symmetrization of spatial integrals at the University of Warwick was funded in the context of the Marie Curie Research Training Network NANOQUANT. The last stage of this project was supported by the Deutsche Forschungsgemeinschaft through the Sonderforschungsbereich 663 “Molecular Response to Electronic Excitation”.

Die hier vorgelegte Dissertation habe ich eigenständig und ohne unerlaubte Hilfe angefertigt. Die Dissertation wurde in der vorgelegten oder in ähnlicher Form noch bei keiner anderen Institution eingereicht. Ich habe bisher keine erfolglosen Promotionsversuche unternommen.

Düsseldorf, den 25.04.2008

(Natalie Gilka)

Zusammenfassung der Dissertation: Electron Spin-Spin Coupling from Multireference CI Wave Functions

Natalie Gilka
Heinrich-Heine-Universität Düsseldorf
April 2008

Die vorliegende Dissertation befasst sich mit der methodologischen Entwicklung und anschließenden Implementation von elektronischer Spin-Spin-Kopplung in ein bestehendes Programmpaket. Elektronische Spin-Spin-Kopplung bezeichnet die Wechselwirkung zwischen den Spins von ungepaarten Elektronen und manifestiert sich spektroskopisch u. a. in der sogenannten Nullfeld-Aufspaltung. Die theoretische Behandlung der Spin-Spin-Kopplung zwischen Elektronen ist bisher stark limitiert, besonderes Interesse bestand in diesem Zusammenhang an einem Ansatz, der auf einer hochkorrelierten Behandlung basiert und die Berechnung größerer Systeme ermöglicht. In der Gruppe von Christel M. Marian an der Universität Düsseldorf wird mit Erfolg ein selektierendes Multireferenz-CI als Korrelationsansatz für molekulare Systeme moderater Größe verwendet. Die hierin erhaltene Wellenfunktion stellt die Basis für eine anschließende Berechnung von Spin-Bahn-Wechselwirkungen dar. Die Aufgabe innerhalb meiner Doktorarbeit bestand in der Erweiterung des Spin-Bahn-Paketes um die Möglichkeit, elektronische Spin-Spin-Kopplung mittels quasi-entarteter Störungstheorie zu berechnen.

Die starke theoretische/methodologische Orientierung der Arbeit umfasste zunächst die Ausarbeitung der entsprechenden Spin-Spin-Kopplungsterme. Beginnend mit den in der Literatur verfügbaren Operatorausdrücken wurden Umformulierungen durchgenommen, die die speziellen mathematischen Eigenschaften des Spin-Spin-Operators ausnutzten. Ziel war hierin eine Vereinfachung der zu berechnenden Terme auf dem Hintergrund der verwendeten Rechenzeit. Des Weiteren waren durch das umgebende Spin-Bahn-Paket Rahmenbedingungen hinsichtlich der möglichen Realisierung gegeben, die in diesen Umformulierungen berücksichtigt werden mussten. Das Spin-Bahn-Paket selbst arbeitet mit einem effizienten Algorithmus zur Berechnung der Spin-Wechselwirkungen im Rahmen einer Ein-Elektronen-Behandlung. Es musste gezeigt werden, dass dieser Algorithmus prinzipiell auf den Zwei-Elektronen-Fall erweiterbar ist und dass dies zudem innerhalb der Programmumgebung realisiert werden kann. Dieser Schritt stellte einen zentralen Aspekt in der Umsetzung der vorliegenden Arbeit dar. In der eigentlichen Programmierung wurden die äußeren Strukturen des Spin-Bahn-Codes als Orientierung für die Spin-Spin-Implementation verwendet. Die Auswahlregeln zwischen beiden Fällen unterscheiden sich jedoch gravierend, so dass das Programmdesign insbesondere in inneren Routinen stark erweitert wurde. Der räumliche Beitrag zur Spin-Spin-Kopplung wurde im Rahmen eines kooperativen Projektes an der University of Warwick (UK) erarbeitet. Dies involvierte Programmentwicklung auf der Ebene der Integralberechnung. Im letzten Teil der Arbeit wurden die Möglichkeiten des Programms in Anwendungsrechnungen demonstriert und erste Einsichten hinsichtlich der Eigenschaften von elektronischer Spin-Spin-Kopplung erhalten.

Summary of Dissertation: Electron Spin-Spin Coupling from Multireference CI Wave Functions

Natalie Gilka
Heinrich-Heine-Universität Düsseldorf
April 2008

The present dissertation concerns the methodological development and subsequent implementation of electron spin-spin coupling into an existing programming package. Electron spin-spin coupling describes the interaction between the spins of unpaired electrons and manifests itself experimentally *inter alia* in the so-called zero-field-splitting. Theoretical considerations of this effect are limited; particular interest in this context lay in the development of an evaluation of this effect based on a high-level correlation treatment, feasible for application on larger systems. The group of Christel M. Marian at the University of Düsseldorf successfully operates with a selecting multireference CI approach in the computation of systems of moderate size. The wave function obtained in the correlation treatment constitutes the starting point for a subsequent calculation of spin-orbit interactions. The task within my thesis was an extension of the capabilities of the spin-orbit package by a computation of spin-spin coupling effects in the framework of quasi-degenerate perturbation theory.

The strong theoretical/methodological emphasis of the work encompassed in the first part the derivation of sets of equations describing electron spin-spin interactions. Expressions available in the literature were reformulated utilizing the particular mathematical properties of this operator, aiming at a simplification of the individual terms on the basis of a reduction in the computational labour. The general framework of the surrounding spin-orbit package imposed further conditions which had to be accounted for in the actual reformulations. The spin-orbit package implements an efficient scheme for the evaluation of the spin part in the formalism of a one-electron mean-field approach. It had to be shown that in principle, this scheme can be extended from the case of a one- to a two-electron spin-operator and furthermore, that this could be incorporated into the existing program environment. This step constituted a crucial aspect in the realization of the present work. In the subsequent program development, the outer structure of the spin-orbit code constituted an orientation for the spin-spin implementation. However, different selection rules as well as additional coupling cases necessitated a substantial extension of the code design, particularly in the innermost routines. The spatial contribution to the spin-spin interaction was obtained through a cooperative project at the University of Warwick (UK). This involved program development on the level of integral evaluation. In the last part of the thesis, the potential of the program was illustrated on application calculations of different molecular systems, obtaining first insights into the characteristics of electron spin-spin coupling.